Molecular Mechanism of Bruton's Tyrosine Kinase Activation by the HIV-1 Nef Virulence Factor

by

Manish Aryal

B.A., The College of Wooster, 2014

Submitted to the Graduate Faculty of the

School of Medicine in partial fulfillment

of the requirements for the degree of

Doctor of Philosophy

University of Pittsburgh

2021

UNIVERSITY OF PITTSBURGH

SCHOOL OF MEDICINE

This dissertation was presented

by

Manish Aryal

It was defended on

December 15, 2021

and approved by

Thomas Smithgall, Ph.D., Professor and Chair of Microbiology and Molecular Genetics, School of Medicine

Rieko Ishima, Ph.D., Associate Professor, Department of Structural Biology, School of Medicine

John Jeff Alvarado, Ph.D., Research Assistant Professor, Department of Microbiology and Molecular Genetics, School of Medicine

Amy Andreotti, Ph.D., University Professor and Chair of Department of Biochemistry, Biophysics, and Molecular Biology, Iowa State University

Dissertation Director: James Conway, Ph.D., Associate Professor, Department of Structural Biology, School of Medicine

Molecular Mechanism of Bruton's Tyrosine Kinase Activation by the HIV-1 Nef Virulence Factor

Manish Aryal, PhD

University of Pittsburgh, 2021

Antiretroviral therapy has significantly boosted the effort in the fight against HIV. However, a cure has still not been found. The shortcomings associated with antiretroviral therapy underscore the need for alternative approaches to eliminate the latent viral reservoirs. HIV-1 Nef represents an attractive drug target in this regard because of its role in immune escape of HIV-infected cells.

I explored the mechanism of interaction between HIV-1 Nef and Bruton's tyrosine kinase (BTK), a member of the TEC tyrosine kinase family previously shown to enhance the HIV-1 life cycle in cells of myeloid lineage. I discovered that HIV-1 Nef activates BTK by a unique mechanism dependent upon SH3-SH2-mediated dimerization. In a solution-based assay, complex formation with HIV-1 Nef increased the stability of the BTK SH3-SH2 dimer. A cell-based bimolecular fluorescence complementation assay also showed increased recruitment of the BTK dimer to the cell membrane in presence of Nef. Alanine substitution of Pro327 in BTK SH2 domain CD-loop reduced the stability of the BTK dimer in solution, and also reduced BTK homodimerization in cells. Introduction of the P327A mutation completely uncoupled BTK from Nef-mediated activation in a kinetic kinase assay, and also prevented BTK dimerization and activation in response to Nef in cells. The effect of the P327A mutation is consistent with molecular modeling studies which identified a novel interface between the SH2 CD loop and the SH3 domain, where Pro327 is predicted to stabilize a specific CD loop conformation for SH3

engagement. An analogous interaction was demonstrated previously by NMR for the related kinase ITK, which also contributes to the HIV life cycle in CD4 T cells.

Remarkably, this mechanism of BTK activation through stabilization of SH3•SH2 interaction is distinct from the SH3 domain displacement mechanism previously described for Nef-mediated activation of SRC-family kinases, indicating that this viral protein has evolved two separate mechanisms for host cell tyrosine kinase activation. Molecular details of the Nef-driven BTK activation process may guide future drug targeting of this unique interaction. The requirement of HIV-1 Nef homodimerization in this model suggests that HIV-1 Nef dimerization can be targeted for potential therapeutic intervention.

Table of Contents

List of Tables

List of Figures

Acknowledgements

I would like to thank everyone who has helped me over the past few years in graduate school. First of all, I would like to thank my mentor Dr. Thomas Smithgall for the opportunity to join his lab and conduct my dissertation research. I am thankful to Tom for allowing me the creative freedom throughout my time to come up with hypotheses and develop experimental techniques. I looked forward to Monday meetings with Tom and discussing the results, and his constant optimism and encouragement motivated me to keep pushing. I am also thankful for Tom's support in pursuing my professional interests.

During my time in Smithgall lab, I have learned not only about what makes a good scientist, but also about teamwork, mentorship, and friendship. I would like to thank Dr. John Jeff Alvarado for his mentorship and friendship. He always found a way to brighten the lab environment and was a reminder to always enjoy the process. I would also like to thank Dr. Lori Emert-Sedlak, Dr. Sherry Shu, Dr. Haibin Shi, Dr. Shoucheng Du, and Dr. Li Chen for constant mentorship and always being available to me. Thank you to fellow graduate students Ari Selzer, Kasia Thomas, and Giancarlo Gonzalez-Areizaga for your friendship and help. It has been such a pleasure to share the highs and lows with you. Thank you to Kiera Regan for your help, enthusiasm, and contribution to this project.

Thank you to former members of Smithgall lab who have helped me over the years as well. Dr. Ryan Staudt, Dr. Ravi Patel, and Winson Li helped me a lot through both experimental designs as well as dealing through the difficult patches. Also, thank you to Kindra Whitlatch and Dr. Heather Rust for their help early on.

Lastly, thank you to my dissertation committee for helping me throughout this process. I have learned a lot from your feedback on my project and it has helped me in keeping focus.

1.0 Introduction

1.1 The global pandemic of HIV infection and AIDS

1.1.1 Origin of the AIDS crisis

In June 1981, a team of clinicians reported a mysterious illness among five homosexual men in Los Angeles [1]. These patients displayed symptoms that were previously seen in immunocompromised people only, including lower T cell counts, defective immunity and decreased lymphocyte proliferative responses, suggesting the new disease mainly targeted the immune system, and may be transmitted through sexual contact. Another report published a month later found similar symptoms in 26 men who have sex with men in New York and California [2]. These patients were also diagnosed with opportunistic infections such as a rare malignant neoplasm associated with immunosuppression called Kaposi's sarcoma (KS), *Pneumocystis carinii* pneumonia (PCP) as seen earlier in the Los Angeles patients, or other infections. This prompted the US Centers for Disease Control (CDC) to form a task force to undertake surveillance and perform epidemiologic and laboratory tests for PCP, KS, and other infections in men who have sex with men. The report documented PCP, KS, and other infections in 159 patients, and sounded the alarm for a rapidly increasing infectious disease with a high mortality rate [3]. As the number of cases grew, more studies were conducted that uncovered the immune dysfunction brought on by this disease, including the loss of CD4+ T cells [4]. A large proportion of the patients also displayed symptoms like fatigue, fever, weight loss, lymphadenopathy, and subsequently displayed KS, PCP, or other infections, including more than one infection at a time. In September

1982, the CDC named the new disease acquired immunodeficiency syndrome (AIDS) and defined it as a disease associated with defects in cellular immunity and occurrence of PCP, KS or other opportunistic infections in people with no known etiology [5]. In the next few months, new infections were found in patients who had received blood-derived products, intravenous drug users, and sexual partners of patients with AIDS. These epidemiological reports suggested the presence of an infectious agent that is transmitted through blood-borne, sexual and vertical transmissions, and thus led the scientific community on a quest to identify the unknown agent behind this pandemic.

1.1.2 Discovery of HIV-1 as the cause of AIDS

This inquest coincided with rapid developments in methods to stably grow cell lines from patients with various leukemias, lymphomas, and sarcomas, allowing the discovery and isolation of complete, well-defined retrovirus particles from various human tissues [6, 7]. In 1980, Gallo and colleagues reported the detection and isolation of the first retrovirus particles in T-cell lines (human T-lymphotropic virus; HTLV) from a patient with a cutaneous T-cell lymphoma, and these particles were found to be associated with abnormal T-cell replication [8]. Abnormal T-cell function and counts are also observed in AIDS patients, leading to the hypothesis that a similar retrovirus that specifically infects T-cells might be the infectious agent behind AIDS.

The first glimpse into this mysterious infectious agent was provided by Luc Montagnier's group in 1983 [9]. Using similar techniques that enabled isolation of HTLV in Gallo's study, they cultured T cells from a lymph node biopsy of a patient displaying symptoms that often precede AIDS (called pre-AIDS). The virus particles obtained were able to infect T cells from healthy donors, but unable to infect other cell types. Reverse transcriptase activity and electron

microscopy-based morphology suggested isolation of an HTLV-related but clearly distinct isolate of a type-C RNA retrovirus (initially designated as HTLV-III). Even though the identity and morphology of the retrovirus isolated from the T cells of a pre-AIDS patient was now known, the virus's clear association with AIDS was still unproven. Gallo's group made another significant contribution by establishing the causal relationship between HTLV-III and AIDS [10]. They isolated HTLV-III from a total of 48 patients including 18 of 21 patients with pre-AIDS, three of four clinically normal mothers of juveniles with AIDS, 26 of 72 adult and juvenile patients with AIDS, and from one of 22 male homosexual patients. Further proof of the causal relationship was provided by another study which detected AIDS-associated retroviruses (ARV) in 22 of 45 randomly selected patients with AIDS in San Francisco [11]. Similar to HTLV-III, ARV could also be propagated in the human T cell line HUT-78. Furthermore, ARV obtained from these patients cross-reacted with antibodies to a lymphadenopathy-associated retrovirus from AIDS patients in France. Antibodies to ARV were also found in all 86 AIDS patients tested. In 1986, the International Committee of the Taxonomy of Viruses recommended that this AIDS-causing virus be called the human immunodeficiency virus-1 (HIV-1) [12].

1.1.3 Simian origin and HIV-1 subtypes

Even though the likely cause of AIDS was now identified, its origin, reasons for sudden emergence and pandemic spread were still a mystery. Clavel *et al*. reported a novel human retrovirus that is morphologically similar but antigenically distinct from HIV-1 in two AIDS patients from West Africa [13]. This new virus was referred to as HIV-2 and found to be recognized by antibodies from a macaque with simian AIDS infected by the simian immunodeficiency virus (SIV_{mac}). HIV-2 was also found to be genetically closer to SIV than HIV-

1 [14]. Over the next few years, additional SIV variants were discovered in primates from sub-Saharan Africa, including African green monkeys, sooty mangabeys, mandrills, and chimpanzees. Genetic comparisons revealed that close simian relatives of HIV-1 and HIV-2 are found in chimpanzees (SIV_{cpz}) and sooty mangabeys (SIV_{sm}), respectively [15, 16]. This suggested that AIDS may have emerged due to cross-species infections with lentiviruses from different primate species. Indeed, subsequent studies confirmed the early suspicions of zoonotic transfer of these viruses from primates in Africa, with SIV_{cpz} and SIV_{sm} as the immediate ancestors of HIV-1 and AIDS in humans [17]. The origins and distributions of primate lentiviruses are discussed in detail elsewhere [18].

The rate of evolution of HIV-1 is estimated to be one million times faster than mammalian DNA due to the short viral generation time and error prone HIV-1 genome replicase called reverse transcriptase [19, 20]. Statistical and phylogenetic analyses have dated the last common ancestor of HIV-1 to around 1910 – 1930 [21], suggesting that HIV-1 had spread for about 50 to 70 years in West Africa before it was identified and characterized as a disease agent. This would allow sufficient time for the virus to spread and create extensive viral diversity. With the increase in urbanization and mass movements in the mid to late twentieth century, and after years of circulating in West Africa, HIV-1 was propelled onto the global stage. Today, four distinct lineages of HIV-1 exist which are known as groups M, N, O, and P which have resulted from four independent cross-species transmissions. HIV-1 groups M and N are of chimpanzee origin, with group M transmitted during the early twentieth century and group N appearing more recently [18, 21]. Group P is of gorilla origin and crossed over to humans recently. The origin of group O is not clear but was transmitted in the early twentieth century. These groups vary in prevalence and pathogenesis in humans. Group M represents the pandemic form of HIV-1 and is present in over

90% of global HIV-1 infections; Group O represents less than 1% of global HIV-1 infections; Group N is even less prevalent than group O; and group P is a new group with only 2 cases in humans so far. Group M is further divided into subtypes (also called clades), which are designated as A1, A2, A3, A4, B, C, D, F1, F2, G, H, J, and K. Genetic variations within a subtype (e.g., subtypes A, F) can be 15 to 20% whereas variation between subtypes can be 25 to 35% [22]. Subtype C is the most common and is responsible for 50% of all infections worldwide [22]. Subtypes A, B, D, and G are present in 12%, 10%, 3% and 6% of patients respectively. Subtypes F, H, J and K are less prevalent and together account for only 0.94% of global infections. Additional genetic diversity is provided by recombination that can occur in individuals infected with more than one subtype leading to formation of a circulating recombinant form (CRF). CRFs CRF01_AE and CRF02_AG are each responsible for 5% of cases globally. To date, over 100 HIV-1 CRFs have been characterized [23]. Recombinant forms that are present in less than three individuals are described as unique recombinant forms (URFs). Regional distribution of HIV-1 subtypes is shown in Figure 1. HIV-1 subtypes not only display differences in their distribution, but also in transmission rates, interactions with the human host and the rates of disease progression. Detailed discussion of HIV-1 subtype diversity and their implications are discussed in detail elsewhere [24].

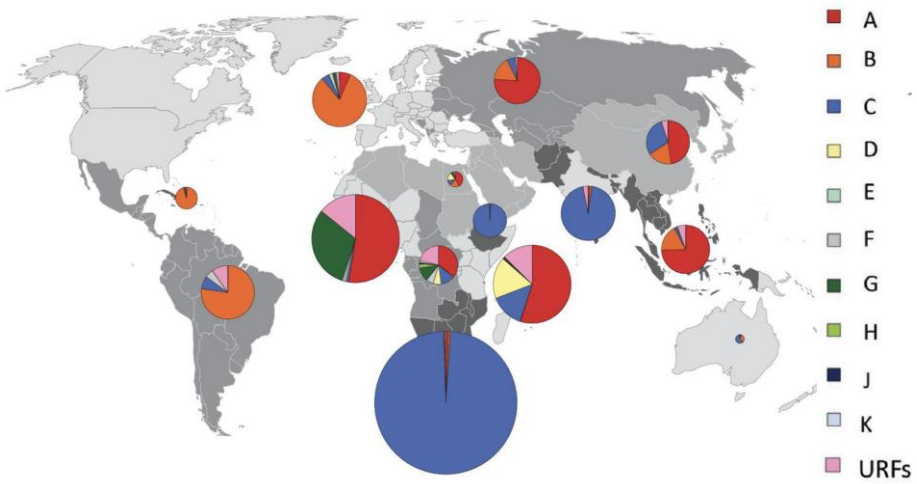

Figure 1. Regional distribution of HIV-1 subtypes.

All countries are grouped into 14 regions and individual regions are shaded differently on the map. The proportion of HIV infections attributed to each subtype in each region is shown in pie charts. The surface area of the pie charts is proportional to the relative number of people living with HIV in each region. Figure obtained and re-published from Elangovan *et al*. [25], and is licensed under the Creative Commons Attribution License (CC BY).

1.1.4 Current status of the pandemic

While AIDS was first recognized in the US in 1981 after originating and spreading from West Africa, the disease has spread globally infecting over 80 million people to date. More than 40 million people have lost their lives due to AIDS-related illnesses. UNAIDS estimates that almost 38 million people were living with HIV in 2019, including 1.7 million new infections and 0.8 million deaths [26]. In the last decade, the rate of new infections and AIDS-related mortality have been steadily decreasing leading to stabilization of the pandemic. However only 53% of infected individuals have access to antiretroviral drugs, meaning about 17 million people with HIV-1 are living without therapy [27]. Moreover, 21% of people with HIV-1 do not know their HIV-1 status, and therefore pose significant hurdles in efforts to curb new HIV-1 infections.

The spread of HIV-1 in resource-limited parts of the world remains a major challenge in the fight against AIDS. Today, more than 70% of HIV-1 positive people live in sub-Saharan Africa

[28]. While the majority of new infections in sub-Saharan Africa occur in heterosexual individuals above age 25, young women are disproportionally affected. More than 4 in 10 infections occur in women aged 19-24 [29, 30]. Adolescent and young sex workers, men who have sex with men, people who inject drugs, transgender youth, and children represent the most vulnerable populations in sub-Saharan Africa [31].

With about 14% of HIV-1 cases, Asia and the Pacific rim represent the second most affected region. Vulnerable populations in this region include men who have sex with men, intravenous drug users, and transgender people [32]. North America and Western and Central Europe represent the third most affected regions with about 2.4 million people living with HIV-1. Vulnerable populations in this region vary for each country, but generally include men who have sex with men, people who inject drugs and their sexual partners, migrants from sub-Saharan Africa, transgender people, prisoners, and sex workers. The Middle East and North African region are the least affected regions with only 0.1% of patients.

Even though the virus was discovered almost 40 years ago, no cure has been found. However, successful prevention and treatment methods have been developed which have slowed the progression of the pandemic. Early strategies of prevention included behavioral changes, condom use, HIV testing, and blood supply safety. Pre-exposure prophylaxis (PrEP) is now recommended by the WHO as a form of prevention in addition to other methods for high-risk populations. HIV-1 treatment involving combination antiretroviral therapy (ART), along with medications to prevent opportunistic infections, have been tremendously successful in lowering transmission and mortality rates across all demographics and HIV-1 subtypes. Individuals on ART also have very low plasma levels of HIV-1 and are less likely to transmit the virus to others. Current methods of HIV-1 treatment and management will be discussed in section 1.2.4.

1.2 HIV-1 genome, structure, and encoded proteins

1.2.1 Genome and Structure

HIV-1 belongs to a class of viruses known as retroviruses and a subgroup of retroviruses known as lentiviruses [33]. HIV-1 is enveloped by the host-derived plasma membrane and contains two copies of a single-stranded positive-sense RNA genome. The viral RNA is enclosed inside a conical capsid composed of the viral capsid protein, p24 [34]. The prototypical HIV-1 RNA is 9,749 nucleotides long and bears a 5´ cap, a 3´ poly(A) tail, and several open reading frames (ORFs) that encode nine proteins, including the Gag, Pol, and Env polyproteins, which are proteolyzed further. Four Gag proteins, MA (matrix or p17), CA (capsid or p24), NC (nucleocapsid or p7), and p6 are viral core proteins. Two Env (envelope) glycoproteins, SU (surface or gp120) and TM (transmembrane or gp41) together form the viral surface along with membrane derived from the host cell. Pol-derived proteins include protease (PR), integrase (IN), and reverse transcriptase (RT) which are enzymes required for viral replication [35]. HIV-1 also encodes the regulatory proteins Tat and Rev, which activate viral transcription and control the splicing and nuclear export of viral transcripts, respectively [36]. Lastly, HIV-1 also encodes four accessory proteins, Vif, Vpr, Vpu, and Nef. Of these, Vif, Vpr and Nef are incorporated into budding virions [37]. The viral genome is flanked by long terminal repeats (LTRs) that are required for viral gene expression, reverse transcription, and integration.

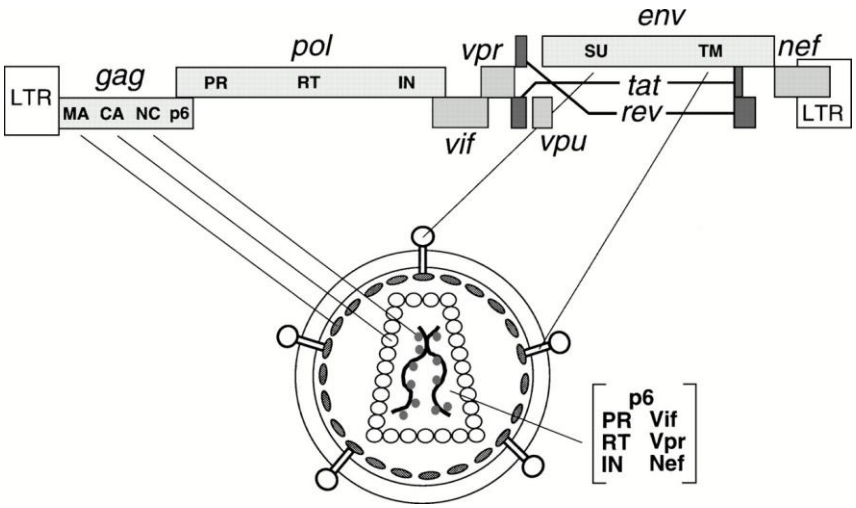

Figure 2. HIV-1 genome and virion.

HIV-1 is a retrovirus that is approximately 90-120 nm in diameter and is enveloped by plasma membrane derived from the host cell during egress. Spikes on the virion surface are formed by the trimeric envelope glycoproteins gp120/gp41 and are embedded on the membrane. The cytoplasmic tail of gp41 interacts with HIV-1 MA. The cone-shaped viral core is formed by p24 capsid protein during maturation. The core contains two copies of positive-strand RNA. The figure shows Nef protein within the capsid, however Nef fucntions are understood in the context of Nef in host cells only, and Nef presence in virus may be passive incorporation than active. Republished with permission of Annual Reviews, Inc., from HIV-1: Fifteen Proteins and an RNA, Frankel *et al*., 1998 [37]; permission conveyed through Copyright Clearance Center, Inc.

HIV-1 capsid viral core and viral membrane

HIV-1 capsid cores form "fullerene cones", which are a family of related structures comprising conical hexagonal nets that close at both ends through the introduction of 12 pentons (Figure 2) [38]. Pentamers can be distributed differently to give different cones. Each capsid core contains approximately 1,500 CA proteins to form the closed structure. Inside the core are two copies of HIV-1 RNA genome, NC, RT, IN, and accessory proteins Vpr, Vif and Nef [39-41]. The capsid core helps to protect the viral genome from host factors which can detect viral nucleic acids and initiate an antiviral response [42]. A matrix composed of p17 surrounds the capsid, which is then surrounded by a lipid envelope.

HIV-1 acquires its envelope from the host cell membrane by assembly and budding at the plasma membrane of the infected cell [43]. Lipid mass spectrometry results have revealed the viral membrane is enriched with "raft lipids" composed of sphingomyelin, cholesterol, and

plasmalogen-phosphatidyl ethanol, with an increase in saturated fatty acids compared to the producer cell membrane. [44, 45]. The membrane also contains glycoproteins gp120 and gp41, which are responsible for binding to and entering the host cell.

1.2.2 HIV-1 proteins

Gag proteins

Group-specific antigen (Gag) is a polyprotein that makes up the core structures of almost all members of the viral order *Ortervirales* (except *Caulimoviridae*) including retroviruses. Gag was named as such because it was believed to be antigenic, however we now know it makes up the viral capsid core and not the exposed envelope. The HIV-1 Gag precursor protein is also called p55 because of its 55 kDa molecular weight. Gag is expressed from the unspliced viral mRNA and is myristoylated at its N-terminus during translation [46]. Myristoylation targets the Gag polyprotein to the inner cell membrane, where it recruits two copies of viral RNA and proteins to trigger budding of viral particles. After budding, Gag is cleaved by the viral protease into four protein products – N-terminally myristoylated matrix (MA or p17), capsid (CA or p24), nucleocapsid (NC or p9), and p6 [47].

Matrix

Since MA is myristoylated, it is involved in targeting Gag and Gag-Pol precursor polyproteins to the plasma membrane prior to viral assembly. MA is 132 residues long and lines the inner surface of the virion membrane (Figure 2). Structural studies of MA show three monomers arranged in a triskelion form [48]. Mutations that interrupt MA trimerization are shown to be virus assembly defective, suggesting biological roles for MA trimerization. MA utilizes basic residues in the first 50 amino acids to interact with phospholipid headgroups, along with the

insertion of three myristoyl groups, in order to localize to the membrane. In addition to membrane targeting of Gag and Gag-Pol, MA also facilitates infection of non-dividing cells with roles in the viral preintegration complex and nuclear localization processes [49-51].

Capsid

Capsid proteins form the conical core that houses the viral genome along with several viral and host proteins. About 1,500 molecules of CA are required to spontaneously form the viral capsid core, where CA molecules assemble predominantly in hexameric forms, with a few pentamers to facilitate the curvature required for fullerene cone closure [52]. Each CA protomer consists of two domains – the N-terminal domain (CA_{NTD}) and C-terminal domain (CA_{CTD}), which are comprised of ~150 and ~80 residues, respectively. After CA monomers assemble into the capsid core, the CA_{NTD} is exposed to the outside whereas CA_{CTD} faces inside the core. The CA_{NTD}-CA_{CTD} interface further stabilizes the oligomeric state, and also forms binding pockets that allow cellular factors to bind and interact in order to facilitate viral infection [53-55]. CA also interacts with the cellular peptidylprolyl isomerase cyclophilin A and incorporates it into the virion. Interaction between CA and cyclophilin A is essential for viral replication and is a drug target for molecules that work by preventing viral assembly [56, 57].

Nucleocapsid

Nucleocapsid is a 55 residue long viral protein that binds nucleic acids through two retroviral-type zinc finger motifs [58]. The zinc finger motifs and other basic residues are involved in interaction with the RNA packaging signal ψ, which is a stable secondary structure of viral mRNA that serves as the first signal for packaging of HIV-1 virions [58, 59]. Initiation of packaging function is carried out by NC as a part of Gag and Gag-Pol proteins, whereas NC can also exist in the capsid core as a fully processed mature protein, where it helps in multiple reverse

transcription steps [60-64]. During virus budding and maturation, cleavage of the Gag polyprotein by viral protease leads to NC maturation, which then binds and stabilizes viral RNA.

p6

p6 comprises the C-terminal 51 residues of Gag and is required for Vpr recruitment to the virion. Residues 32-39 and hydrophobic residues within segment 41-46 in p6 are required for Vpr binding [65, 66]. Even though p6 was originally thought to be unstructured, an N-terminal helix–flexible middle region–C-terminal helix structural configuration was recently reported [67]. p6 regulates the interaction of Gag with components of the cellular endosomal sorting complex required for transport (ESCRT), eventually leading to membrane fission events. Deletion of the primary late assembly domain in p6 resulted in severe budding defects [68-70].

Gag-Pol Precursor polyprotein

Four viral proteins – protease (PR or p10), integrase (IN or p31), RNase H (p15), and reverse transcriptase (RT or p50) are always expressed within the context of a Gag-Pol fusion protein of about 160 kDa. The Gag-Pol fusion protein is encoded by both *gag* and downstream *pol* sequences. These genes lie in different translation frames even though the 3´ end of gag overlaps with the 5´ end of pol gene. Frameshifting by the ribosome generates the Gag-Pol fusion protein [71]. During translation, ribosomes shift approximately 5% of the time, without interrupting translation, to the *pol* reading frame upon encountering a heptanucleotide sequence followed by a short stem loop motif in the distal region of *gag* gene in the viral mRNA [72]. The rare nature of this frame shift is why the Gag and Gag-Pol precursor proteins are produced at approximately a 20:1 ratio. During HIV-1 maturation, the Pol polypeptide is cleaved from Gag by the viral protease to produce the individual Pol proteins described below.

Pol proteins

Protease

HIV-1 protease is a 99-residue aspartyl protease that functions in a dimeric state [73]. PR cleaves Gag and Gag-Pol into smaller viral protein products during viral maturation after budding from the membrane. Large conformational changes occur in the virus particle as PR cleaves the polypeptides. Since PR acts as a part of Pol, PR activity depends on the concentration of Gag-Pol and the rate of autoprocessing, which may be influenced by nearby p6 molecules [74]. Furthermore, cleavage of viral proteins by PR is also influenced by a p2 spacer peptide between CA and NC, and RNA binding of proteins [75, 76]. Therefore, PR is a critically regulated viral enzyme and its overexpression can lower infectivity [77].

Crystal structures of PR reveal that the active site is formed at the dimeric interface with catalytically essential aspartic acid residues (Asp25) from each monomer that closely resemble aspartyl protease active sites with a conserved catalytic triad Asp-Thr-Gly [78, 79]. These structures enabled development of HIV protease inhibitors, which remain as an essential treatment option today for HIV-1 patients.

Reverse transcriptase

RT catalyzes the polymerization reaction that reverse transcribes single-stranded viral RNA into duplex DNA. RT is a heterodimer of 560 residue (p66) and 440 residue (p51) proteins both derived from the Pol polyprotein. Crystal structures of RT, the RT-DNA complex, and RT-inhibitor complexes have greatly improved our knowledge of the RT polymerase mechanism [80-82]. Each subunit of RT contains a polymerase domain with four subdomains often referred to as the fingers, palm, thumb, and connection. p66 also contains an additional RNase H domain, which

removes the original RNA template from the first DNA strand, allowing synthesis of the complementary DNA strand.

Reverse transcription reaction begins when a primer $tRNA_3^{Lys}$ hybridizes with a complementary region in the HIV-1 genome near the 5´ end called the primer binding site. Whether reverse transcription initates within the virus or in the cells is not clearly understood, but majority of the viral DNA synthesis takes place in the infected cells, as there are not abundant dNTPs within the virion. RT adds dNTPs onto the 3´ end of the primer to generate DNA complementary to the U5 (non-coding region) and R (repeats at either ends of viral RNA) regions creating an RNA-DNA duplex, a substrate for RNase H. RNase H then degrades the U5 and R regions on the 5´ end of the viral RNA, exposing the newly synthesized DNA. The newly synthesized minus-strand transfers to 3´ end of R region in viral RNA. Further extension of the cDNA takes place as RNase H degrades the majority of viral RNA leaving only a purine-rich region in viral RNA called the polypurine tract (PP). A second DNA strand is then synthesized by using the PP sequence in the viral RNA as a primer. Then, the tRNA primer leaves and the primer binding site from the second DNA strand hybridizes with the complementary primer binding site on the first DNA strand, allowing the creation of a complete double-stranded DNA copy of the viral genome termed the proviral DNA [83]. HIV-1 RT lacks an exonucleolytic proofreading function, which makes it prone to errors and introduces several point mutations onto each new copy of proviral DNA it generates [84].

Structural and mechanistic insights into RT function led to development of several classes of RT inhibitors that are in clinical use today. Nucleoside analogs such as AZT and ddI lack a 3´ hydroxyl group on their ribose mimetic moiety and act as chain terminators during the RT DNA

elongation process [85, 86]. Non-nucleoside RT inhibitors have also been developed that bind to a hydrophobic pocket close to RT active site, which locks RT in an inactive state [87].

Integrase

Integrase is a 288-amino acid viral protein that mediates a series of reactions to insert HIV-1 proviral DNA into the genomic DNA of human host cells. IN has three domains – an N-terminal multimerization domain that contains an HHCC motif to bind Zn^{2+}, a central catalytic domain that is required for activity, and a C-terminal domain that non-specifically binds to DNA [88-91].

The preintegration complex, composed of proviral DNA and viral proteins, is transported to the nucleus via a yet to be identified mechanism [92]. Then, availability of DNA within the chromosome, rather than a specific DNA sequence, dictates the integration site within the host DNA [93]. Sites with kinks in DNA are suggested to be "hot-spots" for integration in *in vitro* studies [94]. Integrase first removes two 3´ end nucleotides from the long terminal repeats of each strand of the proviral DNA in the cytoplasm. In the second step, which occurs in the nucleus, processed 3´ ends are covalently joined to the 5´ end of non-specifically cut cellular genomic DNA by integrase. In the last step, unpaired nucleotides at the viral 3´ ends are removed, and the ends are joined to human DNA 3´ ends. Cellular enzymes are then required to remove two unpaired nucleotides at the 5´ end of the proviral DNA, fill in the single strand gaps and finally ligate the DNA [95]. The strand transfer step of the integrase mechanism of action is currently targeted by FDA-approved integrase strand transfer inhibitors (INSTIs) [96].

Envelope glycoproteins

HIV-1 envelope glycoproteins are synthesized from a singly spliced mRNA as a single precursor protein gp160 in the rough ER [97]. gp160 contains an N-terminal ER signal sequence that directs it into the rough ER, and also contains a hydrophobic 'stop-transfer' signal that anchors

a portion of it to the ER membrane. This ensures that the ER-lumen portion of gp160 will be ultimately sticking out of the virion, and a transmembrane domain with its C-terminal tail extending into the virion after budding [98]. ER residency also allows for N- and O-linked glycosylation in gp160 [99]. gp160 oligomerizes in the ER to mainly a trimeric state, although dimers and tetramers are also observed [100-102]. Along its passage through the secretory pathway, gp160 acquires further glycosylation in the trans-Golgi network. Also in the Golgi, gp160 is cleaved by cellular furin or furin-like proteases at K/R-X-K/R-R motifs yielding the mature surface (SU) glycoprotein gp120 and the transmembrane glycoprotein gp41 [103, 104]. Following proteolysis, gp120 and gp41 remain weakly associated by noncovalent interactions. Three molecules each of gp120 and gp41 form the trimeric HIV-1 glycoprotein spike, which is rapidly recycled via endocytosis as it reaches the plasma membrane [105]. Weak noncovalent interactions between gp120 and gp41 and rapid recycling by cellular clathrin coated pits explain why there are low levels of Env incorporated into each virus particle (8-10 trimers/virion) [106]. Low-levels of spike glycoproteins may help HIV-1 evade immune responses.

SU glycoprotein

Comparison of genetic variation in HIV-1 isolates reveals surface glycoproteins to be the most variable. There are five constant and five variable domains in the 515-residue gp120 protein. These variable regions in gp120 represent the antigenic sites. In contrast, the constant regions of gp120 are highly conserved [107, 108]. Furthermore, gp120 contains 18 Cys residues that can form covalent disulfide bonds that may change in number and distribution leading to heterogeneous gp120 structure and antigenicity [109]. Moreover, further immune evasion is provided by N-linked glycosylation which masks gp120 from immune cells [110]. Entry of HIV-1 into the host cell is initiated by binding of gp120 to the CD4 receptor, the primary attachment point for all primate

lentiviruses. CD4 binding triggers conformational changes leading to gp120 binding to G protein-coupled chemokine co-receptors CCR5 and CXCR4 depending on the cell type [111]. The CD4 receptor binding site in gp120 is formed by the constant domains. Several crystal structures of HIV-1 gp120 have been solved, in both apo and CD4 bound forms, providing insights into the HIV-1 entry process and leading to the development of HIV-1 entry inhibitors [112-114].

TM glycoprotein

The 345-residue HIV-1 transmembrane protein gp41 mediates the fusion between viral and cellular membranes following gp120-mediated CD4 binding [115]. gp41 consists of three domains – an extracellular domain, a transmembrane domain, and a C-terminal cytoplasmic tail. The extracellular domain contains an N-terminal hydrophobic fusion peptide, a polar region, two coiled-coil structures referred to as heptad-repeat regions HR1 and HR2, and a Trp-rich domain [116-118]. Binding of gp120 to CD4 exposes the normally buried fusion peptide, such that it can extend into the target cell membrane as an alpha-helical structure leading to membrane destabilization and formation of a fusion pore [119]. The transmembrane region plays important roles in Env function, and mutations in TM affect Env-mediated membrane fusion [120]. The C-terminal tail of gp41 is involved in Env incorporation, infectivity, gp120 shedding, and fusion [121-124]. A membrane-proximal GYxxL sequence in gp41 interacts with the clathrin adaptor protein complex 2 (AP-2) to mediate endocytosis of Env [125]. In addition to GYxxL, a dileucine motif also present in the C-terminal tail interacts with AP-1. Mutations in both the GYxxL and dileucine motifs were sufficient to completely inhibit cell surface downregulation of Env protein [126].

Regulatory proteins

Tat

Expression of HIV-1 genes is regulated through binding of both host and viral proteins to the 5´ LTR, which contains the promoter sites for host transcription factors such as Sp1, nuclear factor kappa B (NF-κB), activator protein 1 (AP-1), nuclear factor of activated T cells (NFAT), and CCAAT enhancer binding protein (C/EBP) [127]. However, cellular factors alone are inefficient and need the viral Tat protein to enhance the viral transcript elongation process. The presence of Tat increases the efficiency of transcription by about 100-fold. In the absence of Tat, HIV-1 generates primarily short transcripts that are less than 100 nucleotides. Therefore, Tat plays a role in elongation of transcription and is required to generate the full-length ~9 kb viral genome by assembling a pre-initiation complex.

Tat is found in 72 and 101 residue forms inside the nucleus of infected cells [128]. Tat binds to a short-stem loop structure known as trans-activating response element (TAR) located at the 5´ end of HIV-1 RNA [129]. Tat forms a complex with a cellular co-factor, Cyclin T, which facilitates the recognition of TAR by Tat [130]. The transcription elongation function of Tat is accomplished through recruitment of a host cell serine kinase CDK9, which phosphorylates the C-terminal domain of RNA polymerase II to stimulate its activity [131]. Tat also regulates the activity of transcription factors. Tat promotes phosphorylation of Sp1 which enhances its binding to the LTR [132]. Tat also increases transcription by promoting transcription factors' interactions with the LTR [133, 134].

Rev

Rev is a 116-residue RNA-binding viral protein that induces transition from the early to the late phase of HIV gene expression [135, 136]. Rev binds to a 240 base region of RNA

secondary structure called the Rev response element (RRE). Such binding facilitates the export of unspliced and singly spliced viral mRNAs to the cytoplasm [137]. Rev contains a leucine-rich nuclear export signal, which allows it to shuttle between the nucleus and the cytoplasm, thus allowing Rev to achieve unspliced and singly spliced viral mRNA export function [138].

Rev contains three domains – an arginine-rich RNA binding domain, a multimerization domain, and an effector domain that contains the nuclear export signal (NES) [139]. Rev also interacts with host cell proteins to form Rev/RRE/exportin 1/RanGTP complexes to shuttle viral mRNAs out of the nucleus in a fashion distinct from cellular mRNA export [140]. Rev is required for viral replication, and proviruses that lack Rev are unable to produce late viral proteins [141]. In addition to export of viral mRNA, Rev is also involved in inhibition of splicing of viral mRNAs by preventing the entry of small nuclear ribonucleoproteins (snRNPs) during later stages of spliceosome assembly [142].

Accessory proteins

Vpu

Viral protein U (Vpu) is an 81-residue viral protein that plays crucial roles in CD4 downregulation, along with HIV-1 Nef, and virion release from the cell membrane. Intracellular newly synthesized CD4 molecules interact with HIV-1 gp160 (Env) in the ER lumen. This interaction blocks proteolytic cleavage of gp160 and traps it in ER, effectively lowering the amount of gp160 in the cell membrane for virion assembly. Vpu induces rapid degradation of CD4 in the ER, allowing gp160 cleavage and maturation [143]. In addition to CD4 downregulation, Vpu also enhances the release of the progeny viruses. In the absence of Vpu, large numbers of virus particles are seen in the cell membrane, unable to bud off [144, 145]. However, Vpu is dispensable for viral egress from some cell lines. This discrepancy in Vpu dependency led to the discovery of a host

cell restriction factor, tetherin. Tetherin is an interferon-induced restriction factor that inhibits the release of enveloped viruses by tethering the virus to the host cell membrane. Vpu was shown to bind directly to tetherin and antagonize its antiviral role by displacing it from viral assembly sites and triggering its degradation [146, 147].

Vpr

Viral protein R (Vpr) is a 96 amino acid protein that is expressed late in the viral life cycle. However, Vpr is also present early in infection since it is packaged in significant quantities inside the virion [148]. Vpr allows infection of nondividing cells, where it mediates the nuclear localization of the preintegration complex by interacting with the nuclear transport pathway [149, 150]. This Vpr function is indispensable for HIV-1 infection of macrophages [151]. Vpr also influences the reverse transcription of HIV-1 through interaction and recruitment of uracil DNA glycosylase 2 [152]. Vpr also affects normal cell cycle progression by arresting infected cells in the G2 and M phases of the cell cycle [153]. Sustained expression of Vpr has been shown to kill T cells by apoptosis [154].

Vif

Viral infectivity factor (Vif) is a 192-residue HIV-1 protein that is involved in production of highly infectious mature virions [155]. Vif mutants show defects in infectivity only in some cell types, designated nonpermissive or semi-permissive, but not in permissive cells [156]. This suggested that permissive cells may have a host factor which is antagonized by Vif. Subsequent work identified APOBEC3G as this host restriction factor [157]. In the absence of Vif, APOBEC3G is packaged into the virion and deaminates cytidines in the viral DNA, resulting in lethal G-to-A hypermutation [158]. Moreover, APOBEC3G also inhibits reverse transcription

through a deamination-independent mechanism [159]. Vif recruits an E3 ubiquitin ligase complex to APOBEC3G proteins to promote their ubiquitination and subsequent degradation [160].

Nef

Negative factor (Nef), a 210-residue N-terminally myristoylated protein, is the first viral protein to accumulate to detectable levels following HIV-1 entry, suggesting an early role during HIV-1 infection [135]. The term 'Negative Factor' followed early reports of Nef-mediated downregulation of transcriptional activity. However, a Nef role in transcriptional regulation has since been debunked, and the name is a misnomer given the many positive roles for this accessory factor in the viral life cycle [161]. One of the best characterized properties of Nef is its ability to dramatically reduce the levels of CD4 on the surface of infected cells [162]. Nef-induced CD4 downregulation occurs through internalization of surface CD4 through a conserved dileucine motif in Nef which binds to the clathrin-associated adaptor protein 2 (AP-2) [163]. Another conserved property of Nef is its ability to downregulate MHC class I molecules in order to help the immune evasion of infected cells [164]. Nef-induced MHC-I downregulation involves two distinct molecular mechanisms. The first involves interaction with the endocytic adaptor protein PACS-2, leading to assembly of a multi-kinase signaling complex and activation of PI3K. This PI3K-dependent mechanism results in trapping of MHC-I molecules in the trans-Golgi network, preventing them from reaching the cell surface. Alternatively, Nef binds directly to MHC-I through its cytoplasmic tail as seen in the crystal structure of a Nef/AP-1/MHC tail peptide complex [165, 166]. This interaction leads to downregulation of MHC-I from the cell surface and subsequent trafficking through the endosomal pathway.

In addition to mediating downregulation of MHC-I, CD4 and other cell surface receptors, Nef also interacts directly with several host cell kinase proteins [167]. Even though Nef lacks

intrinsic enzymatic activity, it can exert influence on host cell kinase activity because of its homodimeric state [168, 169]. Additional details of Nef functions, including interactions with adaptor protein complexes, and cellular kinases are discussed in detail in sections 1.3.3, 1.3.4 and 1.3.5 below.

1.2.3 HIV-1 life cycle

Even though several processes necessary for productive HIV-1 infection and replication can be inhibited with small molecule drugs, HIV-1 cannot be completely eradicated, and patients must adhere to lifelong therapy. Moreover, prolonged drug administration can lead to toxicity, drug-drug interactions and drug resistance [170]. Therefore, the fight against HIV-1 must continue to explore novel therapeutic strategies, including detailed understanding of and opportunities for intervention within every stage of the viral life cycle.

The HIV-1 life cycle can be divided into early and late phases. The early phase consists of events that occur from virus-host cell first contact to integration of proviral genome into the host cell genome, while the late phase refers to events from viral gene expression through assembly, egress, and maturation.

HIV-1 entry

In the first step of viral entry, virions specifically or nonspecifically attach to the target cell membrane. In macrophages, Env interacts with negatively charged cell-surface heparin sulfate proteoglycans, which serve as the main class of attachment receptors for HIV-1 [171]. More specific interaction between HIV-1 gp120 and an activated form of integrin $\alpha_4\beta_7$, a cellular adhesion molecule, occurs on CD4+ T lymphocytes [172]. On dendritic cells, a specific C-type lectin (DC-SIGN) promotes efficient infection of cells that also express CD4 and chemokine

receptors by binding to the HIV-1 gp120 [173]. HIV-1 attachment to these cellular factors serves to bring gp120 in close proximity to CD4 and coreceptors, which are required for HIV-1 entry, while the attachment factors themselves are not essential (Figure 3).

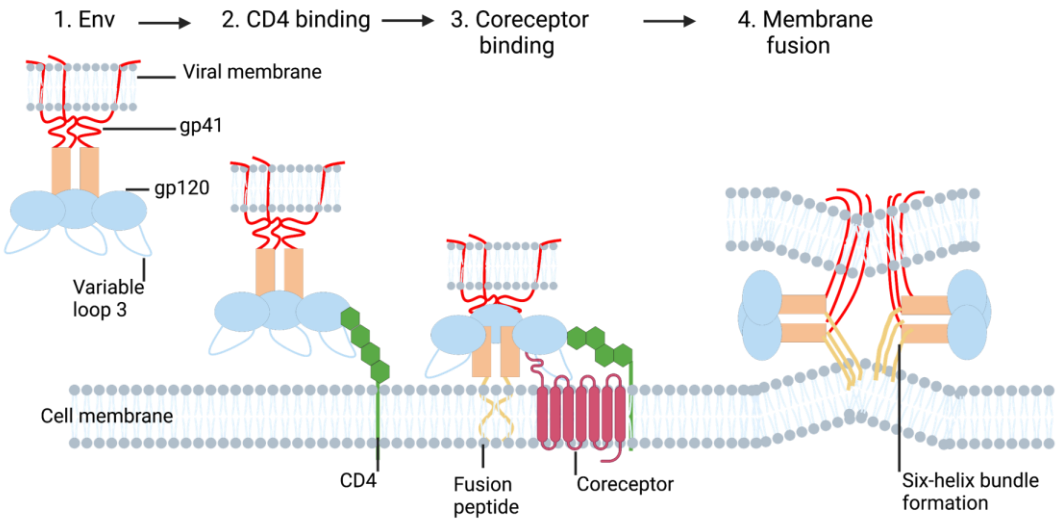

Figure 3. Overview of HIV-1 entry.

HIV-1 Env protein gp120 is the first protein that attaches to the host cell by binding to the CD4 receptor (green). Conformational changes in Env induced by gp120/CD4 interaction leads to co-receptor binding. At this point, membrane fusion begins to occur, initiated by insertion of the fusion peptide of gp41 into the host cell membrane and leading to six-helix bundle formation and complete membrane fusion. This model is adapted from Wilen *et al*. [174], and produced using Biorender.

In the second step, specific binding occurs between Env and the host CD4 receptor protein. CD4 is an immunoglobulin superfamily protein that normally enhances T-cell receptor-mediated signaling. Variable loops in gp120 that are largely responsible for the genetic diversity of HIV-1 epitopes are predominantly on the surface of gp120 and form disulfide loops at their bases [175]. The gp120 protein binds to the most amino-terminal of the four immunoglobulin-like domains of CD4 (green hexagons in Figure 3). This domain in CD4 contains a positively charged pocket lined

with three lysine and one arginine residues, where negatively charged residues in gp120 dock [176]. Residues that are conserved for the CD4/gp120 interaction have been identified in both CD4 and HIV-1 gp120 [176, 177]. Binding to CD4 causes conformational changes in gp120 leading to rearrangements of variable regions 1 and 2, followed by variable region 3. The gp120 rearrangements induced by CD4 interaction contribute to the next step in HIV-1 entry involving cell-specific chemokine receptors.

In the third step of HIV-1 entry, interactions between gp120 and a cellular co-receptor takes place. The major co-receptors for HIV-1 entry are the chemokine receptors CXCR4 and CCR5, which are variably expressed on different HIV host cell types. CD4/gp120 interaction exposes a highly conserved binding site for the co-receptor in gp120 [178]. gp120/co-receptor interactions are mediated by the co-receptor binding site and the rearranged variable loop 3 of gp120. Details of interactions between gp120 and CCR5 are not fully clear. Recently, a structure of CD4/gp120/CCR5-co-receptor complex was reported, which showed the overall structure of gp120 to be very similar to the CD4-only bound form, suggesting that CCR5 co-receptor binding does not induce a major conformational change in the structure of gp120 [179]. Co-receptor binding, through unknown mechanistic processes, triggers changes in gp120, ultimately exposing a 15 hydrophobic residue sequence in gp41. This sequence, called the fusion peptide, in turn triggers rearrangements between trimerized N- and C-terminal heptad repeat sequences in gp41 [180].

Finally, the interaction between the gp41 fusion peptide and host cell membrane produces an intermediate, pre-hairpin state bridging the two membranes. The hairpin then refolds into the six-helix bundle core leading to membrane fusion [181, 182]. Fusion proceeds via lipidic intermediate states, a membrane stalk, opening of the fusion pore and subsequent expansion events

[183, 184]. Energy released during coordinated gp41 refolding is used to overcome the kinetic barrier of the membrane fusion process [185, 186]. The site of membrane fusion is however not completely understood. It is suggested that fusion is achieved through movement of the virus particle to the site where productive membrane fusion occurs by utilizing host cell transport machinery [187]. Retroviruses, including HIV-1, have been shown to "surf" along the cell surface to reach productive entry sites [187, 188]. HIV-1 entry may also involve endosomes via receptor-mediated internalization and dynamin-dependent fusion [189]. Membrane fusion results in delivery of the HIV-1 capsid into the host cell cytoplasm.

HIV-1 post-entry events

Uncoating

Before the viral RNA can be reverse transcribed into proviral DNA and integrated into the host genome, disassembly of the protective capsid core must occur. The capsid core is composed of hexamers and pentamers of CA proteins and contains the two viral RNAs, NC, RT, IN, PR, and the accessory proteins Nef and Vpr. Uncoating of the HIV-1 capsid is not fully understood but represents a highly regulated and critical process in the viral life cycle. Different models have been proposed for the mechanisms of HIV-1 capsid disassembly process. The first model suggests that the HIV-1 capsid is disassembled close to the plasma membrane immediately following entry, and most of the capsid is dissociated from viral RNA/protein complexes [190, 191]. Uncoating may be triggered by the sudden change in local environment or due to loss of high concentrations of free CA protein responsible for maintaining metastable cores [192].

A second model for uncoating proposes that the capsid remains intact for some time post-entry, and that uncoating occurs gradually as the core is transported towards the nucleus and as reverse transcription occurs [193]. This model argues that the combination of successive changes

in the cellular environment as the virion is transported towards the nucleus, effects of several host factors binding, and conformational changes as a result of reverse transcription occurring at the same time, all together lead to gradual uncoating of the capsid core. The strongest arguments for this model come from studies that show a broad range of different shapes and sizes of cytoplasmic HIV-1 capsids, suggesting a step-by-step set of uncoating events accompanying reverse transcription and transport to the nucleus [194-196].

A third model for HIV-1 capsid uncoating suggests that the capsid remains intact until it reaches the nuclear pore, where uncoating takes place following completion of reverse transcription. This model proposes that cyclophilin A (CypA) plays a role in preventing premature uncoating and thus facilitating reverse transcription, which is followed by engagement of host proteins TNPO3 and CPSF6. Subsequently, the nuclear pore proteins NUP358 and NUP153 are involved in uncoating and transport of the pre integration complex through nuclear pores [197, 198]. Recent studies support this model by showing the requirement of nuclear pore proteins for proper uncoating and subsequent nuclear trafficking [199, 200].

Reverse transcription

The RT enzyme by itself is sufficient to carry out DNA synthesis from an RNA template *in vitro*. However, reverse transcription in infected cells is a complex process that is interconnected with many processes like uncoating and transport as described earlier. Reverse transcription is initiated shortly after virus entry and proviral DNA can be detected within hours of infection [201]. Reverse transcription in infected cells occurs through formation of a reverse transcription complex (RTC), which upon completion of reverse transcription, is proposed to transition into the pre-initiation complex (PIC), which is then imported into the nucleus via nuclear pores. Exact mechanism of reverse transcription is quite complex and not clearly understood.

In addition to accumulation of mutations from APOBEC3G-induced deamination and error-prone RT, recombination frequently occurs during reverse transcription of the viral genome [202]. The recombination rate for HIV-1 is higher than other retroviruses [203]. HIV-1 RT is estimated to switch between templates about 8 – 10 times in one cycle [204, 205]. Recombination of the HIV-1 genome during transcription has led to more than 100 circulating recombinant forms that represent a significant proportion of total HIV-1 infections worldwide [22, 206]. Therefore, recombination plays an important role in generating complex viral diversity.

Integration

After successful reverse transcription, a linear double-stranded viral DNA with LTRs at each end is synthesized, which serves as a substrate for integrase. IN catalyzes a reaction where two nucleotides are hydrolyzed at the 3´ LTR, which may also define the transition from RTC to PIC [207]. In the DNA strand transfer reaction, IN uses the 3´ hydroxyl groups to make a double-stranded staggered cut in host DNA. Cellular proteins then repair the 5´ end of viral DNA and seal the single-strand gaps [208]. The PIC is imported into the nucleus without disrupting the nuclear envelope, allowing HIV-1 to infect nondividing cells such as macrophages and microglial cells. Even though the full details of PIC nuclear import are not known, several studies have documented the roles of HIV-1 CA and several host proteins including importins, NUPs, CPSF6, and TNPO3 [198, 209-211]. One model proposes that initial binding of CA to the nuclear pore complex (NPC) constituent proteins nucleoporins NUP358 and NUP153 docks the PIC to the NPC. Once at the NPC, CA interacts with CPSF6 to facilitate the transport through nuclear pores. TNPO3 is required to localize CPSF6 to the nucleus, whereas premature cytoplasmic CPSF6 binding to CA prevents nuclear import [212]. This model is supported by studies showing that CA N74D mutation disrupts

its interaction with MX2, a restriction factor that blocks nuclear import in a CA dependent manner [213].

Once in the nucleus, PIC elements must interact with chromosomal DNA to select the site of proviral DNA insertion. Early analysis of proviral DNA insertion sites of retroviruses suggested that integration is favored near DNAse I hypersensitive sites, indicating preferences for open chromatin [214]. Completion of the first human genome sequence in the early 2000s allowed for the study of HIV-1 integration sites by high-throughput DNA sequencing. Schroder *et al.* mapped 524 sites of HIV-1 integration in the SupT1 T-cell line and showed that HIV-1 favors active transcription units for integration of proviral DNA, which ensures efficient transcription [215, 216].

Viral mRNA biogenesis and transport

Integration of proviral DNA into the host cell genome signals the transition from the early to late phase of HIV-1 replication. Transcription of viral genes requires the Tat protein for efficient elongation of transcripts. Tat recruits positive transcription elongation factor P-TEFb to the viral trans-activation response (TAR) element. P-TEFb consists of Cdk9 kinase and cyclin T1 (CycT1) subunits. Cdk9 phosphorylates Ser2 and Ser5 in the C-terminal domain of RNA polymerase II, which leads to efficient transcription of viral pre-mRNA [217]. Tat binds TAR through an Arg-rich motif, which inserts into the RNA major groove within the stem-loop TAR structure. In binding P-TEFb, Tat primarily interacts with the CycT1 subunit, but also contacts the T loop region of Cdk9, which results in conformational changes in the substrate binding region of the kinase leading to RNA polymerase II phosphorylation and stimulation of polymerase activity [218]. Viral mRNA transcribed in this way must undergo a variety of splicing events prior to export from the nucleus for translation. However, the viral protein Rev binds to the Rev response element located

within the mRNA to facilitate the export of incompletely spliced mRNAs through nuclear pores. Rev forms higher order multimers in a cooperative manner dependent on RNA binding [219]. While bound to unspliced viral mRNA, Tat also binds with the cellular CRM1 nuclear export factor to achieve the export of unspliced viral mRNA for translation by ribosomes [220, 221]. Export of mRNAs with aberrant splicing allows for expression of all HIV-1 proteins, some of which then initiate the process of new virion assembly at the plasma membrane.

HIV-1 assembly

Synthesis of late viral proteins by the ribosome includes the Gag polyprotein, which is transported to the inner lining of the plasma membrane to begin virus assembly. The mechanisms of Gag polyprotein transport to the assembly site is not clearly understood. However, the basic patch of MA (which is myristoylated and membrane associated) was shown to be important for Gag targeting, as mutations in this MA region mistargeted Gag to late endosomes and multivesicular body (MVB) compartments [222]. In addition to the MA basic region, phosphatidylinositol-4,5-biphosphate (PIP_2), a phosphoplipid enriched in the inner leaflet of the plasma membrane, was also shown to play a role, as depletion of PIP_2 also reroutes Gag to late endosomes or MVBs [223]. NMR studies revealed that the basic region of MA in Gag interacts with the soluble negatively-charged headgroup of PIP_2 in order to expose the myristoyl group in the MA N-terminus, allowing myristic acid insertion into the plasma membrane [224]. Therefore, PIP_2 acts as a trigger and a membrane anchor for Gag targeting. Once at the membrane, Gag also induces the formation of lipid rafts by recruiting cholesterol and sphingolipid-enriched membrane microdomains [225].

At this stage of infection, the cytoplasm of the infected cell is filled with multiple forms of viral mRNA, including those that are spliced, incompletely spliced or unspliced. Unspliced

mRNAs arrive in the cytoplasm through the action of the viral Rev protein. Viral RNAs either take part in translation at ribosomes, or pack into newly forming virions. Intron-containing intact viral RNAs have been shown to dimerize in the cytoplasm, forming a recognition motif for packaging into assembling virions [226, 227]. Packaging of viral RNAs is achieved by the NC domain of the Gag polyprotein. Two Cys-Cys-His-Cys zinc-finger-like motifs in the NC domain bind to the packaging signal near the 5´ UTR. This region of the RNA contains many secondary structural elements including the TAR, the primer-binding site, and a site for polyadenylation [34]. Deletions and mutations in the 5´ UTR reduce packaging efficiency, thus establishing the key role of this region of the RNA in interacting with the Gag polyprotein. While the 5´ UTR region undergoes conformational changes to favor packaging instead of translation, events that are biologically relevant for packaging have not been identified [228]. NC-RNA interactions also play a role in promoting Gag assembly.

The major determinant of Gag multimerization is the CA domain of the Gag polyprotein. CA forms hexameric and pentameric lattices of the viral capsid core. The flexible nature of CA along with its curvature has made it difficult to investigate the role of CA during Gag assembly. Mature CA molecules alone have the capacity to assemble *in vitro*, but their assembly as part of the Gag polyprotein is not understood [229]. Recent low resolution cryo-EM and cryo-ET studies on the structure of the immature capsid lattice revealed that retrovirus capsid proteins, while having conserved tertiary structures, adopt different quaternary arrangements during virus assembly [230]. This may account for the heterogeneity observed in CA assemblies of both immature and mature virus particles.

Env incorporation into HIV-1 also remains an incompletely understood process. Compared to other retroviruses, HIV-1 Env contains long cytoplasmic tails, which need to be incorporated

into the virion [231]. Genetic studies suggest that direct or indirect interactions between the gp41 cytoplasmic tail and the MA domain of Gag play a role in Env incorporation [232, 233]. HIV-1 MA forms trimers in crystals, but long-range order is not seen in the MA shell [48, 230]. The structure and assembly of the cytoplasmic tail of gp41 is also not understood, but it is suggested to play a role by imposing steric clashes on trimeric MA. The trimeric MA arrangement is a critical factor in incorporation of Env into the assembling virion [234].

HIV-1 release

After assembly of the Gag lattice at the plasma membrane, the next step in the HIV-1 lifecycle is release of the budding virion from the infected cell. This step is mediated by the cellular endosomal sorting complexes required for transport (ESCRT) machinery. Deletion of the p6 domain of Gag or mutations of a highly conserved Pro-Thr/Ser-Ala-Pro (PTAP) motif resulted in release block and accumulation of particles at the cell membrane, highlighting the importance of this motif in HIV-1 release processes [68, 69]. Several PTAP motifs positioned at various sites along the Gag polyprotein have been identified to drive virus release [235-237]. These PTAP motifs directly interact with a cellular protein known as the tumor susceptibility gene 101 (TSG101), which itself is a part of ESCRT-I. ESCRT-I and ESCRT-II are involved in membrane budding, whereas ESCRT-III is involved in membrane scission. Structures of several sorting proteins and their interactions with so-called viral late domains have offered detailed understanding of virus budding processes, which are almost identical to cellular budding processes, and are discussed in detail elsewhere [238, 239]. Ubiquintinylation of cargo proteins results in recruitment of the ESCRT machinery. HIV-1 Gag proteins are ubiquintinylated and may help in recruitment of ESCRT complexes. Both ubiquintinylation and late viral domains are involved in Gag-mediated ESCRT recruitment [240, 241]. Efficient virus egress is inhibited by

tetherin, which has a dual membrane-bound topology and a dimeric ectodomain, which together lead to inhibition of release of budding virus particles [242]. HIV-1 Vpu counteracts tetherin restriction as described above [145].

HIV-1 maturation

Even though the Gag protein is by itself sufficient to drive virion assembly and release, these immature virions are not infectious. Infectivity requires maturation of the virion, which is brought on by the function of viral protease (PR). PR is expressed and recruited into the virion as part of the Gag-Pol precursor. Activity of PR is critical for viral maturation, and an increase or decrease in PR activity leads to aberrant, non-functional particles [243].

The immature virion contains the Gag molecules organized in a radial manner. Following the activity of PR, where CA domains are cleaved from Gag, CA proteins reassemble into the conical capsid core. Whether this reassembly is facilitated through complete disassembly of CA lattices and reassembly into mature CA lattice, or without much disassembly is not known [244, 245]. Core shell assembly is triggered by a novel β hairpin formed by a salt-bridge between Pro1 and Asp51 in the CA protein [246]. This assembly of CA proteins into the capsid core serves to protect the viral RNA and aid reverse transcription in newly infected cells in the next round of HIV-1 infection.

1.2.4 Treatment options and limitations

The main cell type for HIV-1 attack is the CD4 T-lymphocyte. HIV-1 infection results in the gradual depletion of CD4 T cells, leading to opportunistic infections and cancer if left untreated. However, pathogenesis due to HIV-1 infection varies substantially in different patients, and is considered a host-specific infection [247]. Most patients are successfully treated with a

combination of drugs targeting HIV-1 enzymes, an approach often referred to as combination antiretroviral therapy (ART). ART results in control of virus replication and an increase in CD4 T-cells, thus slowing disease progression and transmission by slowing the asymptomatic phase [248].

1.2.4.1 Reverse transcriptase inhibitors

There are two types of RT inhibitors - nucleoside/nucleotide reverse transcriptase inhibitors (NRTIs) and non-nucleoside reverse transcriptase inhibitors (NNRTIs). NRTIs were the first drugs approved for use against HIV by the FDA [249]. Upon entering the cell, nucleoside inhibitors are phosphorylated into the triphosphate form by cellular kinases, and they compete with cellular purine or pyrimidine nucleotides during viral cDNA synthesis by RT. Unlike natural purine or pyrimidine nucleotides, these drugs lack a 3´-hydroxyl group leading to early termination of reverse transcription activity and incomplete viral cDNA synthesis [250]. The first nucleoside inhibitor for RT was azidothymidine (AZT), which was originally tested as an experimental cancer drug in 1964. The anti-HIV properties of this compound were demonstrated in clinical trials in 1985 [251]. Additional nucleoside inhibitors have been approved by FDA since then that compete with different cellular nucleotides. Nikavir and stavudine, like AZT, compete with dTTP, emtricitabine and lamivudine compete with dCTP, didanosine and tenofovir compete with dATP, while abacavir competes with dGTP [252, 253]. Emtricitabine and tenofovir are two examples of NRTIs that are still in widespread clinical use. They are given in combination as a daily pre-exposure prophylaxis (PReP) formulation (Truvada) designed to prevent HIV-1 transmission.

Despite the roles of these compounds in turning HIV-1 infection into a chronic, non-fatal condition, there is a constant need for newer nucleoside and nucleotide analogs because HIV-1 RT undergoes mutations that enable it to be resistant against these drugs. A significant reduction in

drug efficacy is seen in patients as soon as 6 months after NRTI treatment, leading to the accumulation of viral strains that are fully resistant to these drugs [254, 255]. Resistance to NRTIs can occur in one of two ways: 1) reduced affinity for non-natural substrates of RT, and 2) increased ability of RT to catalyze the pyrophosphorolysis reaction, an excision reaction of incorporated nucleotide analogs [256, 257].

NNRTIs are RT inhibitors that function through a different mechanism than NRTIs. NNRTIs non-competitively form and bind a hydrophobic pocket near the active site of RT leading to configurations that eliminate polymerase activity. Since they are hydrophobic, they can readily enter the cell, and do not require further modifications inside the cell. Several NNRTIs are currently in clinical use – nevirapine, delavirdine, efavirenz, etravirine, and rilpivirine [258, 259]. Despite structural and mechanistic differences, the effects of NNRTIs on RT activity is similar to NRTIs in that both classes of drugs inhibit RT-catalyzed elongation of HIV-1 cDNA. Even though NNRTIs can bind RT in the absence of substrates, they have enhanced affinity for RT in the enzyme-substrate complex state, and they promote binding of substrates to RT [260-262]. One of the shortcomings of NRTIs discussed above included mutations that lead to reduced drug affinity for RT. This can be overcome by combination with NNRTIs, which promote substrate binding to RT. However, mutations in the NNRTIs binding pocket of RT can also lead to NNRTI resistant viruses. Over 40 such mutations have been found in this region of RT. While newer generations of NNRTIs overcame some of these initial mutations, resistance to newer generations of NNRTIs soon followed [263-265]. RT inhibitors produce side effects with chronic use. Early NRTIs were associated with mitochondrial toxicity that manifests as myopathy, lipoatrophy, neuropathy, and lactic acidosis [266]. NNRTIs are also associated with adverse side effects, including skin rashes, Stevens-Johnson syndrome and toxic epidermal necrolysis [267]. In addition, nevirapine has been

shown to cause significant transaminitis, efavirenz can lead to CNS alterations, and delavirdine causes neutropenia when co-administered with AZT [268, 269].

1.2.4.2 Protease inhibitors (PIs)

PIs are often an essential component of combination ART. Inhibition of HIV-1 protease causes the release of immature and noninfectious virus particles. PIs are peptidomimetics that bind to the protease active site in a manner similar to natural substrates [270]. However, unlike natural substrates, current PI inhibitors do not undergo proteolytic cleavage, as they contain hydroxyethylene bonds in place of peptide bonds. Competitive binding of PIs with protease renders the enzyme unable to further process proteolytic cleavage of viral polyproteins, thus leading to noninfectious particles. There are ten HIV-1 protease inhibitors approved by the FDA: saquinavir, indinavir, ritonavir, nelfinavir, amprenavir, fosamprenavir, lopinavir, atazanavir, tipranavir, and darunavir. Inclusion of PIs in combination ART with RT inhibitors greatly improved patient outcomes by reducing viral loads, improving CD4 T cell counts, and slowing AIDS progression [271, 272].

Although PIs significantly improved disease management in combination with RT inhibitors, several pharmacokinetic limitations exist. Ritonavir was found to be a potent inhibitor of cytochrome P450 3A, redefining its use as a pharmacokinetic booster rather than a PI [273, 274]. Another potent PI inhibitor, indinavir, required very frequent doses to maintain low viral loads because it has a half-life of less than 2 hours [275]. Indinavir was discontinued after it was found to be highly toxic, and is no longer used alone in antiretro viral therapy. Therapeutic efficacy was also low for other first-generation PIs like saquinavir, nelfinavir, and amprenavir [276]. Moreover, gastrointestinal distress including nausea, diarrhea, and abdominal pain are also

common with first-generation PIs. Second-generation PIs (lopinavir, atazanavir) demonstrated improved plasma half-lives [277, 278].

Similar to RT inhibitors, PIs are also vulnerable to mutations that render them ineffective. Primary mutations that reduce the interaction between the protease and the PI are found in the active site of the enzyme in response to PI treatment [279]. Out of a total of 99 residues in HIV-1 protease, mutations in 45 residues have been observed to confer drug resistance [280]. Newer inhibitors that were designed to have a higher genetic barrier against resistance mutations were introduced, but problems persist in the form of side effects [281]. Each PI treatment is now associated with a signature resistance mutation, and newer inhibitors with higher genetic barriers have suffered the same fate [282]. This has led to the emergence of multidrug-resistant HIV-1 variants and indicate that drug resistance maybe a perpetual issue [283, 284].

1.2.4.3 Integrase inhibitors

IN stands out among other HIV-1 proteins because it least resembles any human enzyme. This makes IN an attractive target for reducing off-target side effects [285]. Integrase inhibitors (INIs) were developed in 2000 when diketone organic acids were shown to inhibit HIV-1 proviral DNA integration in cell culture [286]. All INIs contain an aromatic hydrophobic region and a chelating region represented by a diketo acid motif or a bioisostere of a diketo acid [287]. The first INI, raltegravir, was approved by the FDA for HIV-1 treatment in 2007. Raltegravir was shown to be a highly effective antiretroviral agent, even against multidrug-resistant viral strains, and quickly became one of the most commonly used anti-HIV-1 drugs [288]. Two other INIs – elvitegravir and dolutegravir - have been recently approved by the FDA for HIV-1 treatment [289, 290]. Elvitegravir combined with other agents was able to overcome the twice-daily dosing limitation of raltegravir, but elvitegravir suffers from cross-resistance with raltegravir [291]. Moreover, the

low genetic barrier for mutations meant that primary and secondary mutations quickly followed to offer resistance to raltegravir and elvitegravir. The need for INIs with a higher genetic barrier against resistance mutations led to the discovery of dolutegravir, which was approved by the FDA in 2019, and offers good tolerability, once-daily dosing without other agents, and low cross-resistance with raltegravir [292]. The long-term implications of dolutegravir treatment are still not known, but it was shown to potently inhibit the renal organic cation transporter OCT2 *in vitro* at concentrations below the peak concentrations demonstrated in clinical trials [293]. Although no significant resistance mutations have been reported for dolutegravir, mutations that made the drug slightly less effective were observed in tissue culture and in patients treated with dolutegravir monotherapy [294]. This underscores the need to constantly look for alternative therapies to keep up with constantly changing needs of HIV-1 treatment.

1.2.4.4 Entry inhibitors

Since the discovery of CD4 as the major receptor of viral entry, efforts were made to target CD4 in order to stop virus entry into the cell. This approach did not initially yield therapeutic benefits because CD4 is essential to many immunologic functions. However, the discovery of CXCR4 and CCR5 as essential coreceptors for HIV-1 entry provided new targets for HIV-1 inhibition [295] [296]. CCR5-tropism is characteristic of viral infection during the asymptomatic stage, and the switch to CXCR4-tropism or dual tropism is associated with rapid depletion of CD4 T cells and disease progression to AIDS [297, 298].

Inhibitors that 1) block interaction of the virus with CD4, 2) block interaction of the virus with CCR5 or CXCR4, and 3) prevent membrane fusion, are collectively called entry inhibitors. The small molecule CCR5 antagonist maraviroc was approved by the FDA in 2007. Maraviroc binds to hydrophobic pockets in the transmembrane helices of CCR5, which induces

conformational changes in the coreceptor making it unrecognizable to HIV-1 gp120 [299]. The resistance profile to a small molecule CCR5 antagonist was anticipated to take a different form than those described earlier, because these small molecules target cellular receptors and not viral proteins. Indeed, two forms of resistance mechanisms were observed for maraviroc: 1) emergence of minor CXCR4-using HIV-1 variants that were not detected in plasma before initiation of maraviroc [300]; 2) evolution of viruses able to bind to the modified maraviroc-induced conformation of CCR5 [301, 302].

Fusion of membranes is a conserved process which is facilitated by the formation of the six-bundle helix at the fusion interface involving the HR1 and HR2 domains in gp41 [303]. This HIV-1 gp41 intramolecular interaction is required to promote fusion, and disruption of this interaction was shown to have antiviral activity [304]. These observations led to the design of enfuvirtide, an HR2 mimetic, which was approved by the FDA in 2003 [305]. Mutations in the HR1 domain were subsequently observed *in vitro* and *in vivo* in response to enfuvirtide treatment [306, 307], although mutations at this site also highly reduces viral infectivity.

1.2.4.5 Monoclonal antibodies

Broadly neutralizing antibodies (bnAbs) antagonize multiple HIV-1 strains through recognition of conserved viral epitopes [308]. While several potential broadly neutralizing antibodies are undergoing clinical trials, only two (ibalizumab, leronlimab) are currently approved by the FDA for the treatment of heavily treatment-experienced patients with multidrug resistant HIV-1 infection in combination with other antiretroviral medicines [309, 310]. Ibalizumab exerts its antiviral effect by binding noncompetitively to extracellular domain 2 of the CD4 receptor, and blocks interaction between the coreceptor and gp120, thus blocking virus entry. Its efficacy was demonstrated in a phase III trial in patients with advanced HIV-1 infection and resistance to other

antiviral drugs [311]. Most patients achieved significantly low viral loads after ibalizumab was added to a failing antiretroviral regimen. After 24 weeks, almost half of all patients achieved an undetectable viral load [312]. The primary mechanism of resistance to ibalizumab is the reduced expression or loss of potential N-linked glycosylation sites in the variable loop 5 of gp120 [313]. Resistance has been observed to occur as soon as 1 - 2 weeks after ibalizumab treatment [314]. The observation that viruses that are resistant to ibalizumab also display higher infectivity is particularly troublesome [315].

1.2.4.6 Stem-cell transplantation cases

The biggest obstacle to HIV cure is the long-lived viral reservoir, which persists despite ART. This reservoir is maintained through transcriptionally silent but replication competent proviruses in resting memory CD4+ T cells that have very long life spans, including central, effector, transitional, and stem memory T cells [316]. These cells can reactivate and seed viral rebound upon discontinuation of ART. In the presence of ART, reservoirs are shown to decay with a half-life of 44 months, implying that about 73 years of ART would be required for complete virus eradication [317]. Therefore, newer strategies are needed to avoid this life-long ART dependency. Only 2 individuals have been effectively cured of HIV infection by a process involving myeloablative therapy for leukemia or lymphoma, which presumably eliminated the viral reservoir present in bone marrow memory T cells. This was followed by allogenic transplantation of hematopoietic stem cells from compatible donors expressing the naturally occurring CCR5Δ32 mutation, which prevents infection of CD4+ T cells by HIV-1 [318, 319]. While these cases demonstrate that HIV-1 cure is possible, widespread application of CCR5Δ32 bone marrow transplantation is not a feasible approach to end the global HIV-1 pandemic.

1.3 Role of HIV-1 Nef in viral pathogenesis

As discussed in earlier sections, major obstacles to HIV-1 cure arise from the virus's ability to adapt quickly to specific therapeutic pressures and to establish a latent proviral reservoir that is unaffected by current antiretroviral drugs. Moreover, many elements within the virus are intricately linked with and successfully adapted to the human immune system as a result of more than 80 years' tussle [320]. Therefore, small victories are the long-term course in the fight against HIV-1. As such, all the possible avenues for HIV-1 targets must be considered. Here, given its several essential roles during HIV-1 pathogenesis, we look at HIV-1 Nef as a target for preventing HIV-1 immune evasion and disease progression.

HIV-1 genome sequencing revealed an ORF overlapping with the 3´ LTR. This 3´ ORF was initially suggested to be a negative factor (*nef*) for viral replication, since overexpression of the 3´ ORF attenuated viral transcription and replication *in vitro* [321, 322]. These conclusions were soon contradicted, and the observed negative influence of Nef in these studies were found to be due to the LTR sequences within the *nef* coding region interfering with HIV-1 gene expression rather than the product of *nef* itself [323, 324]. The role of Nef in viral pathogenicity *in vivo* was first realized in a study that showed deletions in the *nef* gene of SIV greatly reduces the severity of the SIV-associated disease in rhesus macaques [325]. Subsequent studies supporting an essential role for HIV-1 Nef in AIDS pathogenesis was shown through sequence analysis of HIV-1 isolates from long-term non progressors (LTNPs), which revealed *nef*-deleted HIV-1 [326, 327]. LTNPs, sometimes referred to as elite controllers, are individuals infected with HIV-1 that do not progress to AIDS in the absence of ART.

Hanna *et al*. constructed transgenic mice selectively expressing the entire HIV-1 provirus in CD4+ T cells, dendritic cells, and macrophages using a CD4 promoter. These mice developed

AIDS-like symptoms including T cell loss that correlated with the levels of transgene expression and died within a month [328]. This study was followed up with another to identify the individual HIV-1 genes involved in this AIDS-like syndrome. Remarkably, all HIV-1 proteins except Nef were found to be dispensable for the emergence of this phenotype [329], identifying Nef as a major determinant of HIV-1 pathogenesis in this mouse model, indicating Nef may play a critical role in human AIDS, independently of its role in virus replication.

The role of Nef in AIDS progression was subsequently studied in 'BLT' humanized mice that offer a model of the human immune system for studying HIV-1 pathogenesis *in vivo*. These animals are derived from an immunocompromised strain (often NSG) that are transplanted with human fetal bone marrow cells, liver cells, and thymus (hence the BLT designation). Infection of BLT mice with HIV-1 resulted in high plasma viral loads, rapid depletion of human CD4+ T cells in the peripheral blood and elimination of CD4+/CD8+ thymocytes from the implanted human thymic tissue. Nef-defective viruses displayed lower peak viral loads and minimal CD4+ T cell and CD4+/CD8+ thymocyte killing [330]. Together with the transgenic HIV-1 mice, these studies revealed that HIV-1 Nef has key roles in disease progression and is a major determinant of T cell loss. Therefore, a complete understanding of Nef functions that lead to viral replication and AIDS progression *in vivo* is needed to be able to design Nef-based antiviral agents.

Drug targeting of Nef is complicated by the fact that Nef itself possesses no enzymatic properties. Its influence is exerted through a myriad of protein-protein interactions with host cell proteins [161]. Three main activities of Nef have been documented: 1) downregulation of CD4, MHC-I, and other cellular receptors through the endolysosomal pathway; 2) constitutive activation of kinases and other cellular signaling pathways to promote viral transcription and spread; and 3) enhancement of viral infectivity primarily through antagonism of the SERINC family of host

restriction factors [162, 164, 331-334]. Detailed analysis of each of these Nef functions requires an understanding of Nef structure which is described in the next section.

1.3.1 Introduction to structure-function relationships in HIV-1 Nef

Primate lentiviral Nef accessory factors (27-32 kDa depending on the viral isolate) are among the earliest and most abundantly expressed proteins during viral infection [335], where early processes involve virus entry to trasnscription of genes essential for viral replication, whereas late processes involve producing viral structural proteins to viral egress and maturation. Several crystal and solution structures have demonstrated that Nef consists of a globular core domain flanked by a flexible N-terminal arm and a C-terminal disordered loop [336-338]. Figure 4 shows the full-length Nef conformation with some of the conserved motifs important for host protein interactions highlighted.

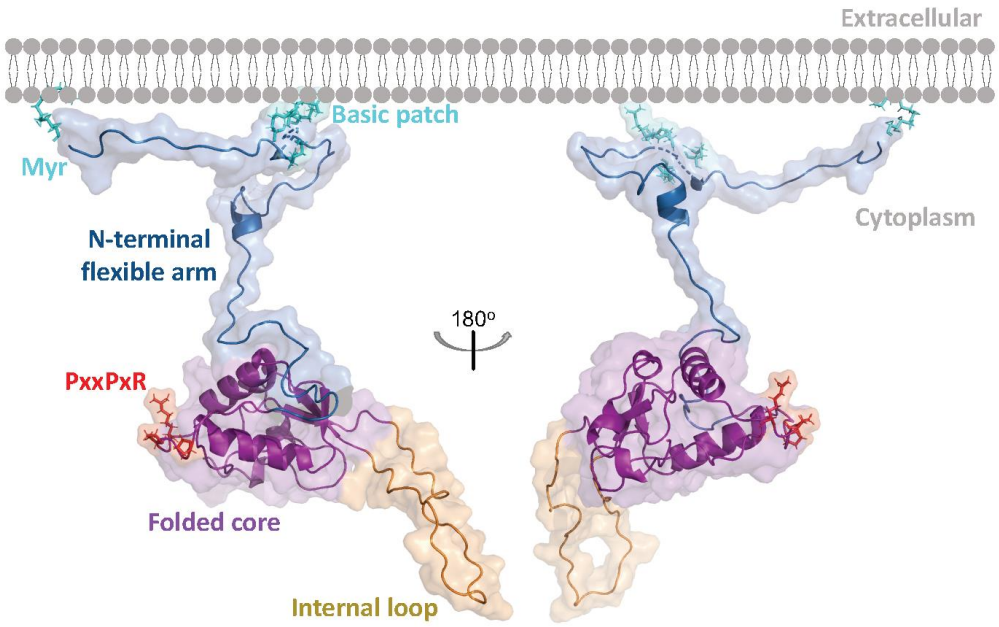

Figure 4. Structural model of HIV-1 Nef at the plasma membrane.

N-terminal myristoylation (Myr) and a basic patch containing four Arg residues target Nef to the inner cell membrane. Residues 2-61 (numbering based on the B-clade SF2 Nef variant) form an extended N-terminal flexible arm (shown in blue). Residues 62-210 fold into a compact Nef core (shown in purple) with a C-terminal flexible internal loop extending outwards (shown in orange). The folded core also contains the PxxPxR motif (shown in red sticks) essential for several Nef-mediated host cell proteins interactions including Src-family kinase recruitment and activation. This model was produced in PyMol using the NMR coordinates of myristoylated HIV-1 Nef anchor domain (PDB: 1QA5), the crystal coordinates of a single Nef core (PDB: 1EFN), and the C-terminal loop is modeled as described in [339].

N-terminal myristoylation

HIV-1 Nef undergoes myristoylation at its N-terminal MGxxx(S/T) sequence. This reaction is carried out co-translationally by the ubiquitous human N-myristoyltransferase (hNMT), which removes the methionine and adds myristate to the glycine residue. This Nef motif is conserved in all HIV-1 variants, and therefore underscores the critical role of membrane localization in Nef-mediated interactions [340]. In addition to the myristoylation site, arginine and lysine clusters in the N-terminal flexible arm also regulate Nef membrane localization [341]. Interestingly, several studies report that Nef is also found in the cytosol [342, 343], suggesting a dynamic equilibrium in which Nef shuttles back and forth from the cell membrane in order to carry

out its functions. Furthermore, myristoylation may also alter Nef conformation and self-assembly leading to myristoylation-dependent functions [168].

Many Nef functions, including downregulation of CD4 and MHC-I as well as T cell activation, involve myristoylation-dependent localization of Nef into lipid rafts [344, 345]. Replacement of Nef Gly2 with alanine (G2A mutant), which prevents myristoylation, also abrogated most Nef functions [346-348]. However, the tendency of Nef to homodimerize was shown to be myristoylation-independent in cell-based bimolecular fluorescence complementation assays, consistent with previous X-ray crystal structures of the un-myrisotylated Nef core lacking the N-terminal anchor domain [169].

EEEE acidic motif and Nef interaction with trafficking proteins

HIV-1 Nef is well known to hijack multiple intracellular trafficking pathways. One mechanism behind this Nef function involves interactions with PACS-1, which controls endosome-to-Golgi trafficking [349]. Nef interaction with PACS-1 involves an acidic cluster of four glutamic acids. However, other proteins that bind PACS-1 contain an additional phosphorylated residue, and lack of phosphorylation sites in Nef initially cast doubt over this function of the tetra-glutamate motif and questions whether PACS-1/Nef interaction is essential for MHC-I downregulation [165, 350]. Subsequent structural work showed that the tetra-glutamic acid motif stabilizes interactions with the MHC-I cytoplasmic tail and μ1 subunit in the AP-1 endocytic adaptor protein. This motif in Nef was shown to form long-range electrostatic interaction with a basic patch in the AP-1 μ1 subunit [166]. Reversing these Nef charges through mutation abolished binding to AP-1 μ1 and validated the importance of this region in MHC-I downregulation as seen in previous functional studies [351, 352]. Additional details of the

pathways involved in MHC-I downregulation by Nef, which is an essential function related to immune escape of HIV-1 infected cells, is provided in section 1.3.3.

PxxPxR motif

The left-handed polyproline helix containing the conserved PxxPxR sequence (Figure 5) is essential for Nef interaction with signaling proteins that induce cellular activation, a required process for viral replication in resting cells [353, 354]. Crystal structures of the Nef core region bound to the FYN wild-type and R96I mutant SH3 domains reveal that this PxxPxR motif is required for SH3 binding [338, 355]. Subsequent work has established that this motif is essential for Nef interaction and activation of HCK and LYN, two members of the Src kinase family expressed in HIV-1 target cells. The structural and mechanistic bases of these interactions are described in detail in section 1.4.1.3.

Dileucine motif

Another conserved Nef sequence motif involved in trafficking includes a pair of leucine residues within the C-terminal flexible loop of Nef. Two negatively charged regions flank the dileucine motif and are involved in internalization of CD4, SERINC5 and other cell surface proteins. The (E/D)xxxLL motif containing the two leucines is absolutely conserved in all Nef variants. This motif takes part in sorting of Nef into clathrin-coated pits through interactions with AP-1 and AP-2 [356, 357]. Nef mutants in which the two leucines are replaced with alanines are defective for CD4 downregulation and infectivity, but not MHC-I downregulation [358]. Additional details of the Nef-AP-2 pathway in CD4 downregulation, as well as recent crystal structures of this complex, are provided in section 1.3.4.

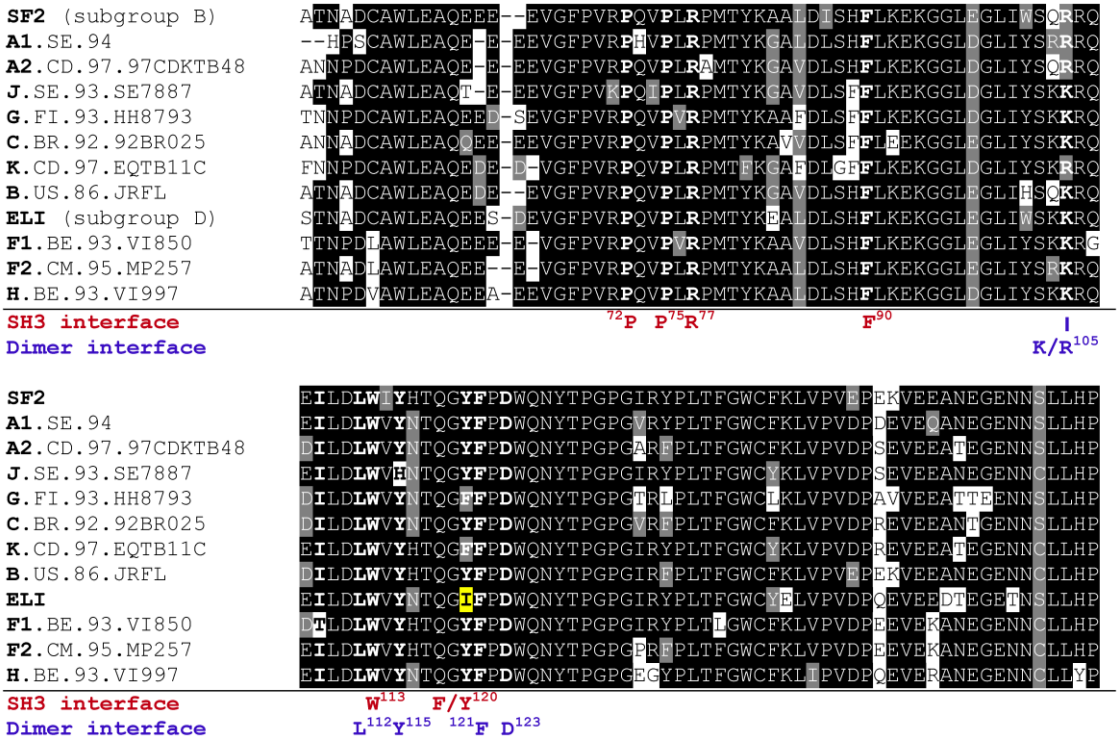

Figure 5. Sequence alignment of Nef alleles.

Nef cDNA clones from all major HIV-1 clades were selected from NIH HIV-1 sequence database and aligned by Clustal W alignment. Nef SF2 is shown in top. Key residues essential for SH3 binding are shown in red, and include the PxxPxR motif and residues hydrophobic residues Phe90, Trp113, Tyr/Phe120. Residues involved in Nef homodimerization are indicated in blue, and include Arg/Lys105, Leu112, Tyr115, Phe121, and Asp123. Flanking N- and C- terminal sequences are not shown for clarity. This figure was obtained and reproduced from Narute *et al.* [359], and is licensed under the Creative Commons Attribution License (CC BY).

1.3.2 HIV-1 Nef homodimerization

While HIV-1 Nef utilizes conserved motifs to engage various host cell proteins, its tendency to self-assemble is also essential for most if not all of its functions [360]. Early crystal structures of the Nef core in complex with SH3 domains showed that Nef not only binds the SH3 domain through its PxxPxR motif, it also forms a homodimer through its αB helix [338, 355]. Four residues in the αB helix form a hydrophobic homodimer interface (Ile109, Leu112, Tyr115, and Phe121; residue numbering as per PDB ID:1EFN) (Figure 6). The hydrophobic dimer interface is flanked by a pair of electrostatic interactions between Arg105 and Asp123. However, interactions

observed in crystal structures can be due to crystal packing and may therefore not represent biological interactions. In order to understand the biological significance of Nef dimerization observed in this crystal structure, Poe *et al*. took a cell-based approach by developing a bimolecular fluorescence complementation (BiFC) assay [169].

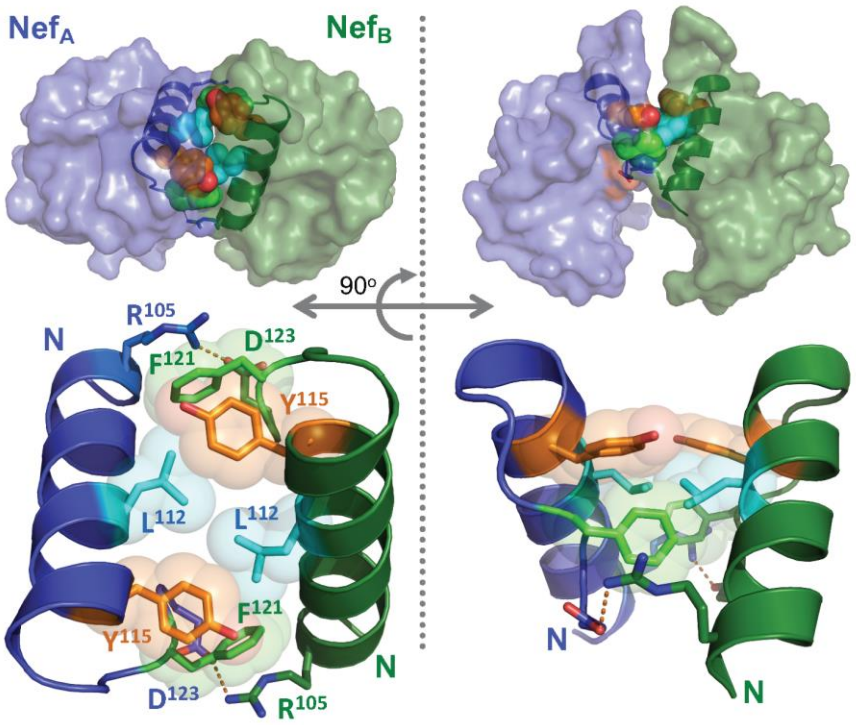

Figure 6. Nef homodimer interface consists of hydrophobic and ionic interactions between αB helix residues.

Overview of the Nef dimer structure is shown in the top panel using the crystal coordinates of Nef bound to the FYN SH3 domain R96I mutant, which is not shown for clarity (PDB: 1EFN). Nef proteins are shown in blue (NefA) and green (NefB), with the αB dimer interface highlighted. Bottom panels show the close-up view of interactions present at the αB dimer interface. Residues Leu112, Tyr115, and Phe121 form hydrophobic interactions, whereas Arg105 in each Nef monomer makes ionic contact with Asp123 in the other Nef monomer. This figure was obtained and reproduced from Staudt *et al*. [360], and is licensed under the Creative Commons Attribution License (CC BY).

For the BiFC assay, HIV-1 Nef was fused to non-fluorescent N- and C-terminal fragments of YFP and expressed in 293T cells. Co-expression resulted in strong membrane-associated fluorescence, consistent with formation of Nef homodimers, juxtaposition and complementation of the YFP fragments. In order to investigate the biological significance of the Nef-Nef crystal contacts, multiple residues in the homodimerization interface were altered including Ile109,

Leu112, Tyr115, Phe121, and Asp123. These mutations, either alone or in combination, substantially reduced the BiFC signal, providing evidence for the role of these amino acids in homodimer formation. Furthermore, these same Nef mutations also reduced HIV-1 infectivity and replication to levels observed with a virus that fails to express Nef. Subsequent studies showed that Nef homodimerization also may play an allosteric role in the downregulation of both CD4 and the SERINC5 restriction factor through the AP-2 endolysosomal pathway [361, 362].

In addition to CD4 and SERINC5 downregulation, Nef oligomerization is also important in the Nef-induced activation of the Src-family tyrosine kinase, HCK [363]. Further support for the role of Nef dimerization in HCK activation was provided by a crystal structure of Nef in complex with the SH3 and SH2 domains of HCK [364]. This structure showed that Nef forms a homodimer using the same αB helical interface, however the orientation and interactions between dimer interface residues were distinct compared to the structures of the Nef homodimer with SH3 domains only. In addition to the residues involved in Nef dimerization in complex with SH3 described above, Val70 and Trp113 are also part of the dimer interface in the SH3-SH2-bound structure. Unlike electrostatic interaction between Arg105 and Asp123 in the SH3-only complex, these residues are not involved in Nef dimerization. Instead Arg105 now contributes to SH3 binding, and Asp123 is solvent exposed where it may facilitate other Nef interactions downstream of HCK activation, as described for Nef-MHC-I interactions in sections 1.3.3 and 1.4.1.3. Recently Li *et al*. also used the BiFC assay to demonstrate the role of Nef dimerization in the activation of T and B cell specific tyrosine kinases, ITK and BTK (described in detail in section 1.4.2.3) [365]. As part of that study, I purified recombinant wild-type Nef along with mutants harboring L112D, Y115D, L112D/Y115D, and F121A mutations, and showed that these mutations shift the oligomerization state of Nef from dimer to monomer in solution.

In addition to signaling and CD4 downregulation, Nef dimerization has also been shown to influence MHC-I downregulation (W. Li and T. Smithgall, unpublished results). Therefore, even though Nef contains an arsenal of sequence motifs that allow it to accomplish diverse interactions, oligomerization has emerged a central requirement for many Nef functions. Mutations that abolish Nef dimerization rescue CD4 and MHC-I levels on the cell surface, abolish Nef-induced signaling cascades, and in turn, lower HIV-1 replication and promote immune system recognition of HIV-infected cells. The therapeutic implication of these mutations may be harnessed by designing small molecules that disrupt HIV-1 Nef dimerization as described in section 1.3.6 [366].

1.3.3 HIV-1 Nef is essential for downregulation of MHC-I

In response to virus infection, host cells mount countermeasures involving innate and adaptive immune responses. Adaptive immunity to HIV-1 infection involves destruction of the infected cell by CD8+ cytotoxic T lymphocytes (CTLs). This essential CTL response depends on the presentation of antigenic viral peptides on the surface major histocompatibility complex class I (MHC-I) receptors [367]. Immunoproteases in the cytoplasm cleave viral peptides and enable their loading onto MHC-I complexes in the ER. This MHC-I complex containing the viral peptide exits the ER and undergoes post-translational modification in the trans-Golgi network (TGNs). From the TGN, vesicles containing MHC-I bud off and travel to the plasma membrane, where they are detected by antigen-specific CTLs [368]. However, interruption of any these processes interferes with the immune response and allows infected cells to remain undetected. In the case of HIV-1 infection, Nef interferes with MHC-I function by interacting with several host trafficking proteins, thus facilitating immune evasion. Clathrin-coated vesicles are responsible for transport of cargo between the TGN and plasma membrane via endosomes. Clathrin-associated adaptor

proteins (APs) are essential to this process and consist of four subunits: two large subunits, β1 (or β2) and γ in AP1 (α in AP-2; δ in AP-3), one medium subunit μ, and a small subunit σ [369]. These four subunits combine to form a heterotetrameric adaptor complex that recognizes Yxxφ (φ= bulky hydrophobic residue), or (E/D)xxxLL based sorting signals in cargo proteins. AP-1 is responsible for mediating transport between the TGN and endosomes, whereas AP-2 is plasma membrane localized and internalizes cargo into endosomes, and finally AP-3 is localized in endosomes and transports proteins into degradative compartments [370-372]. As introduced in a previous section, HIV-1 Nef interacts directly with AP-1 and AP-2 subunits to redirect MHC-I, CD4, and other proteins from the plasma membrane.

In addition to the adaptor proteins, phosphofurin acidic cluster sorting proteins (PACS-1 and PACS-2) represent another important component of the host cell protein trafficking machinery. PACS proteins were originally discovered by studying proteins bound to the phosphorylated cytoplasmic tail of the cellular protease, Furin [373]. PACS-1 and PACS-2 are involved in recruiting AP-1 or AP-3 to cargo containing an acidic cluster and a nearby phosphorylated serine or threonine [374]. Both of these proteins also interact with Nef as described below.

The involvement of Nef in downregulation of MHC-I in HIV-1 infected cells was first reported in 1996 [164]. Currently there are two models proposed for MHC-I downregulation by HIV-1 Nef, both of which entail Nef forming interactions with adaptor proteins or PACS proteins.

The first model, also termed the signaling mode, occurs early during HIV-1 infection and involves targeting of Nef to the TGN through interaction with PACS-2 [375]. Nef's acidic cluster (EEEE) and PxxPxR motif are both required for this process. Firstly, Nef binds to PACS-2 through its acidic cluster, which targets Nef to the TGN [376]. At this site, Nef interacts with a Src-family

kinase (LYN in CD4 T cells; Hck in monocytes) as well as the ZAP70 kinase in CD4 T cells (SYK in monocytes). This multi-kinase complex induces activation of phosphatidylinositol 3-kinase (PI3K) which is essential for Nef-mediated MHC-I downregulation [377]. How PI3K activity drives Nef-mediated MHC-I downregulation is not known. MHC-I is then internalized into endosomes coated with the GTPases ARF6 or ARF1 [378, 379]. Following endocytosis, MHC-I is inhibited from recycling back to the cell surface through complex formation with AP-1 and HIV-1 Nef.

A crystal structure of the trimeric HIV-1 Nef/MHC-I/AP-1 complex reveals new details of this important interaction [166]. To obtain crystals, Nef was fused with the cytoplasmic tail domain (CD) of MHC-I which was previously shown to associate with AP-1 through its μ1 subunit. In the structure of the complex, the MHC-I CD tail is held within a groove formed by Nef and AP-1 μ1 (Figure 7). The MHC-I CD peptide, which contains a Tyr residue, binds via the canonical Yxxφ recognition motif to AP-1 μ1. This assembly closely resembles that of Yxxφ peptide binding to the analogous μ2 subunit of AP-2 [380]. However, AP-1 is not able to bind MHC-I in the absence of Nef. This is because even though the MHC-I tail contains the requisite tyrosine, the bulky hydrophobic group φ is missing. Nef allows MHC-I to bypass the need of this hydrophobic residue by forcing tight association between AP-1 and the MHC-I CD. Furthermore, Nef also allows for stabilization of the active ‘unlatched’ form of AP-1 and promotes tighter association of AP-1 with the membrane.

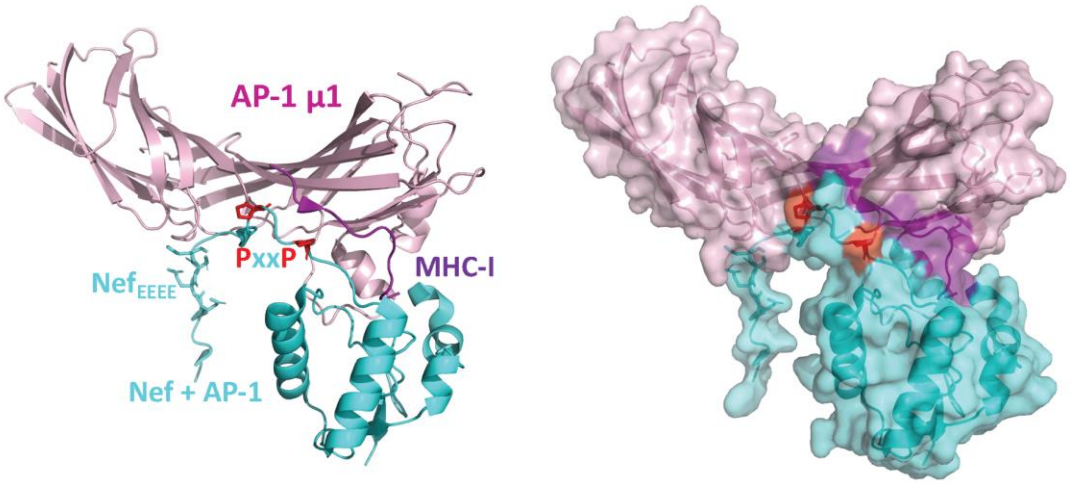

Figure 7. X-ray crystal structure of a fusion protein comprised of Nef and the MHC-I cytoplasmic domain (CD) bound to the AP-1 μ1 subunit.

Ribbon (left) and surface (right) representations of the overall Nef-MHC-I_{CD} fusion protein and AP-1 μ1 complex. Nef is shown in cyan, MHC-I_{CD} is shown in purple, and AP-1 μ1 is shown in pink. The Nef EEEE and PxxP motifs are shown as sticks. MHC-I_{CD} binds the canonical cargo recognition site on μ1, and the Nef PxxP motif helps to force the tight association of MHC-I_{CD} with AP-1 μ1 by forming a side wall of the binding groove and by shaping a binding path between Nef and μ1. This model was produced with PyMol using the crystal coordinates of the complex of HIV-1 Nef with N-terminally fused MHC-I_{CD} and AP-1 μ1(PDB: 4EN2).

The second model of Nef-mediated MHC-I downregulation, also termed the stoichiometric model, occurs later in HIV-1 infection [375]. This model involves blocking the transport of newly synthesized MHC-I molecules from the TGN to the plasma membrane. Nef binds to immature, hypo-phosphorylated MHC-I in the TGN and prevents further transport through MHC-I sequestration [381]. As described in the first model, Nef forms the same ternary complex with MHC-I and AP-1, which is then transported to lysosomes by a β-COPI protein complex. Both Nef mutant deficient in β-COPI binding and siRNA knockdown of β-COPI inhibited MHC-I downregulation by Nef, providing support for this pathway [382].

Taken together, these models suggest two distinct mechanisms that are temporally linked to downregulate MHC-I. At first, Nef facilitates the assembly of the multi-kinase complex, followed by endocytosis and sequestration of MHC-I from the cell surface. After about 48 hours of infection, newly synthesized MHC-I molecules are blocked from transport to the cell membrane

and degraded in lysosomes. The relative contributions of the two models are not known, but it has been suggested that they can occur simultaneously [375].

1.3.4 HIV-1 Nef downregulation of CD4

While Nef-mediated MHC-I downregulation allows HIV-1 to escape immune surveillance, Nef-mediated CD4 downregulation also facilitates critical events during viral pathogenesis [383]. Repeated entry of virus into the same cell induces premature cell death and is detrimental to successful viral replication because of the toxicity of accumulating unintegrated viral genomes [384]. Nef-induced CD4 downregulation not only prevents superinfection due to blocking of further virus particle entry, but also blocks proapoptotic signals delivered through CD4 receptors [385, 386]. Furthermore, downregulation of CD4 also interferes with the immune response and promotes virion release [387, 388]. Early genetic studies showed that downregulation of CD4 depends on both Nef myristoylation and sequences including the C-terminal loop (E/D)xxxLL motif and the diacidic motif Asp174, Asp175 [163, 389, 390]. Myristoylation allows membrane targeting of Nef, and the C-terminal flexible loop containing the dileucine motif engages a clathrin-associated AP-2 complex [163]. Similar to MHC-I downregulation, Nef mediates the interaction of CD4 with AP-2 although the structural details are distinct.

AP-2 is a heterotetrameric complex containing four subunits: α, β2, μ2, and σ2 [391]. In addition to Yxxφ based sorting signal recognition, AP-2 also recognizes the (D/E)xxxL(LIM) signal for endocytosis. The cytosolic portion of CD4 also contains a dileucine motif in the sequence SQIKRLL, and phosphorylation of the serine in this sequence is required for recognition and endocytosis by AP-2 [392]. Nef facilitates the formation of CD4/Nef/AP-2 complex at the plasma membrane in the absence of phosphorylation. Nef binding to AP-2 is inhibited by the mutation of

the Nef dileucine motif as well as the diacidic aspartate residues, suggesting their distinct roles in AP-2 binding. Nef has been shown to bind the AP2 'α-σ2' hemicomplex, which harbors the binding site for (D/E)xxxL(LIM) type signals [393, 394]. A basic patch made up of residues Lys298 and Arg341 in the α subunit of AP-2 is also required for Nef binding and CD4 downregulation [395]. Ren *et al*. first crystallized the HIV-1 Nef core domain in complex with the AP-2 'α-σ2' hemicomplex in which Nef contacts both the α and σ2 subunits. The Nef C-terminal flexible loop, which is not ordered in structures with other proteins, was highly ordered and makes extensive contacts with α and σ2 subunits. Residues previously identified to be involved in AP-2 binding were shown to play key roles, and Nef polar interaction with the AP-2 basic patch was also confirmed. A more recent crystal structure of Nef fused to the C-terminal tail of CD4 and the AP-2 complex revealed the structural foundation behind Nef-mediated CD4 downregulation [396]. Nef functions as a 'connector' between AP-2 and CD4 (Figure 8). In this structure, Nef N-terminal loop and αB helix residues make hydrophobic contacts with CD4 residues that allow AP-2 recruitment and CD4 downregulation. CD4 binds Nef but does not make direct contact with AP-2. On the other hand, Nef associates with AP-2 mainly through the Nef C-terminal loop that contains the dileucine motif, which mimics AP-2 natural ligands. Thus, Nef facilitates CD4 downregulation by acting as a connector between CD4 and AP-2 endocytic machinery.

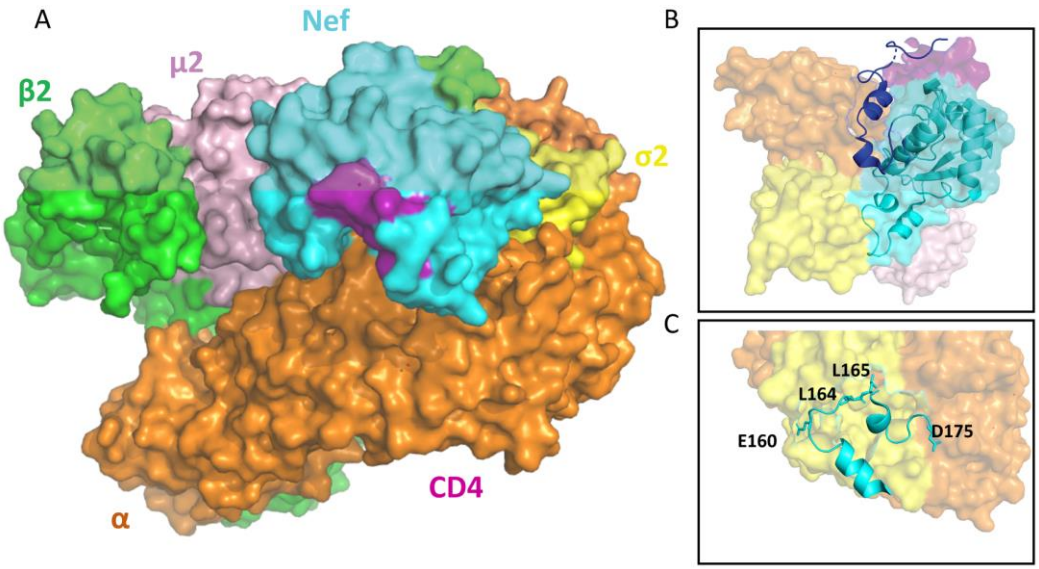

Figure 8. X-ray crystal structure of the fusion protein comprising Nef and the cytoplasmic domain of CD4 bound to the tetrameric AP-2 complex.

A) Overall structure of the Nef-CD4$_{CD}$ fusion and AP-2$^{\Delta\mu2\text{-}CTD}$ complex. Nef (shown in cyan) interacts with CD4 (shown in purple) and AP-2 subunits (β2 shown in green, μ2 shown in pink, α shown in orange, and σ2 shown in yellow). Nef recruits CD4 to a pocket that is opposite to the C-terminal loop, and the CD4 dileucine motif dips into the hydrophobic pocket formed by Nef residues Phe121, Trp124, Met79, Thr138 and Pro78. B) CD4 recruitment is secured by the Nef N-terminal loop (shown in blue), which is highly ordered in the crystal structure and wraps around the Nef core. The N-terminal loop then extends in the N-terminus to support CD4 binding. C) The Nef C-terminal loop containing the dileucine motif required for CD4 downregulation associates with AP-2 through extensive charge-charge and hydrophobic interactions. This model was produced with PyMol using the crystal coordinates of HIV-1 Nef (NL43) fused with cytoplasmic domain of CD4 and the AP-2 complex (PDB: 6URI).

1.3.5 HIV-1 Nef interactions with other proteins

In addition to downregulation of MHC-I and CD4, HIV-1 Nef also downregulates other receptors to ensure efficient immune evasion. MHC-II is expressed on antigen-presenting cells such as macrophages and dendritic cells which are also host cells for HIV infection. Nef downregulation of MHC-II molecules prevents antigen presentation to helper T cells [397]. The MHC-II downregulation function of Nef is conserved among several HIV-1 strains, which suggests that it is important to HIV-1 immune escape [398].

Nef has been reported to decrease surface expression of CCR5, CCR3 and CXCR4 co-receptors in macrophages, T helper 2 cells and microglial cells, and T cells respectively [399]. While the mechanisms by which co-receptors are downregulated by Nef is not fully clear, co-receptor downregulation may also aid in prevention of superinfection [400].

The transmembrane glycoprotein CD8 is also a co-receptor of the CD4 receptor. As for CD4, Nef downregulates the CD8 β chain by recruiting AP-2 followed by clathrin-mediated endocytosis [401]. The role of CD8 molecules in the recognition of antigens in association with MHC-I molecules is very important, and Nef-mediated CD8 downregulation may provide an additional mechanism to avoid antigen recognition [402].

CD80 and CD86 are co-stimulatory proteins found in dendritic cells and macrophages, and provide co-stimulatory signals necessary for T cell activation and survival [403]. Nef mediates CD80/CD86 downregulation by two mechanisms: 1) direct binding of Nef to CD80/CD86 to mark the molecules for Rac-mediated endocytosis; and 2) activation of a PKC-Src-TIAM-Rac pathway to trigger Rac-mediated endocytosis [404]. CD28 is also expressed in T cells and plays a role together with CD80 and CD86 to ensure efficient co-stimulation for the activation of T cells. Nef was shown to downregulate CD28 through an AP-2-dependent mechanism similar to Nef downregulation of CD4 [405]. CD1 is an MHC-I-like molecule that presents lipid and glycolipid antigens to Natural Killer T cells (NKT) [406]. Nef was shown to downregulate at least two out of the five CD1 molecules found in humans [407, 408].

In addition to modulating cell surface receptors and co-receptors, Nef also alters the threshold of T lymphocyte activation by interacting with various signaling cascades [334, 409, 410]. Nef interacts with the p21-activated kinase 2 (PAK2) which has a direct effect on cytoskeletal morphology and apoptotic signaling [411]. Nef based activation of PAK2 was found to increase

HIV replication [412]. The mechanism of Nef activation of PAK2 is not known, but the effect of PAK2 activation on viral replication is attributed to enhancement of virus entry by PAK-driven changes in the actin cytoskeleton [331, 353]. PAK2 activation in viral replication also causes inactivating phosphorylation of the proapoptotic protein Bad through a Nef-PAK2-PI3K complex [413].

In addition to PAK2, Nef also associates with and activates Vav, a protooncogene and guanine nucleotide exchange factor, in order to initiate a signaling cascade and remodel the actin cytoskeleton [353]. Inhibition of Nef-based Vav activation blocked viral replication. Coordinated activation of Src-family tyrosine kinases (discussed in detail in section 1.4.1.3, below), members of PAK family, and Vav drive transcription factor activation resembling TCR stimulation that promotes viral replication. This is accomplished in part through activation of the NFAT and NFκB transcription factors, which are responsible for induction of innate and adaptive immune responses [414, 415]. HIV-1 Nef has a complex relationship with these transcription factors as it both increases and suppresses their activity. In the early stages of infection, Nef is the most highly expressed viral protein and it promotes the nuclear translocation of NFκB and NFAT, which activate viral promoters to induce Tat expression leading to viral replication [416]. In later stages of infection, however, Nef downregulates CD3 from the cell surface, an important determinant of TCR signaling. By downregulating CD3, Nef is able to block stimulation of CD4 T cells by antigen presenting cells and suppress NFκB and NFAT signaling, hence suppressing the antiviral immune response.

1.3.6 HIV-1 Nef as a drug target

Considering the persistent demand for new antiviral therapeutics, and the importance of Nef in HIV-1 immune evasion, replication and infectivity, HIV-1 Nef represents an attractive target for new anti-viral drug discovery and virus eradication. As described in detail in the preceding sections, Nef promotes the HIV-1 life cycle in multiple ways, by promoting infectivity, replication, immune escape and persistence [330, 417]. However, HIV-1 Nef has no targetable enzymatic activity or a single functional motif or active site. Our lab and others have shown the importance of Nef dimerization to several viral processes described above leading to successful viral infection. Inhibition of Nef dimerization therefore presents an opportunity to 1) increase the CD8 CTL response by increasing MHC-I•antigen presentation, 2) stop viral replication by reducing Nef-mediated constitutive activation of host signaling, and 3) induce superinfection and allow antiviral immune responses by increasing CD4 and coreceptor expression on the cell surface.

Our group designed an *in vitro* assay to take advantage of the requirement of Nef dimerization for kinase constitutive activation in order to identify inhibitors of Nef dimerization. Under these assay conditions, recombinant Nef was coupled to activation of the Src-family kinase HCK, which provided a robust read-out compatible with automated high-throughput screening. This kinase-coupled assay was then used to identify small molecule inhibitors of Nef-mediated HCK activation [418, 419]. From a library of more than 220,000 compounds, a unique diphenylpyrazolo diazene compound, referred to simply as ‘B9’, was identified that selectively inhibited Nef-dependent activation of HCK. More importantly, B9 potently inhibited wild-type HIV-1 replication, similar to Nef-defective HIV-1 levels. Furthermore, surface plasmon resonance (SPR) experiments demonstrated direct interaction between HIV-1 Nef and B9 *in vitro* further validating B9 as a promising drug lead. Subsequent studies with B9 and first-generation analogs

showed that pharmacological inhibition of Nef restored MHC-I to the surface of latently infected CD4 T cells, resulting in activation of autologous CD8 T cells and infected cell killing [420]. This result provided an important proof of concept that Nef inhibitors may not only suppress HIV-1 replication, but may also restore the host CTL response to help clear the viral infection.

In subsequent studies, our group synthesized more than 200 analogs of B9 with distinct functional groups. These inhibitors were tested for direct HIV-1 Nef binding by SPR and in a cell-based assay for antiretroviral activity [366]. Cell-based activity and *in vitro* binding kinetics were then together used to identify the analogs with maximum therapeutic potential. The top compounds bound recombinant Nef with K_D values in the 0.1 - 100 nM range, and inhibited HIV-1 replication in donor peripheral blood mononuclear cells (PBMCs) with low nM IC_{50} values. These compounds also inhibited Nef-mediated activation of HCK and ITK (Tec family kinase, discussed in section 4.3) in 293T cells. Lastly, these compounds also rescued cell-surface MHC-I expression in the Nef-transfected CEM-SS T cell line. Therefore, selective inhibitors of HIV-1 Nef present a promising opportunity to overcome the longstanding problem of the latent viral reservoir by restoring cell surface MHC-I expression followed by CTL clearing of infected cells.

1.4 Non receptor protein tyrosine kinases

Pathogens often exploit host cell signaling pathways in order to mount successful infections. These interactions allow pathogens to survive and replicate despite the hosts' innate and adaptive immune responses. In general, critical signaling cascades exploited by viruses include the G-protein-coupled receptor (GPCR) signaling network, PI3K/AKT signaling, and mitogen

activated protein kinase (MAPK) pathways to generate cellular conditions favorable for replication [421-423].

Within these signaling networks, viruses also exploit protein-tyrosine kinases (TKs) for their own advantage as these kinases are critical mediators of diverse cellular functions, including cell growth, viability, motility and metabolism [424]. TKs also play crucial roles in the pathophysiology of cancer, including hematological malignancies, which has led to wide exploration of their functions and regulatory mechanisms.

In humans, the protein-tyrosine kinase family includes 90 enzymes responsible for transmitting signals from the cell membrane to cytoplasmic proteins and the nucleus [425]. They catalyze the transfer of a γ-phosphate group from ATP to target proteins' tyrosine residues in a highly regulated and specific manner. There are two main classes: receptor (RTKs) and non-receptor tyrosine kinases (NRTKs). Well characterized examples of RTKs include platelet-derived growth factor receptors (PDGFR), fibroblast growth factor receptors (FGFR), the epidermal growth factor receptor (EGFR) family, and the insulin receptor (IR). The NRTKs can be classified into nine subgroups according to their sequence similarity as well as the presence of particular regulatory domains. These include the ABL, FES, JAK, ACK, SYK, TEC, FAK, SRC, and CSK kinase families [426].

NRTKs contain homologous kinase catalytic domains comprised of N- and C-terminal lobes. Moreover, they often possess additional protein-protein interaction domains, including Src homology 2 (SH2), Src homology 3 (SH3), and pleckstrin homology (PH) domains, which serve unique purposes in each kinase.

NRTKs are critical components of signaling pathways that mediate both innate and adaptive immune responses. JAK family kinases are associated with cytoplasmic domains of

multiple cytokine receptors that control the growth and differentiation of hematopoietic cells of myeloid lineage as well as interferon receptor signaling in response to viral infections. JAK kinases, upon activation, induce phosphorylation and nuclear translocation of the STAT family of transcription factors [427]. Signaling by activated B and T cells of the immune system is also dependent on multiple NRTKs (described in detail in section 1.4.2.3) [428].

The SRC kinases make up the largest and best studied of the NRTK families. SFKs participate in a variety of signaling events controlling cell growth and survival, DNA synthesis and cell division, actin cytoskeleton rearrangement and motility. Multiple upstream signals stimulate SRC family kinases, including growth factor and cytokine receptors, GPCRs, and cell adhesion receptors [429]. Because of their central roles in immune responses and regulation of cellular events, SFKs are often exploited by viral pathogens [430]. Below I describe SFK structure and regulation, followed by the mechanism of activation by HIV-1 Nef.

1.4.1 SRC family kinases

There are eight mammalian Src-family kinases: SRC, FYN, YES, BLK, FGR, HCK, LCK and LYN. Of these, SRC, FYN, and YES are expressed in almost all cell types. Expression levels vary according to cell type and some family members exist as isoforms due to alternative splicing. For example, platelets, neurons and osteoclasts express 5- to 200-fold higher levels of SRC compared to other cell types [431]. BLK, FGR, HCK, LCK, and LYN are expressed primarily in hematopoietic cells [432]. Expression of FGR is largely limited to monocytes and macrophages [433]. FYN is observed at high levels in T lymphocytes and neuronal tissues [434]. LCK is mostly expressed in T lymphocytes where it is a critical component of the TCR signaling complex as

described below [435]. LYN is expressed in myeloid cells and B lymphocytes [436]. HCK is largely limited to myeloid cells, while BLK is present in high levels in B lymphocytes [437, 438].

1.4.1.1 Structure of SFKs

Because SFKs modulate signal transduction in a variety of cellular processes, SFKs contain multiple structural modules to facilitate protein-protein interactions. There are five distinct domains present in all SFKs. Starting from the N-terminus, these domains include an SH4 and unique region, the SH2 and SH3 domains, the kinase domain (sometimes referred to as the SH1 domain), and a C-terminal negative regulatory tail [439]. Structural features and regulatory functions of these domains are described briefly below.

SH4 and unique domains

The N-termini of all Src family kinases contain the consensus sequence MGxxxST, where myristoylation takes place on the Gly residue after removal of Met during this co-translational modification [431]. N-terminal myristoylation is required for membrane association as well as oncogenic transforming activity by v-SRC [431, 440]. The first 15-residue segment containing the myristoylation signal sequence is also referred to as the SH4 domain. All SFKs (except SRC and BLK) contain cysteine residues in the SH4 domain that undergo palmitoylation which also contributes to membrane association [441].

Following the SH4 domain is the unique region, which contains non-homologous sequences of different lengths for each SFK member. The SH4 and unique domains are highly disordered and resistant to crystallization or other structural studies. The functions of these disordered regions are still obscure. SH4 domains are mainly responsible for binding to lipids, except in LCK, where the unique domain is responsible for interactions with T cell CD4 and CD8 co-receptors via a zinc finger motif. [442]. Recently, unique domains have been implicated in

protein-protein interactions, and multiple phosphorylation sites found in this region may also play important biological roles [443]. A regulatory role for the unique domain in c-SRC was proposed that involves intramolecular interactions with the SH3 domain [444]. Recent SAXS and NMR studies suggested that the N-terminal regulatory region of c-SRC comprised of the SH4, unique and SH3 domains form a compact, but highly dynamic, intramolecular 'fuzzy' complex [445]. While the nature of this fuzzy complex is unique to each SFK member, the authors suggest that there may be a shared regulatory function of this region. The N-terminal region of SRC has also been reported to bind to a hydrophobic pocket in the kinase domain, resulting in dimerization [446]. Interference with this dimerization event by introducing mutations abrogated SRC activation, suggesting a regulatory role for this intrinsically disordered N-terminal region.

SH3 domain

SFK SH3 domains are about 50-70 amino acids in length and participate in intra- and inter-molecular protein-protein interactions [447]. Alternatively spliced forms of SRC containing 6- or 11-residue insertions in the SH3 domain are found in CNS neurons [448]. SH3 domains consist of a β-barrel architecture with five antiparallel β-strands and two loops, the RT loop and the n-SRC loop [449]. These loops flank the hydrophobic and aromatic residues that make up the binding site for proline-rich sequences bearing a 'PxxP' motif. SH3-binding sequences form a polyproline type II (PPII) helix with a left-handed orientation. These helices have a triangular cross section, where the prolines form the base of the triangle and interact with aromatic residues on the SH3 domain surface. Additional specificity is provided by Lys or Arg residues following or preceding the PxxP motif. This allows two high affinity binding modes with respect to the N to C orientation of the PPII helix: class I ligands share the general motif RxxPxxP while class II ligands bind with PxxPxR in the opposite orientation [450]. In intracellular signaling, SFKs SH3 domains have been shown

to bind to the RNA binding protein p68 Sam, the p85 subunit of phosphatidylinositol-3' kinase (PI3K), and paxillin [451-453]. Moreover, SFK SH3 domains also participate in intramolecular regulatory interactions which are discussed in detail below.

SH2 domain

SFKs SH2 domains are typically 100 residues in length and are responsible for association with tyrosine phosphorylated proteins. SH2 domains contain a central antiparallel β-sheet flanked by two α-helices. These secondary structural elements and the loops that connect them form two binding pockets, one that binds phosphotyrosine and another that binds hydrophobic residues C-terminal to the phosphotyrosine [454]. The phosphotyrosine recognition pocket is highly conserved among SH2 domains with an essential arginine residue that forms electrostatic interactions with the phosphotyrosine. The other pocket is not conserved, allowing protein-specific targeting of phosphotyrosine-containing partner proteins [447]. SFKs preferentially bind to a pYEEI motif coordinating the phosphotyrosine and isoleucine in the respective binding pockets. Glu residues are favored at pY+1 and pY+2 positions, but other residues can be accommodated at these positions in SFK SH2 domains [455]. The Src SH2 domain has been shown to interact with tyrosine phosphorylated sites on the focal adhesion kinase (FAK), p130 cas, the PI3K p85 subunit, and p68 Sam [451, 453, 456]. SFK SH2 domains are also essential for autoregulation of kinase activity through intramolecular recognition of C-terminal tail phosphotyrosine as described in more detail below.

SH1 or kinase domain

SFKs share the bilobed protein kinase domain fold found in all other tyrosine and serine/threonine kinases [457]. The smaller N-terminal lobe of the kinase domain is primarily involved in binding and orienting ATP for the phosphotransfer reaction. The N-lobe consists of

five β-strands and a single α-helix, termed the C-helix. The C-helix is an important determinant of kinase activity. The larger C-terminal lobe is predominantly helical and responsible for binding to substrates. It also contains another important determinant of kinase activity, the activation loop. Nucleotide binding and transfer of phosphate occurs in the cleft between the N-lobe and the C-lobe of the kinase domain. The two lobes move relative to each other and can open or close the cleft as necessary. The open form is required for ATP binding to the catalytic site and release of ADP, while the closed form orients the catalytic residues required for transfer of phosphate to substrate. Insights into the SFK phosphorylation mechanism were facilitated by the crystal structure of the LCK kinase domain in an active conformation [458]. This structure revealed that phosphorylation of the activation loop tyrosine is required to maintain the active conformation.

Several residues from both lobes of the kinase domain are involved in the phosphotransfer reaction. The N-lobe contains a glycine-rich motif (GxGxφG) that binds the ATP phosphates and is also called the P loop. These glycine residues are involved in coordinating the ATP phosphates via backbone interactions. Substrate binding takes place in an open conformation, where the activation loop offers a platform for peptide substrates. Autophosphorylation of the Tyr in the activation loop stabilizes the kinase in this open and extended conformation as described above for LCK. In the absence of phosphorylation, however, the activation loop collapses back into the active site and interacts with the C-helix, and blocks binding of both nucleotides and substrate [459]. This forces the C-helix to rotate outward in order to accommodate the activation loop, which assumes a partially helical conformation in downregulated structures of HCK and SRC. Inward and outward motion of the C-helix coupled with phosphorylation of the activation loop rearranges the catalytic Asp-Phe-Gly sequence in the active site as required for transfer of phosphate in a crankshaft-like motion [460].

C-terminal tail

The C-terminal tail consists of 15-17 amino acids that have a role in regulating kinase activity through intramolecular SH2 domain binding. The conserved Tyr in the tail is phosphorylated by C-terminal Src kinase (CSK) or CSK-homologous kinase (CHK) [461, 462]. When phosphorylated, the tail phosphotyrosine binds to the SH2 domain in order to regulate the kinase activity. Songyang *et al*. carried out a phosphopeptide library screening study to determine the sequence specificity of the peptide-binding sites of SFK SH2 domains [455]. Binding specificity varied between the kinases for different peptides signifying kinase specific substrates that may bind SH2 domain. Furthermore, flexibility in some residue placements and different extents of binding suggest *in vivo* competition between substrates. Under basal conditions *in vivo*, 90-95% of SRC is phosphorylated on the tail Tyr residue, making the enzyme inactive. However, mutation of tail Tyr residue in SRC renders the kinase active, leading to anchorage-independent growth *in vitro* and tumor formation *in vivo* [463-465].

1.4.1.2 Regulatory mechanisms of SFKs

Crystal structures of SFKs in the autoinhibited state show that both the SH2 and SH3 domains bind to the back of the kinase domain to lock the kinase domain in an inactive state. This inactive conformation is characterized by the tucking of the dephosphorylated activation loop Tyr into the active site, and outward rotation of the C-helix [459, 466-469]. The SH3 domain interacts with the N-terminal lobe and SH2 domain interacts with the C-terminal lobe of the kinase domain. This autoinhibited state is stabilized through contacts between the regulatory domains and flexible segments within the protein. The SH3 domain binds the linker segment that connects the SH2 domain with the N-lobe of kinase domain, and the SH2 domain binds the phosphorylated C-

terminal tail of the protein as described above. Importantly, these intramolecular interactions are not of high affinity, and may be easily destabilized by binding partners including HIV-1 Nef.

Despite their locations away from the catalytic cleft, SH2 and SH3 domains are capable of communicating and exerting conformational pressure on the catalytic site of the kinase domain. The SH3 domain regulates the kinase domain by modulating the position of the C-helix to be either inward or outward by pinning the linker segment against the N-lobe of the kinase domain. Conserved residue Trp260 is located at the C-terminal end of the SH2-kinase linker and points into a hydrophobic region in the N-lobe of the kinase domain in the autoinhibited structures of HCK and SRC in order to help stabilize the C-helix in an outward position unsuitable for catalysis. An HCK mutant in which Trp260 was replaced with alanine showed higher specific activity than wild type HCK, confirming the importance of this residue in coupling SH3-linker interaction with regulation of the kinase domain [470]. The crystal structure of the LCK kinase domain showed that this residue has a different conformation in the activated state.

In addition to stabilizing effects on the autoinhibited state, the SH2 and SH3 domains also communicate to the C-helix via activation loop helix formation. Release of the SH2-SH3 clamp is likely to disorder the helical activation loop and lead to activating phosphorylation of the Tyr residue. The clamp also restricts the mobility required for catalysis between N- and C-lobes of the kinase domain. A tight coupling between the SH2 and SH3 domains is also required to maintain the autoinhibited conformation of the kinase domain, even though the relative orientations of SH2 and SH3 in isolation may not be conserved [471, 472]. Furthermore, assembly of these domains to downregulate the kinase also involves inward facing and occupancy of their respective binding pockets. Therefore, the assembled downregulated confirmation also restricts the availability of the regulatory domains for other ligands, implying a bidirectional regulatory mechanism [473]. The

weak nature of the intramolecular bonds holding the inactive structure together suggests that it is like a precariously set mousetrap, waiting to spring to the active conformation through factors that outcompete the intramolecular binding sites of SH2 and SH3 domains [474].

Several lines of evidence support an essential role for C-terminal tail phosphorylation and intramolecular SH2 domain engagement in the cellular regulation of SFK activity. Perhaps the earliest examples come from studies of the v-SRC and v-YES oncogenes associated with the Rous and Yamaguchi sarcoma retroviruses, respectively. Both viral tyrosine kinases lack the C-terminal tail residues required for phosphorylation by CSK and CHK, and are therefore constitutively active and transformation competent [475]. The weak nature of the SH2:phosphotail interaction is also overcome during SRC activation by platelet-derived growth factor (PDGF). Autophosphorylation of Tyr 579 in the juxtamembrane region of the PDGF receptor allows PDGF binding to the SH2 domain of SRC with high affinity leading to displacement of the negative regulatory tail and activation of SRC [476]. SFKs in turn can phosphorylate the receptor and thus play a role in promoting mitogenesis. In another example, closely spaced PxxP and phosphotyrosine motifs in focal adhesion kinase (FAK) bind both the SH2 and SH3 domains of SRC and FYN [477]. FAK is involved in dynamic regulation of actin and determines cell migration, and the FAK-SRC connection may therefore contribute to cancer cell metastasis. In cancer cells, other protein-protein interactions overcome the inhibitory conformation of SFKs by disrupting the tail phosphotyrosine-SH2 interactions. SFK SH2 domains bind to activated receptors such as FLT3 and oncogenic proteins such as BCR-ABL in AML and CML, respectively [478]. Furthermore, cancer cells can also overcome inhibitory interactions in SFKs by suppression of CSK, leading to a higher proportion of activated SFKs [479, 480].

In addition to competitive SH2:phosphotail disruptions, another method to overcome SFK autoinhibition involves the activity of phosphatases. Protein tyrosine phosphatases (PTPs) such as PTPα, PTPγ, SHP-1, SHP-2, and PTP1B are involved in regulation of SFKs through dephosphorylation of SFK activation loop tyrosine or C-terminal tail tyrosine. PTPα and PTPγ play a dual role by dephosphorylating both the activation loop and the C-tail phosphotyrosines [481, 482]. SHP-1 has been shown to dephosphorylate the SRC phosphotail resulting in kinase activation. Mice expressing loss-of-function SHP-1 mutations show increased levels of SRC tail phosphorylation [483]. SHP-2 is another PTP that dephosphorylates the SRC tail. Moreover, SHP-2 also activates SRC in a phosphatase-independent manner by associating with its SH3 domain [484]. PTP-1B also activates SRC activity through specificity for C-tail pTyr dephosphorylation [485].

Another mechanism for activation of downregulated SFKs involves the disruption of intramolecular SH3:polyproline helix binding. Interaction between SH3 and the SH2-kinase linker segment allosterically hinders the formation of an essential salt bridge involving a conserved glutamate in the C-helix and a lysine in the β-sheet of the kinase domain N-lobe. The activity of the SRC SH3 domain is required for the mitogenic effects of PDGF and EGF in fibroblasts [486]. SH3 deletion or mutation of an essential residue within the binding surface of SH3 inhibited PDGF-induced signaling through SRC in fibroblasts. SFK SH3 domains also regulate the activation of the transcription factor, STAT3 [487]. SRC, HCK, LYN, FYN, and FGR were all shown to transiently engage STAT3 and become activated in a SH3-domain dependent manner. SH3 domain-dependent substrate recruitment was enough to induce SFK activation. The activated kinases returned to the inactive state after release of phosphorylated STAT3, suggesting that SFKs can be activated without disruption of the SH2:phosphotail interaction or tail dephosphorylation.

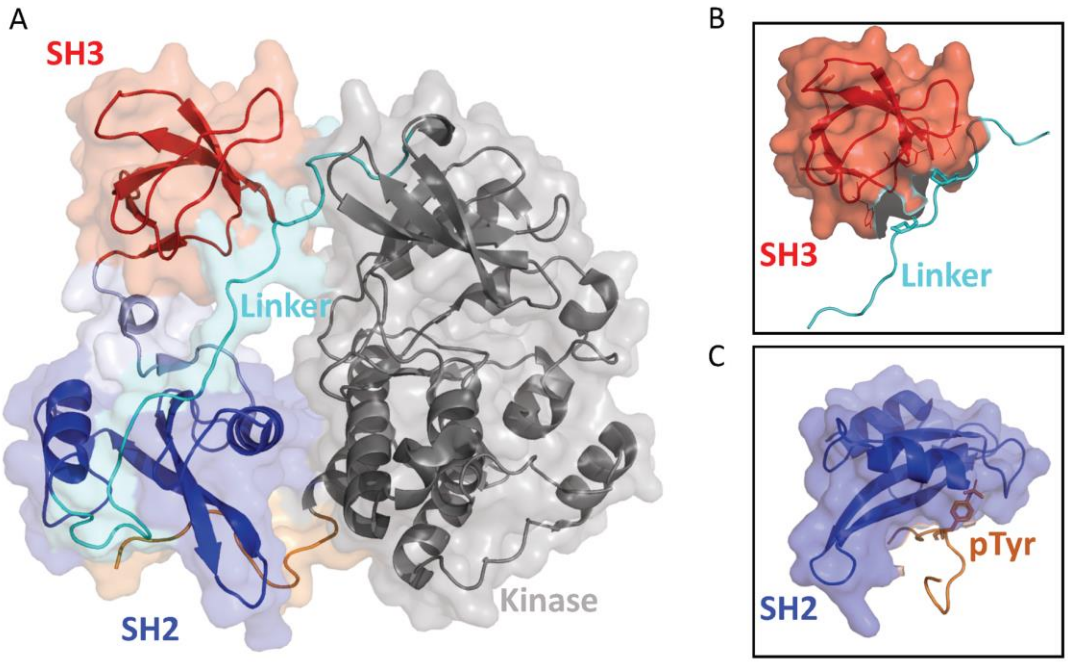

Figure 9. Autoinhibited structure of HCK.

A) X-ray crystal structure of inactive HCK (PDB: 1QCF) showing the compact autoinhibited conformation where the SH3 (shown in red) and SH2 (shown in blue) domains engage the back of the kinase domain (shown in grey) to maintain the inactive conformation. The linker segment that connects the SH2 and N-lobe of the kinase domain is shown in cyan. The c-terminal tail is shown in orange. B) Close-up view of autoinhibitory interactions maintained by the PPII helix in the SH2-kinase linker (cyan sticks) binding to the SH3 domain. C) Close-up view of autoinhibitory interactions maintained by phosphorylated Tyr (show in orange sticks) in C-terminal tail binding to the phosphotyrosine binding pocket in the SH2 domain. This model was produced in PyMol using the crystal coordinates of autoinhibited HCK.

To determine whether SH3:linker displacement was required for SFK activation in cells, Lerner *et al*. made high affinity linker (HAL) mutants of HCK in which additional prolines were added to the SH2-kinase linker to increase its intramolecular affinity for the SH3 domain [488]. HCK HAL was further modified to include a C-terminal tail Tyr to Phe (Y501F) substitution to disrupt SH2:phosphotail binding. The resulting HCK-HAL-Y501F mutant showed equivalent transforming and kinase activities as HCK-Y501F with a wild-type linker in fibroblasts, suggesting that SH3:linker interaction does not need to be disrupted to achieve kinase activation. These observations suggest that SFKs can exist in multiple active conformations in which the SH3:linker, SH2:phosphotail, or both interactions are disrupted. Different modes of activation may determine

unique downstream signaling events. Meng *et al*. used Markov state modeling to simulate the SFKs activation, and observed extensive conformational sampling and transitions [489].

1.4.1.3 Activation of SFKs by the HIV-1 Nef accessory protein

The highly conserved PxxPxR motif in HIV-1 and SIV Nef closely resembles the sequences that bind SH3 domains in cellular signaling proteins. This observation led to the discovery that HIV-1 Nef binds to a subset of SFK SH3 domains, namely those derived from HCK and LYN [354]. In the same study, HIV-1 mutants lacking the Nef PxxPxR motif compromised viral replication in monocytic U937 cells. This early observation provided the first evidence that HIV-1 Nef evolved to exploit SH3-containing signaling proteins like SFKs to enhance the viral life cycle. Interestingly, subsequent work showed that isolated peptides containing the Nef PxxPxR sequence were not able to bind to SH3 domains with affinities as high as the intact Nef protein, suggesting an additional layer of interaction [490]. This possibility was confirmed in a subsequent crystal structure of the Nef:SH3 complex as described in the next section. Nef exhibited weaker affinity for the FYN SH3 domain compared to the HCK SH3, despite the high similarity between the FYN and HCK SH3 domain structures (K_D = 0.25 μM for the HCK SH3 vs. > 20 μM for the FYN SH3). Mutation of Arg96 to Ile in the RT loop of the FYN SH3 domain enhanced Nef binding (K_D = 0.38 μM), suggesting that this RT loop residue may also play a key role in Nef interaction.

Lee *et al*. determined the crystal structure of the Nef core (residues 54-205, HIV-1 NL43 isolate) bound to the R96I mutant of the FYN SH3 domain to shed light on the structural mechanism of this interaction (Figure 10) [338]. The crystal structure shows two Nef-SH3 complexes in the asymmetric unit. The structure of the FYN SH3 domain is unchanged upon interaction with Nef, with the SH3 β-barrel structure presenting an array of conserved hydrophobic residues that are spaced appropriately for interaction with the Nef PxxPxR motif. Residues 71-77

in HIV-1 Nef form the PPII helix, with conserved prolines Pro72 and Pro75 packing against a hydrophobic interface provided by Tyr91, Trp119, Pro134, and Tyr137 of SH3.

In addition to the prolines, the arginine residue in the PxxPxR motif (Arg77) is also highly conserved in HIV-1 Nef variants. This arginine forms a salt bridge with Asp100 in the RT loop of the SH3 domain to orient and stabilize the interaction. The RT loop extends over the Nef surface, such that Ile96 of SH3 is inserted into a pocket formed by helices αA and αB of Nef. Ile96 interacts with the conserved side chains of Leu87, Phe90, Trp113, and Ile114 of Nef. This structure demonstrates that the high affinity interaction of Nef with SH3 requires not only the PxxPxR motif, but is also dependent upon the three-dimensional fold of the Nef core, which creates the hydrophobic binding pocket for Ile96 in the SH3 RT loop. Note that isoleucine is present in this position in HCK and LYN, but not in any other SRC-family members. Apart from the hydrophobic interactions involving SH3 Ile96 and the Nef PxxP motif, the rest of the 1200 $Å^2$ interface between Nef and SH3 is polar.

Interaction between Arg77 in Nef and Asp100 in SH3 is further enhanced by interactions with SH3 Trp119. In addition, Asp100 forms a hydrogen bond with Gln118 in Nef which in turn hydrogen bonds with SH3 Tyr93. These SH3 residues that take part in hydrogen bonding with Nef play a key part in positioning the RT loop in a defined orientation to allow specificity of interaction with Nef. The extensive hydrogen bond network between HIV-1 Nef and SH3 also explains why Nef:SH3 interaction is more than 300-fold tighter compared to SH3 interaction with the isolated Nef PxxPxR peptide. Crystal structures of Nef in the bound vs. unbound states of the FYN SH3 domain further showed that the Nef polyproline motif is partially disordered when unbound and is fully folded when bound to SH3. Similarly, Nef maintains the flexible SH3 RT loop in a rigid conformation through hydrogen bonding interactions [355].

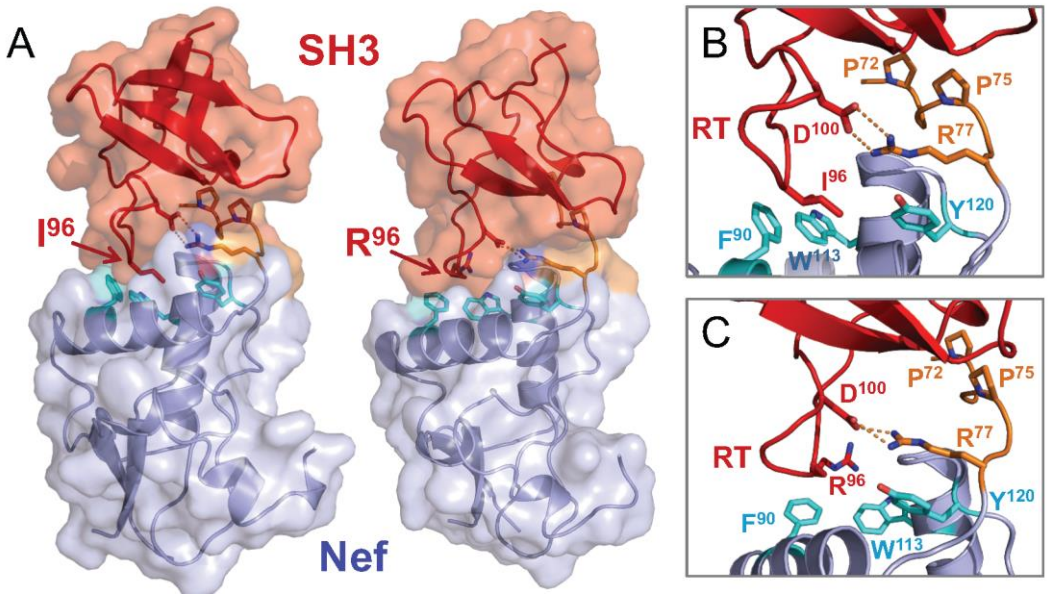

Figure 10. X-ray crystal structures of HIV-1 Nef in complex with wild-type and R96I mutant forms of the SH3 domain of Src-family kinase FYN.

A) Overall structure of the HIV-1 Nef core with the wild-type SH3 domain of FYN (right) and the high-affinity mutant, R96I (left). Both SH3 domains are shown in red, and Nef is shown in blue. The PxxPxR motif in Nef is shown in orange where it contacts Nef. Nef forms homodimers across the αB interface in both structures (not shown for clarity; see Figure 6 for dimer interface). B) Close-up view of the interactions between Nef and the FYN SH3 R96I mutant. Pro72 and Pro75 in Nef form a type II polyproline helix that contacts the SH3 domain surface and is stabilized by ionic interaction between Nef Arg77 and FYN SH3 Asp100. Ile96 in FYN SH3 mutant accesses a hydrophobic pocket on the Nef surface formed in part by residues Phe90, Trp113, and Tyr120 (cyan). C) Close-up view of the interactions between Nef and FYN SH3 wild-type. In contrast to the R96I mutant, Arg96 in wild-type FYN SH3 RT loop cannot take part in hydrophobic interaction with Nef, even though the rest of the interactions are maintained as in the R96I mutant. This figure was reproduced from Staudt *et al*. [360], and is licensed under the Creative Commons Attribution License (CC BY).

The structure of HIV-1 Nef in complex with both the SH3 and SH2 domains of HCK was later solved by Alvarado *et al*. in our group (Figure 11, top center panel) [364]. Even though the structures of the individual SH3, SH2 and Nef proteins were conserved, important differences were observed in their relative orientations along with additional contacts. For example, an additional salt bridge was observed between SH3 and Nef involving Nef residue Arg105 and SH3 residue Glu93. Mutation of Glu93 interfered with Nef binding and kinase activation in cells, indicating that this interaction is functionally relevant. Even though the Nef dimer interface in this structure still involved the αB helix, important differences were observed with respect to the orientation and

residues involved compared to earlier Nef:SH3 structures. Unlike the Nef:SH3 complex, the orientation of the Nef dimer interface seen in this structure exposes Nef Asp123 to solvent, where it may be available for interaction with the C-terminal tail of MHC-I and AP-1. Remarkably, the position of Nef Asp123 in the crystal complex with HCK SH3-SH2 is almost identical to its position in the crystal structure of Nef in complex with the MHC-I C-terminal tail and the μ1 subunit of AP-1 (Figure 11, right panels) [360]. In addition, residues in the SH2 domain make an extensive network of Van der Waals contacts with both Nef molecules. Loops connecting the β-sheets and α-helices of the SH2 domain contact residues Phe68, Pro69, Leu76, and Tyr115 in both Nef molecules. The biological implication of these Nef:SH2 contacts are not known but may stabilize this 'functionally important' Nef dimer conformation, and also may help position the PxxPxR motif for interaction with the SH3 domain.

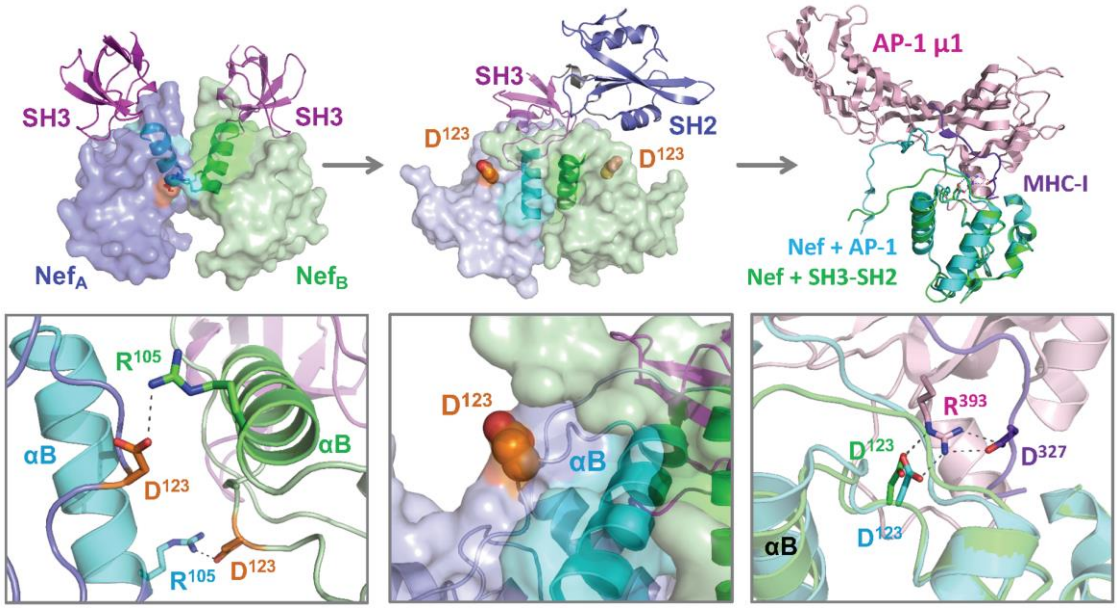

Figure 11. Interaction with HCK may induce an HIV-1 Nef conformation compatible with MHC-I/AP-1 recruitment.

Nef core in a 2:2 complex with the HCK SH3-SH2 dual domain (PDB: 4U5W). HCK SH3 (purple) and SH2 (blue) both make contacts with Nef (only one SH3-SH2 is shown for clarity). The Nef αB dimer interface is reoriented relative to the Nef-FYN SH3 R96I structure with Nef Asp123 pointing outward to the solvent instead of taking part in charge-charge interactions with Nef Arg105 (shown by orange spheres in center bottom panel in close-up view). Right) Structural alignment between one of the Nef cores in the Nef-HCK SH3-SH2 complex (green) with Nef in complex with MHC-I_{CD}/AP-1 µ1 (cyan) (Top right panel; PDB: 4EN2). MHC-I_{CD} is shown in purple and AP-1 µ1 is shown in pink. Close-up view of the alignment shows that Nef Asp123 positioning is nearly identical between the two structures (bottom right panel). Nef Asp123 forms charge-charge interaction with Arg393 in AP-1 µ1 and Asp327 in MHC-I_{CD}. Mutation of Nef Asp123 completely abolishes downregulation of MHC-I. Figure is obtained and reproduced from Staudt *et al*. [360], and is licensed under the Creative Commons Attribution License (CC BY).

Wales *et al*. performed hydrogen-deuterium exchange mass spectrometry (HDX MS) to study the conformational changes to the overall HCK structure that result from Nef interaction. Remarkably, only subtle changes in the N-lobe of the HCK kinase domain were observed upon Nef binding [491]. On the flip side, conformational rearrangement was observed in the quaternary structure of Nef as a result of HCK SH3 vs. SH3-SH2 domain interactions [492]. This subsequent HDX MS study revealed that the Nef αB helical interface is protected from deuterium exchange when in complex with the HCK SH3 or SH3-SH2 domain proteins in a manner consistent with αB-interfaced Nef dimerization revealed in the crystal structures. However, when HDX MS was

performed on the Nef Asp123 mutant, only the complexes with the HCK SH3-SH2 dual domain protein and not the SH3 domain alone resulted in protection of the dimer interface, supporting the conclusion that the different dimer arrangements observed in the crystal structures are also present in solution. Furthermore, Nef interaction with HCK may expose Nef Asp123 for recruitment of AP-1 and MHC-I for downregulation. These structural observations are consistent with biological data described above which demonstrate an essential role for HCK (and LYN) as essential components of the MHC-I downregulation pathway. Taken together, these structural studies suggest that interaction of HCK with Nef has at least two significant outcomes: 1) activation of the kinase to facilitate viral replication, and 2) stabilization of a dimeric conformation of Nef that facilitates MHC-I downregulation.

Several lines of evidence support a role for Nef:HCK interactions in HIV-1 pathogenesis. Enhanced expression of HCK in monocyte-derived macrophages was shown to correlate to high titer replication of HIV-1 [493]. Furthermore, selective expression of Nef in the T cells and macrophages of transgenic mice caused depletion of CD4+ T cells and AIDS-like pathology, whereas expression of a PxxP Nef mutant, which cannot interact with HCK, caused no such effects [329, 494]. The AIDS-like syndrome observed in Nef-transgenic mice was delayed in *HCK*-null mice, highlighting the importance of the Nef:HCK interaction to HIV-1 pathogenesis.

In addition to HCK, HIV-1 Nef has been reported to interact with several other members of the SRC kinase family. HIV-1 Nef binds to the LYN SH3 domain as tightly as to the HCK SH3 domain [354]. HIV-1 Nef interaction with FYN has been controversial, where SH3 binding was observed *in vitro* but did not lead to kinase activation [495]. Nef also interacts with the SRC SH3 domain albeit with lower avidity compared to HCK [496]. Trible *et al*. tested whether direct functional interaction takes place between HIV-1 Nef and each of the eight human SFKs using

yeast as a model expression system. Yeast do not express homologs of SFKs or other mammalian protein-tyrosine kinases, and ectopic expression of SFKs in yeast cells results in growth arrest which is reversed by co-expression of CSK. Co-expression of HIV-1 Nef strongly activated the downregulated HCK and LYN in yeast as well as SRC to some extent, but not FGR, FYN, LCK, or YES. This study clearly identified HCK and LYN, and SRC to a lesser extent, as the direct targets for Nef. A subsequent study used the same system to demonstrate that activation of these SFKs is a feature conserved across representative Nef variants from all major HIV-1 subtypes [359].

Reports also exist arguing for both activation and suppression of LCK by Nef [497, 498]. The LCK SH2 domain but not the HCK SH2 domain binds HIV-1 Nef in a phosphotyrosine-independent manner [499]. The added interaction provided by SH2 binding was sufficient to overcome the low affinity between Nef and the LCK SH3 domain. Furthermore, SIV Nef has been shown to bind both HCK and LCK SH2 domains [500]. The observations of SIV and HIV-1 Nef binding to SH2 domains of SFKs combined with the crystal contacts between Nef and SH2 domain of HCK raises the possibility that Nef may have evolved more than an SH3-displacement based mechanism to override SFKs autoinhibition. However, no other accounts of SFKs SH2 domain interactions with Nef have been reported. The inability of Nef to stimulate full-length LCK activity in the yeast system described above also argues against direct Nef-mediated activation of this T cell kinase.

1.4.2 Tec family kinases (TFKs)

Another family of NRTKs that play key roles in relaying and integrating signals produced at the cell membrane are the Tec family kinases. TFKs are responsible for transmitting signals

generated from SFKs, as well as PI3K, protein kinase C (PKC), Jak kinases, and G proteins [501]. There are five members of the TEC kinase family, namely TEC, BTK, ITK, BMX, and TXK. Study of novel protein tyrosine kinases in mouse liver led to the identification of *Tec* [502], which is also expressed in spleen, kidney and heart but at lower levels in other tissues. In less than five years, four other novel protein kinases related to TEC were identified. BTK was identified as the deficient protein in human X-linked agammaglobulinemia (XLA) [503], consistent with its essential role in B cell receptor signal transduction (more below). ITK was identified as a developmental regulator in T-lymphocyte differentiation [504]. BMX is expressed in endothelial cells and has roles in growth and differentiation of hematopoietic cells [505]. Finally, TXK was identified as the final member of the family and found to play a role in intra-thymic T cell development and mature T cell signaling [506].

Subsequent studies have shown that TEC is expressed in both T and B cells, in myeloid cells, and in liver, but its role in lymphocytes is not clearly understood. Reduced TEC expression in primary T cells led to a reduction of interleukin-2 (IL-2) production in response to T cell receptor stimulation, suggesting a role for TEC in TCR signaling [507]. Overexpression of TEC also enhances IL-2 and IL-4 promoter activity through the TCR/CD3 pathway or CD28 engagement [508]. However, *Tec* knockout mice were reported to have no defects in lymphocyte function, suggesting potential compensatory roles of other TFKs [509]. Intercrossing of *Tec* knockout mice with *Btk* knockout mice indicated that *Btk* compensates for the lack of *Tec* activity. Expression of TEC was reported to be relatively low in T and B cells compared to that of ITK and BTK, but TEC is upregulated following T-cell activation and in Th1 and Th2 cells [510]. Furthermore, overexpression of TEC, but not other TFKs, induced NFAT activation in lymphocyte cell lines. Therefore, Tec kinases may play a unique role in effector T cells.

BTK (Bruton's tyrosine kinase) is expressed in a variety of hematopoietic cells including B cells, mast cells, and macrophages, but not in T cells [503]. XLA in humans is characterized by a marked reduction in mature B cells, which established BTK's role in B cell maturation. *Btk* knockout mice develop X-linked immunodeficiency (*xid*), similar to XLA in humans [511]. BTK is also the only TFK associated directly with human disease. BTK is involved in signal transduction downstream of the B cell receptor (BCR). In addition, BTK regulates other signaling pathways in B cells, including chemokine receptor, Toll-like receptor (TLR), and F_c receptor signaling [512]. Due to its essential role in B cell maturation and several signaling pathways, BTK is an important therapeutic target in B cell malignancies. The small molecule BTK inhibitor ibrutinib is associated with high response rates in patients with relapsed/refractory chronic lymphocytic leukemia (CLL) and mantle-cell lymphoma (MCL) in which BTK is constitutively active.

ITK (IL-2 inducible T-cell kinase), also known as TSK (T-cell-specific kinase) or EMT (expressed in mast cells, myeloid cells and T lymphocytes), is expressed predominantly in T cells. ITK mRNA levels were shown to increase in response to IL-2 treatment [513]. *Itk* knockout mice had decreased numbers of mature thymocytes, and had reduced proliferative responses to allogenic MHC stimulation and to anti-TCR cross-linking, but responded normally to stimulation with IL-2 [514]. Therefore, ITK is involved in T cell development and also plays a role in TCR-mediated signaling pathways.

Bone marrow kinase on chromosome X (BMX) is expressed in hematopoietic cells of myeloid lineage like granulocytes and monocytes, as well as endocardial and endothelial cells of the heart [515, 516]. BMX has been shown to play roles in differentiation, motility, and cell survival [516-518]. *Bmx* deficient mice do not show spontaneous phenotypes, but *Bmx* has been

shown to play a crucial role in ischemia-induced arteriogenesis and angiogenesis, as well as VEGF-induced lymphangiogenesis [519-521]. BMX also regulates TLR-induced IL-6 production, a driver of chronic inflammation such as rheumatoid arthritis and Crohn's disease [522].

TXK, also referred to as RLK (resting lymphocyte kinase), is found preferentially within the T cell lineage and in the thymus as well as in resting mature peripheral T lymphocytes [506]. The role of TXK in cells is not completely characterized. Homozygous knockout of *Txk* by itself has few functional consequences, but deletion in combination with *Itk* is functionally important to Th1 cells. Compound $Txk^{-/-}Itk^{-/-}$ mice also display defects in TCR responses in mice [523]. The TCR utilizes TXK in the phosphorylation of key sites in the adaptor protein SLP-76, leading to upregulation of the Th1 preferred cytokine, IL-2 [524]. Deletion of both ITK and TXK also affects Th17 differentiation and IL-17 production [525]. ITK and TXK may also have overlap in functionality, as overexpression of *Txk* in *Itk*-null mice rescues the Th2 response [526].

As described above for the SFKs, the TFKs are also highly versatile in terms of their functions. The variation in functionality of different kinases mainly stems from differences in regulatory mechanisms since the kinase domains are highly conserved across different families. As such, TEC family kinases exhibit several distinct domains that confer variability in their functions. Next, I'll describe structural units that compose TFKs.

1.4.2.1 Structure of TFKs

The overall domain structure of the TEC family kinases resembles that of SRC family kinases, albeit with important differences. Similar to SFKs, TFKs also contain an SH3 domain, an SH2 domain, an SH2-kinase linker segment, and a kinase domain. Instead of the N-terminal unique region and SH4, TFKs contain pleckstrin homology (PH) and Tec homology (TH) domains (Figure 12). The presence of a PH domain is a characteristic unique to the TFKs among all protein-tyrosine

kinases [527]. One exception is TXK, which does not contain a consensus PH domain. PH domains are associated with membrane localization, and this function in TXK may be replaced with a cysteine-rich motif which is palmitoylated *in vivo* [528]. Another characteristic feature of TFKs is the TH domain. Within the TH domain, a BTK motif is found in the N-terminal half and a proline-rich region is found in the C-terminal half. TXK also lacks the BTK motif. However, TXK shares several functionalities with BTK and ITK *in vivo*, suggesting common ancestry and therefore membership in the TEC kinase family [523, 529].

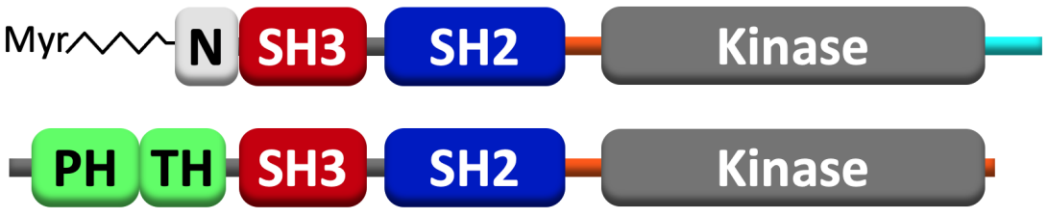

Figure 12. Domain arrangement in SFKs and TFKs.

SFKs (shown on top) and TFKs (shown on bottom) share similar domain arrangement in their structures. SFKs are myristoylated at the N-terminus, whereas PH and TH domains are present in the N-terminus of TFKs. The PH dimain targets TFKs to membrane in response to PIP_3 production.

Pleckstrin homology (PH) domain

PH domains are small signal transduction modules found in over 100 different eukaryotic proteins [530]. Although PH domains share low sequence conservation, their three-dimensional structures share a common fold and remarkable electrostatic polarization. Several structures of PH domains have been solved by X-ray crystallography, including the BTK PH domain [530-532]. Similar to other PH domains, the BTK PH domain structure is composed of a strongly bent seven-stranded antiparallel β-sheet which packs against a C-terminal α-helix. The BTK PH domain also contains a long insertion in the loop between β-strands 5 and 6 which includes a short 1.5-residue turn α-helix (α1).

PH domains show preference for binding different phosphatidylinositols in a canonical binding pocket located at the positive pole of the highly polarized PH domain [533]. BTK PH domain binds PtdIns(3,4,5)P3 and Ins(1,3,4,5)P4 with K_D values of 800 nM and 40 nM, respectively [534, 535]. Comparison of the structure of the BTK PH domain with and without Ins(1,3,4,5)P4 shows that upon ligand binding, the PH domain undergoes conformational changes, including stabilization of β1- β2 loop. Residues in the β1-β2 loop contact and stabilize the 5-phosphate. Residue Lys12 contacts both 3- and 4-phosphates with two and one hydrogen bonds, respectively. The Arg28 sidechain contacts the 3-phosphate with two hydrogen bonds. Spontaneous mutation of Arg28 to cysteine causes *xid* in mice [511], supporting a critical role of lipid interactions with this PH domain. The BTK PH domain also binds to hexakisphosphate (IP_6) in another peripheral site in addition to the IP_4 binding site [532]. The peripheral site is on the surface formed by an elongated β hairpin involving strands β3 and β4 and includes residues Lys36, Tyr40, Arg49, and Lys52. However, the peripheral site is less well defined and is present in the groove between two PHTH monomers in the crystal structure (TH domain discussed below). This interface between the two PHTH monomers is called the 'Saraste dimer' interface (first described by Saraste and co-workers) and is observed in all BTK PHTH crystal structures (Figure 13). Mutation of residues Arg49 and Lys52 abrogates IP_6 dependent BTK activation. Thus, it is suggested that transient dimerization of PH domains takes place due to IP_6 binding. Chung *et al*. later showed that BTK dimerizes in a PH domain-dependent manner at the cell surface in the presence of PIP_3, a property found to be absent in other TFKs [536].

In addition to phospholipids, PH domains also take part in protein-protein interactions. The BTK PH domain also serves as a binding site for the Gα and the βγ subunits of heterotrimeric G-proteins [537]. The BTK PH domain also associates with protein kinase C (PKC), transcription

factor TFII-I/BAP-135, and actin [538-540]. Furthermore, PH domains in TFKs are involved in autoinhibitory intramolecular interactions with the kinase domain [541, 542].

Tec homology (TH) domain

The TH domain contains a BTK motif, which packs against the PH domain, and a proline-rich region. ITK, BMX, and TXK each contain one proline-rich region (PRR), whereas BTK and TEC contain two proline-rich regions. The BTK motif includes three conserved cysteines and a histidine residue that has a globular fold [530]. The BTK motif is also known as the BTK-type zinc finger and is formed by a long loop which is held together by a zinc ion [543]. Together with the PH domain, the BTK motif forms a binding site for the GTP-bound "active" Gα subunit of heterotrimeric G-proteins. The C-terminal half of the TH domain contains the polyproline sequences. SFK SH3 domains have been shown to bind to this region of TFKs [544, 545]. Furthermore, TFKs are activated as a result of such association with SFKs [546, 547]. Lastly, proline-rich regions in TFKs are also involved in intramolecular interactions to regulate kinase activity as described below [548].

Src homology 3 (SH3) domain

TFK SH3 domains adopt a prototypical SH3 structure with two three-stranded β-sheets juxtaposed at right angles. The SH3 domains of TFKs also contain a conserved tyrosine residue (Y180 in ITK, Y223 in BTK) that undergoes autophosphorylation in the context of the full-length kinase. Mutation of this residue has no effect on kinase activity *in vitro* but does affect BTK and ITK signaling in cells [549-551]. Thus, phosphorylation of this position *in vivo* may alter SH3-mediated ligand interactions rather than directly influencing kinase activity. Tyr180 in ITK is within the aromatic proline binding surface of the SH3 domain. Phosphorylation (mimicked by Y180E mutation) of this site causes structural perturbations that lead to diminished affinity for

proline-rich ligands, and increased affinity for non-canonical ligands [549]. Phosphorylation of Tyr223 in BTK is also shown to alter its ligand preferences [552]. Therefore, phosphorylation of TFK SH3 domains plays a role in determining ligand-specificity for interactions.

Interactions have also been noted between TFK SH3 domains and the proline-rich region (PRR) in the TH domain. Such an association exists exclusively intramolecularly in ITK, whereas only intermolecularly in TXK [553]. Detailed NMR and biophysical studies showed that a complex equilibrium exists between intra- and inter-molecular associations in TFK SH3 domains [554, 555]. Determination of intramolecular association constants revealed that TXK is the only member in which an intramolecular association is unfavored, mainly due to the short 10-residue linker between the PRR and the SH3 domain of TXK. ITK, on the other hand contains a 15-residue linker between the PRR and the SH3 domain and only takes part in intramolecular PRR-SH3 association. Furthermore, the TEC SH3 domain can bind its PRR intra- or inter-molecularly, and the inter-molecular association leading to dimerization is favored [555]. This suggests that an intricate set of coupled monomer-dimer equilibria may alter quaternary structure to regulate TFK activity.

Src homology 2 (SH2) domain

Structures of the BTK and ITK SH2 domains have been solved in isolation, but their functional roles are still being determined [556-558]. An NMR-based structure of the ITK SH2 domain showed that a conformationally heterogeneous Pro residue mediates different functional states of the SH2 domain [558]. The Asn286-Pro287 imide bond can undergo *cis-trans* isomerization and the corresponding SH2 conformers are called the *cis* and *trans* conformers respectively. Both the *cis* and *trans* conformers of the ITK SH2 adopt the typical SH2 domain fold. The most prominent difference arises in the positioning of the CD loop, where the bend at Pro287

and the corresponding cross-strand residue Lys280 rotates the CD loop by about 60°. The *cis* conformer generates a conformation which is chemically similar to polyproline motifs that bind the SH3 domain. ITK SH2 residues Thr279, Ala281, Ile282, Cys288, Val330, Thr331, and Arg332 undergo large chemical shift changes upon addition of the SH3 domain. About 65% of the SH2 species in solution adopt a *trans* conformation, and 35% adopt the *cis* conformation of Asn286-Pro287 imide bond. Functional studies of *cis-trans* isomerization of this Pro residue revealed that it serves as an important regulatory switch to determine intra- or inter-molecular assembly and ligand associations [559-562]. As discussed earlier, ITK only forms intra-molecular association between the SH3 domain and the proline-rich motif. However, the *cis* SH2 conformer tightly binds SH3 from another molecule, allowing ITK to form intermolecular associations as well. Because of intermolecular SH3 and SH2 association, the binding site in the SH3 domain is also masked, which prevents the SH3 domain from making contacts with exogenous ligands. These points are highly relevant to my own work on the mechanism of Nef-mediated activation of TFKs. As described in Chapter 2, my work supports a model in which Nef homodimers stabilize this type of SH3-SH2-mediated interaction as a unique mode of BTK activation.

On the other hand, an X-ray crystal structure of the ITK SH2 domain showed domain-swapped dimers [557]. The EF loop and F strand of each SH2 monomer adopts an extended conformation that results in a detached C-terminal B helix. The typical SH2 fold of each monomer is reconstituted by the B-helix of the other monomer. The dimer interface consists of extensive hydrophobic contacts throughout the domain. The *cis-trans* state of Asn286-Pro287 could not be resolved in this structure, leaving open the question of functional relevance of the domain swapped dimer of ITK SH2 domain. The domain-swapped structure is sterically incompatible with the ITK SH2-SH3 structure when overlaid [562]. The SH3-binding site on the SH2 domain includes the

CD, BG, and EF loops, whereas the CD and BG loops are completely occluded in the domain-swapped dimer. However, analysis of purified ITK SH2 that crystallized as a domain swapped dimer revealed only the monomeric state in solution [557]. Therefore, the domain-swapped dimer may represent a partially unfolded state that emerges solely during the crystallization process.

The global fold of the BTK SH2 domain resembles that of ITK SH2 domain, with some localized differences [556]. The *cis-trans* isomerization of the prolyl imide bond in the CD loop of ITK SH2 is not observed in the structure of BTK SH2. Only the *trans* conformer was detected in solution. Furthermore, another crystal structure containing the SH3-SH2-kinase fragment of BTK showed an SH2 domain-swapped dimer state [532]. This SH2 domain swapping is distinct from the ITK SH2 domain swapped dimer and closely resembles the Grb2 SH2 domain swapped dimer [563]. This dimeric state was observed in solution as well, since the protein was purified as a dimer and a monomer, and only the dimer crystallized. However, lack of functional correlates of BTK multimerization suggests that this may represent another partially unfolded state that is stabilized by crystal formation.

Kinase domain

TEC-family kinase domains share a similar conserved architecture with the SFKs [564], with their N-terminal lobes consisting of five β-strands and one helix – the C-helix. The C-terminal lobe consists of multiple α-helices, and the ATP binding site is located between the two lobes as described above for SFKs. The activation loop, containing autophosphorylation sites at Tyr511 and Tyr551 in ITK and BTK respectively, tugs between the two lobes. Activation is triggered by phosphorylation of these residues, and the resulting conformational changes create a substrate docking site in the activation loop. The C-helix also rotates inward during activation leading to a salt bridge between Glu445 in the C-helix and Lys430 in BTK. The crystal structure of the inactive

kinase domain of BTK showed that the activation loop adopts an extended conformation that does not block the active site, and closely resembles the active LCK structure described above [565]. However, Glu445 and Lys430 are separated by about 10Å, and Glu445 forms a hydrogen bond with Arg544 instead. This hydrogen bond is proposed to function as a general mechanism for TFK regulation. Structures of ITK kinase domains in the phosphorylated and unphosphorylated states show similar configurations [566].

1.4.2.2 Regulation of TFKs activity

Crystal structure of near-full length (SH3-SH2-kinase) fragment of SFKs is solved, but full-length TFKs have so far resisted crystallization efforts. *In vitro* experiments and crystallization of fragments have enabled models of TFK autoinhibition [532, 567]. Crystal structures of an SH3-SH2-kinase fragment of mouse *Btk* (spanning residues 214 to 659) lacking the PHTH domain, along with an artificial PHTH-kinase construct lacking the SH3 and SH2 domains of bovine BTK were separately crystallized. Together, these structures provide important clues to overall TFK regulation.

In the BTK SH3-SH2-kinase crystal structure, the SH3 domain fold is identical to those determined previously for the isolated domain by NMR [568]. The SH2 domain forms a domain-swapped dimer as discussed earlier. In a manner consistent with previous observations in SRC, HCK, and ABL, the BTK SH3 domain binds to a PPII helix adopted by residues 383-387 in the SH2-kinase linker segment. This observation suggests a similar role for SH3:linker interaction in the autoinhibition of TFKs as observed for these other NRTKs. The SH3 domain also makes contacts with the back of the N-lobe of the kinase domain, and the SH2 domain makes contacts with the back of the C-lobe of the kinase domain. Alignment of the kinase domain C-lobe structures from autoinhibited ABL and BTK showed relative differences in SH3 domain

orientation of about 20° and SH2 domain orientation of about 15°. Therefore, even though SH3:polyproline-linker interaction is a shared mechanism of autoinhibition, coupling between the SH2 and SH3 domains may be different in BTK and other kinases.

The same study reported a crystal structure of bovine BTK containing the PHTH domain artificially connected directly to the kinase domain by a 13-residue segment that normally links the SH2 and kinase domains. In this structure, the PHTH domain directly contacts the N-lobe of the kinase domain. In particular, Tyr134 in the PHTH α2 helix packs into a pocket between Trp395 at the linker-kinase junction and the C-helix in the kinase domain N-lobe. This interaction was suggested to stabilize the autoinhibited state of BTK by hindering the inward swing of the C-helix accompanying kinase activation. Interestingly, both the canonical and peripheral lipid binding sites in the PHTH domain are oriented away from the kinase interacting α2 helix interface.

Computational combination of the two structures allowed for an overall model of the autoinhibited BTK structure. Overlap was detected between the PHTH domain and SH3 domain loops. The structure was relaxed by performing MD simulation to avoid clashes. Inhibitory interactions between each of the regulatory domains and the kinase domain were tested by making mutations and measuring kinase activity. This autoinhibited full-length BTK model was subsequently tested by solution NMR by Joseph *et al*. [567]. Analysis of the isolated SH3 and SH2 domains and the same domains in full-length BTK showed that the PPII-binding surface of the SH3 and phosphotyrosine-binding pocket in SH2 are sequestered on the back of the kinase domain in the autoinhibited state. Furthermore, even though TFKs lack a C-terminal phosphotyrosine, a similar inhibitory mechanism is provided by Asp656 salt bridge formation with Arg307 in the binding pocket of the SH2 domain, which is conserved in all TFKs. Mutation of Asp656 was shown to promote activity of BTK in a manner similar to mutation of the PPII helix.

Furthermore, the proline-rich region in BTK also directly regulates BTK activity. Mutation of the proline residues in the PRR sequence to alanine decreased the rate of BTK autophosphorylation, suggesting a positive role ('on' switch) of the PRR in regulating the activity of TFKs. One possibility is that the PRR sequesters the SH3 domain away from its negative regulatory position on the back of the kinase domain.

The crystal structure of the BTK PHTH-kinase module showed that the PHTH makes autoinhibitory contacts in the N-lobe of the kinase domain. In the autoinhibited model, a binding site for PIP_3 is exposed on the surface. However, solution NMR studies indicated that PIP_3 binding disrupts autoinhibitory contacts in BTK and leads to large scale allosteric changes to fully expose the open configuration of BTK [567]. This closely matches the linear arrangement of open BTK observed in a low-resolution small-angle X-ray scattering (SAXS) study [569]. Together, these findings suggest that contacts between the PHTH and kinase domains serve as a unique regulatory mechanism for the TFKs.

Interaction between the kinase domain and the PHTH domain have been observed for ITK as well [542]. Devkota *et al*. showed an interplay between PIP_3 production at the cell membrane and ITK PH domain-mediated autoinhibition. A cluster of residues adjacent to the PIP_3 binding pocket were shown to directly bind the kinase domain. In the absence of a PIP_3 signal at the cell surface, the lipid-binding interface of PHTH turns its autoinhibitory face towards the kinase domain. In doing so, it blocks the activation loop tyrosine from acquiring an activating phosphorylation. Amatya *et al*. later utilized a combination of HX MS, NMR and sequence alignments to suggest that the PHTH domain causes dynamical allosteric perturbations around the C-lobe activation loop, the active site, and the distal face of the N-lobe of the kinase domain [541]. Taken together with the structural model that positions the PHTH domain next to the N-lobe of

the kinase domain in autoinhibited BTK, these observations suggest that BTK may assume multiple autoinhibitory conformations through multiple intramolecular interactions. Such interactions may have evolved specifically in each kinase to serve unique functions in substrate recognition. Similar autoinhibitory contacts between regulatory domains and the kinase domain that mask the activation loop are also observed in protein kinase C, AKT, and PTK2 [570-572].

In addition to PIP_3 mediated displacement of PHTH, another layer of self-regulation of TFKs activity may involve multimerization. As discussed earlier, a variety of multimeric forms of the TFKs including ITK and BTK have been observed. Shah *et al*. suggest the possibility of a monomeric form of autoinhibited BTK, as well as a dimeric form, which might be promoted at the membrane before activation [573]. However, while higher order associations are observed in truncated regulatory domains, no such interactions have been reported for full-length kinases. That may be because: 1) higher order associations of full-length kinases are not sterically/functionally relevant, or 2) higher order associations involving full-length kinases are too transient to detect and stably isolate.

Structural and biophysical studies suggest the latter case to be true. Crystal structures of the BTK PHTH domain reveal formation of a 'Saraste dimer' even though such a dimer could not be detected in solution (Figure 13). Mutations in this dimer interface are known to cause XLA, however, and thus this dimer is hypothesized to play a role in the activation of BTK. Biophysical studies showed that BTK undergoes PHTH domain-mediated dimerization in reconstituted membranes and subsequent activation by *trans*-phosphorylation [536]. BTK dimerization is achieved in a switch-like manner dependent on the PIP_3 concentration. Furthermore, PIP_3 binding at both peripheral and canonical sites is required for dimerization. Unlike BTK, ITK and TEC were not found to dimerize on the membrane. This shows that TEC family members may have evolved

independently to regulate their kinase activity through higher order self-assemblies. The extent and importance of self-association of TFKs and the implications for their regulation and function is a very important question that remains to be fully understood.

A final note regards the activation loop sequence and its influence on TFK specific activity. Recombinant purified BTK has higher specific activity than ITK, and replacement of the ITK activation loop sequence with that of BTK increased ITK activity [574]. One interpretation of this result is that BTK may be better able to self-associate and auto-activate by *trans*-phosphorylation, whereas ITK may be more reliant on LCK-mediated phosphorylation of its activation loop as observed in the TCR signaling pathway.

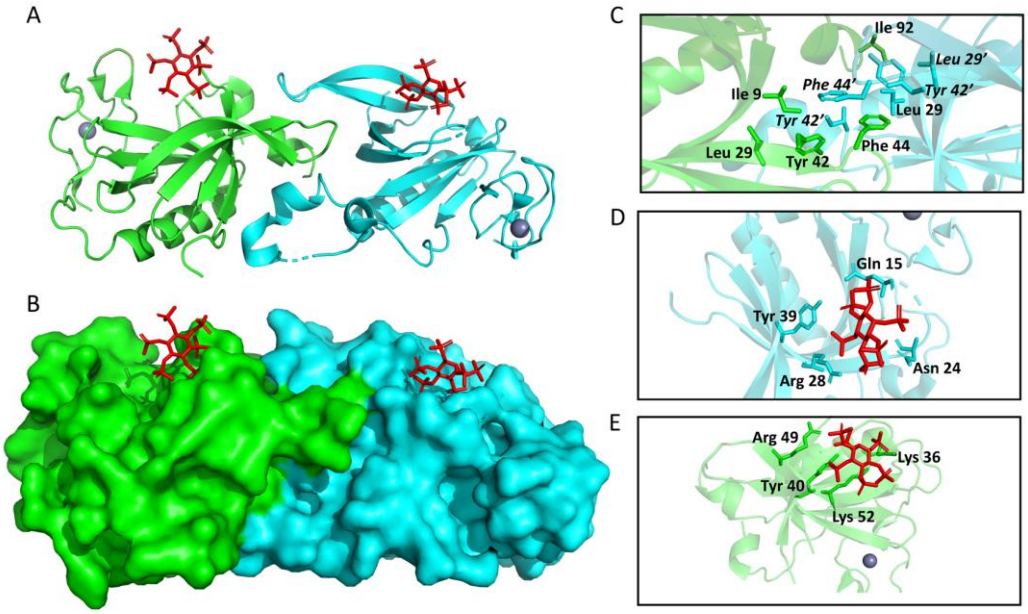

Figure 13. X-ray crystal structure of BTK PHTH domain bound to IP_6.

Cartoon (A) and surface (B) representations of structure of BTK PHTH domain bound to two IP_6 molecules (PDB: 4Y94). The two PHTH domains that form the homodimer are shown in green and cyan. IP_6 bound to each monomer is shown in red. The Zn^{2+} ion bound each domain is shown as blue dot. C) Close-up view of the dimer interface. Residues that mediate dimerization are shown as sticks and labeled. Residues from the second PHTH monomer are labeled in italics and indicated by a single quotation mark '′'. D) Close-up view of IP_6 (red) bound to the canonical lipid binding site. E) Close-up view of IP_6 (red) bound to the peripheral lipid binding site. These models were produced in PyMol using the crystal coordinates of the bovine BTK PHTH domain bound to IP_6.

1.4.2.3 Role of ITK and BTK in HIV-1 infected cells

T cell signaling is initiated upon interactions between T-cell receptors (TCRs) and MHC complexes on antigen-presenting cells. Such interaction leads to co-receptor (CD4/CD8)-associated LCK activation [575]. LCK then phosphorylates conserved tyrosines in the immunoreceptor tyrosine-based activation motifs (ITAMs) of the TCR CD3 and ζ chains. Phosphorylation of ITAMs leads to binding of SYK family kinase ZAP-70 through its tandem SH2 domains, which is further activated by LCK phosphorylation. Activation of LCK and ZAP-70 leads to phosphorylation of the Linker for Activation of T cells (LAT) [576], which in turn activates PI3K. Production of PIP_3 at the cell membrane by PI3K then recruits ITK and its substrate phospholipase Cγ1 (PLCγ1) through their PH domains. Activation of ITK, which is mediated by LCK in *trans*, leads to phosphorylation and activation of PLCγ1, which in turn generates the second messengers, inositol 1,4,5-triphosphate (IP_3) and diacylglycerol (DAG).

Similar regulatory mechanisms also exists in B cells during B-cell receptor (BCR) signaling. Antigen binding to the BCR triggers activation of LYN, SYK, and BTK [577]. In B cells, the Src-family member LYN phosphorylates the ITAMs within the Ig-α/β chains associated with the BCR as well as CD19. Phosphorylated ITAMs activate SYK, which then phosphorylates the B-cell adaptor protein for PI3K (BCAP). Phosphorylation of BCAP and CD19 then activates PI3K, which leads to PIP_3 production, PH domain-mediated recruitment and activation of BTK and its substrate PLCγ2. Activation of PLCγ2 generates the second messengers IP_3 and DAG [578].

The second messengers IP_3 and DAG raise intracellular calcium levels and activate protein kinase C (PKC) isozymes and the Erk and Jnk MAPK pathways. These kinases ultimately stimulate upregulation of genes essential to T- and B-cell maturation and proliferation by

activating or promoting nuclear translocation of key transcription factors including nuclear factor-κB (NFκB) and nuclear factor of activated T cells (NFAT) [579].

Interestingly, NFκB and NFAT are also required for transcription from the LTRs of integrated primate lentiviruses, including HIV-1. This observation suggests that lentiviruses may have evolved to hijack this pathway to promote transcription of genes essential for the viral life cycle. Along these lines, Readinger *et al*. provided evidence that ITK activity is required for efficient HIV transcription and replication [580]. Suppression of ITK function using ITK-specific siRNA, an ITK inhibitor, and expression of kinase-inactive ITK all blocked multiple steps in the HIV replication cycle, although the exact mechanism and the viral protein required for ITK modulation was not reported. BTK has also been implicated in HIV-1 replication in cells of myeloid origin [581]. HIV-1 Nef, which is packaged in the virus and is one of the earliest HIV proteins to be produced, also contributes to HIV-1 transcription through the NFκB pathway [414].

Given the established relationship between HIV-1 Nef and kinase signaling, these observations suggested that HIV-1 may enhance TCR signaling for its own benefit by stimulation of Tec family kinases. The first evidence for a direct connection between Nef and Tec family kinases was provided by Tarafdar *et al*. This study used a cell-based BiFC assay to investigate whether HIV-1 Nef interacts with individual members of the Tec kinase family [582]. This approach revealed that Nef interacted with BMX, BTK, and ITK, but not TEC or TXK. Furthermore, a selective small molecule inhibitor of ITK (BMS-509744) potently blocked wild-type HIV-1 infectivity and replication, but not that of a Nef-defective mutant, suggesting Nef-induced ITK activation is required for the viral life cycle. Our recent work has shown that Nef directly activates ITK and BTK at the plasma membrane, and that activation of both kinases requires Nef homodimers. Importantly, HIV-1 mutants with dimerization-defective Nef replicated

poorly in T cell lines and donor PBMCs, and failed to activate endogenous ITK. These studies support an essential role for Nef as the molecular bridge between HIV-1 and host cell TFK activation. Nef-mediated short-circuiting of this pathway in HIV-infected cells [365] is likely to boost viral gene expression through the NFAT and NFkB pathways as illustrated in Figure 14. A primary goal of my thesis research, therefore, was to determine the molecular mechanism by which Nef induces TFK activation to enhance the viral life cycle.

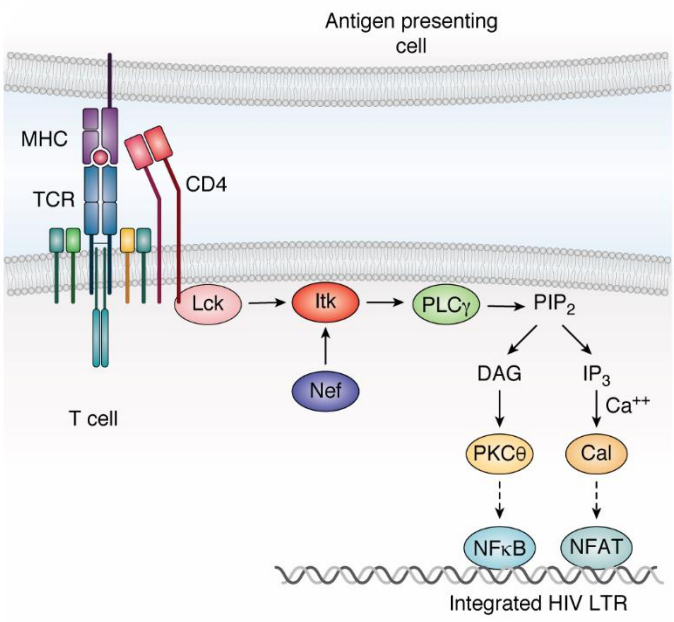

Figure 14. Nef-mediated ITK activation short-circuits TCR signaling to enhance HIV-1 transcription in T cells.

In this simplified scheme, the T-cell receptor (*TCR*) is activated by specific MHC•antigen complexes, which induces activation of the T cell-specific Src-family kinase Lck. Active Lck phosphorylates the ITK activation loop, which in turn phosphorylates phospholipase Cγ (*PLCγ*). Active PLCγ generates diacylglycerol (*DAG*) and inositol triphosphate (IP_3) from membrane phosphatidylinositol 4,5-bisphosphate (PIP_2), leading to activation of protein kinase C isozymes and calcineurin (*Cal*), respectively. Protein kinase Cθ promotes activation of NF-κB via the CARMA1/BCL10/MALT1 complex (*not shown*), whereas calcineurin dephosphorylates NFAT to induce nuclear localization. NF-κB and NFAT both induce transcription of the HIV-1 provirus via its LTR. This Figure was reproduced from Li *et al*. [365], and is licensed under the Creative Commons Attribution License (CC BY).

1.5 Hypotheses and Specific Aims

Previous studies, outlined above, demonstrate that HIV-1 Nef interacts with specific members of the SRC and TEC kinase families in HIV-1 target cells, leading to constitutive kinase activation that supports the viral life cycle. While the structural and mechanistic basis of SRC-family kinase activation by Nef is well known, the mechanisms behind TEC-family kinase activation by this HIV-1 accessory factor is less clear. Previous studies have shown that Nef recruits ITK and BTK to the plasma membrane in cell-based assays, leading to their autophosphorylation. However, the question of whether interaction with Nef is sufficient for kinase activation has not been explored, nor has the requirement for the Nef SH3-binding motif essential for SRC-family activation been addressed in the context of TEC-family kinases. Because of the importance of Nef-mediated ITK and BTK activation to the HIV-1 life cycle, this thesis project explored the mechanisms behind TEC-family kinase activation by Nef using complementary biochemical and cell-based approaches. These studies tested the following hypothesis with these Specific Aims:

1.5.1 Hypothesis 1

Previous studies have shown that HIV-1 Nef selectively binds the SH3 domains of the SFKs HCK and LYN *in vitro* and induces constitutive kinase activation in HIV target cells. This interaction is dependent on high affinity interactions involving the PxxPxR motif in Nef as well as the RT loop in HCK SH3 domain. Unlike HIV-1 Nef, SIV Nef does not bind or activate HCK since the amino acids required for hydrophobic interactions with HCK SH3 are not present in SIV Nef [583]. Besides SFKs, HIV-1 Nef also interacts with select members of the TEC kinase family in HIV target cells [582]. Mutation of the HIV-1 Nef PxxPxR motif required for HCK engagement

only partially reduced interaction with BTK and ITK in cells, suggesting the possibility of alternative modes of Nef recruitment. Recent studies have shown that both HIV-1 and SIV Nef retain the ability to bind and activate BTK and ITK at the cell membrane [365]. Therefore, *I hypothesized that HIV-1 Nef activates TEC-family kinases through direct interaction via a mechanism distinct from Nef-mediated SRC-family kinase activation*. To address this hypothesis, I used a series of continuous kinase assays, purified recombinant individual and tandem BTK regulatory domains, and performed quantitative binding experiments to explore the following experimental aims.

1.5.2 Specific Aims for Hypothesis 1

1.5.2.1 Aim 1: Develop an *in vitro* kinase assay for TEC family kinase activity and determine the kinetics of HCK- and BTK-mediated phosphorylation in presence and absence of Nef.

In this Aim, I measured the enzymatic steady state and autophosphorylation rates of HCK and BTK in a continuous kinase assay. First I validated this assay using HCK, whose interaction with HIV-1 Nef is well characterized. Using this approach, I found that while HIV-1 Nef rapidly accelerated autophosphorylation and kinase activity of HCK, SIV Nef had no effect. In contrast, I found that both HIV-1 and SIV Nef not only robustly accelerated BTK autophosphorylation, but also enhanced the steady state rate of BTK substrate phosphorylation. In order to directly test whether the PxxPxR motif in Nef plays a part in BTK activation, I measured the enzymatic rates of HCK and BTK in the presence of wild-type and mutant (2PA) Nef harboring alanines in place of the conserved prolines in the PxxPxR motif. I found that the Nef-2PA mutant failed to activate HCK, which is consistent with previous observations. However, the Nef-2PA mutant stimulated

BTK steady state and autophosphorylation rates to the same extent as wild-type Nef, suggesting that the Nef-mediated mechanism of activation is distinct for HCK and BTK. Allelic variants of Nef representative of all major HIV-1 clades also activated BTK, suggesting the mechanism of BTK activation is a conserved property among primate lentiviruses.

1.5.2.2 Aim 2: Identify the structural domains of BTK responsible for Nef interaction and investigate the mechanism of interaction.

Interaction between the HCK SH3 domain and HIV-1 Nef has been observed in solution by analytical size-exclusion chromatography (SEC) to form a 2:2 complex with HIV-1 Nef [364, 492], with Nef forming the dimer interface. To test whether HIV-1 Nef interacts similarly with the BTK SH3 domain, I first performed analytical SEC experiments to detect stable complex formation. I mixed either HCK SH3 or BTK SH3 with Nef in equimolar ratios, and injected them onto an analytical SEC column. HCK SH3 formed a stable complex with HIV-1 Nef, but BTK SH3 showed no evidence of complex formation. The individual PH and SH2 domains of BTK also did not yield a stable complex with Nef. Interestingly, the BTK SH3-SH2 dual domain did form a stable complex with HIV-1 Nef, provided that both proteins are in the dimeric state prior to mixing, suggesting a novel mechanism of Nef-mediated kinase association. To further validate this observation, I measured real time binding kinetics using surface plasmon resonance. HCK SH3 and BTK SH3 were immobilized on SPR biosensor chip at equal density, and HIV-1 Nef was injected at various concentrations. The HCK SH3 domain bound Nef with submicromolar affinity as expected, whereas the BTK SH3 showed no evidence of Nef interaction. In contrast, the immobilized BTK SH3-SH2 dual domain protein bound the HIV-1 Nef dimer with low micromolar affinity, while the HIV-1 Nef monomer bound to a lesser extent and with 5-fold lower affinity. On the other hand, the individual BTK SH3 and SH2 domains showed no interaction with

Nef either as dimer or monomer. These results suggest that Nef-mediated BTK activation involves 2:2 complex formation between homodimers of HIV-1 Nef and BTK SH3-SH2 dual domain.

1.5.2.3 Aim 3: Determine whether Nef dimerization is required for BTK activation *in vitro* as previously observed in cells.

To determine the impact of Nef dimer interface mutations on BTK activation, I used the enzymatic assay developed in Aim 1 to measure steady state BTK activity towards a peptide substrate and the rate of BTK autophosphorylation in the presence of Nef wild-type and three dimer interface mutants (L112D, Y115D, F121A). All dimerization-defective mutations diminished the level of BTK activation compared to the wild-type Nef. This observation is in accordance with the analytical SEC observation of 2:2 complex formation, and suggests that homodimerization of HIV-1 Nef through the αB helical interface is required for BTK recruitment and activation. In summary, these studies support a mechanism in which HIV-1 Nef forms a 2:2 dimer complex with the BTK SH3-SH2 domain leading to activation by trans-phosphorylation. While the mechanism of BTK recognition by Nef is distinct from that of HCK, activation of both kinases requires the Nef homodimer.

1.5.3 Hypothesis 2

B cell receptor (BCR) signaling is a tightly regulated cascade, where BTK is activated upon PIP_3 production at the membrane by activated PI3-K after a sequence of events triggered by antigen presentation. PIP_3-mediated recruitment and dimerization of BTK PH domains at the membrane is a required step for BTK activation during BCR signaling. Our previous work has shown that HIV-1 Nef recruits BTK to the cell surface to induce constitutive kinase activation.

Nef-mediated recruitment bypasses the need for complex signaling involving PIP_3 production, and directly drives BTK to the membrane for subsequent Nef-dependent activation [365]. Furthermore, dimerization-defective Nef mutants failed to induce BTK activation suggesting a mechanism where two BTK molecules may be recruited by the Nef dimer to promote activation by trans-autophosphorylation mechanism. BTK has also been shown to form natural dimers through multiple mechanisms, as described in sections 1.4.2.1 and 1.4.2.2. Based on our earlier observation (Aim 1) that Nef dimers are required to form a stable complex with BTK SH3-SH2, it is appealing to consider the possibility that unique SH3-SH2-mediated dimerization represents a natural mechanism of BTK activation. Therefore, *I hypothesized that HIV-1 Nef exploits a natural mechanism of BTK dimerization to induce constitutive kinase activation in the absence of a lipid bilayer and* PIP_3. To address this hypothesis, I utilized complementary cell-based and biochemical studies to investigate the significance of BTK SH3-SH2 dimerization to Nef-mediated interaction and kinase activation.

1.5.4 Specific Aims for Hypothesis 2

1.5.4.1 Aim 1: Determine whether the BTK SH3-SH2 region forms homodimers through a mechanism previously reported for ITK involving a unique SH3•SH2 interface.

Even though the crystal structures of individual BTK domains have been solved, tandem domains consisting of multiple domains have resisted crystallization efforts. Apart from the murine BTK SH3-SH2-kinase fragment, which crystallized as an SH2 domain-swapped dimer, these structures have not revealed the intricacies of the regulatory domain interfaces. This may be because BTK exists as an ensemble of conformations mediated by constantly changing intra- and inter-molecular interactions. In the absence of a crystal structure of BTK SH3-SH2 module, we

turned to the crystal structure of ITK SH3•SH2, which shows an inter-molecular interaction between the SH3 and SH2 domains mediated by SH2 CD loop Pro287 *cis/trans* isomerization as described in section 1.4.2.1. In this aim, I substituted an analogous proline in the BTK SH2 CD loop (Pro327) with alanine to determine whether BTK SH3-SH2 adopts a similar dimer conformation as the ITK SH3•SH2 mediated by the SH2 CD loop and the SH3 domain. First, I showed that the SH2 P327A mutation reduces the stability of the BTK SH3-SH2 homodimer at room temperature. To validate this observation further, I performed a cell-based BiFC experiment, which showed that the P327A mutation in the BTK SH2 CD loop significantly reduced the level of full-length BTK dimerization compared to wild-type BTK. Next, I investigated whether dimerization mediated by SH3-SH2 represents an activating mechanism for BTK. Using the *in vitro* kinase assay, I found that the BTK P327A mutant exhibited lower specific activity compared to BTK wild type. A similar observation was also made using the BiFC assay, where the BTK P327A mutant exhibited less autophosphorylation compared to wild-type BTK at the membrane. These observations support the idea that dimerization involving the SH3-SH2 interface represents a functional activation mechanism for BTK.

1.5.4.2 Aim 2: Investigate the role of BTK SH3-SH2-mediated dimerization in Nef interaction and kinase activation *in vitro* and in cell-based assays.

In this Aim, I measured the effect of Nef association on the stability of the BTK SH3-SH2 dimer in solution at room temperature. Incubation with the HIV-1 Nef dimer stabilized the BTK SH3-SH2 dimer and slowed the rate of dimer to monomer transition, suggesting a role for HIV-1 Nef in promoting the BTK dimer population and allowing sustained kinase activity through dimer stabilization. In order to investigate whether the dimeric state corresponded to the active state of BTK, I performed *in vitro* kinase assays to measure steady state substrate phosphorylation as well

as the autophosphorylation rates of BTK wild-type and the dimerization-defective P327A mutant in the presence and absence of HIV-1 Nef. I observed that HIV-1 Nef robustly increased the steady state rate of BTK wild-type activity and the rate of autophosphorylation, whereas Nef had no effect on the BTK P327A mutant. To validate this observation further, I performed a cell-based BiFC experiment to determine the effect of Nef on BTK homodimer formation at the membrane. HIV-1 Nef significantly increased recruitment and dimerization of BTK at the membrane. In contrast, the BTK P327A mutant showed no change in dimerization levels in absence or presence of Nef. Lastly, I also observed that interaction of wild-type BTK with HIV-1 Nef in the membrane correlated with kinase activation, as reported in our earlier study [365]. However, the BTK P327A mutant showed significantly less Nef association at the membrane and no change in activation state. These results together suggest that HIV-1 Nef selectively interacts with and stabilizes BTK dimers at the cell membrane, leading to sustained kinase activation in the absence of PIP_3 signaling.

1.5.4.3 Aim 3: Determine the X-ray crystal structure of HIV-1 Nef in complex with the BTK SH3-SH2 dual domain protein.

In this Aim, I attempted to crystallize the BTK SH3-SH2 dual domain alone and in a 2:2 complex with HIV-1 Nef. Since crystal structures of full-length HIV-1 Nef have not been reported, I also produced complexes of the HIV-1 Nef core region (lacking the N-terminal anchor domain) and BTK SH3-SH2 for crystallization experiments. Conditions tested for crystallization of BTK SH3-SH2 and HIV-1 Nef core complex are described in section 3.2, and unfortunately none of these conditions resulted in crystal formation. From earlier experiments, I found that the BTK SH3-SH2 dimer, which is required for complex formation with the Nef dimer, rapidly dissociates into monomers which do not form stable complexes with Nef. Therefore, to add stability to the

BTK SH3-SH2 dimer, I made the BTK SH3-SH2 proteins fused separately at either the N- or C-termini to the well-characterized yeast GCN4 leucine zipper separated by a flexible linker. This leucine zipper motif readily dimerizes as a parallel coiled-coil domain predicted to stabilize the interaction between the fused SH3-SH2 dimer partners. While fusion to these GCN4 leucine zippers added stability to SH3-SH2 dimer, the fused protein could not be sufficiently concentrated for crystallization screening. Therefore, I made another construct with BTK SH3-SH2 fused to a GST tag at its N-terminus separated by a flexible linker. The GST-tagged BTK SH3-SH2 also formed a dimer as well as higher order oligomers. Analysis of the dimer fraction revealed that the GST-tagged BTK SH3-SH2 protein is stable in solution as a dimer at room temperature. However, the complex of the HIV-1 Nef core with the GST-tagged BTK SH3-SH2 dimer also did not yield crystals under the conditions described in section 3.2.3.

2.0 HIV-1 Nef Activates the Tec-Family Kinase BTK by Stabilizing Intermolecular SH3-SH2 Domain Interaction

2.1 Chapter 2 Summary

The Nef proteins encoded by HIV-1 and SIV are critical for efficient viral replication and AIDS progression. In addition to downregulating cell-surface immune and viral receptors, Nef induces constitutive activation of host cell tyrosine kinases of the Src and Tec families. Nef-mediated activation of ITK and BTK enhances the viral life cycle in CD4 T cells and macrophages, respectively. ITK and BTK share a similar domain organization consisting of PH, SH3, SH2 and kinase domains. Both HIV-1 and SIV Nef strongly enhanced recombinant full-length BTK autophosphorylation and steady-state kinase activity *in vitro*, demonstrating that interaction with Nef is sufficient to induce kinase activation. Surprisingly, a mutant of Nef lacking the conserved motif required for SH3 domain binding (PxxPxR) activated BTK to the same extent as wild-type Nef. This mutant failed to activate the Src-family kinase HCK, demonstrating that Nef activates Tec and Src family kinases by distinct mechanisms. Size-exclusion chromatography coupled to multi-angle light scattering analysis of recombinant BTK PH, SH3, and SH2 domain proteins as well as an SH3-SH2 tandem domain protein revealed that the BTK SH3-SH2 region naturally forms a dimer mediated by the SH2 domain CD loop. The dimeric BTK SH3-SH2 protein was stabilized in the presence of Nef homodimers, while alanine substitution of Pro327 in the SH2 domain CD loop completely abolished SH3-SH2 dimerization and interaction with Nef. Introduction of the SH2 P327A mutation into full-length BTK resulted in complete loss of activation by Nef, supporting a mechanism in which Nef interaction stabilizes BTK dimers via the

SH3-SH2 interface to promote kinase activity. Bimolecular fluorescence complementation assays showed that Nef stabilizes wild-type but not P327A BTK homodimerization at the membrane in cells, providing support for this mechanism *in vivo*. These data reveal a unique mechanism of BTK kinase regulation independent of the PH domain and show that the Nef protein of HIV-1 has evolved two independent mechanisms to interact with and activate non-receptor tyrosine kinases important to the viral life cycle.

2.2 Introduction

Despite the significant progress in HIV treatment and prevention by combination antiretroviral therapy (ART) and pre-exposure prophylaxis, many challenges persist in the path to a cure for AIDS through complete elimination of latent viral reservoirs [584]. Chronic antiretroviral therapy itself poses risks, including metabolic disturbances, organ damage, and the potential for emergence of drug resistance [585]. To overcome these shortcomings, strategies employing enhanced methods for the detection of infected cells and clearance of the latent viral reservoir are urgently needed.

While most existing ART drugs target viral enzymes including reverse transcriptase (RT), protease and integrase, HIV-1 also encodes four accessory factors (Vpr, Vpu, Vif, and Nef) that promote the viral life cycle and progression to AIDS [586]. The HIV-1 Nef protein represents a promising alternative target for antiretroviral drug development because of its diverse functions promoting the viral life cycle and immune escape of HIV-infected cells. Early work identified a subset of individuals infected with Nef-defective HIV-1 that showed low to undetectable plasma viremia and stable $CD4^+$ T cell counts in the absence of ART [326, 327]. Parallel observations

have been made in animal studies, in which infection of rhesus macaques or humanized mice with Nef-defective mutants of SIV or HIV-1, respectively, reduced viremia and T cell loss [587, 588]. These and many other studies suggest that inhibition of Nef function with small molecule antagonists may not only provide antiretroviral efficacy but also eliminate HIV-infected cells restoring the host anti-HIV CTL response [589, 590].

Nef is a relatively small protein (~25-30 kDa depending upon the viral isolate) with a central folded core flanked by a flexible N-terminal arm and C-terminal loop. Myristoylation of the N-terminal arm targets Nef to the plasma membrane, which is essential for function [591]. Nef lacks intrinsic enzymatic or biochemical activity and works instead through a complex array of interactions with host cell proteins including endocytic trafficking adaptors, viral and immune receptors, restriction factors, and non-receptor tyrosine kinases, which are the focus of the present study [360, 592, 593].

Arguably the best studied kinase interaction with HIV-1 Nef involves the Src-family member, HCK [360]. HCK is primarily expressed in cells of the myeloid lineage [594] which includes macrophages and other HIV target cells. In the inactive state, HCK adopts an assembled conformation with the SH3 domain bound intramolecularly to the SH2-kinase linker which forms a polyproline type II helix [466, 595]. Nef binds directly to HCK through its SH3 domain, displacing the linker and causing constitutive kinase activation [596, 597]. Interaction requires a conserved Nef PxxPxR motif as well as other contacts that confer specific interaction with HCK and LYN out of the eight mammalian Src-family members [598, 599]. Pharmacological inhibition of Nef-dependent HCK activation suppresses HIV-1 replication, supporting a role for this pathway in the viral life cycle [600, 601].

Several members of the Tec non-receptor tyrosine kinase family are also expressed in HIV target cells where they facilitate the viral life cycle. The Tec-family kinases ITK and BTK regulate antigen receptor signaling pathways in T and B cells, respectively, serving as critical rheostats controlling adaptive immune responses [501, 602]. Initial studies established a role for ITK in the HIV-1 life cycle in T cells [603], while BTK has been linked to HIV-1 replication in cell lines of myeloid origin [581]. Selective inhibition of ITK kinase activity as well as siRNA-mediated ITK knockdown both interfered with viral transcription, assembly and spread [603]. Subsequent studies established a role for HIV-1 Nef as the mediator of ITK and BTK activation. Using bimolecular fluorescence complementation, Nef was shown to selectively interact with ITK, BTK and BMX among the five Tec-family members [604]. Interaction occurred predominantly at the plasma membrane and led to constitutive kinase activation through a mechanism dependent upon Nef homodimerization [365]. Small molecule Nef inhibitors were later shown to suppress ITK activation by Nef in T cells, providing a plausible explanation for their potent antiretroviral activity [605].

In the present study, we explored the molecular mechanisms by which HIV-1 Nef induces constitutive activity of Tec- family kinases. We focused primarily on BTK, because of the detailed structural information available for this Tec family member [532, 606, 607]. BTK shares a similar core domain architecture with HCK and other Src-family kinases, with the SH3, SH2 and kinase domains adopting an assembled conformation in the inactive state [532]. Unique to BTK and other Tec-family kinases are N-terminal pleckstrin homology (PH) and Tec homology (TH) domains. When BTK is inactive, the PH domain interacts with the kinase domain to suppress kinase activity [606]. During physiological activation of BTK, phosphatidylinositol 3-kinase (PI3-K) produces PIP_3 in the lipid bilayer, which in turn directs BTK to the membrane via the PH domain while

simultaneously relieving its inhibitory action on the kinase domain. The PH domain also drives BTK activation by promoting homodimer formation [536].

Here we provide evidence that HIV-1 Nef activates BTK by a unique mechanism dependent upon SH3-SH2-mediated dimerization of BTK and distinct from the mechanism of Nef-induced HCK activation. Using recombinant purified Nef, HCK and BTK, we first investigated the kinetics of Nef-mediated kinase activation. Nef activated HCK through an SH3-dependent mechanism involving acceleration of kinase autophosphorylation, consistent with previous studies [596, 597, 608]. Unlike HCK, activation of BTK by Nef did not require the Nef PxxPxR motif associated with SH3 binding, with Nef increasing the steady-state rate of BTK kinase activity. BTK was activated by Nef proteins derived from a wide range of M-group HIV-1 isolates and by SIV Nef, which does not activate HCK. Nef mutants defective for homodimerization failed to activate BTK, consistent with a role for dimer formation in the activation mechanism. Using analytical size exclusion chromatography (SEC) and surface plasmon resonance (SPR), we observed that Nef failed to interact with the individual PH, SH2, or SH3 domains of BTK. However, Nef did interact with a BTK SH3-SH2 dual domain protein, provided both partner proteins were present as pre-formed dimers prior to mixing and analysis. Based on alignments with a previous structure of an ITK SH3-SH2 dimer, we observed an intrinsic capacity for the BTK SH3-SH2 protein to form dimers that required a single proline residue in the SH2 domain CD-loop (Pro327). Substitution of Pro327 with alanine destabilized the BTK SH3-SH2 dimer as well as interaction with Nef dimers. Introduction of the P327A mutation into full-length BTK completely uncoupled BTK from Nef-mediated activation in vitro and BTK homodimer stabilization in cells. These findings show that the Nef proteins of primate lentiviruses have evolved independent mechanisms for the activation of two distinct yet related families of non-receptor protein tyrosine

kinases for the benefit of the virus, and suggest an additional layer of Tec family kinase regulation that involves intermolecular interaction between the SH3 and SH2 domains.

2.3 Results

2.3.1 Nef activates HCK and BTK through distinct kinetic mechanisms

Previous studies using endpoint kinase assays have shown that purified recombinant HIV-1 Nef proteins activate recombinant downregulated HCK *in vitro* [600, 609]. However, the kinetics of Nef-mediated enhancement of HCK activity have never been measured. To address this question, we used the ADP-Quest continuous kinase assay [610] to track the rates of HCK autophosphorylation and steady state activity towards a peptide substrate in the presence and absence of Nef. In both cases, activity is detected as the production of ADP through a series of coupled reactions that regenerate ATP while producing a fluorescent product. Each kinase reaction was performed with the ATP and peptide substrate concentrations set to their respective K_m values (Table 1). Figure 15A shows representative progress curves for substrate phosphorylation by HCK either alone or in the presence of HIV-1 or SIV Nef. HCK reached maximal steady state activity more rapidly in the presence of HIV-1 Nef, while SIV Nef had no effect. This observation is consistent with the progress curve for HCK autophosphorylation, which was also accelerated in the presence of HIV-1 Nef (Figure 15B). The steady state rates of HCK activity in the presence and absence of Nef, determined as the slope of the linear portion of each curve from multiple experiments, were not significantly different (Figure 15E, red bars). The effect of Nef on acceleration of HCK activity was measured as the time to reach approximately 10% of maximal

activity (~50 pmol ADP produced) in presence and absence of HIV-1 Nef (Figure 15F, red bars). The presence of HIV-1 Nef significantly shortened this threshold from 92.3 ± 7.4 min for HCK alone vs. 35.1 ± 5.3 min in presence of HIV-1 Nef. SIV Nef had no significant effect, consistent with prior reports demonstrating the inability of SIV Nef to interact with the SH3 domain of HCK [611]. Altogether, these kinetic analyses suggest that the primary impact of HIV-1 Nef binding is to accelerate HCK autophosphorylation, resulting in rapid and sustained kinase activity *in vitro*.

We next investigated the effect of Nef on recombinant full-length BTK using a similar kinase assay with a peptide substrate optimized for BTK (Table 1). Representative progress curves show that both HIV-1 and SIV Nef enhanced BTK kinase activity and autophosphorylation (Figures 15C and 15D). Unlike HCK, the steady state rate of BTK-mediated substrate phosphorylation was significantly increased in presence of HIV-1 and SIV Nef compared to BTK alone (Figure 15E, blue bars). In addition, the time to reach the 50 pmol ADP threshold was also significantly shorter in presence of both HIV-1 and SIV Nef (Figure 15F, blue bars). Unlike HCK, these kinetic assays demonstrate that Nef proteins not only accelerate BTK autophosphorylation but also enhance steady state BTK kinase activity. Furthermore, BTK activation may be more broadly conserved among Nef proteins from primate lentiviruses, with HCK activation limited to HIV-1 Nef.

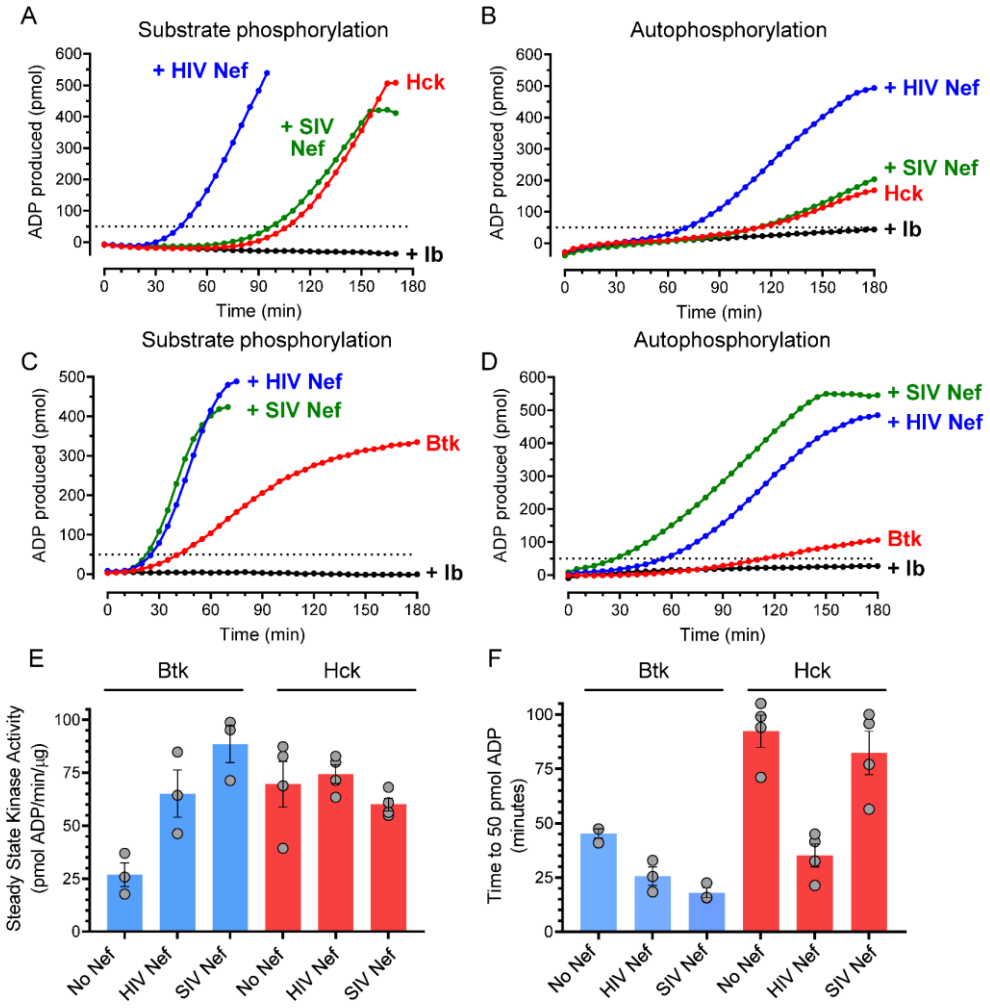

Figure 15. Lentiviral Nef proteins activate HCK and BTK by kinetically distinct mechanisms *in vitro*.

The ADP-Quest assay was used to measure ADP production by HCK or BTK in the presence of a peptide substrate (A and C) or as kinase autophosphorylation (B and D) either alone or in presence of HIV-1 or SIV Nef as shown. Both kinases were co-expressed with phosphatases to prevent autophosphorylation prior to assay (see Materials and Methods). Negative control reactions were run in the presence of HIV-1 Nef and ibrutinib (1 µM). Each data point is the average of 4 technical replicates. In A and C, the dotted line indicates the 50 pmol ADP threshold. E) Steady-state kinase activity was calculated for BTK (blue bars) and HCK (red bars) either alone or in presence of HIV-1 or SIV Nef from 4 independent experiments (grey points). The height of each bar indicates the mean ± S.E; HIV-1 and SIV Nef both significantly increased the rate of BTK activity ($p < 0.05$) but not HCK activity. F) The time to reach the 50 pmol ADP threshold was calculated for BTK (blue bars) and HCK (red bars) either alone or in presence of HIV-1 or SIV Nef from three (BTK) or four (HCK) independent experiments. The height of each bar indicates the mean ± S.E. For BTK, both HIV-1 and SIV Nef shortened the time to 50 pmol ADP ($p < 0.05$); only HIV-1 Nef significantly shortened the time for HCK ($p < 0.01$).

Autophosphorylation of activation loop Tyr551 is a key step in the BTK activation mechanism. To determine whether Nef induced BTK activation loop autophosphorylation at this site, BTK was expressed in the presence of the YopH phosphatase to allow purification in the

dephosphorylated state. Kinase reactions were then performed with BTK alone or in presence of HIV-1 or SIV Nef, with the kinase and ATP concentrations as per Figure 15. Reactions were initiated by adding ATP, and activation loop phosphorylation was monitored by immunoblotting with a phosphospecific antibody at various time points. Both HIV-1 and SIV Nef increased BTK Tyr551 phosphorylation, which was reversed by the presence of the BTK inhibitor, ibrutinib (Figure 16). The pTyr551 and BTK protein levels were quantified and plotted as pY551/BTK protein ratios for each of two independent experiments (Figure 16B). Both HIV-1 and SIV Nef increase BTK autophosphorylation on a time scale like that observed in the kinetic kinase assay (Figure 16B).

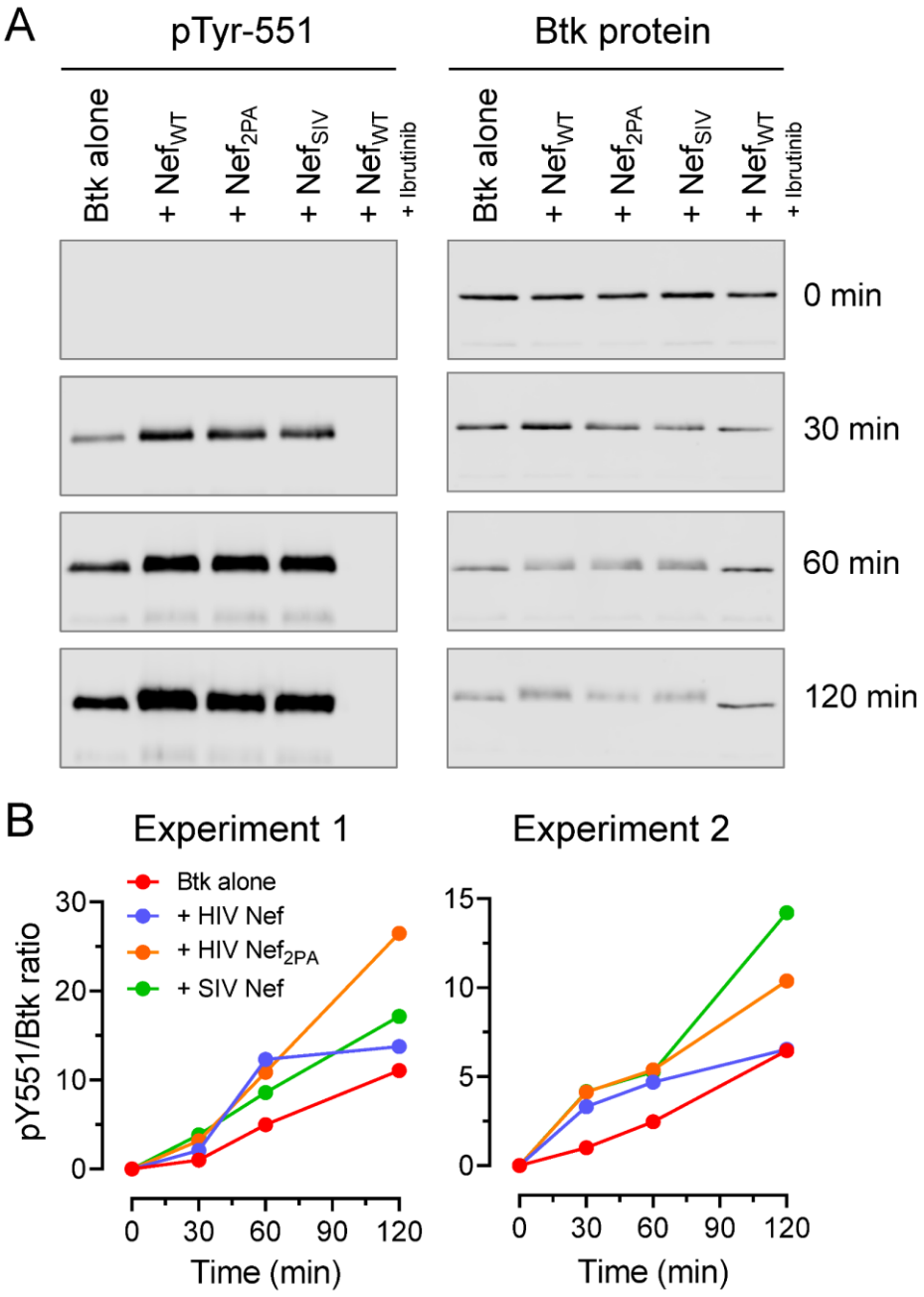

Figure 16. Nef induces BTK autophosphorylation on activation loop Tyr551.

Each kinase reaction was performed with BTK alone or in presence of HIV-1 Nef wild-type (WT), the PxxP to AxxA mutant (2PA), SIV Nef, or wild-type Nef plus 1 µM ibrutinib as a negative control. Aliquots were collected after 0, 30, 60, and 120 minutes, resolved by SDS-PAGE, and transferred to nitrocellulose membranes for immunoblot analysis. A) Left panels show representative immunoblots of BTK activation loop tyrosine phosphorylation (pTyr-551) while the right panels show BTK protein levels using an antibody against the His-tag fused to the BTK C-terminus. B) Immunoreactive band intensities for BTK autophosphorylation normalized to BTK protein levels (pTyr-551/BTK protein ratio) for 2 independent experiments. Band intensities were quantified using the Odyssey infrared imaging system.

2.3.2 BTK activation is a conserved property of M-group HIV-1 Nef proteins

Results presented thus far were generated with recombinant Nef from the SF2 isolate of HIV-1, a commonly used laboratory allele of the B-subtype. To determine if BTK activation is a property shared by Nef proteins derived from other HIV-1 M-group subtypes, we expressed and purified Nef from representative isolates of HIV-1 clades A1, F1, G, J, and K [609] as well as three C-clade Nef alleles derived from clinical isolates of transmitter/founder viruses (CH185, Cz249M, and Cz3618M). We also included Nef from HIV-1 NL4-3, another common laboratory HIV-1 strain of the B subtype. Together, these ten Nef proteins are representative of HIV-1 subtypes responsible for over 90% of global infections, with subtype C strains accounting for the largest proportion [612].

BTK activation by each of these Nef variants was then determined using the kinetic kinase assay (Figure 17). All ten Nef subtypes significantly enhanced steady state BTK activity *in vitro*, with enhancement ranging from 2-fold for Nef-NL4-3 to more than 4-fold for Nef-G. This result indicates that all major HIV-1 subtypes responsible for global HIV infections have retained the ability to activate BTK and may share a common mechanism to achieve BTK activation. Conservation of BTK activation by diverse HIV-1 Nef proteins as well as SIV Nef strongly suggest that Tec-family kinase activation is important to the HIV-1 life cycle.

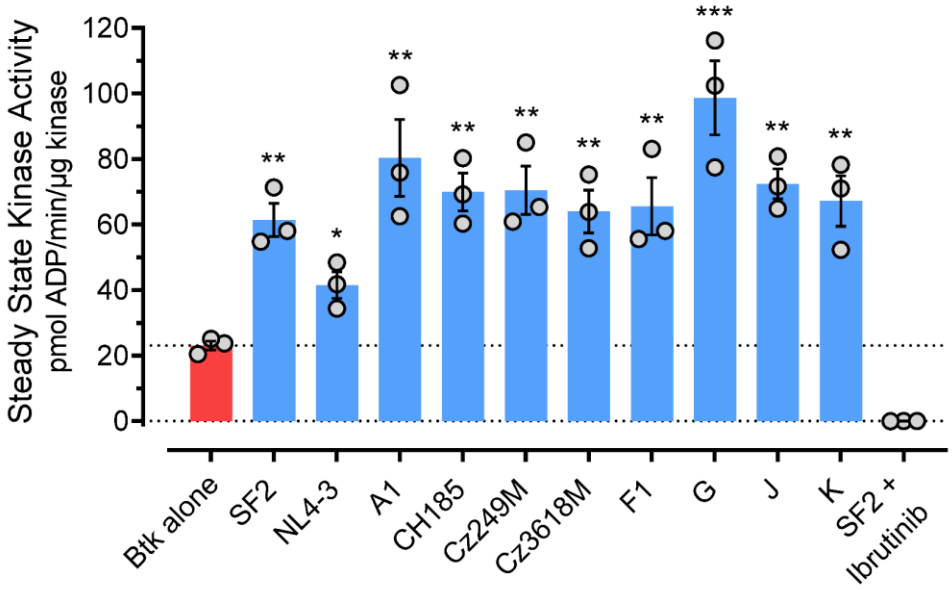

Figure 17. Recombinant Nef proteins from major HIV-1 subtypes induce BTK activation.

Steady state kinase activity was calculated from three independent experiments for BTK alone (red bar) or in presence of Nef from the indicated HIV-1 subtypes (blue bars). Bar heights indicate the mean rates ± S.E. Student's t-tests were performed for steady state rates observed with BTK alone vs. BTK in presence of each Nef subtype; * $p < 0.05$; ** $p < 0.01$; *** $p < 0.001$. Activation of BTK by Nef-SF2 was completely suppressed in the presence of 1.0 µM ibrutinib (far right).

2.3.3 BTK activation does not require the conserved Nef PxxPxR motif

Recruitment of HCK by HIV-1 Nef requires a conserved PxxPxR motif, which engages the HCK SH3 domain and displaces it from the SH2-kinase linker as part of the activation mechanism [360]. To explore the role of the Nef PxxPxR motif in BTK activation, we purified recombinant HIV-1 Nef-SF2 harboring alanine mutations in place of the conserved prolines required for HCK SH3 engagement (Nef-2PA). Kinetic kinase assays showed that the HIV-1 Nef-2PA mutant had no effect on HCK kinase activity, consistent with previous *in vitro* and cell-based studies (Figure 18A) [597, 598, 609]. In contrast, HIV-1 Nef-2PA stimulated steady state BTK activity to the same extent as wild-type Nef (Figure 18B). The Nef-2PA mutant also enhanced

BTK autophosphorylation on Tyr551 (Figure 16). This surprising result demonstrates that HIV-1 Nef induces BTK activation by a distinct mechanism that does not require the PxxPxR motif.

The observation that the Nef-2PA mutant activates BTK but not HCK implies that the BTK SH3 domain alone may not be sufficient for Nef interaction. To explore this possibility, we purified recombinant HCK and BTK SH3 domains and tested their interaction with HIV-1 Nef using analytical size-exclusion chromatography (SEC). We have previously shown that the HCK SH3 domain forms a stable complex with HIV-1 Nef in solution using this approach [613]. Purified Nef eluted as a mixture of monomers and dimers, while the HCK SH3 domain eluted as a monomer (Figure 18C). When the Nef and SH3 proteins were mixed prior to SEC, both dimer and monomer Nef peaks shifted to the left, indicative of stable complex formation. In contrast, SEC of a mixture of the BTK SH3 domain with Nef showed no evidence of complex formation (Figure 18D), demonstrating that the BTK SH3 domain alone is not sufficient for interaction with Nef in solution, unlike HCK where Nef engagement with SH3 is sufficient. We also analyzed the interactions of Nef with the HCK and BTK SH3 domains by SPR. Purified recombinant HCK and BTK SH3 domains were immobilized on an SPR biosensor surface at equal density, and recombinant HIV-1 Nef was injected over a range of concentrations. The HCK SH3 domain bound to HIV-1 Nef in a concentration-dependent manner yielding a kinetic K_D value of 0.14 μM (Figure 18E), consistent with a published K_D value of 0.18 μM reported previously [610]. Unlike HCK, the BTK SH3 domain failed to bind HIV-1 Nef by SPR even at the highest Nef concentration tested (10 μM; Figure 18F). Taken together, these experiments suggested that interaction and subsequent activation of BTK by HIV-1 Nef requires more than SH3 domain engagement as observed previously for HCK or other Src-family kinases.

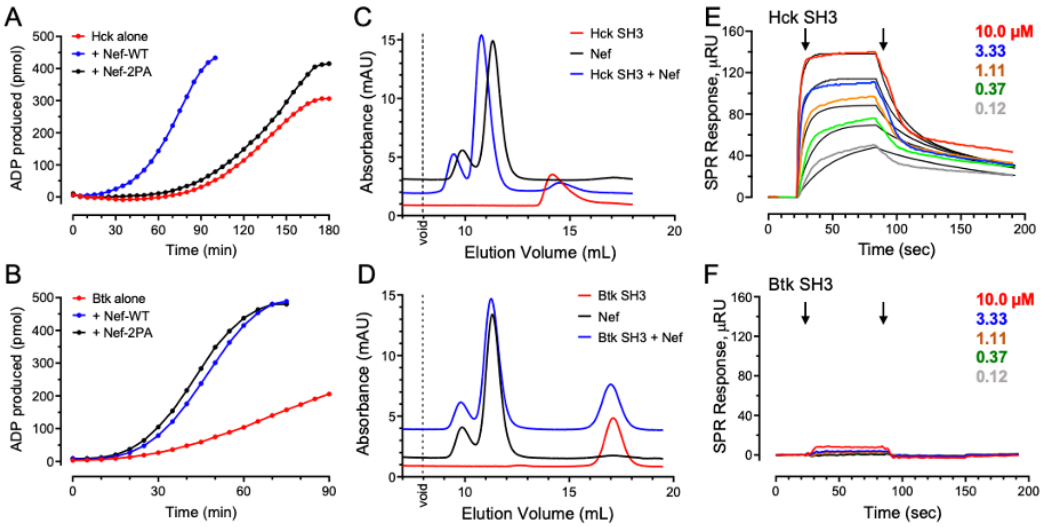

Figure 18. Nef-induced BTK activation is independent of the SH3-binding PxxP motif.

A) Representative progress curves of ADP produced by HCK (A) or BTK (B) either alone or in presence of HIV-1 Nef wild-type (WT) or the Nef PxxP to AxxA (2PA) mutant. Analytical SEC elution profiles of the HCK (C) or BTK (D) SH3 domains alone, HIV-1 Nef alone, or an equimolar mixture of each SH3 domain with Nef. The total protein concentration in each sample was 12 µM; the void volume is indicated by the dotted line. Protein-protein interactions were also measured in real time by SPR. Recombinant HCK SH3 (E) and BTK SH3 (F) domains were immobilized on a carboxymethyl dextran chip at the same density. HIV-1 Nef was injected over the range of concentration shown (*left arrow*) and interaction was monitored to equilibrium followed by a dissociation phase (*right arrow*). HCK SH3 binding to HIV-1 Nef in E) was fitted with 1:1 two-state binding model.

2.3.4 Nef homodimerization is required for BTK activation

Crystal structures of HIV-1 Nef in complexes with a Src-family kinase SH3 domain or an SH3-SH2 dual domain protein show that Nef forms homodimers mediated by the αB helix in each Nef monomer [360]. Cell-based bimolecular fluorescence complementation assays demonstrated that Nef forms homodimers at the plasma membrane [169, 365], and that mutagenesis of residues involved in homodimer packing in the crystal structures are essential for dimer integrity in cells [365]. Amino acids crucial to Nef homodimer stability include Leu112, Tyr115, and Phe121 (Figure 19A). Purified recombinant HIV-1 Nef proteins with substitutions at these positions (L112D, Y115D, and F121A) were previously shown to elute exclusively as monomers by SEC [365]. All three dimerization-defective Nef mutants showed significantly diminished levels of

BTK activation compared to wild-type Nef in the kinetic kinase assay (Figure 19B, 19C), indicating that Nef homodimerization is required for BTK activation *in vitro*. These results suggest that BTK activation requires formation of a 2:2 dimer complex with HIV-1 Nef, resulting in kinase autophosphorylation by a *trans*-mechanism. To control for the impact of these mutations on the overall structure of recombinant Nef, we evaluated their interaction with the HCK SH3 domain by SPR. All three mutants demonstrated similar interaction kinetics as wild-type Nef, consistent with proper folding as HCK SH3 engagement requires not only the Nef PxxPxR motif but also a hydrophobic pocket dependent upon a specific three dimensional fold of the Nef core region [614] (Figure 20).

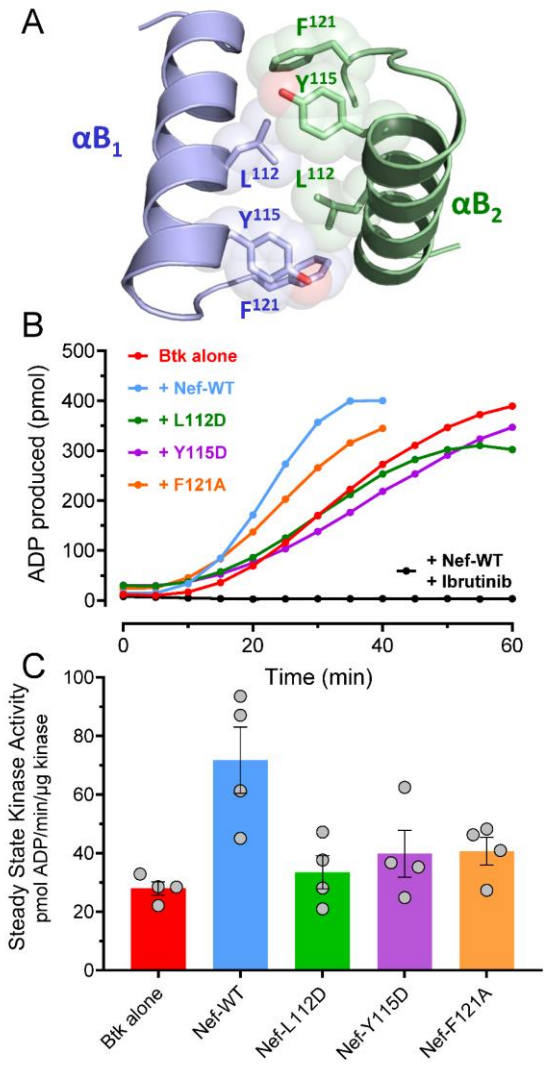

Figure 19. Dimerization-defective Nef mutants do not activate BTK.

A) Dimer interface present in the crystal structure of HIV-1 Nef in complex with a Src-family kinase SH3 domain (PDB: 1EFN). Reciprocal hydrophobic interactions of the side chains of Leu112, Tyr115, and Phe121 form the interface between the αB helices of the Nef cores (blue and green, respectively). B) Representative progress curves for ADP produced by BTK alone, in presence of wild-type HIV-1 Nef (WT), or the indicated dimerization-defective Nef mutants. BTK activity in the presence of wild-type Nef and ibrutinib (1 µM) is included as a negative control. C) Steady-state kinase activity was calculated from four independent experiments for BTK alone or in presence of wild-type or mutant Nef proteins as indicated. The height of each bar indicates the mean rate ± S.E. Wild-type Nef significantly increased BTK activity vs. BTK alone ($p < 0.01$) while the Nef mutants were without significant effect ($p > 0.05$ in all three cases).

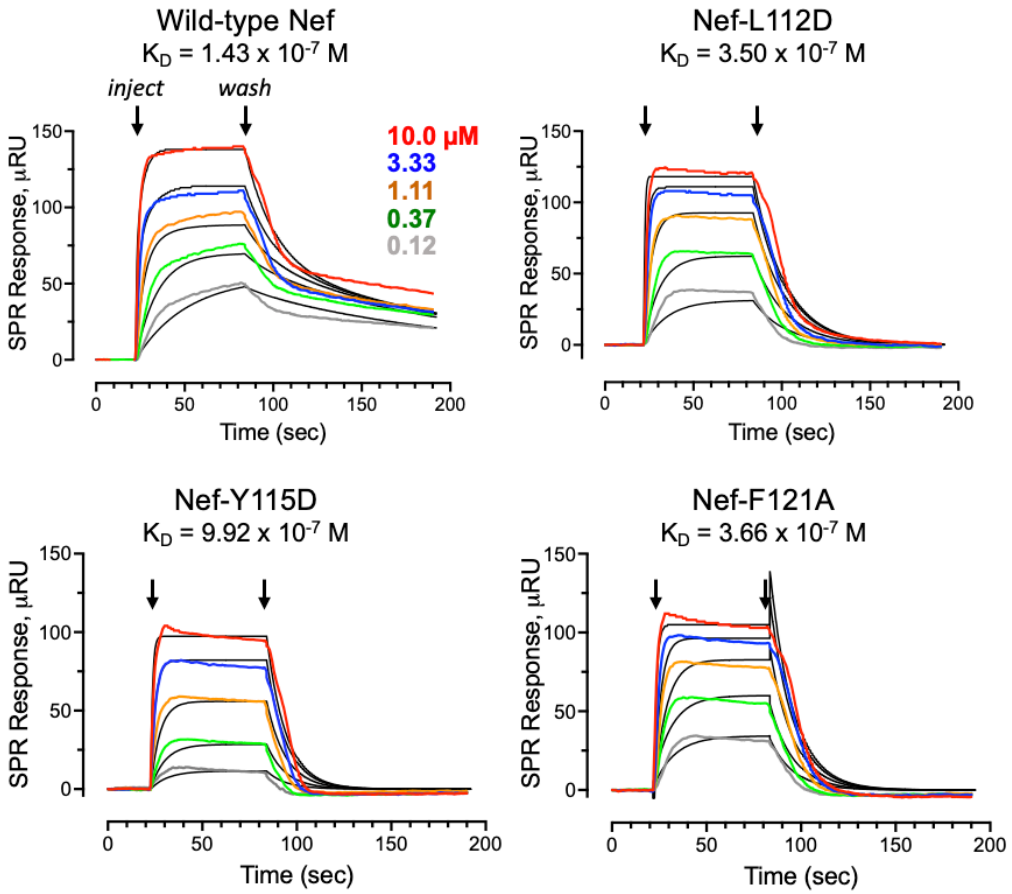

Figure 20. Kinetics of HIV-1 Nef interactions with the HCK SH3 domain.

Recombinant HCK SH3 domain protein was immobilized on a carboxymethyl dextran SPR biosensor chip. Wild-type HIV-1 Nef as well as the dimerization-defective mutants L112D, Y115D, and F121A were injected in triplicate over the range of concentrations shown in the upper left panel (0.12 µM to 10 µM; *inject*). Binding was recorded until equilibrium reached, followed by a switch to running buffer to induce dissociation (*wash*). Kinetic rate constants were calculated from reference-corrected sensorgrams by fitting with a 1:1 Langmuir binding model. Kinetic K_D values derived from the resulting rate constants and the formula $K_D = k_d/k_a$ are shown. Binding between HCK SH3 and HIV-1 Nef wild-type was fitted using the simplest model of 1:1 two-state, whereas binding between HCK SH3 and HIV-1 Nef mutants were fitted using 1:1 Langmuir model.

2.3.5 Nef forms a 2:2 dimer complex with BTK SH3-SH2 dual domain

The observation that BTK activation is dependent on Nef homodimers led us to explore the regions of BTK responsible for interaction with Nef. To this end, we expressed and purified recombinant BTK regulatory domain proteins including the individual PH, SH3, and SH2 domains as well as tandem constructs consisting of the PH-SH3, SH3-SH2, and PH-SH3-SH2. Bth TH

domain are part of the folded PH domains and are included with PH domains. All proteins behaved as homogeneous monomers during purification, except the SH3-SH2 dual domain protein which eluted as two distinct peaks during SEC. Each SH3-SH2 peak was isolated, concentrated, and evaluated further by SEC-multiangle light scattering (SEC-MALS) which confirmed the presence of monomeric and dimeric forms (Figure 21A, 21B). In addition to BTK SH3-SH2, SEC-MALS also confirmed the presence of HIV-1 Nef monomers and dimers (Figure 21C, 21D). The isolated Nef dimer and monomer preparations retained a small amount of the other species, which is likely due to partial re-equilibration during chromatography.

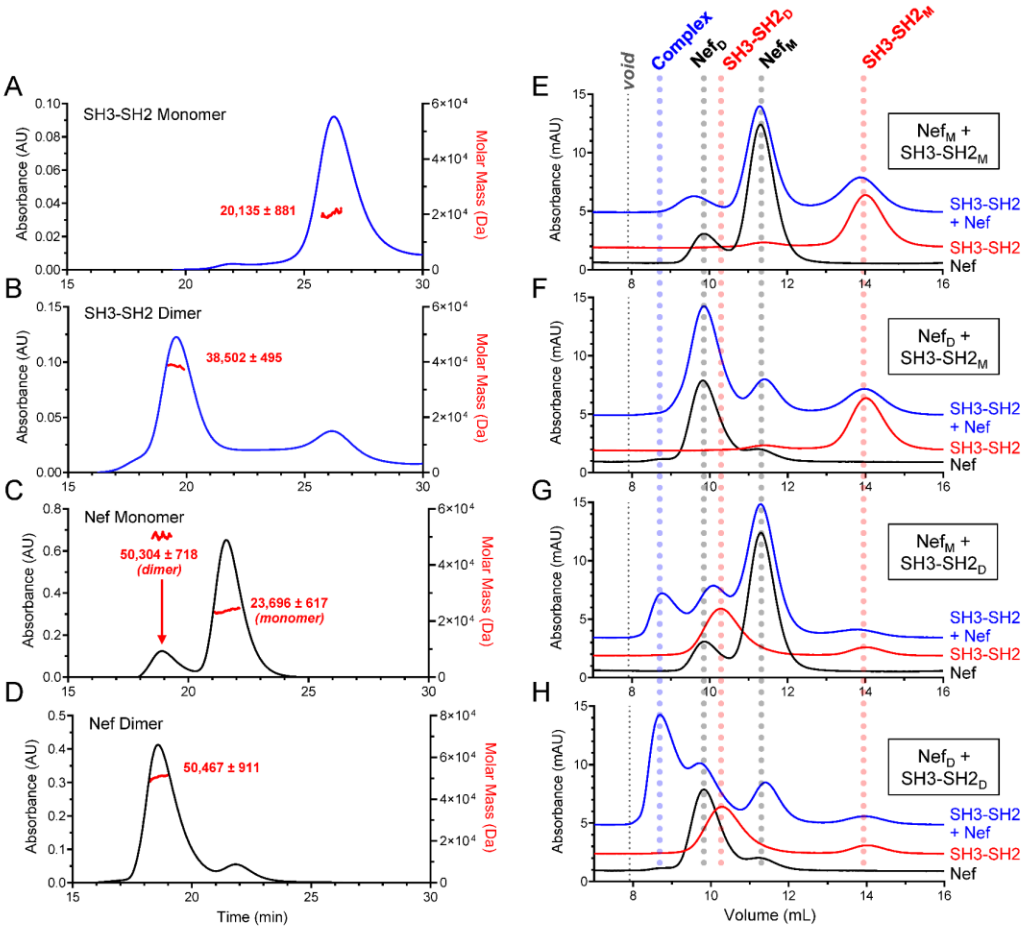

Figure 21. Preformed homodimers of the BTK SH3-SH2 dual domain and HIV-1 Nef form a 2:2 complex.

A-D: SEC followed by multi-angle light scattering (MALS) were used to analyze the A) BTK SH3-SH2 monomer, B) the BTK SH3-SH2 dimer, C) the Nef monomer, and D) the Nef dimer. Protein absorbance at 280 nm and molar mass (Da) are shown on the left and right axes, respectively, with the mass of each peak calculated from MALS is shown in red. All proteins were analyzed at 100 µM concentrations. E-H: Monomeric (M) and dimeric (D) forms of BTK SH3-SH2 and Nef were mixed in equal proportions followed by analytical SEC at 4 °C. In each experiment, the proteins were run individually for comparison. Each protein was present in the sample at a final concentration of 12 µM. Elution profiles shown are E) Nef monomer + SH3-SH2 monomer; F) Nef dimer + SH3-SH2 monomer; G) Nef monomer + SH3-SH2 dimer; H) Nef dimer + SH3-SH2 dimer. The red vertical dotted lines indicate the peak elution positions for the SH3-SH2 monomer (SH3-SH2$_M$) and dimer (SH3-SH2$_D$). The black dotted lines indicate the peak elution positions for the Nef monomer (Nef$_M$) and dimer (Nef$_D$). The blue dotted line indicates the peak elution position for the complex of the Nef and SH3-SH2 dimers (Complex).

We next investigated whether the recombinant BTK domain proteins formed stable complexes with HIV-1 Nef in solution. None of the individual BTK domains (PH, SH3, SH2) formed complexes with Nef by SEC analysis (Figure 22). However, the BTK SH3-SH2 dual domain protein did form a stable complex with Nef provided that each protein was present in the

homodimeric form prior to mixing and SEC analysis. As shown in Figure 21E, the BTK SH3-SH2 monomer and Nef monomer did not associate when incubated together prior to SEC analysis. Similarly, monomeric SH3-SH2 did not associate with dimeric Nef (Figure 21F) while dimeric SH3-SH2 and monomeric Nef largely eluted unassociated, except for a small peak consistent with higher order complex formation (Figure 21G). However, when dimeric BTK SH3-SH2 was mixed with dimeric Nef, a new SEC peak was observed that is consistent with a 2:2 Nef:SH3-SH2 dimer (Figure 21H). These analytical SEC results indicate that HIV-1 Nef and BTK SH3-SH2 associate to form a stable complex when both proteins are initially present as pre-formed dimers.

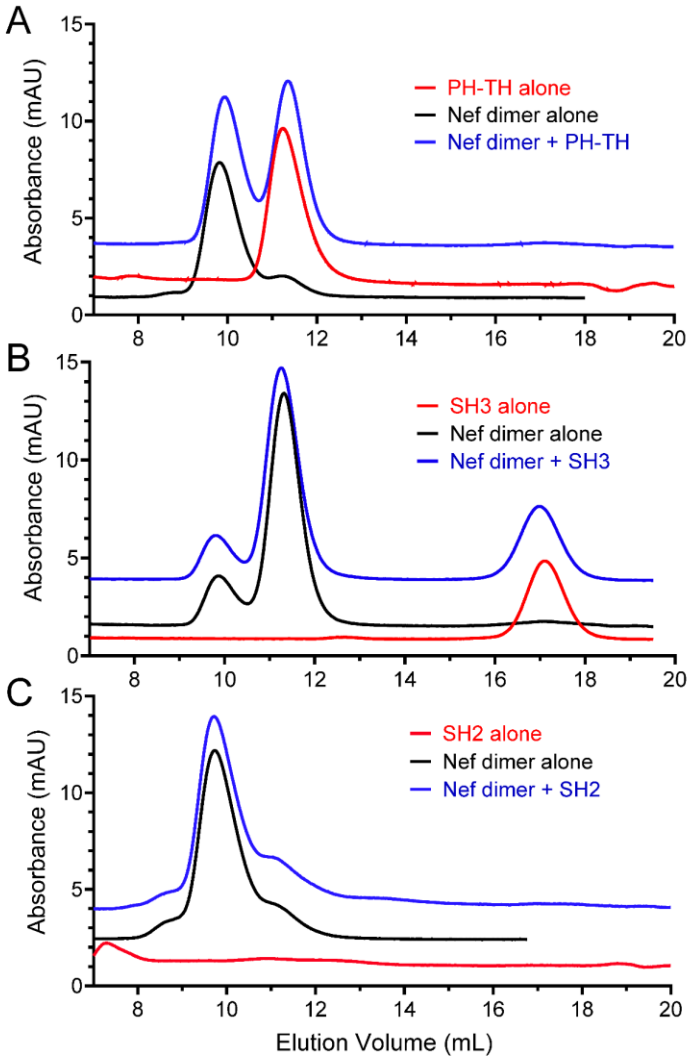

Figure 22. Individual BTK regulatory domains do not form complexes with Nef.

Individual domains of BTK (PHTH, SH3, SH2) were injected alone or following preincubation with the Nef homodimer at 4 °C. All proteins were present at a final concentration of 12 µM in each sample. Protein elution profiles at 280 nm of BTK PHTH (A), SH3 (B) and SH2 (C) alone, Nef homodimer alone, and in combination. Note that the BTK SH2 domain does not contain Trp residues and does not absorb at 280 nm.

To validate the SEC data using an orthogonal approach, we also performed SPR experiments. Equal amounts of the BTK dual domain SH3-SH2 protein, as well as the individual SH3 and SH2 domains, were immobilized on an SPR biosensor chip. The BTK dual domain protein was isolated as the homodimeric fraction by SEC prior to immobilization on the SPR chip surface. Purified recombinant HIV-1 Nef proteins, isolated as their monomeric and dimeric forms,

were then injected over a range of concentrations. The Nef homodimer bound robustly to the BTK SH3-SH2 dual domain with a kinetic K_D value of 1.75 μM and maximum response of 411 μRU with the highest Nef concentration of 10 μM (Figure 23A). The Nef monomer also bound SH3-SH2, although with reduced affinity (K_D = 7.64 μM) and a lower maximum response of 199 μRU (Figure 23B). Neither monomeric nor dimeric Nef interacted with the isolated SH3 or SH2 domain proteins alone (Figure 23C-23F). Together with the SEC data, these observations support a model in which Nef homodimers selectively interact with pre-formed BTK SH3-SH2 dimers as an initial step in the BTK activation sequence.

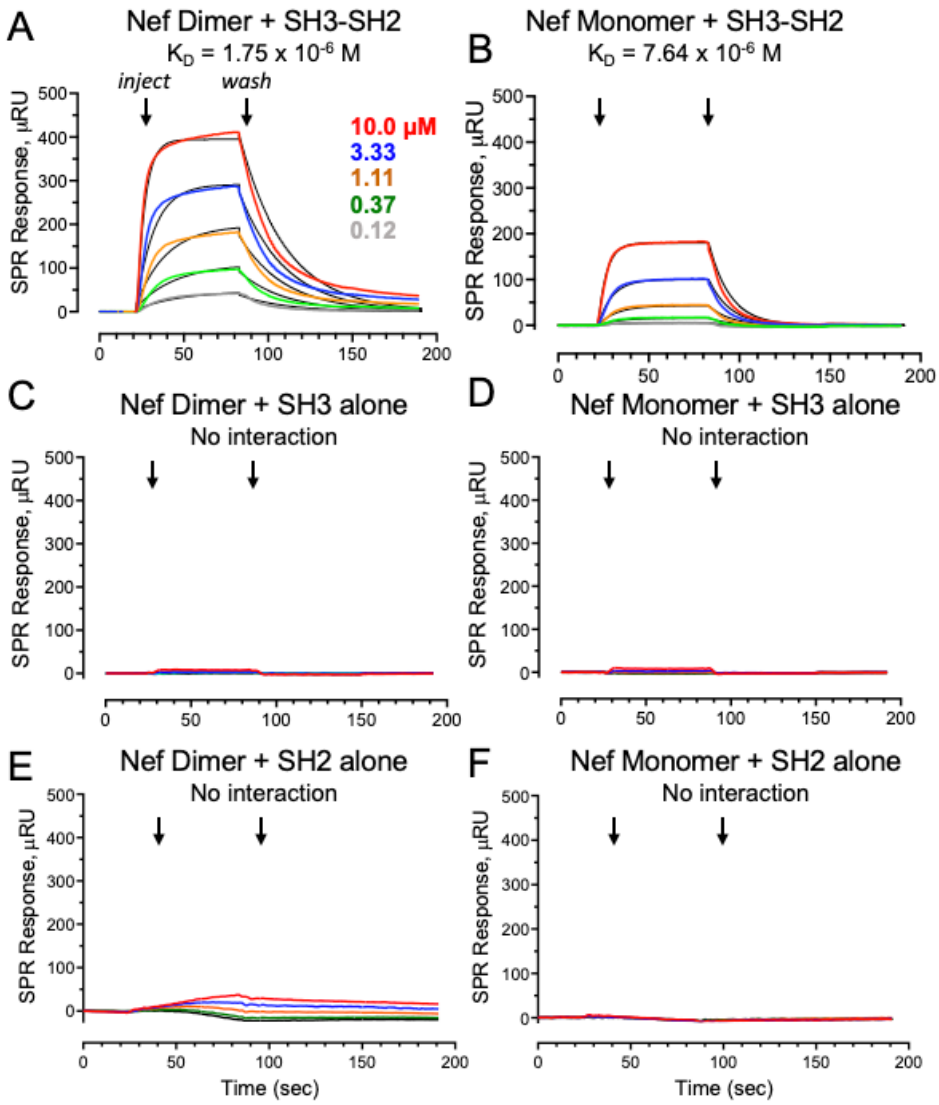

Figure 23. The BTK SH3-SH2 dual domain preferentially interacts with HIV-1 Nef homodimers by SPR.

The BTK SH3-SH2 dual domain along with the individual SH3 and SH2 domains were immobilized at equal density on a carboxymethyl dextran SPR biosensor chip. Purified Nef homodimers or monomers were then injected over the range of concentrations shown in panel A (0.12 µM to 10 µM; *inject*). Binding was recorded until equilibrium reached, followed by a switch to running buffer to induce dissociation (*wash*). Each Nef protein concentration was tested in triplicate and best fit by a 1:1 two-state binding model to calculate the kinetic K_D. values shown. Representative sensorgrams are shown for the BTK SH3-SH2 with the Nef dimer (A) or monomer (B); the BTK SH3 domain with the Nef dimer (C) or monomer (D); and the BTK SH2 domain with the Nef dimer (E) or monomer (F). SPR bindings were recorded in Reichert 4-channel SPR instrument.

2.3.6 Interaction with HIV-1 Nef stabilizes the BTK SH3-SH2 dimer

Differential scanning fluorimetry analysis revealed no significant difference between the melting temperatures of the monomeric vs. dimeric forms of the BTK SH3-SH2 dual domain protein, suggesting that the intrinsic stability or folding of the individual domains is not influenced by dimerization (Figure 24). In this experiment, however the dimer to monomer transition of BTK SH3-SH2 protein at higher temperature may be more rapid than observed at room temperature. The observation of similar melting point between monomer and dimer BTK SH3-SH2 suggest this may be true. To determine the kinetic barrier associated with dimer to monomer transition at room temperature, BTK SH3-SH2 dimer was then incubated at room temperature over 24 hours, followed by determination of oligomerization status by SEC (Figure 25A). Under these conditions, the BTK SH3-SH2 dimer completely dissociated into the monomeric form within 24 hours. Whether such conversion proceeds via complete or partial unfolding substates is not known. In contrast to SH3-SH2, similar SEC analysis showed that the HIV-1 Nef dimer was stable at room-temperature up to 96 hours with no change in the SEC elution profile (Figure 25B). Addition of the Nef dimer to the BTK SH3-SH2 dimer prior to the shift to room temperature resulted in a stable dimer complex that dissociated more slowly over time, with the complex still present after 24 hours at room temperature (Figure 25C). The influence of the Nef dimer on the stability of the Nef:SH3-SH2 complex at room temperature is also evident in the rate of appearance of SH3-SH2 monomer in Figure 25C compared to that in the absence of Nef in Figure 25A. Moreover, Figure 25C shows that dissociation of BTK SH3-SH2 and HIV-1 Nef 2:2 complex yields peak consistent with HIV-1 Nef monomer. SPR interactions between HIV-1 Nef and BTK SH3-SH2 is best fitted by 1:1 two-state binding model, suggesting that conformational changes may take place in HIV-1 dimer upon BTK SH3-SH2 binding, which is consistent with HIV-1 Nef binding with HCK SH3

and HCK SH3-SH2 domains. Furthermore, appearance of second species within the BTK SH3-SH2 and Nef 2:2 complex is noticed in 24 hours, suggesting further conformational sampling may take place within the complex at room temperature over 24 hours. These results support the idea that Nef dimers stabilize BTK dimers through SH3-SH2-mediated interaction.

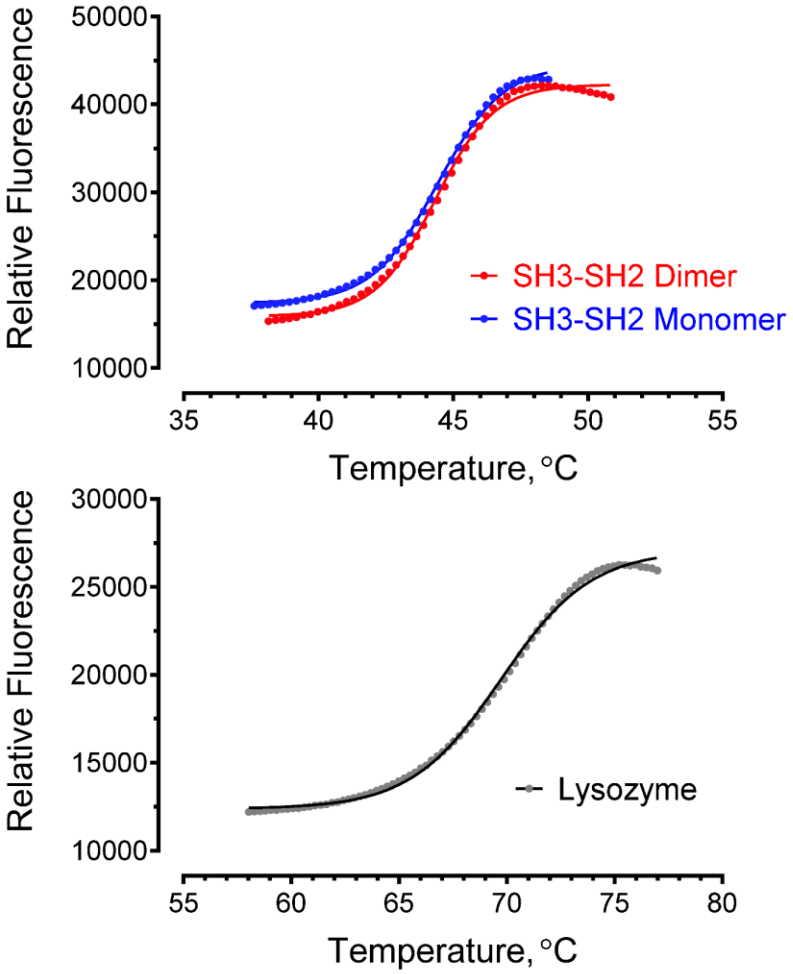

Figure 24. Differential scanning fluorimetry (DSF) shows no difference in intrinsic thermal stability of the BTK SH3-SH2 dimer and monomer.

A thermal shift assay was conducted to monitor the thermal stability of the BTK SH3-SH2 protein in the dimeric vs. monomeric forms. Each form of the BTK SH3-SH2 protein (5 µM) was combined with SYPRO orange. As the temperature increases and the protein unfolds, SYPRO orange binds hydrophobic patches with the protein resulting in an increase in fluorescence. Each thermal shift curve was fit by non-linear regression analysis, yielding T_m values of 44.4 °C for the SH3-SH2 dimer and 44.3 °C for the monomer (upper panel). DSF of lysozyme was also performed as a control, yielding a T_m value of 69.7 °C (lower panel).

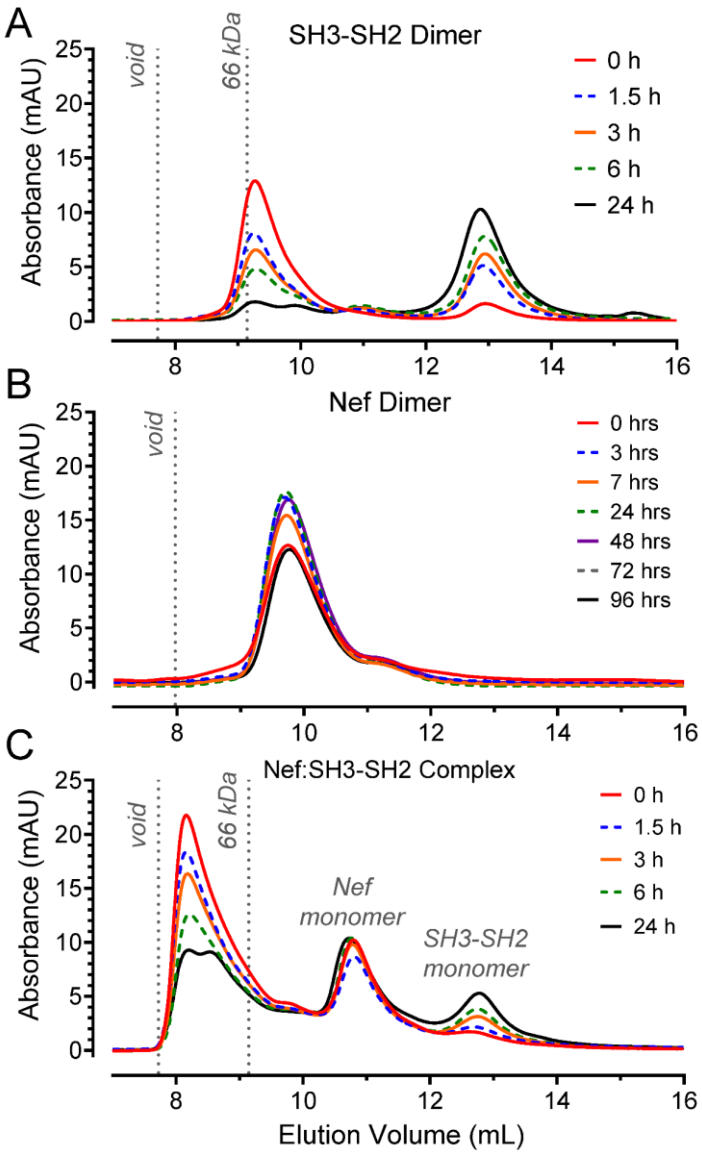

Figure 25. Stability of the HIV-1 Nef:SH3-SH2 dimer complex in solution.

A) BTK SH3-SH2 homodimer stability was determined by monitoring the dimer to monomer transition by SEC following incubation at room-temperature for each of the time points shown. B) Nef homodimer stability at room temperature was also measured by SEC for up to 96 hours; no evidence of the Nef monomer was observed at any of the time points sampled. C) Stability of the Nef:SH3-SH2 dimer complex was assessed at room temperature as in panel A. The starting concentration of each protein in all samples was 18 µM. The elution position of a 66 kDa molecular weight standard as well as the void volume are indicated by vertical dotted lines.

2.3.7 The BTK SH2 domain CD Loop regulates BTK SH3-SH2 dimerization

We next explored the structural basis of SH3-SH2 dimerization in BTK, and the mechanism by which Nef enhances this interaction. While a dimer interface between the BTK SH3-SH2 dual domain protein has not been reported, the SH3-SH2 unit of the closely related Tec-family member ITK, which is also activated by Nef in cell-based assays, has been shown to dimerize by NMR. In these experiments, the ITK SH3 domain interacts with several loops connecting secondary structural elements of the ITK SH2 domain [615]. Specifically, a single prolyl amide bond in the CD loop of the ITK SH2 domain (Pro287) dictates the conformation necessary for ITK SH3-SH2 dimerization with interaction requiring the *cis* conformation [558, 562]. Using the NMR structure of the ITK SH3•SH2 interface as a starting point, we aligned existing NMR structures of the individual BTK SH3 and SH2 domains to gain structural insight regarding a potential BTK SH3•SH2 interface (Figure 26A). This model suggests that Pro327 in the BTK SH2 domain may structure the CD loop for interaction with the BTK SH3 domain, along with intra-loop polar contacts between Glu326 and Gln328. Predicted stabilizing contacts are also possible between BTK SH2 Pro327 and SH3 Tyr223; SH2 His362 and SH3 Asn229, and SH2 Lys349 and SH3 Tyr263.

To test for SH2-mediated interaction with SH3 in the context of SH3-SH2 dual domain proteins, we first expressed and purified the SH3-SH2 region of ITK. This protein gave rise to both dimeric and monomeric forms by analytical SEC (Figure 26B), as well as higher order oligomers, consistent with previous observations [562]. Replacement of Pro287 with alanine in the ITK SH2 domain, which structures the CD loop for engagement of SH3 as described above, led to a single monomeric species of ITK SH3-SH2 by SEC (Figure 26B). This observation demonstrates that intermolecular interaction of the SH2 and SH3 domains also occurs in the

context of the ITK SH3-SH2 dual domain protein. We then expressed and purified an analogous mutant of the BTK SH3-SH2 protein, in which Pro327 in the SH2 domain CD loop was replaced with alanine. SEC analysis of the dimer fraction of the BTK SH3-SH2 P327A mutant over time revealed more rapid dissociation than the wild-type dimer, with estimated half-lives of 40.8 minutes vs. 105.6 minutes for the P327A mutant and wild-type, respectively (Figure 26C). Although the activation enthalpy associated with dimer to monomer transition was not measured, the observation of rapid dissociation of BTK SH3-SH2 P327A dimer compared to the wild-type dimer suggests that the kinetic barrier for dimer to monomer transition is lower for the mutant BTK SH3-SH2 (Figure 27). While this observation suggests that Pro327 stabilizes BTK SH3-SH2 dimerization, additional interactions are likely present at the SH3-SH2 dimer interface since P327A mutation did not prevent dimer formation as observed with the ITK SH3-SH2 dimer. Nevertheless, subsequent experiments demonstrated a critical role for Pro327 in BTK activation by Nef as described in the following sections.

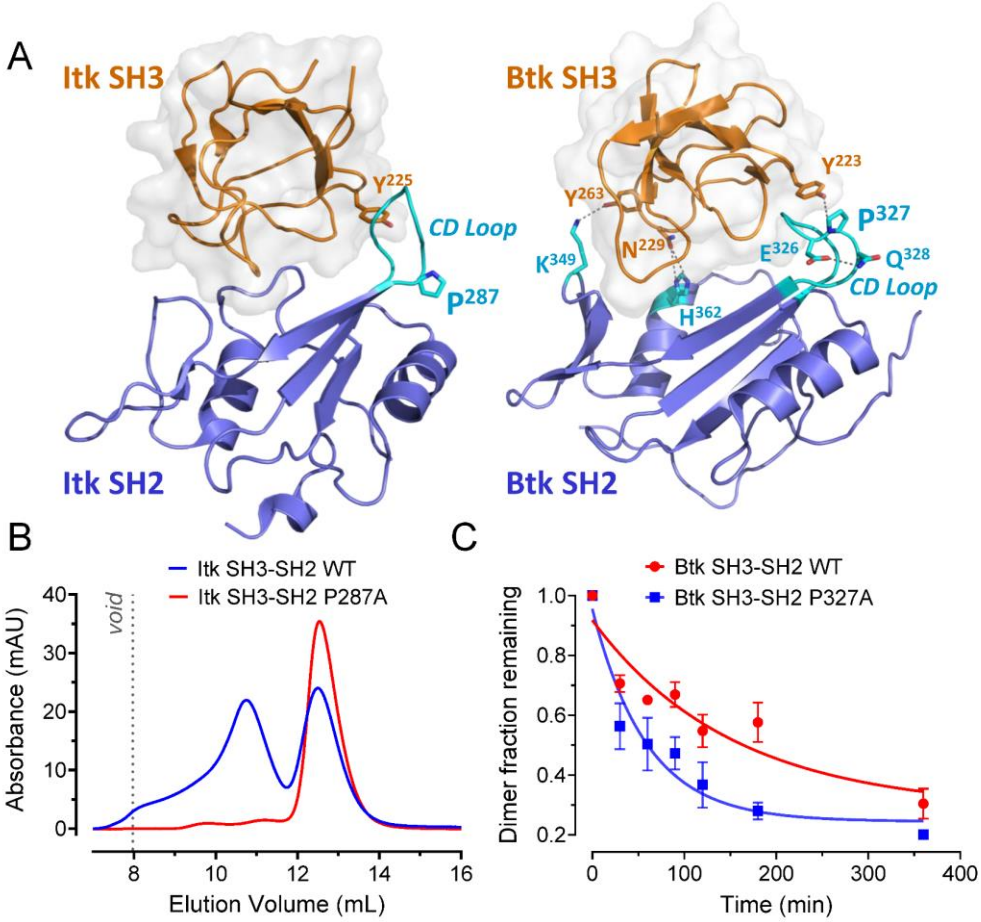

Figure 26. The BTK SH2 domain CD loop influences BTK SH3-SH2 dimerization.

A) Model of the ITK SH3•SH2 interface based on the NMR structure (PDB: 2K79; *left*). Pro287 in the CD loop of the ITK SH2 domain (cyan) adopts the *cis* conformation for dimerization. NMR structures of the individual BTK SH3 (PDB: 1QLY) and SH2 (PDB: 2GE9) domains were aligned to the ITK SH3•SH2 interface to model a potential BTK SH3•SH2 dimer (*right*). Pro327 in the BTK SH2 domain may structure the CD loop for interaction with the BTK SH3 domain. Intra-loop polar contacts are also observed between Glu326 and Gln328. In addition to the CD loop, stabilizing contacts are also possible between SH2 Pro327 and SH3 Tyr223; SH2 His362 and SH3 Asn229; and SH2 Lys349 and SH3 Tyr263. B) Wild-type and P287A mutant ITK SH3-SH2 proteins were expressed in bacteria, purified, and their oligomeric states determined by analytical SEC. The initial protein concentration in each sample was 50 µM. C) The stability of the wild-type and P327A BTK SH3-SH2 homodimers was assessed by analytical SEC following incubation for various times at room temperature. The proportion of dimer remaining at each time point was estimated from the height of each peak and the average value is plotted ± SE vs. time for three independent determinations. The data were fit by single-phase exponential decay (GraphPad Prism) and yielded a half-life of 105.6 minutes for the wild-type SH3-SH2 dimer vs. 40.8 minutes for the P327A mutant. The initial protein concentration in each sample was 50 µM. Representative SEC elution profiles are shown in Figure 27.

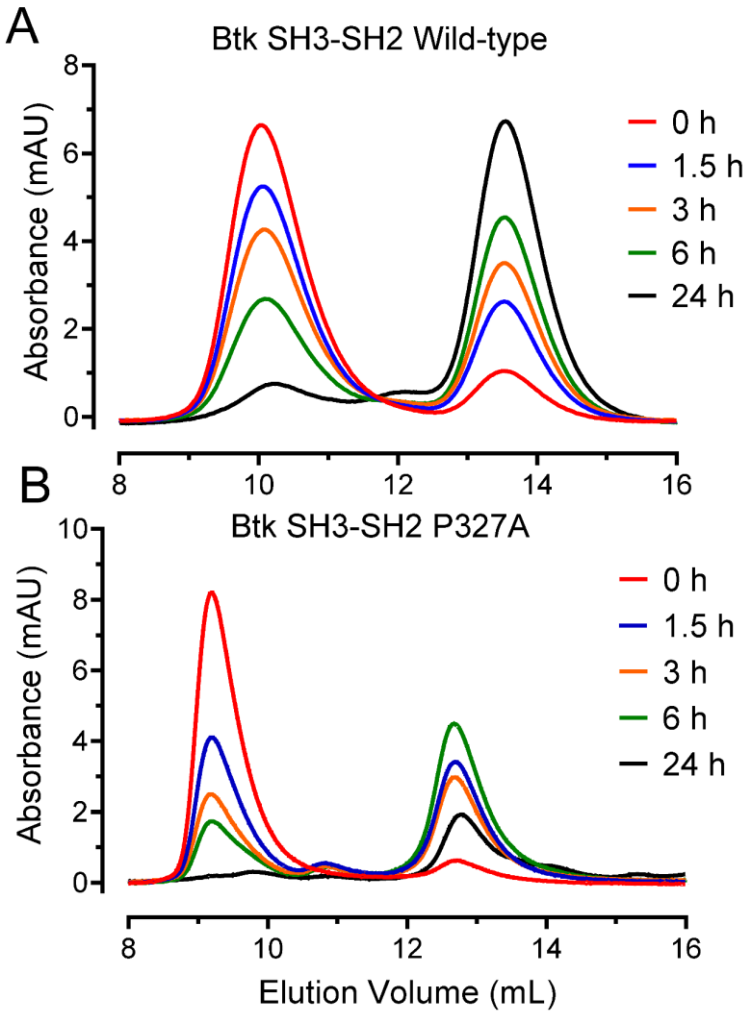

Figure 27. Dissociation of wild-type BTK SH3-SH2 homodimers vs. the SH3-SH2 P327A mutant by SEC.

Representative SEC elution profiles for the wild-type and P327A mutant forms of the BTK SH3-SH2 dimer protein. Equivalent sample volumes (100 µL) with each protein at a starting concentration of 12 µM were loaded onto a Superdex 75 10/300 GL size exclusion column after incubation at room temperature for each of the time points indicated. Purified protein elution was monitored as absorbance at 280 nm. A) The wild-type homodimer dissociated completely to the monomeric form after 24 hours. B) The P327A dimer dissociated into the monomeric form more rapidly. This experiment was repeated in triplicate, and the dimer to monomer ratio was estimated from the height of each peak. Plots of peak height vs. time are presented in Figure 26C.

2.3.8 Nef stabilizes BTK dimer formation at the cell membrane

Previous work has demonstrated that HIV-1 and SIV Nef proteins recruit BTK to the plasma membrane in transfected cells, resulting in activation loop autophosphorylation and

constitutive kinase activation [365]. While BTK activation by Nef at the membrane was shown to require Nef homodimers, the mechanism of Nef interaction with BTK was not explored. Based on our observation that recombinant HIV-1 Nef homodimers stabilize the BTK SH3-SH2 dimer *in vitro* (Figure 25), we hypothesized that Nef may also promote BTK dimerization at the cell membrane as an initial step in kinase activation. To test this hypothesis, we combined bimolecular fluorescence complementation (BiFC) and immunofluorescence (IF) microscopy to visualize and quantify BTK dimerization in absence and presence of HIV-1 Nef. Human BTK was fused to each of two complementary, non-fluorescent fragments of the Venus variant of YFP (VN and VC). BTK-VN and BTK-VC were then expressed either alone or together with Nef in 293T cells, followed by immunostaining with antibodies to Nef or to a V5 epitope tag on BTK. Three-color confocal microscopy allowed us to assess BTK homodimer formation as BiFC of the Venus fluorophore as well as Nef and BTK protein expression in individual cells. In the absence of Nef, BTK showed diffuse cytoplasmic staining with a weak BiFC signal, consistent with low levels of BTK homodimerization. Co-expression with Nef resulted in a stronger, membrane-localized BiFC and BTK signals (representative images shown in Figure 28A). To quantify the result, we determined the BiFC and BTK expression fluorescence intensities for at least 100 cells and found that the BiFC to BTK expression ratios were significantly higher in the presence of Nef (Figure 28B). These results show that Nef promotes BTK dimerization at the cell membrane.

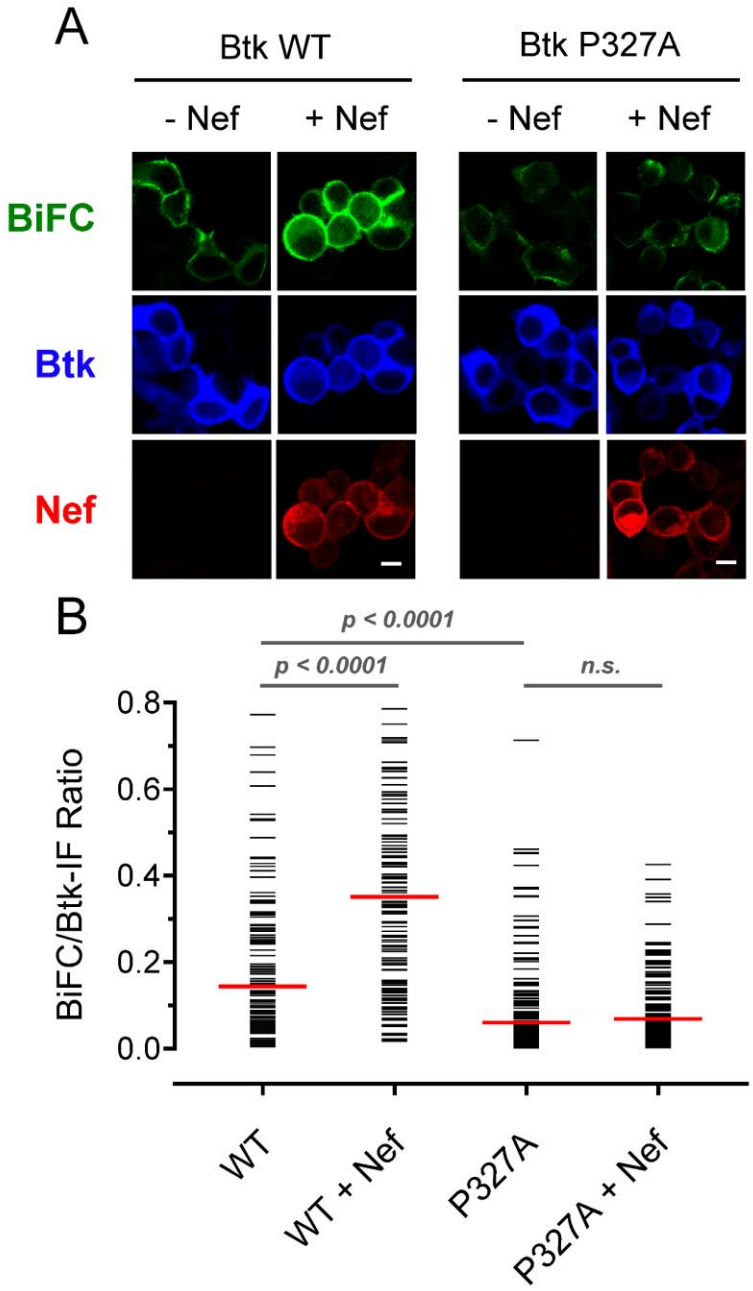

Figure 28. Nef-induced BTK dimerization at the cell membrane requires SH2 domain CD loop Pro327.

Wild-type and SH2 P327A mutant forms of BTK were expressed as BiFC pairs either alone or in the presence of Nef in 293T cells. The cells were immunostained for Nef and BTK protein expression and imaged by confocal microscopy to detect BTK dimerization (BiFC, green), Nef (red), and BTK (blue). A) Representative images. Scale bar, 10 µm. B) Single-cell image analysis. Mean fluorescence intensities for the BiFC and BTK signals were determined for at least 100 cells from each condition using ImageJ. The fluorescence intensity ratio (BiFC:BTK expression) for each cell is shown as a horizontal bar, with the median value indicated by the red bar. Student's t tests were performed on the groups indicated by horizontal lines above the plot; $p > 0.0001$ in each case (***). Scale bar, 10 µm.

We next investigated whether an intact BTK SH2 domain CD loop was required for BTK dimerization at the cell membrane. BiFC expression constructs of BTK harboring the CD loop P327A mutation were co-expressed in 293T cells in the presence and absence of Nef, and the BiFC (BTK homodimerization) and BTK expression signals were acquired by confocal microscopy as before (representative images shown in Figure 28A). Single-cell image analysis showed that BiFC to BTK expression ratios for cells expressing BTK P327A were significantly lower than those observed with wild-type BTK (Figure 28B). The presence of Nef did not significantly alter the BiFC to BTK expression ratios for BTK P327A despite the presence of membrane-localized Nef. These observations suggest that BTK Pro327 and by extension SH2•SH3 interaction promotes BTK homodimerization at the membrane in the presence of Nef.

2.3.9 BTK homodimerization promotes kinase activation

Data presented above demonstrate that interaction with Nef stabilizes BTK homodimers at the cell membrane. Stabilization requires BTK Pro327 in the SH2 domain CD loop, suggesting a unique SH3•SH2 interaction mechanism of Nef-mediated kinase activation. To test this hypothesis, we compared the effect of Nef on BTK kinase activity using the kinetic kinase assay described earlier. First, the recombinant full-length BTK P327A mutant was expressed in bacteria and purified using the same protocol developed for wild-type BTK. Kinetic analysis showed that the K_m values for both ATP and the peptide substrate were very similar for each kinase (Table 1). Next, the initial kinase reaction velocities were determined over a range of kinase amounts. The reaction rates were then fit by linear regression to determine kinase specific activity (Table 1). The specific activity of BTK P327A was approximately 68% of that observed for wild-type BTK, suggesting that homodimerization involving Pro327 may influence kinase activity *in vitro*.

Next, we performed kinetic kinase assays to determine the effect of Nef on the rates of peptide substrate phosphorylation by BTK P327A as well as autophosphorylation in comparison to wild-type BTK. Representative progress curves are shown in Figures 29A and 29B, and a statistical comparison of replicate steady state peptide phosphorylation rates are presented in Figure 29C. Nef enhanced both substrate and autophosphorylation of wild-type BTK as observed previously but had no effect on the kinase activity of the P327A mutant. This result shows that the BTK SH2 domain CD loop is essential for Nef-mediated kinase activation *in vitro*.

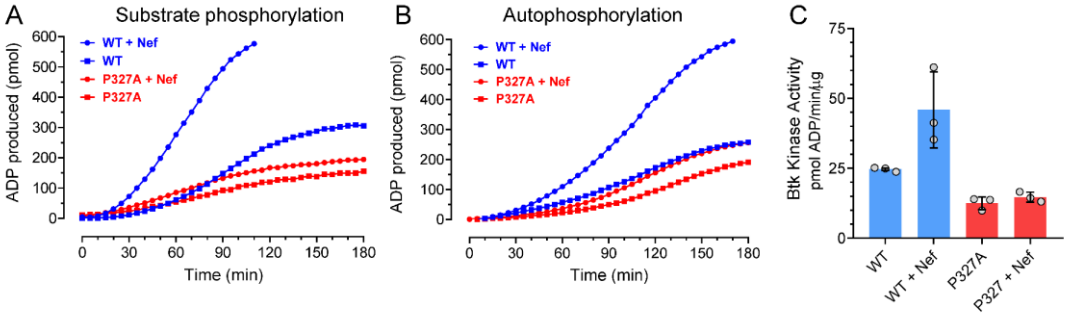

Figure 29. The BTK SH2 domain CD loop is required for Nef-mediated activation *in vitro*.

The ADP-Quest assay was used to measure ADP production by wild-type and P327A mutant forms of BTK in the presence of a peptide substrate (A) or as kinase autophosphorylation (B) either alone or in presence of HIV-1 Nef as shown. Each data point is the average of four technical replicates. ATP and peptide substrate concentrations were set to the respective K_m values for each kinase (see Table 1). C) Steady-state kinase activity was determined for 3 independent experiments (grey points). The height of each bar indicates the mean value ± SE; addition of Nef significantly increased the rate of wild-type BTK activity ($p < 0.05$) but did not impact BTK P327A activity.

To extend these studies to a cellular context, we combined analysis of Nef-BTK interaction by BiFC with antiphosphotyrosine (pTyr) antibody staining using an approach previously developed for wild-type ITK and BTK [365]. In this approach, the BTK wild-type and P327A mutant coding sequences were fused to a non-fluorescent C-terminal fragment of Venus (VC) while the HIV-1 Nef sequence was fused to the N-terminal Venus fragment (VN). The kinase-VC fusions were then expressed in 293T cells either alone or together with Nef. When expressed alone, wild-type BTK exhibited diffuse subcellular localization and low levels of anti-pTyr

immunoreactivity (Figure 30A). In comparison, the BTK P327A mutant alone exhibited even lower anti-pTyr signals compared to wild-type consistent with the *in vitro* kinase assay data. In the presence of Nef, wild-type BTK exhibited strong anti-pTyr fluorescence at the cell periphery, consistent with Nef-mediated kinase recruitment and activation at the cell membrane as reported previously [365]. In contrast, the BTK P327A mutant showed no change in anti-pTyr fluorescence intensity or subcellular localization in presence of Nef. Single cell image analysis shows that cells expressing wild-type BTK alone have significantly higher pTyr to BTK protein fluorescence intensity ratios compared to cells expressing the BTK P327A mutant (Figure 30B). Moreover, while co-expression with Nef resulted in a significant increase in the pTyr to BTK fluorescence ratio, Nef had no effect on the BTK P327A ratio. This result strongly suggests that BTK activation by Nef requires the formation of the SH3•SH2 dimer that is regulated by SH2 Pro327.

We also compared the BiFC signal originating from interaction of each BTK-VC protein with Nef-VN. Co-expression of wild-type BTK produced a clear membrane-associated BiFC signal with Nef, indicative of Nef-mediated BTK recruitment to the plasma membrane as reported previously [365]. However, co-expression of Nef-VN with the BTK-VC P327A mutant showed a comparatively lower BiFC signal (Figure 30A) that was confirmed in single cell image analysis of the BiFC to BTK protein fluorescence intensity ratios (Figure 30C). Reduced interaction of wild-type Nef with full-length BTK P327A in the cell-based BiFC assay is consistent with our observation that Nef•BTK SH3-SH2 complex formation *in vitro* requires that both partners are homodimerization competent (see Figure 21).

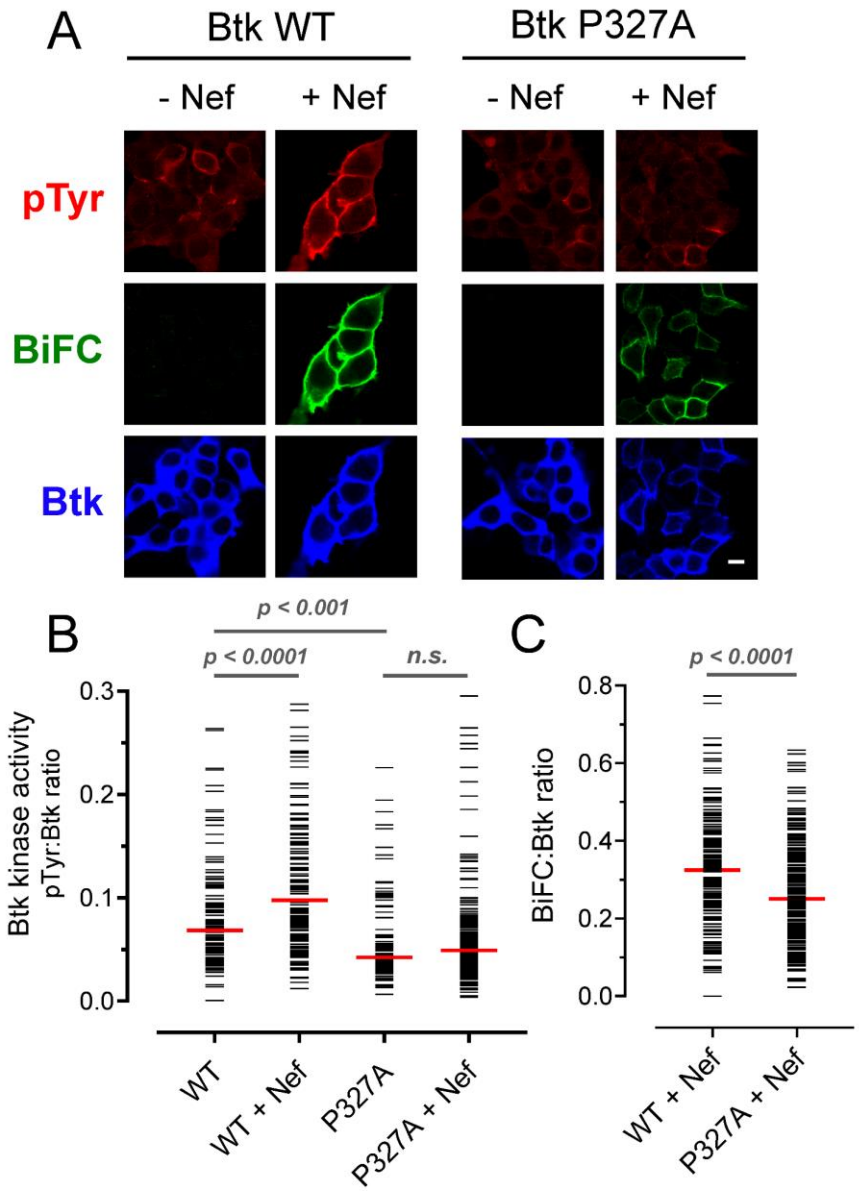

Figure 30. Nef-induced BTK activation at the cell membrane requires SH2 domain CD loop Pro327.

A) Wild-type and SH2 P327A mutant forms of BTK were expressed either alone or as a BiFC pair with Nef in 293T cells. The cells were immunostained with anti-phosphotyrosine (pTyr) antibodies and for BTK protein expression followed by confocal microscopy to detect pTyr (red), BTK•Nef interaction (BiFC, green), and BTK expression (blue). A) Representative images. Scale bar, 10 µm. B) Single-cell image analysis of BTK activity. Mean fluorescence intensities for the pTyr and BTK signals were determined for at least 100 cells from each condition using ImageJ. The fluorescence intensity ratio (pTyr to BTK expression) for each cell is shown as a horizontal bar, with the median value indicated by the red bar. C) Single cell image analysis of BTK•Nef interaction. Mean fluorescence intensities for BTK•Nef BiFC interaction and BTK expression were measured for at least 100 cells by ImageJ. The normalized BTK•Nef BiFC intensity ratio for each cell is shown as a horizontal bar with the median value indicated by the red bar. Student's t tests were performed on the groups indicated by horizontal lines above the plot and the p values are shown; n.s., not significant. Scale bar, 10 µm.

2.3.10 P327A mutation does not affect PIP_3 mediated BTK activation

BTK downregulation is maintained through several intramolecular interactions involving the SH3 domain and the SH2-kinase linker, the C-tail terminal tail and the SH2 domain, as well as the PHTH and kinase domains [607]. While BTK can be activated by ligand perturbation of these autoinhibitory interactions, physiological BTK activation is mainly triggered in response to PIP_3 generation in the cell membrane by activation of PI3K following antigen receptor stimulation [616]. To test whether BTK activation by PIP_3 involves dimerization mediated by interaction of SH3 and SH2 as observed with Nef, we compared the activation loop autophosphorylation of wild-type and P327A mutant forms of BTK in response to PIP_3-containing liposomes. Incubation with liposomes containing 100% 1,2-dioleoyl-*sn*-glycero-3-phosphocholine (DOPC) and ATP had no detectable effect on autophosphorylation of either kinase under these conditions. However, both the wild-type and P327A mutant kinases were readily activated following a five-minute incubation with liposomes containing 95% DOPC and 5% PIP_3 plus ATP (Figure 31). This observation suggests that BTK SH3•SH2 dimerization is not required for PIP_3-mediated BTK activation at the cell membrane. Instead, Nef may have evolved a unique mechanism to recruit BTK to the membrane and trigger its constitutive activation by stabilizing a homodimer involving the SH3•SH2-mediated interface.

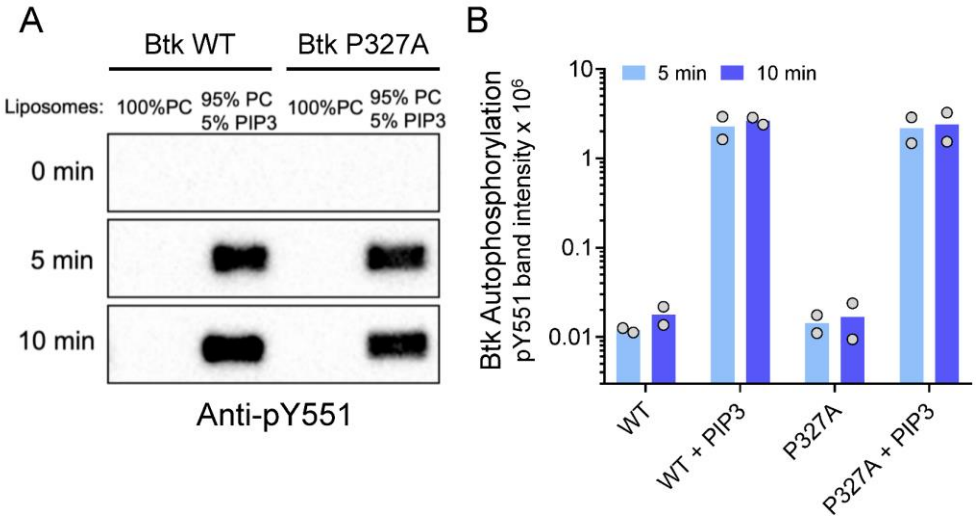

Figure 31. An intact BTK SH2 domain CD loop is not required for PIP_3-mediated activation *in vitro*.

Wild-type and P327A mutant forms of BTK were incubated in the presence of ATP and phosphatidylcholine (PC) liposomes with or without 5% PIP_3. A) Aliquots were taken from each kinase reaction at the time points shown and BTK autophosphorylation was assessed by immunoblotting with phosphospecific antibodies to the activation loop phosphotyrosine (Anti-pY551). A representative set of immunoblots is shown; bands present in the control lanes (100% PC liposomes) are not visible in this exposure. B) BTK anti-pY551 band intensities from two independent experiments were corrected for background and plotted; bar height represents the mean value.

2.4 Discussion

This study builds on previously reported observations of Nef-induced constitutive activation of ITK and BTK at the cell membrane [365] with the discovery of the unique molecular mechanisms that govern Nef interaction and activation of these Tec family members. Using a kinetic kinase assay, we showed that HIV-1 and SIV Nef proteins increase both steady-state substrate phosphorylation and autophosphorylation rates of BTK. Unexpectedly, an HIV-1 Nef mutant harboring alanine residues in place of the prolines in the conserved PxxPxR motif activated BTK to the same extent as wild-type Nef. This finding contrasts with the inability of this mutant to activate the Src-family kinase HCK and suggests that Nef-induced activation of BTK does not

require displacement of the intramolecular regulatory contact between the SH3 domain and the SH2-kinase linker found in both kinases [617]. Older work has pointed to alternative modes of interactions between Nef and the regulatory domains of other Src-family kinases. Nef has been reported to interact with the SH3 and SH2 domains of Lck, with SH2 interaction compensating for the low affinity of SH3 interaction [499]. Nef interaction with the Lck SH2 domain is independent of Nef tyrosine phosphorylation and does not require the phosphotyrosine binding pocket of the Lck SH2 domain. However, these interactions do not stimulate Lck kinase activity *in vitro* [618]. SIV Nef also interacts with select Src-family members via their SH2 domains, independently of the Nef SH3-binding motif [619]. Our work with BTK clearly shows that interaction with Nef requires the tandem SH3-SH2 unit as a preformed homodimer, suggesting a complex recognition surface for Nef distinct from that observed with Src-family kinase SH3 and SH2 domains. These observations underscore the remarkable versatility of this viral accessory protein in terms of hijacking diverse host cell kinase signaling pathways.

Quantitative binding measurements by SPR and analytical SEC provided new insights regarding the molecular mechanisms underpinning not only Nef interactions with BTK but also additional intermolecular contacts within the kinase itself. SEC analysis of the BTK regulatory domains revealed that while the individual SH3 and SH2 domains exist as monomers in solution, the SH3-SH2 dual domain protein forms a mixture of monomers and dimers. In the absence of a crystal or NMR structure of the BTK SH3-SH2 fragment, we turned to the related ITK SH3-SH2 NMR structure for clues to the basis of BTK SH3-SH2 dimerization. In this NMR structure, ITK SH3 and SH2 individual domains were observed to interact in a mechanism consistent with dimerization and not intramolecular association. Previous work has shown that Pro287 in the ITK SH2 domain CD loop domain is subject to peptidyl prolyl *cis*/*trans* isomerization, with the *cis*

conformer preferentially binding to the SH3 domain of another monomer to form a dimer [562]. Structural alignment of the BTK SH3 and SH2 domains onto the ITK SH3•SH2 dimer interface formed by individual ITK SH3 and SH2 domains in NMR, identified an analogous role for Pro327 in the BTK SH2 domain CD loop for SH3 domain contact and dimer formation in BTK SH3-SH2 dual domain protein. Substitution of BTK Pro327 with alanine reduced the stability of BTK SH3-SH2 homodimers by SEC analysis. This regulatory role for Pro327 was also observed with full-length BTK in a cell-based BiFC assay, where the P327A mutation reduced homodimerization at the membrane in comparison to wild-type BTK. The BTK P327A mutant also showed lower specific activity than wild-type BTK *in vitro*, suggesting a role for homodimerization mediated by SH3•SH2 interaction in the regulation of BTK kinase activity.

To our knowledge, a role for an SH3-SH2 interface in BTK dimerization has not been reported before, although alternative dimerization mechanisms involving the PHTH and SH3 domains have been described. For example, BTK has been shown to form an asymmetric homodimer where the N-terminal proline-rich region of one BTK monomer contacts the SH3 domain in the other monomer [554]. In addition, crystal structures and membrane-binding kinetics show that the PHTH domain mediates BTK dimerization at the membrane in a PIP_3-dependent manner [532, 536]. These observations support a model in which membrane recruitment in response to PI3K activation and kinase dimerization are coordinated by the PHTH domain. Finally, a crystal structure of the BTK SH3-SH2-kinase core region revealed a domain-swapped dimer involving the SH2 domain [532]. This dimeric state was observed in solution as well, since the protein was purified as a monomer-dimer mixture although only the dimer was present in the crystal. The SH2 domain region involved in the swap does not involve Pro327, suggesting that this mechanism is not directly related to the Nef effects on kinase stabilization reported here.

Our results support a model in which Nef dimers directly recruit and stabilize BTK homodimers at the cell membrane leading to sustained kinase activation (Figure 32). None of the individual BTK regulatory domains (PHTH, SH3, SH2) interacted with HIV-1 Nef by SPR or analytical SEC. However, the dual SH3-SH2 domain protein bound Nef both by SPR and in solution, with SEC data supporting a 2:2 complex stoichiometry as observed previously for the SH3-SH2 region of HCK when complexed to Nef [620]. Interestingly, complex formation in solution as measured by SEC required that both the Nef and BTK SH3-SH2 proteins exist as preformed homodimers. Cell-based BiFC assays are also consistent with this observation, where Nef interacted with wild-type BTK but had no effect on the P327A mutant, which is dimerization-defective in cells. Previous studies have shown that wild-type Nef forms homodimers through an interface involving conserved hydrophobic residues Leu112, Tyr115, and Phe121 [169] as observed in previous crystal structures. Mutation of these residues reduces Nef homodimer formation by BiFC assay and compromises activation of both BTK and ITK in cells [365], an observation confirmed here with the same Nef mutants and BTK using an *in vitro* kinase assay. Interestingly, while each of these dimerization-defective Nef mutants retained interaction with BTK and ITK in cells, the extent of interaction compared to wild-type Nef was reduced (Li et al., 2020). These observations suggest that Nef homodimer formation at the cell membrane is a necessary prerequisite for recruitment and activation of BTK.

BTK plays a critical role in B-cell development and B-cell receptor (BCR) signaling. Engagement of the BCR by specific class II MHC-antigen complexes triggers a signaling cascade that results in BTK activation through an intricate series of molecular events [616]. First, the Src-family kinase LYN phosphorylates BCR immunoreceptor-tyrosine-based activation motifs (ITAMs). The phosphorylated ITAMs recruit and activate SYK through its SH2 domains, which

in turn phosphorylates the B-cell adaptor protein for PI3K (BCAP) to promote activation of PI3K. Activated PI3K produces PIP_3 in the membrane, which then recruits BTK. PIP_3 recruitment of BTK to the membrane results in BTK activation through dimerization mediated by the PHTH domain as described above [536]. In the present study, we observed that PIP_3-containing liposomes equally activated wild-type BTK as well as the P327A mutant, suggesting that the unique SH3•SH2-mediated dimerization event utilized by Nef may not contribute to BTK activation during BCR signaling. That said, BTK is known to sample many different conformational ensembles [616] that may include the SH3•SH2-mediated dimers described here. The opportunistic presence of Nef homodimers in the membrane of HIV-infected cells may stabilize this BTK dimer conformation, thereby shifting the equilibrium towards this unique active form of BTK.

In addition to B cells, BTK is also expressed in HIV-1 host cells of myeloid lineage where HIV-1 infection enhances BTK expression and autophosphorylation [581]. Inhibitors of BTK as well as siRNA knockdown of BTK expression selectively induced apoptosis of HIV-1-infected cells but not their uninfected counterparts, supporting a specific role for BTK in the HIV-1 lifecycle [581]. Proteomic profiling of a latently infected T cell line also revealed the presence of BTK, suggesting that HIV-1 infection of T cells may induce BTK expression for the benefit of the virus [621]. In T cells, ITK, which normally regulates TCR signaling, contributes to multiple facets of the HIV-1 lifecycle. Using both pharmacological inhibitors and siRNA knockdown, Readinger *et al.* established a key role for ITK activity in viral transcription, particle assembly, and viral spread [603]. Subsequent work showed that HIV-1 Nef is responsible for ITK activation, as replication of Nef-defective HIV-1 was not affected by an ITK-specific kinase inhibitor [604]. Both HIV-1 and SIV Nef activate BTK and ITK following recruitment to the membrane and

formation of a 2:2 dimer complex [365]. The finding that activation of both ITK and BTK is dependent on Nef dimerization suggests a common mechanism in which Nef exploits SH3•SH2 interaction as described here. Unlike BTK, however, the ITK PHTH domain does not dimerize at cell membrane in response to PIP_3 generation by PI3K [536]. This observation raises the possibility that in absence of a stabilizing PHTH dimer, SH3•SH2 mediated dimerization might play a greater role in physiological ITK activation.

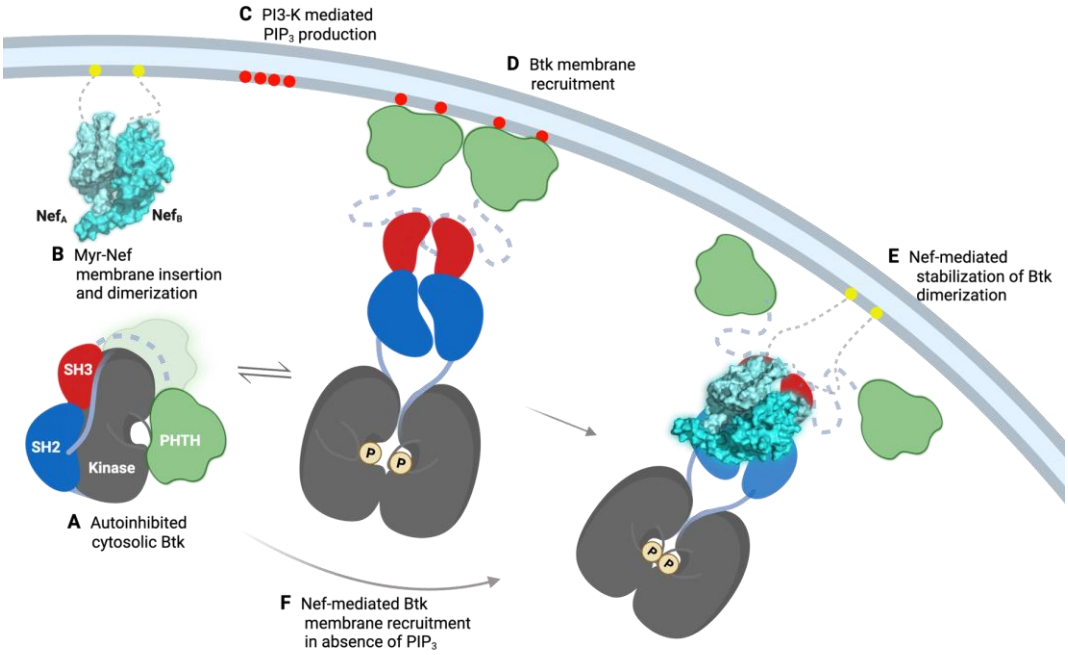

Figure 32. Proposed model of Nef-induced BTK activation.

A) Autoinhibited BTK adopts a closed structure with multiple intramolecular interactions between the kinase domain and the regulatory PHTH, SH3, and SH2 domains. In this downregulated state, the PHTH domain has been observed to occlude the BTK activation loop by NMR (green position) while docking on the N-lobe of kinase domain in crystal structure (light green position). B) HIV-1 Nef is targeted to the membrane by virtue of myristoylation (yellow circles) where it forms homodimers (Nef_A and Nef_B monomers rendered in light and dark cyan). C) Under physiological conditions, PI3K generates PIP_3 (red circles) in the cell membrane which D) recruits BTK via its PHTH domain which also mediates homodimer formation and kinase activation. E) In HIV-infected cells, Nef homodimers recruit and stabilize BTK dimers through SH3-SH2 interactions to stimulate kinase activity in the absence of PIP_3. F) Membrane recruitment and stabilization of the BTK dimer by Myr-Nef may represent a mechanism by which Nef bypasses the PI3K/PIP_3 requirement for BTK activation.

Table 1. Kinetic parameters for recombinant HCK and BTK kinase proteins used in this study.

Respective K_m values were calculated from 3 independent experiments. Peptide and ATP K_m values for HCK are from Moroco *et al*. [610].

Kinase	Peptide Substrate	Substrate K_m	ATP K_m	Specific activity pmol ADP/min/µg kinase
HCK	YIYGSFK	84 µM	56 µM	39.2 ± 2.8
BTK-WT	EQEDEPEGIYGVLF	112 µM	96 µM	23.6 ± 1.5
BTK-P327A	EQEDEPEGIYGVLF	124 µM	99 µM	16.2 ± 1.4

2.5 Materials and Methods

2.5.1 Expression vectors

Construction of full-length murine BTK with a stabilizing Y617P mutation and a C-terminal His6-Tag in the bacterial expression plasmid pET-20b (+) has been described elsewhere [607]. Site-directed mutagenesis was performed to create the BTK SH2 domain P327A mutant using the QuikChange II XL site-directed mutagenesis kit (Agilent). The murine BTK PHTH domain (residues Met1-Lys176), SH3 domain (Glu215-Ser275), SH2 domain (Trp281-Ser378), and SH3-SH2 dual domain (Glu215-Ser378) coding sequences were PCR-amplified and subcloned into the pET-SMT3 expression vector, which fuses a His6-SUMO tag to the N-terminus of each protein. The coding region of full-length HIV-1 Nef (SF2 variant) was subcloned into the

bacterial expression vector pET-21b and used to generate mutants (2PA, L112D, Y115D, F121A) via site-directed mutagenesis (Agilent). SIV Nef (mac239 variant) was subcloned into pET-21a for bacterial expression. Construction of bacterial expression vectors for the representative M group HIV-1 Nef subtypes A1, NL4-3, F1, G, J, and K is described elsewhere [609]. The coding regions for the C-clade Nef genes from the transmitter/founder proviral clones ZM249M, Z3618M and CH185 were PCR-amplified and subcloned into pET-Smt3. All coding regions generated by PCR were confirmed by Sanger sequencing.

For BiFC experiments, a full-length cDNA clone of human BTK was obtained from the Dana-Farber/Harvard Cancer Center PlasmID DNA Resource Core (BTK, #HsCD00346954). Using PCR, the 3´ end of the coding region of BTK was fused with a V5 epitope tag followed by the C-terminal coding fragment of the Venus variant of YFP (residues Ala154 to Lys238) to create the BTK-VC fusion construct in mammalian expression vector pCDNA3.1(-) (Invitrogen). The 3´ end of the BTK coding region was similarly fused to the complementary N-terminal coding fragment of Venus (Val2 to Ala154) to create the BTK-VN construct in pCDNA3.1(-). Site-directed mutagenesis was performed to obtain the P327A mutants using both BTK BiFC constructs as templates (Agilent). Mammalian expression vectors for HIV-1 Nef (SF2 variant) either untagged or C-terminally tagged to the N-terminal fragment of Venus (Nef-VN) in the plasmid pCDNA3.1(-) have been described [604].

2.5.2 Recombinant protein expression and purification

E. coli strain Rosetta2(DE3)pLysS (EMD Millipore) was used for all recombinant protein expression. Expression and purification of His6-tagged Nef proteins, HCK SH3, and near-full-length HCK-YEEI is described in detail elsewhere [365, 613, 620]. *E. coli* cells were co-

transformed with murine BTK (Y617P) and the *Yersinia pestis* tyrosine phosphatase gene, YopH, and a single colony was used to inoculate a 5 mL LB starter culture. After overnight culture at 37 °C, the starter culture was used to inoculate 2x 1 L of LB in 2 baffeled flasks and grown to an A_{600} of 0.6. The culture was cooled at 18 °C for 1 h, IPTG was added to 0.1 mM, followed by 16 h incubation for recombinant protein induction. The bacterial cells were collected by centrifugation and stored at -80 °C until purification.

Induced cell pellets were resuspended in 50 mL His-Trap binding buffer (50 mM KH_2PO_4, 75 mM NaCl, 20 mM Imidazole, pH 8.0) in presence of cOmplete EDTA-free protease inhibitor cocktail (Sigma). The resuspended cells were passed through an M110P microfluidizer (Microfluidics) 10 times at 4 °C and the lysate was clarified by centrifugation at 100,000 x g for 1 h at 4 °C. The supernatant was loaded onto a 5 mL HisTrap HP column (Cytiva). Bound protein was washed with 100 mL of binding buffer with 40 mM imidazole and eluted using a linear gradient of 20 to 500 mM imidazole in binding buffer. Fractions containing BTK were pooled to a volume of 10 mL and dialyzed against 4 L ion-exchange buffer A (20 mM Tris-HCl, 40 mM NaCl, 10% (v/v) glycerol, pH 8.0) for 8 hours. Dialyzed protein was loaded onto a 5 ml Hi-TrapQ HP column (Cytiva) pre-equilibrated with ion-exchange buffer A. Bound proteins were eluted with a linear gradient of 40 mM to 500 mM NaCl using ion-exchange buffer B (ion-exchange buffer A with 500 mM NaCl). The fractions containing BTK were pooled and dialyzed against 4 L gel filtration buffer (20 mM Tris-HCl, 150 mM NaCl, 10% (v/v) glycerol, pH 8.0) for 8 hours. After dialysis, BTK was purified by gel chromatography using Hi-Load 16/60 Superdex 75 column (Cytiva). Fractions containing BTK were pooled, concentrated to 5.96 mg/mL and stored at -80 °C. BTK P327A was purified by the same method and concentrated to 1.07 mg/mL.

The individual BTK domains (PHTH, SH3, SH2) and the dual domain SH3-SH2 protein were expressed as N-terminal His6-SUMO fusion proteins. The BTK fragment proteins were expressed and purified using the same protocol as full-length BTK with the following modification to remove the SUMO tag. After elution from the His-TrapHP column, proteins were dialyzed against 1 L His-Trap binding buffer without imidazole for 8 h followed by incubation with recombinant His6-Ubl-specific protease 1 (Ulp1) for 2 h while rocking at 4 °C. This mixture was reloaded onto the His-TrapHP column, where the Ulp1-cleaved and now untagged BTK proteins were collected in the flow-through while the His6-Ulp1 and His6-SUMO tag remained bound to the column. The BTK fragment proteins were further purified by ion-exchange and size exclusion chromatography as described above for full-length BTK. All BTK domains eluted as a single peak corresponding to the monomer species, except for the dual domain BTK SH3-SH2 (wild-type and P327A mutant) which eluted as a mixture of dimers and monomers. Fractions corresponding to dimers and monomers were separately pooled, concentrated, and stored at -80 °C. The concentrations of the final proteins are as follows: BTK PHTH, 2.08 mg/mL; BTK SH3, 4.56 mg/mL; BTK SH2, 0.37 mg/mL; BTK SH3-SH2 wild-type monomer, 3.5 mg/mL; BTK SH3-SH2 wild-type dimer, 3.05 mg/mL; BTK SH3-SH2 P327A monomer, 1.3 mg/mL; BTK SH3-SH2 P327A dimer, 0.58 mg/mL.

Purification of the clade-C Nef proteins involved a similar approach. Each induced bacterial cell pellet resuspended in 50 mL Ni-IMAC binding buffer (25 mM Tris-HCl, 0.5 M NaCl, 20 mM Imidazole, 10% (v/v) glycerol, 2 mM β-mercaptoethanol, pH 8.3) supplemented with the cOmplete protease inhibitor cocktail and lysed by five microfluidizer passes. The lysate was clarified by ultracentrifugation (100,000 x g) for 1 hour and loaded onto a 5 mL HisTrap HP column and washed with 20 column volumes of binding buffer. The His6-Smt3-Nef protein was

eluted with a linear gradient from 0% to 50% of Ni-IMAC elution buffer (binding buffer plus 0.5 M imidazole) over 32 column volumes. Fractions containing the His6-Smt3-Nef protein were pooled and dialyzed against Nef SEC buffer (20 mM Tris-HCl, 150 mM NaCl, 10% (v/v) glycerol, 2 mM TCEP, pH 8.3). Recombinant purified His6-Ulp1 protease was added followed by rocking at 4 °C for 3 h to cleave the His6-Smt3 tag from the Nef N-terminus. Following protease treatment, the proteins were loaded onto a 5 mL HisTrap HP column, and the cleaved Nef protein was collected in the flow-through fractions. The Nef protein concentrated to 5 mL using a 50 mL stirred cell concentrator (Amicon) with a 10 kDa molecular weight cutoff membrane (Millipore) and loaded onto a HiLoad Superdex 75 26/600 prep-grade SEC column. Fractions containing the purified C-clade Nef proteins were pooled and concentrated to 7.0 – 10.0 mg/mL, aliquoted, snap frozen in liquid nitrogen and stored at -80 °C.

2.5.3 In vitro kinase assay

Kinetic kinase assays were performed using the ADP Quest Assay (Eurofins) [622]. In this assay, production of ADP resulting from phosphorylation is coupled to generation of pyruvate from phosphoenolpyruvate (PEP) by pyruvate kinase and regeneration of ATP. Pyruvate is then converted to hydrogen peroxide by pyruvate oxidase. Hydrogen peroxide then oxidizes Amplex Red to the fluorescent product, resorufin (Ex 530 nm/Em590 nm) which is monitored over time. All assays were performed in quadruplicate in black 384-well microplates (Corning Catalog no. 3571). ATP stock was prepared at 50 mM in 10 mM Tris-HCl, pH 7.0. Kinase substrate peptide stocks (HCK, YIYGSFK 5.0 mM; BTK, EQEDEPEGIYGVLF, 3.2 mM) were prepared in ADP Quest assay buffer (15 mM HEPES, pH 7.4, 20 mM NaCl, 1 mM EGTA, 0.02% Tween-20, 10 mM $MgCl_2$, 0.1 mg/mL BSA). Reactions (50 µL) were initiated by adding ATP and contained 125

ng kinase protein with the final ATP and peptide substrate concentrations at their respective K_m values. Nef proteins were included at a 10-fold molar excess over each kinase protein. Plates were read at 5 min intervals for 3 h on a Molecular Devices SpectraMax M5 microplate reader. Each experiment contained four replicate wells per condition and all experiments were repeated three times.

Analysis of fluorescence data to yield reaction rates was performed as described [610]. Each kinase assay included controls for non-enzymatic production of ADP (no kinase added) and kinase autophosphorylation (no peptide substrate). Raw fluorescence data from four wells for each condition were averaged and corrected for non-enzymatic ADP production and autophosphorylation. Corrected fluorescence units were plotted against time to determine the steady-state rates of reaction. Linear regression analysis (GraphPad Prism) was performed on the linear portion of each reaction progress curve to yield reaction rate as the slope. Fluorescence units (FU) were converted to pmol ADP produced/min using the correction factor of 4.18 FU/pmol ADP which was generated from a standard curve in which ADP was added to the reaction components in the absence of kinase protein.

2.5.4 Immunoblot analysis of BTK autophosphorylation

In vitro phosphorylation reactions were performed by incubating 125 ng BTK in kinase assay buffer (50 mM HEPES, pH 7.0, 10 mM $MgCl_2$, 1 mM DTT, 1 mg/mL BSA) at room temperature with Nef proteins added in 10-fold molar excess where indicated. The reactions were initiated by adding ATP to a final concentration of 96 µM, and aliquots were removed at various time points and quenched by heating to 95 °C for 5 min in SDS-PAGE sample buffer. The samples were separated by SDS-PAGE, transferred to nitrocellulose membranes, and immunoblotted with

rabbit monoclonal anti-BTK pY551 (Abcam, catalog no. ab40770) and mouse monoclonal anti-His6 (Abcam, catalog no. ab18184) antibodies. Secondary antibodies included anti-mouse or anti-rabbit IgG conjugated to 680 nm and 800 nm fluorophores, respectively (LI-COR). Blots were scanned using a LI-COR Odyssey imager, and signal intensities were quantified using the Image Studio Lite software. Data were plotted as ratios of BTK activation loop Tyr551 phosphorylation to BTK protein (His6) signals.

2.5.5 Surface plasmon resonance

Recombinant, purified HCK and BTK proteins were exchanged into SPR buffer (10 mM HEPES, pH 7.4, 150 mM NaCl, 3 mM EDTA, 0.05% (v/v) Surfactant P20). The proteins were covalently immobilized onto carboxymethyl dextran SPR chips (Reichert) using standard EDC/NHS amine coupling chemistry. HIV-1 Nef proteins were also dialyzed against SPR buffer and then injected in triplicate over a range of concentrations (0.123 to 10 µM) at a rate of 30 µL/min for one min followed by dissociation for 2 min. Kinetic rate constants were calculated from reference-corrected sensorgrams using the TraceDrawer software and best fit by 1:1 Langmuir binding models to yield kinetic K_D values.

2.5.6 Analytical size-exclusion chromatography and multi-angle light scattering

Analytical size-exclusion chromatography (SEC) was conducted using Superdex 75 10/300 GL and Superdex 75 Increase 10/300 GL columns (Cytiva). Proteins were dialyzed in SEC running buffer (20 mM Tris-HCl, 150 mM NaCl, 10% (v/v) glycerol, 2 mM TCEP, pH 8.0) for 4 h at 4 °C prior to SEC. All SEC runs were conducted at a flow rate of 0.4 mL/min.

Multi-angle light scattering was performed using a Superdex 75 10/300 GL column with in-line multiangle light scattering (Wyatt DAWN HELEOS II). Individual BTK SH3-SH2 and HIV-1 Nef proteins were run at 100 µM final concentration in SEC running buffer with glycerol at 5% (v/v). The molecular masses of eluted protein species were determined using the Wyatt ASTRA software.

2.5.7 BiFC assay and immunofluorescence

Human embryonic kidney 293T cells were cultured in Dulbecco's modified Eagle's medium supplemented with 10% fetal bovine serum (FBS; Gemini Bio-Products). Cells (1.5 x 10^5) were plated in 35-mm microwell dishes (MatTek, catalog no. P35G-1.5-14-C) and cultured overnight and transfected with X-tremeGENE 9 DNA transfection reagent (Sigma Aldrich) according to manufacturer's protocol. Forty hours post-transfection, the cells were fixed with 4% paraformaldehyde for 10 min, washed with PBS, permeabilized with 0.2% Triton X-100, followed by 2 additional PBS washes. The cells were then blocked with 2% BSA in PBS overnight. Cells were immunostained for 1 h at room temperature with anti-V5 (Thermo Fisher, catalog no. R960-25), anti-pTyr (Santa Cruz, catalog no. sc-7020), or anti-Nef antibodies (NIH AIDS Reagent Program, catalog no. 1539) diluted 1:1000 in PBS with 2% BSA. The cells were washed 3 times in PBS for 5 min each and stained with secondary antibodies conjugated to Pacific Blue (Thermo Fisher/Molecular Probes, catalog no. P10994) or Texas Red (Southern Biotech, catalog no. 1031-07), at dilutions of 1:1000 and 1:500, respectively. Immunostained images were acquired using a Nikon C2+ confocal microscope with a 20x objective using *x-y* scan mode. Single-cell image analysis was performed with the ImageJ software and the detailed protocol of Shu *et al*. [623]. Immunofluorescence intensity for at least 100 cells were measured with each antibody, and single-

cell data were calculated as the mean fluorescence intensity ratio of either kinase activity (pTyr) or BiFC (interaction) intensity to the BTK immunofluorescence (expression level).

2.5.8 Preparation of liposomes and kinase assay

To prepare control and 5% PIP_3 liposomes, 1,2-dioleoyl-sn-glycero-3-phosphocholine (DOPC) and 1,2-dioleoyl-sn-glycero-3-[phosphoinositol-3,4,5-trisphosphate] (tetra-ammonium salt) (PIP_3) (Avanti Polar Lipids) were dissolved in chloroform and mixed in glass test tubes at a molar ratio of 100:0 and 95:5. Chloroform was removed by blowing a gentle stream of nitrogen gas until no solvent was visible. The lipids were transferred to a vacuum desiccator and dried overnight at room temperature. Dry lipid films were hydrated in a buffer containing 50 mM HEPES pH 7.4, 150 mM NaCl, 5% (v/v) glycerol to a final concentration of 12.5 mM. The hydrated liposomes were subject to three freeze–thaw cycles using liquid nitrogen followed by 10 passes through 100-nm filters (Millipore) to generate small unilamellar vesicles.

Kinase assays were performed in 50 mM HEPES pH 7.4, 150 mM NaCl, 5% (v/v) glycerol, 1mM DTT, 10 mM $MgCl_2$ and 1 mM ATP. BTK wild-type and P327A mutant proteins (1 µM) were incubated with 500 µM control or PIP_3 liposomes for 10 min at room temperature. Samples from the reactions were collected and quenched with SDS sample buffer followed by SDS-PAGE and immunoblotting with the anti-pY551 antibody (EMD Millipore). The western blots were quantified using the ChemiDoc detection system (BioRad).

3.0 Crystallization screening of BTK SH3-SH2 in complex with HIV-1 Nef

3.1 Introduction

As discussed earlier in this document, Nef is essential for high-titer replication of HIV-1 *in vivo* and for disease progression to AIDS. This is underscored by the observation that a subset of HIV-infected individuals that do not progress to AIDS (long-term non-progressors) have mutated Nef alleles. Even though Nef does not have enzymatic properties, Nef mediates diverse functional effects by interacting with various host cell factors, like the MHC-I/AP-1 complex, the CD4/AP-2 complex, and the members of the SRC and TEC kinase families. Crystal structures of the HIV-1 Nef core in complex with the SH3 or dual SH3-SH2 domains of SFKs revealed the molecular basis of Nef-mediated SFK activation, where the highly conserved Nef PxxPxR motif plays a major role in SH3 binding. Inhibition of this pathway blocked Nef-mediated enhancement of HIV-1 replication, infectivity, and MHC-I downregulation [375, 624]. The complexes of the HIV-1 Nef core with the HCK SH3 and SH3-SH2 domains showed a 2:2 stoichiometry in solution, which was observed in crystal structures as well. In this study, HIV-1 Nef also formed a 2:2 complex with the BTK SH3-SH2 dual domain protein in solution, although the mechanism of interaction of Nef with the BTK SH3-SH2 region was clearly different and more complex than that observed with the HCK SH3 and SH3-SH2 domains. Crystallization of the HIV-1 Nef:BTK SH3-SH2 complex was therefore one of the major aims of this study.

Full-length BTK has resisted previous crystallization efforts as discussed under section 1.4.2.1. However, the structures of individual BTK domains have all been reported by either crystallography or NMR (PHTH, PDB: 4Y94; SH3, PDB: 1QLY; SH2, PDB: 2GE9; kinase, PDB:

3K54). Lack of a structure of the tandem SH3-SH2 domain of BTK suggests that the domains may exist in an equilibrium mixture of an ensemble of structures. In this study, I observed that the BTK SH3-SH2 protein exists as a mixture of monomers and dimers in solution, where the dimer rapidly transitions into monomeric form at room temperature. Therefore, the BTK SH3-SH2 requires a stabilizing factor in order to preserve the functional dimer conformation. I also showed that the HIV-1 Nef dimer binds and stabilizes the dimer conformation of the BTK SH3-SH2 protein. Mechanism of Nef-mediated BTK activation contrasts with Nef-mediated SFKs activation, even though the Nef homodimerization is a pre-requisite in both cases. Interacting surfaces in BTK or Nef is not yet known, and further studies are required to elucidate the molecular mechanism of Nef-mediated BTK activation at an atomic level. In this study, I attempted to crystallize a complex of the Nef and BTK interacting partners, and utilized several strategies to promote complex stability and crystal formation.

3.2 Results and Discussion

3.2.1 Co-crystallization of BTK SH3-SH2 and HIV-1 Nef

I purified the HIV-1 full-length Nef:BTK SH3-SH2 complex by co-expression in *E. coli*, which yielded a dimer complex of BTK SH3-SH2 and HIV-1 Nef. This complex was purified following protocol to purify BTK SH3-SH2 alone described before. SEC analysis at the end of the purification as well as SDS-PAGE indicated purification of BTK SH3-SH2 in complex with HIC-1 Nef in roughly equimolar ratio. This complex was concentrated to 8.16 mg/mL (Figure 33A), and I attempted to crystallize this complex first using the conditions summarized in Table 2. HIV-

1 Nef in full-length form has resisted crystallization as observed previously in our lab and by others; this is likely due to the flexible N-terminal anchor domain (residues 1-61). Therefore, I also co-expressed and purified the BTK SH3-SH2:HIV-1 Nef core domain complex containing only the folded core region of Nef (SF2 Nef residues 62-209); this complex was concentrated to 5.87 mg/mL (Figure 33A). Complexes of BTK SH3-SH2 with both full-length and the core region of HIV-1 Nef failed to produce crystals. About 50% of the individual crystallization conditions for both complexes resulted in precipitation immediately following incubation with crystallization solution, however no crystals were observed in either 4 °C or room temperature. This result was not completely unexpected as I also observed dissociation of the complex into monomer over time in solution (see section 2.3.6). Therefore, I first attempted to stabilize the BTK SH3-SH2:HIV-1 Nef core complex by performing differential scanning fluorimetry (DSF) using the complex with components of a crystallization additive screen (Hampton Research). This screening kit is designed to allow rapid evaluation of 96 unique additives and their ability to influence the stability of the sample [625]. A summary of the stability screens for the BTK SH3-SH2:HIV-1 Nef core complex is shown in Figure 33B. In this DSF stability assay, the BTK SH3-SH2:Nef core complex was incubated with several classes of additives and a thermal shift assay was conducted to monitor the thermal stability of the complex. In this experiment, melting point of the Nef:BTK SH3-SH2 complex was measured in buffer only or in presence of an additive according to method described in figure 24. All of the groups of additives tested failed to significantly improve the complex stability as measured by differential scanning fluorimetry (DSF) (Figure 33B). The melting-temperature of the complex in the buffer control was 48.3 °C, and the melting-temperatures measured across all the additive classes varied by less than 2 °C. Stabilization of proteins up to 7 °C was observed by others using this assay [625], and my observation of less than 2 °C

improvement suggests none of the additives significantly improved the BTK SH3-SH2:Nef core complex stability.

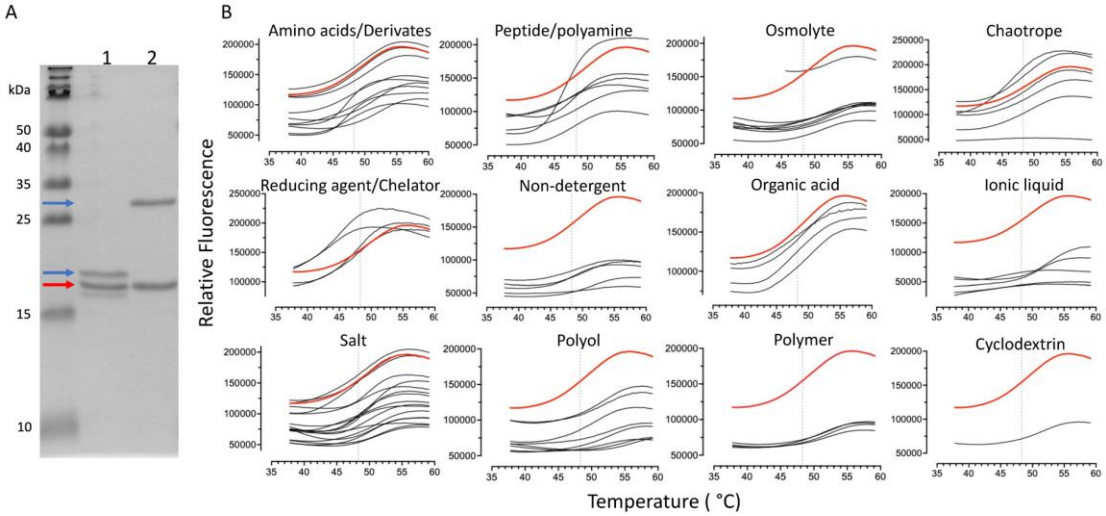

Figure 33. Purification and stability additive screening of BTK SH3-SH2 and HIV-1 Nef complex.

A) Purified complex of BTK SH3-SH2 domain with HIV-1 Nef core (Lane 1) and full-length Nef (Lane 2) run on a 16% SDS-PAGE gel followed by Coomassie staining shows an approximately equimolar mixture of each protein in the complexes. Reference molecular weights are indicated on the left. Red arrow indicates the position of BTK SH3-SH2, blue arrows indicate positions of respective Nef constructs. B) DSF experiments to measure the stability of the BTK SH3-SH2:Nef core complex in the presence of the indicated classes of additives. Thermal melt profile of the BTK SH3-SH2:Nef core complex alone is indicated by red melt curves in each experiment. Grey dotted line indicates the complex T_m of 48.3 °C in buffer only. Thermal melt profile of the complex in the presence of indicated class of additives are shown in black curves. Each black curve represents the thermal melt profile of the complex in presence of a single additive belonging to that class. Class of additives included: amino acids/derivates (x10), peptide/polyamine (x6), osmolytes (x9), chaotropes (x6), reducing agent/inhibitor/chelator (x4), non-detergent (x5), organic acid (x4), ionic liquid (x5), salt (x18), polyol (x9), polymer (x4), cyclodextrin (x1). None of the conditions yielded a significant increase in BTK SH3-SH2:Nef core complex thermal stability.

3.2.2 Co-crystallization of a GCN4-tagged BTK SH3-SH2:HIV-1 Nef core Complex

After the attempt to stabilize the BTK SH3-SH2:Nef core complex by additive screening was not successful, I generated constructs designed to promoted BTK SH3-SH2 dimer stability. We have previously used the yeast GCN4 leucine zipper coiled-coil to promote homodimerization of Nef in our lab. I fused this leucine zipper coiled-coil to the N- and C-termini of BTK SH3-SH2 separated by a flexible 10-residue Gly-Ser linker (Figure 34A). The N- and C-terminally leucine

zipper fused BTK SH3-SH2 proteins eluted as a mixture of monomer, dimer and higher order oligomers in analytical SEC. This is in accordance with previous reports suggesting a high-tendency for oligomerization in the GCN4 leucine-zipper domains [626]. Robust Nef association was observed upon addition of the HIV-1 Nef dimer; however, significant precipitation was also observed upon complex formation (Figure 34B). Furthermore, neither the leucine zipper-fused BTK SH3-SH2 by itself or in the complex with HIV-1 Nef core could be concentrated beyond 0.78 mg/ml. Complexes of the GCN4 coiled coil-tagged BTK SH3-SH2 with the HIV-1 Nef core, although at low concentration, was used for crystallization screens as described in Table 2. Less than 5% of the crystallization conditions resulted in immediate precipitation upon addition of crystallization solution, suggesting the complex concentration may be too low to induce crystal formation. No crystals were observed with this screen.

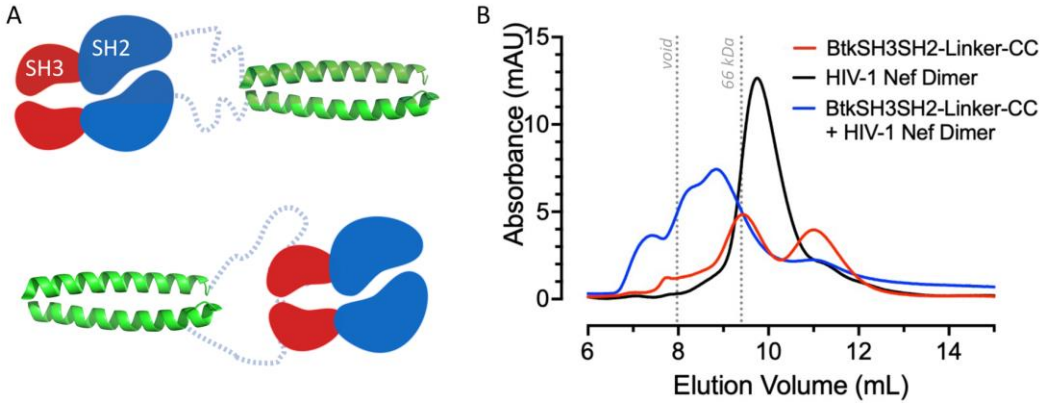

Figure 34. Purification of coiled-coil tagged BTK SH3-SH2.

A) Cartoon representation of BTK SH3-SH2 fused to yeast GCN4 leucine zipper coiled-coil in the C-terminus (top) (BTK SH3-SH2-Linker-CC) or N-terminus (bottom) (CC-Linker-BTK-SH3-SH2) separated by a flexible Gly-Ser linker. B) Analytical SEC of BTK SH3-SH2 fused to GCN4 coiled-coil at the C-terminus shows a mixture of dimer and monomer (red). Equimolar mixtures with the HIV-1 Nef dimer led to complex formation (blue), including precipitate formation seen as the peak that eluted earlier than void volume. Analytical SEC of GCN4 coiled-coil fused to N-terminus of BTK SH3-SH2 also formed complex and precipitate with Nef at low concentration but could not be concentrated beyond 0.3 mg/mL (not shown). All proteins were run at 12 µM final concentration on a Superdex 75 10/300 GL column.

3.2.3 Co-crystallization of Glutathione S-transferase (GST) tagged BTK SH3-SH2: HIV-1 Nef core Complex

Finally, after efforts to stabilize the BTK SH3-SH2 dimer by fusion to a GCN4 coiled coil domain did not yield protein concentrations suitable for crystallization, I attempted to stabilize the dimer using a soluble GST tag fusion approach. Crystal structures demonstrate that GST forms a homodimer with the C-termini exposed to solvent in close proximity to one another, supporting the suitability of this fusion approach (Figure 35A). Similar to yeast GCN4, I made a construct with the GST tag fused to the N-terminus of BTK SH3-SH2 separated by a 10 residue Ser-Gly linker (Figure 35A). GST tagged BTK SH3-SH2 eluted as a mixture of dimers and higher order oligomers. The dimer fraction was concentrated to 3.21 mg/ml, and was stable up to 24 hours in solution at room temperature (Figure 35B), unlike the untagged BTK SH3-SH2 dimer. This protein was isolated as a dimer and used for crystallization screens as described in Table 2. Isolation of the GST-BTK SH3-SH2 dimer fraction and equimolar full-length Nef incubation resulted in a strong complex formation demonstrated by analytical SEC (Figure 35C). A complex of GST-tagged BTK SH3-SH2 and the HIV-1 Nef core was then formed by incubating equimolar mixture of GST tagged BTK SH3-SH2 and HIV-1 Nef core (SF2). Some precipitation was observed, which was cleared by centrifuging at 13,000 rpm at 4 °C for 15 minutes. This concentration of the soluble complex was 4.08 mg/mL. GST tagged BTK SH3-SH2 and Nef core complex eluted earlier than the GST tagged BTK SH3-SH2 only in analytical SEC using Superdex 200 10/300 GL column, suggesting association, although the molar mass of the complex was not determined. This complex was isolated and used for crystallization experiments as described in Table 2. Two conditions triggered crystal formation, although the crystals were too small for harvesting onto nylon loops for X-ray diffraction experiments (Figure 35D). The conditions that led to microcrystal formation

are indicated in Figure 35. Both conditions were set up at 4 °C and microcrystals were observed in about 3 weeks time. UV- fluorescence from these crystals was detected using a UV microscope and confirmed the protein makeup of these crystals (Figure 35E and 35F). In order to optimize these crystallization conditions, an additive screen (Hampton Research) was used in an attempt to induce larger crystal formation. However, optimization screenings failed to induce crystal formation suitable for looping and subsequent X-ray diffraction experiments.

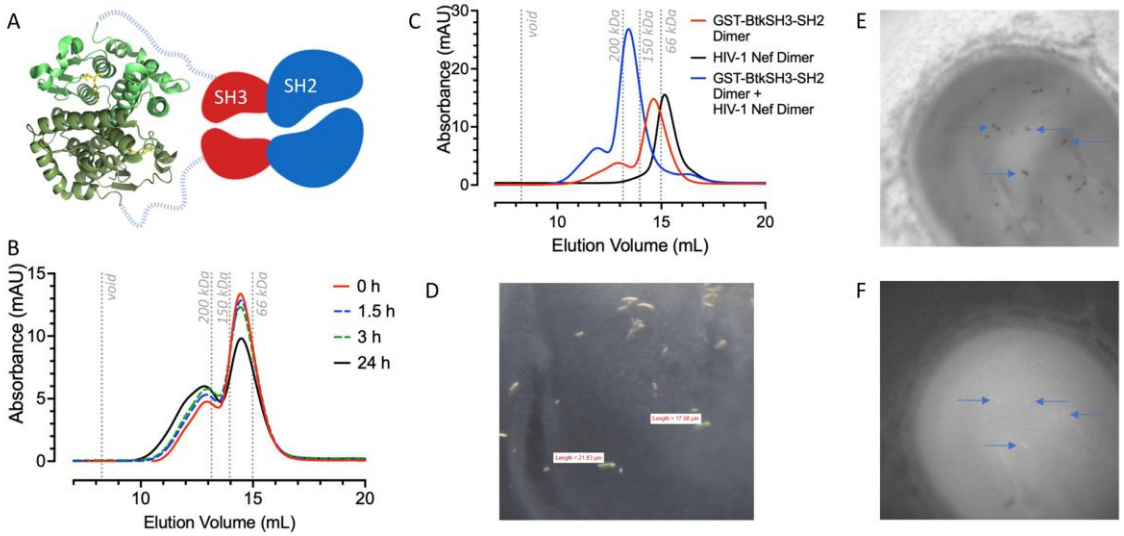

Figure 35. Purification of GST-tagged BTK SH3-SH2 for crystallization with Nef core.

A) Cartoon representation of BTK SH3-SH2 fused at the N-terminus to glutathione S-transferase (GST) from Pseudomonas sp. Ag1. in presence of glutathione (yellow) (PDB: 4ECJ). The GST monomers are shown in dark and light green, respectively. B) Analytical SEC shows that GST-tagged BTK SH3-SH2 elutes predominantly as species consistent with dimer (predicted dimer molecular weight:96 kDa), but also as higher order soluble oligomers. Stability analysis showed that GST tagged BTK SH3-SH2 is stable as a dimer at room temperature in solution for at least 24 h. C) GST tagged BTK SH3-SH2 dimer fraction formed a stable complex with HIV-1 Nef dimer in solution. Both B) and C) were performed on Superdex 200 10/300 GL column. D) Complex of GST tagged BTK SH3-SH2 with HIV-1 Nef yielded crystals measuring up to 20 µm but were too small for harvesting onto nylon loops for diffraction experiments. Crystallization conditions for this drop included 0.17M Ammonium sulfate, 25.5% (w/v) PEG 4000, 15% (v/V) Glycerol at 4 °C (JCSG+ RT, well D9). E) Brightfield and F) UV- fluorescence images showing micro-crystals of the GST-tagged BTK SH3-SH2:Nef core complex. Blue arrows indicate the positions of the microcrystals. The crystallization condition for this drop was 1.6 M lithium sulfate, 0.1 M Tris, pH 8.0 at 4 °C.

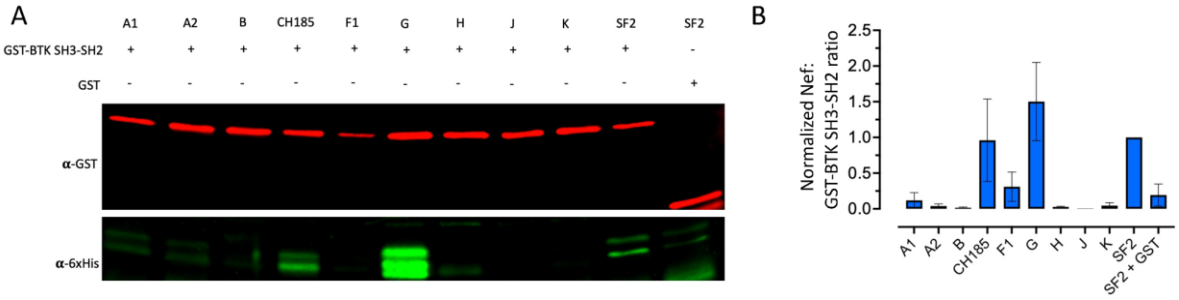

Figure 36. Coimmunoprecipitation of Nef core of HIV-1 subtypes with GST tagged BTK SH3-SH2.

A) Nef core proteins of indicated HIV-1 subtypes were coexpressed with GST tagged BTK SH3-SH2 or GST tag only (last lane) in *E.coli*. Coimmunoprecipitation by anti-GST antibody showed similar levels of GST tagged BTK SH3-SH2 expression (red bands). Anti-6xHis antibody (green bands) showed highest levels of 6x-His-SUMO tagged Nef core G and CH185 proteins present in the anti-GST antibody- GST tagged BTK SH3-SH2 complex. B) Quantification of the bands using Image Studio Lite software was performed and ratio of Nef core levels: GST tagged BTK SH3-SH2 level was obtained for three experiments, and normalized to the SF2 Nef core levels. Last bar shows the ratio of SF2 Nef core: GST tag without BTK SH3-SH2.

Table 2. List of crystallization screens and protein complexes used in this study.

For each screen, each of the 96 screen conditions was mixed in a 1:1 ratio with the HIV-1 Nef:BTK complex. Each crystallization screen was set up in duplicate for incubation at both 4 °C and room temperature to induce crystal formation.

Crystallization screen	Protein complex (mg/mL)	Conditions screened (No. of screens * unique conditions per screen * duplicates)	Conditions with crystals
The JCSG+ Suite (Qiagen)	SH3-SH2:Nef full-length (8.16)	6 * 96 * 2 (4 °C, RT)	0 (1152)
The Protein Complex Suite (Qiagen)	SH3-SH2:Nef core (5.87)	6 * 96 * 2 (4 °C, RT)	0 (1152)
The MbClass Suite (Qiagen)	SH3-SH2-Linker-CC:Nef core (0.78)	6 * 96 * 2 (4 °C, RT)	0 (1152)
The MbClass II Suite (Qiagen)	CC-Linker-SH3-SH2:Nef core (0.38)	6 * 96 * 2 (4 °C, RT)	0 (1152)
PACT Premier (Molecular Dimensions)	GST-Linker-SH3-SH2 (3.16)	6 * 96 * 2 (4 °C, RT)	0 (1152)
ProPlex (Molecular Dimensions)	GST-Linker-SH3-SH2:Nef core (4.08)	6 * 96 * 2 (4 °C, RT)	2 (1152)

3.3 Summary and Conclusions

In this study, I strived to uncover the structural basis of Nef-mediated BTK activation. Coexpression of the BTK SH3-SH2 dual domain and the Nef core protein resulted in a homogenous complex of the two proteins in solution by SEC. However, subsequent crystallization experiments did not yield protein crystals at room temperature or at 4 °C. This may be due to the unstable nature of the BTK SH3-SH2 dimer in solution. In order to stabilize this complex, I pursued several strategies involving additive screening with a thermal shift assay, and stabilizing BTK SH3-SH2 by fusing to natural dimer partners. One such strategy involving fusion with an N-

terminal GST tag considerably improved dimer stability. When combined with the Nef core, the GST-tagged BTK SH3-SH2 complex produced microcrystals in two conditions as described in Figure 33. These microcrystals were too small to loop and analyze by X-ray diffraction. Optimization of these microcrystals did not noticeably improve crystal size.

Although I did not obtain crystals of the BTK SH3-SH2 and Nef complex suitable for X-ray diffraction, progress was made towards generating a stable complex. The complex of GST-tagged BTK SH3-SH2 with the Nef core represents a promising target for future crystallization efforts. Evidence of microcrystal formation shown above suggests that microcrystal electron diffraction (MicroED) may provide an alternative path to the structure of Nef core and BTK SH3-SH2 dimer complex. This technique has benefitted from advances in highly sensitive cryo-electron microscopy detection methods to determine structures of proteins from nano and microcrystals [627].

Moreover, an undergraduate student (Kiera Regan) in our lab also produced core domain versions of the Nef proteins from diverse HIV-1 isolates discussed in section 2.3.2. In subsequent experiments, Nef core proteins derived from a representative G-clade clone as well as the transmitter/founder C-clade isolate CH185 showed the highest levels of co-immunoprecipitation with GST-tagged BTK SH3-SH2 among the ten Nef isolates tested (Figure 34). In this experiment, constructs encoding the core regions of each of the Nef subtypes (based on crystal structure of SF2 Nef) fused to SUMO tag at the N-terminus were coexpressed with GST tagged BTK SH3-SH2 in *E.coli* cells. The lysates were collected, and the GST tagged BTK SH3-SH2 expression was quantified by immunoblotting with anti-GST antibody (catalog no. MA4-004, ThermoFisher). Then, the anti-GST antibody was used to pull down GST tagged BTK SH3-SH2 and co-immunoprecipitation followed by immunoblotting was performed to detect the level of Nef core

in complex with GST-tagged BTK SH3-SH2. GST tag without BTK SH3-SH2 was included as a negative control with SF2 Nef core. These experiments showed that HIV-1 Nef G core and HIV-1 Nef CH185 core form the most stable complex with GST tagged BTK SH3-SH2. Therefore, these two Nef core variants also represent an alternative for crystallization screens with GST-tagged BTK SH3-SH2.

Lastly, members of our lab as well as others have utilized the random microseed matrix screening (rMMS) technique to generate new and improved protein crystals. In this technique, seed crystals are added to random screens. This complementary method has been shown to improve the crystallization success rate and also the quality of X- ray diffraction [628]. This technique can be applied by using the crystals of HIV-1 Nef core (SF2) or HCK SH3-SH2 for seeding.

4.0 Overall Discussion

4.1 Summary and discussion of major findings

For my dissertation project, I set forth to uncover the molecular mechanism by which the HIV-1 Nef accessory protein induces the activation of BTK, which is commonly expressed in HIV-1 target cells including macrophages and dendritic cells. As described in detail in the Introduction, previous studies have implicated both BTK and ITK in the HIV-1 life cycle [580, 581], and subsequent studies from our lab showed that Nef mediates activation of both kinases at the cell membrane [365]. However, the mechanism of kinase activation by Nef was not understood, and assumed to be similar to the mechanism of HCK.

For this study, I utilized an *in vitro* continuous kinase assay previously developed in our lab [610] to directly measure and compare the effect of Nef on BTK and HCK enzymatic properties. While ITK is expressed in primary host cell type for HIV-1, the CD4+ T cell, unlike BTK, ITK is not easily expressed in purified recombinant form and very little structural information is known about ITK compared to BTK. Therefore, my investigation of the mechanism of activation of BTK by HIV-1 Nef, which turned out to be experimentally tractable, provides a model of the general principles governing ITK activation by Nef as well.

While Nef-based HCK activation has been demonstrated in several previous studies, to my knowledge the kinetics of Nef-based enhancement of HCK kinase activity have not been previously reported. I showed that while Nef enhances the activity of both kinases, the mechanisms of activation are distinct. Surprisingly, the presence of HIV-1 Nef had no significant impact on the steady state rate of HCK activity. Instead, Nef significantly reduced the time to reach maximal

kinase activity, suggesting the primary impact of HIV-1 Nef binding is to accelerate HCK autophosphorylation. In contrast, HIV-1 Nef enhanced the steady state rate of BTK activity and reduced the time required to reach maximal activity. I validated these observations by directly measuring BTK activation loop Tyr551 autophosphorylation which was enhanced in the presence of both HIV-1 and SIV Nef proteins. This observation is consistent with our previous study, which reported that SIV Nef can also activate BTK at the cell membrane [365]. Interestingly, the Nef-2PA mutant harboring alanine substitutions in place of conserved prolines in PxxPxR motif also activated BTK but not HCK *in vitro*. Quantitative SPR and analytical SEC experiments also supported this observation. The HCK SH3 domain readily bound to HIV-1 Nef forming a stable complex, but no such interaction was observed between the BTK SH3 and Nef either by SPR or by analytical SEC. Thus recognition of and activation of BTK by Nef requires more than simple engagement of the SH3 domain, which is the case for HCK.

Next, using analytical SEC, I demonstrated that HIV-1 Nef forms a 2:2 dimeric complex with the BTK SH3-SH2 dual domain. This observation was confirmed using SPR, which also showed clear interaction between the BTK SH3-SH2 dual domain and the HIV-1 Nef dimer, while no interaction was observed between Nef and the individual BTK regulatory domains. In order to test the role of Nef dimerization in BTK activation, I showed that dimerization-defective Nef mutants failed to activate BTK *in vitro*. This observation is in accordance with our previous cell-based BiFC study which reported suppressed levels of BTK activation by these Nef mutants compared to wild-type Nef at the cell membrane [365]. Suppression of BTK activity by these Nef mutants suggests that they bind to BTK and prevent autophosphorylation in *trans*. While the dimerization-defective mutants failed to activate BTK *in vitro*, they did not suppress basal kinase activity as observed in the cell-based assay. In the SPR assay, the Nef dimer mutants exhibited

markedly reduced interaction with immobilized BTK SH3-SH2 (K_D about 10-fold less than wild-type Nef) but did not lose interaction completely. This observation suggests that the Nef dimer mutants still retain some degree of interaction with BTK, which may be because multiple residues govern the Nef dimer interface interactions, and the single mutations present in the mutant proteins may not eliminate Nef dimerization completely. However, such an interaction is non-productive and does not lead to kinase activation as observed in the previous study.

In the course of studying the mechanism of BTK regulation by HIV-1 Nef, I also discovered that BTK SH3-SH2 dimerization represents a potential activating mechanism for BTK. While efforts to crystallize a BTK SH3-SH2 dimer did not succeed, alignment of the individual BTK SH3 and SH2 domain structures with an NMR structure of the ITK SH3•SH2 dimer formed by individual SH3 and SH2 in trans suggested a potential role for the BTK SH2 domain CD loop in mediating dimerization by contacting the SH3 domain away from its peptide-binding ligand interface. Substitution of Pro327 with alanine in the BTK SH2 domain CD loop did not eliminate dimerization, but yielded a dimer that was less stable than the wild-type dimer in solution at room temperature. The contribution of Pro327 towards full-length BTK dimerization was established in cells using a BiFC assay, which showed significantly diminished BTK dimerization as a result of P327A mutation in the SH2 CD loop in the absence of Nef.

I also showed that the stability of BTK SH3-SH2 dimer in solution is increased by complex formation with the HIV-1 Nef homodimer. The same observation was also made in cells using the BiFC assay, where the presence of HIV-1 Nef significantly increased the BTK dimer-positive cell population, with the BTK dimers localized most strongly to the cell membrane. No such Nef effect was seen for P327A BTK, suggesting that HIV-1 Nef recruits BTK by forming a 2:2 dimer complex with its SH3-SH2 domains.

I next analyzed whether such Nef-mediated recruitment and dimerization of BTK leads to constitutive kinase activation. First, I measured the steady state rates of the wild-type and P327A mutant forms of BTK in the presence and absence of Nef. Unlike wild-type BTK, the dimerization-deficient P327A mutant showed no change in steady-state substrate phosphorylation or autophosphorylation in the presence of Nef. Importantly, control experiments showed that the P327A mutation did not significantly affect the K_m values for either ATP or the peptide substrate, arguing against a general effect of this mutation on kinase domain function. However, the specific activity of recombinant BTK-P327A was about two-thirds of that observed with wild-type BTK, suggesting that the proposed SH2 to SH3 dimerization mechanism may also contribute to BTK activity in the absence of Nef. A complementary cell-based study using the BiFC assay was consistent with the *in vitro* kinase assay data. In this case, HIV-1 Nef increased BTK wild-type phosphorylation levels at the cell membrane as seen in our previous study [365], while phosphorylation of the BTK P327A mutant did not significantly change in presence of Nef. Interestingly, the interaction of Nef with the P327A BTK mutant was also significantly reduced in the BiFC assay on a per-cell basis, consistent with the requirement for preformed Nef and BTK dimers for interaction as observed *in vitro* by SEC.

Previous studies have shown that BTK forms a PHTH-mediated dimer at the cell membrane in response to PIP_3 production. Rapid recruitment of BTK driven by PIP_3 in the membrane and the proximity between the domains may promote multiple BTK self-assemblies, since BTK has been suggested to adopt an ensemble of multiple conformations in solution [617]. One such intermolecular BTK self-assembly may be mediated through the interactions observed between the SH3 domain and the amino terminal proline-rich region in BTK leading to an asymmetric homodimer as observed by NMR [554]. The BTK dimer formed by the SH3•SH2

interactions observed in this study may represent another such intermolecular association mechanism. This SH3•SH2-mediated BTK dimerization may be transient in nature and unable to remain as a dimer molecule for an extended period of time. My data show that HIV-1 Nef selectively interacts with and stabilizes this dimeric form of BTK at the membrane in absence of PIP_3 signaling. The consequence of this interaction is to provide pathogen-specific, sustained BTK activation that facilitates downstream signaling events that lead to NFκB and NFAT activation in absence of exogenous antigen presentation. These signals are essential for efficient transcription of viral genes from the integrated HIV provirus, where binding sites for these and other transcription factors normally regulated by antigen receptor signaling are present in the HIV-1 LTR.

4.2 Future directions

4.2.1 Exploring the mechanism of Nef-mediated ITK recruitment and activation

Our previous work showed that Nef recruits both BTK and ITK to the cell membrane, leading to constitutive kinase activation [365]. While the specific mechanisms behind Nef interaction with these TEC-family members were not explored in this previous study, the requirement of Nef homodimer formation and the observation that SIV Nef can also activate both kinases prompted the hypothesis that *both ITK and BTK may be recruited and activated by Nef through a common mechanism*. In this study, I utilized the structure of the ITK SH3•SH2 dimer formed by individual SH3 and SH2 in trans to gain insights into the dimerization of the homologous BTK domains. While investigation of the ITK domains responsible for Nef

interaction was not part of my study, the observation that both kinases have the potential to form dimers through a common SH3-SH2 mediated mechanism and that Nef dimers selectively bind the BTK dimer suggest the possibility of a similar mechanism of interaction between HIV-1 Nef and ITK. This possibility could be tested using similar experimental techniques and approaches used in this study. In preliminary experiments, a former graduate student in our lab (Kindra Whitlatch, MS) utilized SPR to show that HIV-1 Nef selectively interacts with the recombinant ITK SH3-SH2 dual domain, but not the individual SH3 and SH2 domains. This result is entirely consistent with my own findings with BTK. Conservation of tertiary and quaternary structures, as well as the regulatory mechanism between these kinases, suggest that ITK may also interact with HIV-1 Nef through a similar mechanism as BTK. Unlike BTK however, the ITK PHTH domain does not form PHTH-mediated dimers in response to PIP_3. This suggests that SH3-SH2 mediated dimerization might play a greater role in physiological ITK activation. Investigating Nef-mediated ITK activation by utilizing the *in vitro* enzymatic experiments performed in this study may be difficult because expression of recombinant ITK in *E. coli* is challenging and the basal activity of the recombinant purified kinase is quite low compared to BTK (my own unpublished observations). However, cell-based studies using BiFC and FAST protein systems (described below) may allow further investigation of Nef-mediated ITK activation in a cellular environment.

4.2.2 Exploring the membrane effects in Nef-BTK interaction

My data suggest that HIV-1 Nef constitutively activates BTK at the cell membrane in the absence of PIP_3 by stabilizing a unique BTK SH3•SH2 dimer interface. In order to further elaborate on the mechanism of Nef-mediated BTK recruitment, a study of BTK mutants harboring PHTH mutations involved in dimerization (F42Q, F44Q) would be helpful. F42Q/F44Q PHTH

mutations abrogate the natural BTK activation mechanism by PIP_3 [536] and may provide a clearer picture of Nef-mediated BTK recruitment, dimer formation, and activation as the PHTH dimer mutants would be unable to self-associate. Furthermore, lipid bilayer SPR experiments with and without PIP_3 could be done to quantitatively measure the dynamics of Nef-mediated BTK membrane recruitment. In this approach, we could measure the rate of Nef membrane recruitment by using recombinant N-terminal myristoylated HIV-1 Nef and monitoring the dynamics of association in model lipid bilayers. Following association of myristoylated Nef with the lipid bilayer, we could then inject the BTK SH3-SH2 dual domain to measure the rate of Nef-mediated BTK membrane recruitment. Finally, we could also measure the rate of autoinhibited BTK and BTK PHTH domain recruitment in presence of PIP_3 to compare rates and dynamics of BTK recruitment by PIP_3 and HIV-1 Nef. In collaboration with Frank Heinrich and Mathias Lösche at Carnegie Mellon University, we demonstrated that recombinant myristoylated Nef interacts strongly with sparsely-tethered lipid bilayer membranes using custom SPR chips produced in the Löeshe laboratory. The difference in membrane bilayer association between myristoylated and non-myristoylated forms of Nef was dramatic, with myristoylated Nef displaying at least 100-fold greater affinity for the bilayer compared to unmyristoylated Nef. In addition, the binding curves for myristoylated Nef were best-fit by a cooperative Hill model, consistent with the formation of Nef homodimers in the membrane. This system could theoretically be extended to model Nef interactions with TEC family kinases on the lipid bilayer. My contributions to this study, which involved expression and purification of myristoylated wild-type and mutant Nef proteins in *E. coli*, will be part of the following manuscript, which is currently in preparation: Heinrich F, Eells, R, Alvarado, JJ, Whitlatch KM, Aryal M, Lösche M and Smithgall TE: Neutron Reflectometry and Molecular Simulations Support Nef Homodimer Formation on Model Lipid Bilayers.

4.2.3 Investigate the role of BTK SH3-SH2 dimerization in BTK activation and Nef interaction using a dynamic cell-based assay

Our previous study showed that Nef homodimer formation in donor PBMCs infected with wild-type HIV-1 leads to constitutive ITK activation and facilitates viral replication [365]. HIV-1 that fails to express Nef (ΔNef) as well as viruses expressing dimerization-defective Nef mutants failed to activate ITK and suppressed viral replication, presumably through a dominant-negative mechanism. My study presents the first evidence that HIV-1 Nef regulates BTK activation *in vitro* by a mechanism involving BTK homodimer formation. In a collaborative study with David Lin and Amy Andreotti (Iowa State University, Ames, IA), we also observed that the BTK P327A mutation does not affect PIP_3-mediated BTK activation in a system that models physiological BCR signaling. In this study, dimerization-deficient P327A BTK was activated to the same extent as wild-type BTK in the presence of PIP_3-containing liposomes, suggesting SH3•SH2 mediated dimerization may not play a role during physiological BTK activation. This implies that Nef utilizes a unique mechanism to recruit and activate BTK. One concern of my study is that the *in vitro* observations were made using recombinant purified proteins in the absence of the cellular environment, especially the cellular membrane where BTK normally operates. Moreover, the irreversibility of fluorophore formation in BiFC assays prevented us from capturing the dynamic interactions of BTK with Nef and with itself at the cell membrane. Future studies may address this issue using a newer fluorescence complementation system known as 'SplitFAST', which provides a reversible readout of protein-protein interactions via fluorescence complementation [629]. The SplitFAST system is based on a small (14 kDa) fluorogenic protein engineered from the photoreceptor of the halophilic bacterium, *Halorhodospira halophila* [630]. This protein, referred to as 'FAST' (fluorescence-activating absorption shifting tag), produces strong fluorescence upon

binding to various hydroxybenzylidene rhodanine fluorogen [629, 631]. Analogous to YFP-based BiFC, the FAST protein can be split into non-fluorescent N- and C-terminal fragments (nFAST and cFAST). Fusion of these fragments to interacting partner proteins results in FAST protein complementation and fluorescence in the presence of the added fluorogen. With this SplitFAST system, we could theoretically follow the rate of BTK wild-type recruitment by HIV-1 Nef and compare that to the BTK P327A recruitment to understand the role of BTK dimerization during HIV-1 infection. Similar to the approach described in section 4.2.2, we could also track the rate of BTK recruitment to the membrane in response to PIP_3 production by cotransfecting with the activated form of PI3K that produces PIP_3 at the cell membrane. In both scenarios, we could also monitor the cell-based dimerization of BTK at the membrane. Together through these dynamic cell assays, we could establish the role and contribution of BTK SH3-SH2 dimerization and activation during HIV-1 infection.

4.3 Closing remarks

It has been nearly 40 years since HIV was identified as the agent that led to AIDS. In this time, about 79 million people have been infected, and about 36 million people have died of HIV. About 38 million people are living with HIV in 2021. Advent of therapeutics discussed in section 1.2.4 have largely contributed to reducing spread and mortality rates, but are limited in eradicating the virus completely. Therefore, novel therapeutic strategies that eliminate latent viral reservoirs are urgently needed. As discussed earlier, HIV-1 Nef is an essential virulence factor in promoting viral pathogenesis, and contributing to its evasion from immune cells. Even though Nef lacks enzymatic property, the essential role of homodimerization across Nef functions provides an

attractive target for drug discovery. I showed that Nef dimerization is essential to hijack and constitutively activate tyrosine kinase signaling cascades that are likely to lead to HIV-1 proviral gene expression. Targeting of Nef dimerization will disrupt Nef activity leading to disruptions in multiple stages of viral life cycle and will promote immune detection of infected cells. Our lab is developing strategies towards disrupting Nef activity by introducing small molecule inhibitors of Nef dimerization as well as targeting Nef for proteasomal degradation. I hope to have contributed in deciphering yet another role of Nef dimerization that promotes the viral life cycle.

Abbreviations

AIDS..... Acquired immunodeficiency syndrome

AP-1/2..... Activator protein 1/2

BiFC..... Bimolecular fluorescence complementation

BSA..... Bovine Serum Albumin

CA..... Capsid

CCR/CXCR..... Chemokine receptors

CD4..... Cluster of differentiation 4

cDNA..... complementary DNA

Csk..... c-Src tyrosine kinase

CypA..... Cyclophilin A

FAK..... Focal adhesion kinase

GEF..... GTP exchange factor

GFP..... Green fluorescent protein

HAART..... Highly active antiretroviral therapy

HIV..... Human immunodeficiency virus

HLA..... Human leucocyte antigen

HTLV..... Human T-lymphotrophic virus

IC_{50}..... half maximal inhibitory concentration

IF..... Immunofluorescence

IFN..... Interferon

IL-2..... Interleukin-2

IN..... Integrase

ITAM..... Immunoreceptor tyrosine-based activation motif

JAK..... Janus kinase

kb..... kilobase

K_D..... dissociation constant

kDa..... kilo-daltons

LAT..... Linker of activated T cells

LTR..... Long terminal repeat

M..... Molar

MA..... Matrix

MAPK..... Mitogen-activated protein kinase

MHC..... Major histocompatibility complex

N/NRTI..... non-/nucleoside reverse transcriptase inhibitor

NC..... Nucleocapsid

NFAT..... Nuclear factor of activated T cells

NFκB..... Nuclear factor kappa-light-chain-enhancer of activated B cells

ORF..... open reading frame

PACS-2..... Phosphofurin acidic cluster sorting protein 2

PAK2..... p21 protein- activated kinase 2

PBMC..... Peripheral blood mononuclear cells

PH..... Pleckstrin homology

PI..... protease inhibitor

PI3K..... phosphoinositide 3- kinase

PIC..... preintegration complex

PIP3..... phosphatidylinositol (3,4,5) triphosphate

PKC..... Protein kinase C

PLCγ..... Phospholipase C gamma

PPII..... polyproline type II

PR..... Protease

PTK..... protein tyrosine kinase

pTyr/pY..... phosphotyrosine

RT..... Reverse transcriptase

RU…….Response units

SEM..... Standard error of mean

SFK..... Src family kinase

SH3..... Src-homology 3

SIV..... Simian immunodeficiency virus

STAT..... Signal transducer and activator of transcription

SU..... Surface

TCR..... T cell receptor

TGN..... trans-Golgi network

TH..... Tec homology

TM..... transmembrane

VC..... C-terminal fragment of Venus

VN..... N-terminal fragment of Venus

vs..... versus

WT..... wild type

XLA..... X-linked agammaglobulinemia

YFP..... Yellow fluorescence protein

Bibliography

1. *Pneumocystis pneumonia--Los Angeles.* MMWR Morb Mortal Wkly Rep, 1981. **30**(21): p. 250-2.

2. *Kaposi's sarcoma and Pneumocystis pneumonia among homosexual men--New York City and California.* MMWR Morb Mortal Wkly Rep, 1981. **30**(25): p. 305-8.

3. *Epidemiologic aspects of the current outbreak of Kaposi's sarcoma and opportunistic infections.* N Engl J Med, 1982. **306**(4): p. 248-52.

4. *Persistent, generalized lymphadenopathy among homosexual males.* MMWR Morb Mortal Wkly Rep, 1982. **31**(19): p. 249-51.

5. *Update on acquired immune deficiency syndrome (AIDS)--United States.* MMWR Morb Mortal Wkly Rep, 1982. **31**(37): p. 507-8, 513-4.

6. Gallagher, R.E. and R.C. Gallo, *Type C RNA tumor virus isolated from cultured human acute myelogenous leukemia cells.* Science, 1975. **187**(4174): p. 350-3.

7. Panem, S., E.V. Prochownik, F.R. Reale, and W.H. Kirsten, *Isolation of type C virions from a normal human fibroblast strain.* Science, 1975. **189**(4199): p. 297-9.

8. Poiesz, B.J., F.W. Ruscetti, A.F. Gazdar, P.A. Bunn, J.D. Minna, and R.C. Gallo, *Detection and isolation of type C retrovirus particles from fresh and cultured lymphocytes of a patient with cutaneous T-cell lymphoma.* Proc Natl Acad Sci U S A, 1980. **77**(12): p. 7415-9.

9. Barre-Sinoussi, F., J.C. Chermann, F. Rey, M.T. Nugeyre, S. Chamaret, J. Gruest, . . . L. Montagnier, *Isolation of a T-lymphotropic retrovirus from a patient at risk for acquired immune deficiency syndrome (AIDS).* Science, 1983. **220**(4599): p. 868-71.

10. Gallo, R.C., S.Z. Salahuddin, M. Popovic, G.M. Shearer, M. Kaplan, B.F. Haynes, . . . et al., *Frequent detection and isolation of cytopathic retroviruses (HTLV-III) from patients with AIDS and at risk for AIDS.* Science, 1984. **224**(4648): p. 500-3.

11. Levy, J.A., A.D. Hoffman, S.M. Kramer, J.A. Landis, J.M. Shimabukuro, and L.S. Oshiro, *Isolation of lymphocytopathic retroviruses from San Francisco patients with AIDS.* Science, 1984. **225**(4664): p. 840-2.

12. Coffin, J., A. Haase, J.A. Levy, L. Montagnier, S. Oroszlan, N. Teich, . . . et al., *What to call the AIDS virus?* Nature, 1986. **321**(6065): p. 10.

13. Clavel, F., D. Guetard, F. Brun-Vezinet, S. Chamaret, M.A. Rey, M.O. Santos-Ferreira, . . . et al., *Isolation of a new human retrovirus from West African patients with AIDS.* Science, 1986. **233**(4761): p. 343-6.

14. Chakrabarti, L., M. Guyader, M. Alizon, M.D. Daniel, R.C. Desrosiers, P. Tiollais, and P. Sonigo, *Sequence of simian immunodeficiency virus from macaque and its relationship to other human and simian retroviruses.* Nature, 1987. **328**(6130): p. 543-7.

15. Hirsch, V.M., R.A. Olmsted, M. Murphey-Corb, R.H. Purcell, and P.R. Johnson, *An African primate lentivirus (SIVsm) closely related to HIV-2.* Nature, 1989. **339**(6223): p. 389-92.

16. Huet, T., R. Cheynier, A. Meyerhans, G. Roelants, and S. Wain-Hobson, *Genetic organization of a chimpanzee lentivirus related to HIV-1*. Nature, 1990. **345**(6273): p. 356-9.

17. Hahn, B.H., G.M. Shaw, K.M. De Cock, and P.M. Sharp, *AIDS as a zoonosis: scientific and public health implications.* Science, 2000. **287**(5453): p. 607-14.

18. Sharp, P.M. and B.H. Hahn, *Origins of HIV and the AIDS Pandemic*, in *Cold Spring Harb Perspect Med*. 2011.

19. Li, W.H., M. Tanimura, and P.M. Sharp, *Rates and dates of divergence between AIDS virus nucleotide sequences.* Mol Biol Evol, 1988. **5**(4): p. 313-30.

20. Wei, X., S.K. Ghosh, M.E. Taylor, V.A. Johnson, E.A. Emini, P. Deutsch, . . . et al., *Viral dynamics in human immunodeficiency virus type 1 infection.* Nature, 1995. **373**(6510): p. 117-22.

21. Korber, B., M. Muldoon, J. Theiler, F. Gao, R. Gupta, A. Lapedes, . . . T. Bhattacharya, *Timing the ancestor of the HIV-1 pandemic strains.* Science, 2000. **288**(5472): p. 1789-96.

22. Hemelaar, J., E. Gouws, P.D. Ghys, and S. Osmanov, *Global and regional distribution of HIV-1 genetic subtypes and recombinants in 2004.* Aids, 2006. **20**(16): p. W13-23.

23. Los Alamos National Laboratory. *HIV Circulating Recombinant Forms (CRFs)*. 2021 [cited 2021 November 14]; Available from: https://www.hiv.lanl.gov/content/sequence/HIV/CRFs/CRFs.html.

24. Taylor, B.S., M.E. Sobieszczyk, F.E. McCutchan, and S.M. Hammer, *The Challenge of HIV-1 Subtype Diversity.* N Engl J Med, 2008. **358**(15): p. 1590-602.

25. Elangovan, R., M. Jenks, J. Yun, L. Dickson-Tetteh, S. Kirtley, J. Hemelaar, . . . R. Zhang, *Global and Regional Estimates for Subtype-Specific Therapeutic and Prophylactic HIV-1 Vaccines: A Modeling Study.* Frontiers in Microbiology, 2021. **12**(1636).

26. UNAIDS. *Global HIV & AIDS statistics - Fact sheet*. n.d. [cited 2020 March 20]; Available from: https://www.unaids.org/en/resources/fact-sheet.

27. The, L., *The global HIV/AIDS epidemic-progress and challenges.* Lancet, 2017. **390**(10092): p. 333.

28. UNAIDS. *The Gap Report*. 2014 [cited 2020 March 20]; Available from: https://www.unaids.org/en/resources/documents/2014/20140716_UNAIDS_gap_report.

29. Dellar, R.C., S. Dlamini, and Q.A. Karim, *Adolescent girls and young women: key populations for HIV epidemic control.* J Int AIDS Soc, 2015. **18**(2 Suppl 1): p. 19408.

30. Karim, Q.A., A.B. Kharsany, J.A. Frohlich, L. Werner, M. Mashego, M. Mlotshwa, . . . S.S. Abdool Karim, *Stabilizing HIV prevalence masks high HIV incidence rates amongst rural and urban women in KwaZulu-Natal, South Africa.* Int J Epidemiol, 2011. **40**(4): p. 922-30.

31. Bekker, L.G., L. Johnson, M. Wallace, and S. Hosek, *Building our youth for the future*, in *J Int AIDS Soc*. 2015: Switzerland. p. 20027.

32. UNAIDS. *HIV in Asia and the Pacific: UNAIDS report 2013*. 2013 [cited 2020 March 20]; Available from: https://www.unaids.org/en/resources/documents/2013/20131119_HIV-Asia-Pacific.

33. Chiu, I.M., A. Yaniv, J.E. Dahlberg, A. Gazit, S.F. Skuntz, S.R. Tronick, and S.A. Aaronson, *Nucleotide sequence evidence for relationship of AIDS retrovirus to lentiviruses.* Nature, 1985. **317**(6035): p. 366-8.

34. Lu, K., X. Heng, and M.F. Summers, *Structural Determinants and Mechanism of HIV-1 Genome Packaging.* J Mol Biol, 2011. **410**(4): p. 609-33.

35. Freed, E.O., *HIV-1 replication.* Somat Cell Mol Genet, 2001. **26**(1-6): p. 13-33.

36. Jablonski, J.A., A.L. Amelio, M. Giacca, and M. Caputi, *The transcriptional transactivator Tat selectively regulates viral splicing.* Nucleic Acids Res, 2010. **38**(4): p. 1249-60.

37. Frankel, A.D. and J.A. Young, *HIV-1: fifteen proteins and an RNA.* Annu Rev Biochem, 1998. **67**: p. 1-25.

38. Ganser-Pornillos, B.K., M. Yeager, and W.I. Sundquist, *The structural biology of HIV assembly.* Curr Opin Struct Biol, 2008. **18**(2): p. 203-17.

39. Accola, M.A., A. Ohagen, and H.G. Gottlinger, *Isolation of human immunodeficiency virus type 1 cores: retention of Vpr in the absence of p6(gag).* J Virol, 2000. **74**(13): p. 6198-202.

40. Kotov, A., J. Zhou, P. Flicker, and C. Aiken, *Association of Nef with the human immunodeficiency virus type 1 core.* J Virol, 1999. **73**(10): p. 8824-30.

41. Welker, R., H. Hohenberg, U. Tessmer, C. Huckhagel, and H.G. Krausslich, *Biochemical and structural analysis of isolated mature cores of human immunodeficiency virus type 1.* J Virol, 2000. **74**(3): p. 1168-77.

42. Yan, N., A.D. Regalado-Magdos, B. Stiggelbout, M.A. Lee-Kirsch, and J. Lieberman, *The cytosolic exonuclease TREX1 inhibits the innate immune response to human immunodeficiency virus type 1.* Nat Immunol, 2010. **11**(11): p. 1005-13.

43. Aloia, R.C., H. Tian, and F.C. Jensen, *Lipid composition and fluidity of the human immunodeficiency virus envelope and host cell plasma membranes.* Proc Natl Acad Sci U S A, 1993. **90**(11): p. 5181-5.

44. Brugger, B., B. Glass, P. Haberkant, I. Leibrecht, F.T. Wieland, and H.G. Krausslich, *The HIV lipidome: a raft with an unusual composition.* Proc Natl Acad Sci U S A, 2006. **103**(8): p. 2641-6.

45. Lorizate, M., B. Brugger, H. Akiyama, B. Glass, B. Muller, G. Anderluh, . . . H.G. Krausslich, *Probing HIV-1 membrane liquid order by Laurdan staining reveals producer cell-dependent differences.* J Biol Chem, 2009. **284**(33): p. 22238-47.

46. Bryant, M. and L. Ratner, *Myristoylation-dependent replication and assembly of human immunodeficiency virus 1.* Proc Natl Acad Sci U S A, 1990. **87**(2): p. 523-7.

47. Gottlinger, H.G., J.G. Sodroski, and W.A. Haseltine, *Role of capsid precursor processing and myristoylation in morphogenesis and infectivity of human immunodeficiency virus type 1.* Proc Natl Acad Sci U S A, 1989. **86**(15): p. 5781-5.

48. Hill, C.P., D. Worthylake, D.P. Bancroft, A.M. Christensen, and W.I. Sundquist, *Crystal structures of the trimeric human immunodeficiency virus type 1 matrix protein: implications for membrane association and assembly.* Proc Natl Acad Sci U S A, 1996. **93**(7): p. 3099-104.

49. Bukrinskaya, A.G., A. Ghorpade, N.K. Heinzinger, T.E. Smithgall, R.E. Lewis, and M. Stevenson, *Phosphorylation-dependent human immunodeficiency virus type 1 infection and nuclear targeting of viral DNA.* Proc Natl Acad Sci U S A, 1996. **93**(1): p. 367-71.

50. Bukrinsky, M.I., S. Haggerty, M.P. Dempsey, N. Sharova, A. Adzhubel, L. Spitz, . . . M. Stevenson, *A nuclear localization signal within HIV-1 matrix protein that governs infection of non-dividing cells.* Nature, 1993. **365**(6447): p. 666-9.

51. Gallay, P., S. Swingler, J. Song, F. Bushman, and D. Trono, *HIV nuclear import is governed by the phosphotyrosine-mediated binding of matrix to the core domain of integrase.* Cell, 1995. **83**(4): p. 569-76.

52. Briggs, J.A., M.N. Simon, I. Gross, H.G. Krausslich, S.D. Fuller, V.M. Vogt, and M.C. Johnson, *The stoichiometry of Gag protein in HIV-1.* Nat Struct Mol Biol, 2004. **11**(7): p. 672-5.

53. Bhattacharya, A., S.L. Alam, T. Fricke, K. Zadrozny, J. Sedzicki, A.B. Taylor, . . . M. Yeager, *Structural basis of HIV-1 capsid recognition by PF74 and CPSF6.* Proc Natl Acad Sci U S A, 2014. **111**(52): p. 18625-30.

54. Ganser-Pornillos, B.K., A. Cheng, and M. Yeager, *Structure of full-length HIV-1 CA: a model for the mature capsid lattice.* Cell, 2007. **131**(1): p. 70-9.

55. Price, A.J., D.A. Jacques, W.A. McEwan, A.J. Fletcher, S. Essig, J.W. Chin, . . . L.C. James, *Host cofactors and pharmacologic ligands share an essential interface in HIV-1 capsid that is lost upon disassembly.* PLoS Pathog, 2014. **10**(10): p. e1004459.

56. Franke, E.K. and J. Luban, *Inhibition of HIV-1 replication by cyclosporine A or related compounds correlates with the ability to disrupt the Gag-cyclophilin A interaction.* Virology, 1996. **222**(1): p. 279-82.

57. Franke, E.K., H.E. Yuan, and J. Luban, *Specific incorporation of cyclophilin A into HIV-1 virions.* Nature, 1994. **372**(6504): p. 359-62.

58. Schmalzbauer, E., B. Strack, J. Dannull, S. Guehmann, and K. Moelling, *Mutations of basic amino acids of NCp7 of human immunodeficiency virus type 1 affect RNA binding in vitro.* J Virol, 1996. **70**(2): p. 771-7.

59. Harrison, G.P. and A.M. Lever, *The human immunodeficiency virus type 1 packaging signal and major splice donor region have a conserved stable secondary structure.* J Virol, 1992. **66**(7): p. 4144-53.

60. Bampi, C., S. Jacquenet, D. Lener, D. Decimo, and J.L. Darlix, *The chaperoning and assistance roles of the HIV-1 nucleocapsid protein in proviral DNA synthesis and maintenance.* Int J Biochem Cell Biol, 2004. **36**(9): p. 1668-86.

61. Levin, J.G., J. Guo, I. Rouzina, and K. Musier-Forsyth, *Nucleic acid chaperone activity of HIV-1 nucleocapsid protein: critical role in reverse transcription and molecular mechanism.* Prog Nucleic Acid Res Mol Biol, 2005. **80**: p. 217-86.

62. Tisne, C., B.P. Roques, and F. Dardel, *Heteronuclear NMR studies of the interaction of tRNA(Lys)3 with HIV-1 nucleocapsid protein.* J Mol Biol, 2001. **306**(3): p. 443-54.

63. Tisne, C., B.P. Roques, and F. Dardel, *The annealing mechanism of HIV-1 reverse transcription primer onto the viral genome.* J Biol Chem, 2004. **279**(5): p. 3588-95.

64. You, J.C. and C.S. McHenry, *Human immunodeficiency virus nucleocapsid protein accelerates strand transfer of the terminally redundant sequences involved in reverse transcription.* J Biol Chem, 1994. **269**(50): p. 31491-5.

65. Checroune, F., X.J. Yao, H.G. Gottlinger, D. Bergeron, and E.A. Cohen, *Incorporation of Vpr into human immunodeficiency virus type 1: role of conserved regions within the P6 domain of Pr55gag.* J Acquir Immune Defic Syndr Hum Retrovirol, 1995. **10**(1): p. 1-7.

66. Kondo, E. and H.G. Gottlinger, *A conserved LXXLF sequence is the major determinant in p6gag required for the incorporation of human immunodeficiency virus type 1 Vpr.* J Virol, 1996. **70**(1): p. 159-64.

67. Solbak, S.M., T.R. Reksten, F. Hahn, V. Wray, P. Henklein, O. Halskau, . . . T. Fossen, *HIV-1 p6 - a structured to flexible multifunctional membrane-interacting protein.* Biochim Biophys Acta, 2013. **1828**(2): p. 816-23.

68. Gottlinger, H.G., T. Dorfman, J.G. Sodroski, and W.A. Haseltine, *Effect of mutations affecting the p6 gag protein on human immunodeficiency virus particle release.* Proc Natl Acad Sci U S A, 1991. **88**(8): p. 3195-9.

69. Huang, M., J.M. Orenstein, M.A. Martin, and E.O. Freed, *p6Gag is required for particle production from full-length human immunodeficiency virus type 1 molecular clones expressing protease.* J Virol, 1995. **69**(11): p. 6810-8.

70. Strack, B., A. Calistri, S. Craig, E. Popova, and H.G. Gottlinger, *AIP1/ALIX is a binding partner for HIV-1 p6 and EIAV p9 functioning in virus budding.* Cell, 2003. **114**(6): p. 689-99.

71. Jacks, T., M.D. Power, F.R. Masiarz, P.A. Luciw, P.J. Barr, and H.E. Varmus, *Characterization of ribosomal frameshifting in HIV-1 gag-pol expression.* Nature, 1988. **331**(6153): p. 280-3.

72. Parkin, N.T., M. Chamorro, and H.E. Varmus, *Human immunodeficiency virus type 1 gag-pol frameshifting is dependent on downstream mRNA secondary structure: demonstration by expression in vivo.* J Virol, 1992. **66**(8): p. 5147-51.

73. Ashorn, P., T.J. McQuade, S. Thaisrivongs, A.G. Tomasselli, W.G. Tarpley, and B. Moss, *An inhibitor of the protease blocks maturation of human and simian immunodeficiency viruses and spread of infection.* Proc Natl Acad Sci U S A, 1990. **87**(19): p. 7472-6.

74. Zybarth, G. and C. Carter, *Domains upstream of the protease (PR) in human immunodeficiency virus type 1 Gag-Pol influence PR autoprocessing.* J Virol, 1995. **69**(6): p. 3878-84.

75. Krausslich, H.G., M. Facke, A.M. Heuser, J. Konvalinka, and H. Zentgraf, *The spacer peptide between human immunodeficiency virus capsid and nucleocapsid proteins is essential for ordered assembly and viral infectivity.* J Virol, 1995. **69**(6): p. 3407-19.

76. Sheng, N., S.C. Pettit, R.J. Tritch, D.H. Ozturk, M.M. Rayner, R. Swanstrom, and S. Erickson-Viitanen, *Determinants of the human immunodeficiency virus type 1 p15NC-RNA interaction that affect enhanced cleavage by the viral protease.* J Virol, 1997. **71**(8): p. 5723-32.

77. Luukkonen, B.G., E.M. Fenyo, and S. Schwartz, *Overexpression of human immunodeficiency virus type 1 protease increases intracellular cleavage of Gag and reduces virus infectivity.* Virology, 1995. **206**(2): p. 854-65.

78. Miller, M., M. Jaskolski, J.K. Rao, J. Leis, and A. Wlodawer, *Crystal structure of a retroviral protease proves relationship to aspartic protease family.* Nature, 1989. **337**(6207): p. 576-9.

79. Navia, M.A., P.M. Fitzgerald, B.M. McKeever, C.T. Leu, J.C. Heimbach, W.K. Herber, . . . J.P. Springer, *Three-dimensional structure of aspartyl protease from human immunodeficiency virus HIV-1.* Nature, 1989. **337**(6208): p. 615-20.

80. Esnouf, R., J. Ren, C. Ross, Y. Jones, D. Stammers, and D. Stuart, *Mechanism of inhibition of HIV-1 reverse transcriptase by non-nucleoside inhibitors.* Nat Struct Biol, 1995. **2**(4): p. 303-8.

81. Kohlstaedt, L.A., J. Wang, J.M. Friedman, P.A. Rice, and T.A. Steitz, *Crystal structure at 3.5 A resolution of HIV-1 reverse transcriptase complexed with an inhibitor.* Science, 1992. **256**(5065): p. 1783-90.

82. Rodgers, D.W., S.J. Gamblin, B.A. Harris, S. Ray, J.S. Culp, B. Hellmig, . . . S.C. Harrison, *The structure of unliganded reverse transcriptase from the human immunodeficiency virus type 1.* Proc Natl Acad Sci U S A, 1995. **92**(4): p. 1222-6.

83. Hu, W.S. and S.H. Hughes, *HIV-1 Reverse Transcription*, in *Cold Spring Harb Perspect Med*. 2012.

84. Roberts, J.D., K. Bebenek, and T.A. Kunkel, *The accuracy of reverse transcriptase from HIV-1.* Science, 1988. **242**(4882): p. 1171-3.

85. Johnson, M.A. and A. Fridland, *Phosphorylation of 2',3'-dideoxyinosine by cytosolic 5'-nucleotidase of human lymphoid cells.* Mol Pharmacol, 1989. **36**(2): p. 291-5.

86. Mitsuya, H., K.J. Weinhold, P.A. Furman, M.H. St Clair, S.N. Lehrman, R.C. Gallo, . . . S. Broder, *3'-Azido-3'-deoxythymidine (BW A509U): an antiviral agent that inhibits the infectivity and cytopathic effect of human T-lymphotropic virus type III/lymphadenopathy-associated virus in vitro.* Proc Natl Acad Sci U S A, 1985. **82**(20): p. 7096-100.

87. Pata, J.D., W.G. Stirtan, S.W. Goldstein, and T.A. Steitz, *Structure of HIV-1 reverse transcriptase bound to an inhibitor active against mutant reverse transcriptases resistant to other nonnucleoside inhibitors.* Proc Natl Acad Sci U S A, 2004. **101**(29): p. 10548-53.

88. Cai, M., R. Zheng, M. Caffrey, R. Craigie, G.M. Clore, and A.M. Gronenborn, *Solution structure of the N-terminal zinc binding domain of HIV-1 integrase.* Nat Struct Biol, 1997. **4**(7): p. 567-77.

89. Lodi, P.J., J.A. Ernst, J. Kuszewski, A.B. Hickman, A. Engelman, R. Craigie, . . . A.M. Gronenborn, *Solution structure of the DNA binding domain of HIV-1 integrase.* Biochemistry, 1995. **34**(31): p. 9826-33.

90. Maignan, S., J.P. Guilloteau, Q. Zhou-Liu, C. Clement-Mella, and V. Mikol, *Crystal structures of the catalytic domain of HIV-1 integrase free and complexed with its metal cofactor: high level of similarity of the active site with other viral integrases.* J Mol Biol, 1998. **282**(2): p. 359-68.

91. Zheng, R., T. Jenkins, and R. Craigie, *Zinc folds the N-terminal domain of HIV-1 integrase, promotes multimerization, and enhances catalytic activity*, in *Proc Natl Acad Sci U S A.* 1996. p. 13659-64.

92. Jayappa, K.D., Z. Ao, and X. Yao, *The HIV-1 passage from cytoplasm to nucleus: the process involving a complex exchange between the components of HIV-1 and cellular machinery to access nucleus and successful integration.* Int J Biochem Mol Biol, 2012. **3**(1): p. 70-85.

93. Muller, H.P. and H.E. Varmus, *DNA bending creates favored sites for retroviral integration: an explanation for preferred insertion sites in nucleosomes.* Embo j, 1994. **13**(19): p. 4704-14.

94. Pruss, D., F.D. Bushman, and A.P. Wolffe, *Human immunodeficiency virus integrase directs integration to sites of severe DNA distortion within the nucleosome core.* Proc Natl Acad Sci U S A, 1994. **91**(13): p. 5913-7.

95. Van Maele, B., K. Busschots, L. Vandekerckhove, F. Christ, and Z. Debyser, *Cellular co-factors of HIV-1 integration.* Trends Biochem Sci, 2006. **31**(2): p. 98-105.

96. Smith, S.J., X.Z. Zhao, T.R. Burke, Jr., and S.H. Hughes, *HIV-1 Integrase Inhibitors That Are Broadly Effective against Drug-Resistant Mutants.* Antimicrob Agents Chemother, 2018. **62**(9).

97. Freed, E.O. and M.A. Martin, *The role of human immunodeficiency virus type 1 envelope glycoproteins in virus infection.* J Biol Chem, 1995. **270**(41): p. 23883-6.

98. Berman, P.W., W.M. Nunes, and O.K. Haffar, *Expression of membrane-associated and secreted variants of gp160 of human immunodeficiency virus type 1 in vitro and in continuous cell lines.* J Virol, 1988. **62**(9): p. 3135-42.

99. Capon, D.J. and R.H. Ward, *The CD4-gp120 interaction and AIDS pathogenesis.* Annu Rev Immunol, 1991. **9**: p. 649-78.

100. Earl, P.L., R.W. Doms, and B. Moss, *Oligomeric structure of the human immunodeficiency virus type 1 envelope glycoprotein.* Proc Natl Acad Sci U S A, 1990. **87**(2): p. 648-52.

101. Pinter, A., W.J. Honnen, S.A. Tilley, C. Bona, H. Zaghouani, M.K. Gorny, and S. Zolla-Pazner, *Oligomeric structure of gp41, the transmembrane protein of human immunodeficiency virus type 1.* J Virol, 1989. **63**(6): p. 2674-9.

102. Schawaller, M., G.E. Smith, J.J. Skehel, and D.C. Wiley, *Studies with crosslinking reagents on the oligomeric structure of the env glycoprotein of HIV.* Virology, 1989. **172**(1): p. 367-9.

103. Freed, E.O., D.J. Myers, and R. Risser, *Mutational analysis of the cleavage sequence of the human immunodeficiency virus type 1 envelope glycoprotein precursor gp160.* J Virol, 1989. **63**(11): p. 4670-5.

104. Hallenberger, S., V. Bosch, H. Angliker, E. Shaw, H.D. Klenk, and W. Garten, *Inhibition of furin-mediated cleavage activation of HIV-1 glycoprotein gp160.* Nature, 1992. **360**(6402): p. 358-61.

105. Egan, M.A., L.M. Carruth, J.F. Rowell, X. Yu, and R.F. Siliciano, *Human immunodeficiency virus type 1 envelope protein endocytosis mediated by a highly conserved intrinsic internalization signal in the cytoplasmic domain of gp41 is suppressed in the presence of the Pr55gag precursor protein.* J Virol, 1996. **70**(10): p. 6547-56.

106. Zhu, P., E. Chertova, J. Bess, Jr., J.D. Lifson, L.O. Arthur, J. Liu, . . . K.H. Roux, *Electron tomography analysis of envelope glycoprotein trimers on HIV and simian immunodeficiency virus virions.* Proc Natl Acad Sci U S A, 2003. **100**(26): p. 15812-7.

107. Starcich, B.R., B.H. Hahn, G.M. Shaw, P.D. McNeely, S. Modrow, H. Wolf, . . . et al., *Identification and characterization of conserved and variable regions in the envelope gene of HTLV-III/LAV, the retrovirus of AIDS.* Cell, 1986. **45**(5): p. 637-48.

108. Willey, R.L., R.A. Rutledge, S. Dias, T. Folks, T. Theodore, C.E. Buckler, and M.A. Martin, *Identification of conserved and divergent domains within the envelope gene of the acquired immunodeficiency syndrome retrovirus.* Proc Natl Acad Sci U S A, 1986. **83**(14): p. 5038-42.

109. Jobes, D.V., M. Daoust, V. Nguyen, A. Padua, S. Michele, M.D. Lock, . . . P.W. Berman, *High incidence of unusual cysteine variants in gp120 envelope proteins from early HIV type 1 infections from a Phase 3 vaccine efficacy trial.* AIDS Res Hum Retroviruses, 2006. **22**(10): p. 1014-21.

110. Montefiori, D.C., W.E. Robinson, Jr., and W.M. Mitchell, *Role of protein N-glycosylation in pathogenesis of human immunodeficiency virus type 1.* Proc Natl Acad Sci U S A, 1988. **85**(23): p. 9248-52.

111. Berger, E.A., P.M. Murphy, and J.M. Farber, *Chemokine receptors as HIV-1 coreceptors: roles in viral entry, tropism, and disease.* Annu Rev Immunol, 1999. **17**: p. 657-700.

112. Kwong, P.D., R. Wyatt, J. Robinson, R.W. Sweet, J. Sodroski, and W.A. Hendrickson, *Structure of an HIV gp120 envelope glycoprotein in complex with the CD4 receptor and a neutralizing human antibody.* Nature, 1998. **393**(6686): p. 648-59.

113. Liu, J., A. Bartesaghi, M.J. Borgnia, G. Sapiro, and S. Subramaniam, *Molecular architecture of native HIV-1 gp120 trimers.* Nature, 2008. **455**(7209): p. 109-13.

114. Wu, S.R., R. Loving, B. Lindqvist, H. Hebert, P.J. Koeck, M. Sjoberg, and H. Garoff, *Single-particle cryoelectron microscopy analysis reveals the HIV-1 spike as a tripod structure.* Proc Natl Acad Sci U S A, 2010. **107**(44): p. 18844-9.

115. Hernandez, L.D., L.R. Hoffman, T.G. Wolfsberg, and J.M. White, *Virus-cell and cell-cell fusion.* Annu Rev Cell Dev Biol, 1996. **12**: p. 627-61.

116. Bosch, M.L., P.L. Earl, K. Fargnoli, S. Picciafuoco, F. Giombini, F. Wong-Staal, and G. Franchini, *Identification of the fusion peptide of primate immunodeficiency viruses.* Science, 1989. **244**(4905): p. 694-7.

117. Dubay, J.W., S.J. Roberts, B. Brody, and E. Hunter, *Mutations in the leucine zipper of the human immunodeficiency virus type 1 transmembrane glycoprotein affect fusion and infectivity.* J Virol, 1992. **66**(8): p. 4748-56.

118. Salzwedel, K., J.T. West, and E. Hunter, *A conserved tryptophan-rich motif in the membrane-proximal region of the human immunodeficiency virus type 1 gp41 ectodomain is important for Env-mediated fusion and virus infectivity.* J Virol, 1999. **73**(3): p. 2469-80.

119. Brasseur, R., M. Vandenbranden, B. Cornet, A. Burny, and J.M. Ruysschaert, *Orientation into the lipid bilayer of an asymmetric amphipathic helical peptide located at the N-terminus of viral fusion proteins.* Biochim Biophys Acta, 1990. **1029**(2): p. 267-73.

120. Shang, L., L. Yue, and E. Hunter, *Role of the membrane-spanning domain of human immunodeficiency virus type 1 envelope glycoprotein in cell-cell fusion and virus infection.* J Virol, 2008. **82**(11): p. 5417-28.

121. Affranchino, J.L. and S.A. Gonzalez, *Mutations at the C-terminus of the simian immunodeficiency virus envelope glycoprotein affect gp120-gp41 stability on virions.* Virology, 2006. **347**(1): p. 217-25.

122. Gabuzda, D.H., A. Lever, E. Terwilliger, and J. Sodroski, *Effects of deletions in the cytoplasmic domain on biological functions of human immunodeficiency virus type 1 envelope glycoproteins.* J Virol, 1992. **66**(6): p. 3306-15.

123. Kalia, V., S. Sarkar, P. Gupta, and R.C. Montelaro, *Rational site-directed mutations of the LLP-1 and LLP-2 lentivirus lytic peptide domains in the intracytoplasmic tail of human immunodeficiency virus type 1 gp41 indicate common functions in cell-cell fusion but distinct roles in virion envelope incorporation.* J Virol, 2003. **77**(6): p. 3634-46.

124. Lee, S.J., W. Hu, A.G. Fisher, D.J. Looney, V.F. Kao, H. Mitsuya, . . . F. Wong-Staal, *Role of the carboxy-terminal portion of the HIV-1 transmembrane protein in viral transmission and cytopathogenicity.* AIDS Res Hum Retroviruses, 1989. **5**(4): p. 441-9.

125. Boge, M., S. Wyss, J.S. Bonifacino, and M. Thali, *A membrane-proximal tyrosine-based signal mediates internalization of the HIV-1 envelope glycoprotein via interaction with the AP-2 clathrin adaptor.* J Biol Chem, 1998. **273**(25): p. 15773-8.

126. Byland, R., P.J. Vance, J.A. Hoxie, and M. Marsh, *A conserved dileucine motif mediates clathrin and AP-2-dependent endocytosis of the HIV-1 envelope protein.* Mol Biol Cell, 2007. **18**(2): p. 414-25.

127. Kilareski, E.M., S. Shah, M.R. Nonnemacher, and B. Wigdahl, *Regulation of HIV-1 transcription in cells of the monocyte-macrophage lineage*, in *Retrovirology*. 2009. p. 118.

128. Feng, S. and E.C. Holland, *HIV-1 tat trans-activation requires the loop sequence within tar*. Nature, 1988. **334**(6178): p. 165-7.

129. Roy, S., U. Delling, C.H. Chen, C.A. Rosen, and N. Sonenberg, *A bulge structure in HIV-1 TAR RNA is required for Tat binding and Tat-mediated trans-activation.* Genes Dev, 1990. **4**(8): p. 1365-73.

130. Tiley, L.S., S.J. Madore, M.H. Malim, and B.R. Cullen, *The VP16 transcription activation domain is functional when targeted to a promoter-proximal RNA sequence.* Genes Dev, 1992. **6**(11): p. 2077-87.

131. Southgate, C.D. and M.R. Green, *The HIV-1 Tat protein activates transcription from an upstream DNA-binding site: implications for Tat function.* Genes Dev, 1991. **5**(12b): p. 2496-507.

132. Chun, R.F., O.J. Semmes, C. Neuveut, and K.T. Jeang, *Modulation of Sp1 phosphorylation by human immunodeficiency virus type 1 Tat.* J Virol, 1998. **72**(4): p. 2615-29.

133. Biswas, D.K., T.R. Salas, F. Wang, C.M. Ahlers, B.J. Dezube, and A.B. Pardee, *A Tat-induced auto-up-regulatory loop for superactivation of the human immunodeficiency virus type 1 promoter.* J Virol, 1995. **69**(12): p. 7437-44.

134. Hidalgo-Estevez, A.M., E. Gonzalez, C. Punzon, and M. Fresno, *Human immunodeficiency virus type 1 Tat increases cooperation between AP-1 and NFAT transcription factors in T cells.* J Gen Virol, 2006. **87**(Pt 6): p. 1603-12.

135. Kim, S.Y., R. Byrn, J. Groopman, and D. Baltimore, *Temporal aspects of DNA and RNA synthesis during human immunodeficiency virus infection: evidence for differential gene expression.* J Virol, 1989. **63**(9): p. 3708-13.

136. Zapp, M.L. and M.R. Green, *Sequence-specific RNA binding by the HIV-1 Rev protein.* Nature, 1989. **342**(6250): p. 714-6.

137. Felber, B.K., C.M. Drysdale, and G.N. Pavlakis, *Feedback regulation of human immunodeficiency virus type 1 expression by the Rev protein.* J Virol, 1990. **64**(8): p. 3734-41.

138. Meyer, B.E. and M.H. Malim, *The HIV-1 Rev trans-activator shuttles between the nucleus and the cytoplasm.* Genes Dev, 1994. **8**(13): p. 1538-47.

139. Pollard, V.W. and M.H. Malim, *The HIV-1 Rev protein.* Annu Rev Microbiol, 1998. **52**: p. 491-532.

140. Fischer, U., J. Huber, W.C. Boelens, I.W. Mattaj, and R. Luhrmann, *The HIV-1 Rev activation domain is a nuclear export signal that accesses an export pathway used by specific cellular RNAs.* Cell, 1995. **82**(3): p. 475-83.

141. Malim, M.H., S. Bohnlein, J. Hauber, and B.R. Cullen, *Functional dissection of the HIV-1 Rev trans-activator--derivation of a trans-dominant repressor of Rev function.* Cell, 1989. **58**(1): p. 205-14.

142. Kjems, J. and P.A. Sharp, *The basic domain of Rev from human immunodeficiency virus type 1 specifically blocks the entry of U4/U6.U5 small nuclear ribonucleoprotein in spliceosome assembly.* J Virol, 1993. **67**(8): p. 4769-76.

143. Willey, R.L., F. Maldarelli, M.A. Martin, and K. Strebel, *Human immunodeficiency virus type 1 Vpu protein induces rapid degradation of CD4.* J Virol, 1992. **66**(12): p. 7193-200.

144. Klimkait, T., K. Strebel, M.D. Hoggan, M.A. Martin, and J.M. Orenstein, *The human immunodeficiency virus type 1-specific protein vpu is required for efficient virus maturation and release.* J Virol, 1990. **64**(2): p. 621-9.

145. Neil, S.J., S.W. Eastman, N. Jouvenet, and P.D. Bieniasz, *HIV-1 Vpu promotes release and prevents endocytosis of nascent retrovirus particles from the plasma membrane.* PLoS Pathog, 2006. **2**(5): p. e39.

146. McNatt, M.W., T. Zang, and P.D. Bieniasz, *Vpu binds directly to tetherin and displaces it from nascent virions.* PLoS Pathog, 2013. **9**(4): p. e1003299.

147. Neil, S.J., T. Zang, and P.D. Bieniasz, *Tetherin inhibits retrovirus release and is antagonized by HIV-1 Vpu.* Nature, 2008. **451**(7177): p. 425-30.

148. Cohen, E.A., G. Dehni, J.G. Sodroski, and W.A. Haseltine, *Human immunodeficiency virus vpr product is a virion-associated regulatory protein.* J Virol, 1990. **64**(6): p. 3097-9.

149. Fouchier, R.A.M., B.E. Meyer, J.H.M. Simon, U. Fischer, A.V. Albright, F. González-Scarano, and M.H. Malim, *Interaction of the Human Immunodeficiency Virus Type 1 Vpr Protein with the Nuclear Pore Complex*, in *J Virol*. 1998. p. 6004-13.

150. Heinzinger, N.K., M.I. Bukrinsky, S.A. Haggerty, A.M. Ragland, V. Kewalramani, M.A. Lee, . . . M. Emerman, *The Vpr protein of human immunodeficiency virus type 1 influences nuclear localization of viral nucleic acids in nondividing host cells.* Proc Natl Acad Sci U S A, 1994. **91**(15): p. 7311-5.

151. Subbramanian, R.A., A. Kessous-Elbaz, R. Lodge, J. Forget, X.J. Yao, D. Bergeron, and E.A. Cohen, *Human immunodeficiency virus type 1 Vpr is a positive regulator of viral transcription and infectivity in primary human macrophages.* J Exp Med, 1998. **187**(7): p. 1103-11.

152. Guenzel, C.A., C. Herate, E. Le Rouzic, P. Maidou-Peindara, H.A. Sadler, M.C. Rouyez, . . . S. Benichou, *Recruitment of the nuclear form of uracil DNA glycosylase into virus particles participates in the full infectivity of HIV-1.* J Virol, 2012. **86**(5): p. 2533-44.

153. Jowett, J.B., V. Planelles, B. Poon, N.P. Shah, M.L. Chen, and I.S. Chen, *The human immunodeficiency virus type 1 vpr gene arrests infected T cells in the G2 + M phase of the cell cycle.* J Virol, 1995. **69**(10): p. 6304-13.

154. Emerman, M., *HIV-1, Vpr and the cell cycle.* Current Biology, 1996. **6**(9): p. 1096-1103.

155. Strebel, K., D. Daugherty, K. Clouse, D. Cohen, T. Folks, and M.A. Martin, *The HIV 'A' (sor) gene product is essential for virus infectivity.* Nature, 1987. **328**(6132): p. 728-30.

156. Simon, J.H., D.L. Miller, R.A. Fouchier, M.A. Soares, K.W. Peden, and M.H. Malim, *The regulation of primate immunodeficiency virus infectivity by Vif is cell species restricted: a role for Vif in determining virus host range and cross-species transmission.* Embo j, 1998. **17**(5): p. 1259-67.

157. Sheehy, A.M., N.C. Gaddis, J.D. Choi, and M.H. Malim, *Isolation of a human gene that inhibits HIV-1 infection and is suppressed by the viral Vif protein.* Nature, 2002. **418**(6898): p. 646-50.

158. Harris, R.S., K.N. Bishop, A.M. Sheehy, H.M. Craig, S.K. Petersen-Mahrt, I.N. Watt, . . . M.H. Malim, *DNA deamination mediates innate immunity to retroviral infection.* Cell, 2003. **113**(6): p. 803-9.

159. Bishop, K.N., M. Verma, E.Y. Kim, S.M. Wolinsky, and M.H. Malim, *APOBEC3G inhibits elongation of HIV-1 reverse transcripts.* PLoS Pathog, 2008. **4**(12): p. e1000231.

160. Stanley, B.J., E.S. Ehrlich, L. Short, Y. Yu, Z. Xiao, X.F. Yu, and Y. Xiong, *Structural Insight into the Human Immunodeficiency Virus Vif SOCS Box and Its Role in Human E3 Ubiquitin Ligase Assembly ▿†*, in *J Virol*. 2008. p. 8656-63.

161. Geyer, M., O.T. Fackler, and B.M. Peterlin, *Structure--function relationships in HIV-1 Nef.* EMBO Rep, 2001. **2**(7): p. 580-5.

162. Garcia, J.V. and A.D. Miller, *Serine phosphorylation-independent downregulation of cell-surface CD4 by nef.* Nature, 1991. **350**(6318): p. 508-11.

163. Lindwasser, O.W., W.J. Smith, R. Chaudhuri, P. Yang, J.H. Hurley, and J.S. Bonifacino, *A diacidic motif in human immunodeficiency virus type 1 Nef is a novel determinant of binding to AP-2.* J Virol, 2008. **82**(3): p. 1166-74.

164. Schwartz, O., V. Marechal, S. Le Gall, F. Lemonnier, and J.M. Heard, *Endocytosis of major histocompatibility complex class I molecules is induced by the HIV-1 Nef protein.* Nat Med, 1996. **2**(3): p. 338-42.

165. Atkins, K.M., L. Thomas, R.T. Youker, M.J. Harriff, F. Pissani, H. You, and G. Thomas, *HIV-1 Nef binds PACS-2 to assemble a multikinase cascade that triggers major histocompatibility complex class I (MHC-I) down-regulation: analysis using short interfering RNA and knock-out mice.* J Biol Chem, 2008. **283**(17): p. 11772-84.

166. Jia, X., R. Singh, S. Homann, H. Yang, J. Guatelli, and Y. Xiong, *Structural basis of evasion of cellular adaptive immunity by HIV-1 Nef*, in *Nat Struct Mol Biol*. 2012. p. 701-6.

167. Moarefi, I., M. LaFevre-Bernt, F. Sicheri, M. Huse, C.H. Lee, J. Kuriyan, and W.T. Miller, *Activation of the Src-family tyrosine kinase Hck by SH3 domain displacement.* Nature, 1997. **385**(6617): p. 650-3.

168. Breuer, S., H. Gerlach, B. Kolaric, C. Urbanke, N. Opitz, and M. Geyer, *Biochemical indication for myristoylation-dependent conformational changes in HIV-1 Nef.* Biochemistry, 2006. **45**(7): p. 2339-49.

169. Poe, J.A. and T.E. Smithgall, *HIV-1 Nef dimerization is required for Nef-mediated receptor downregulation and viral replication.* J Mol Biol, 2009. **394**(2): p. 329-42.

170. Desai, M., G. Iyer, and R.K. Dikshit, *Antiretroviral drugs: Critical issues and recent advances*, in *Indian J Pharmacol*. 2012. p. 288-98.

171. Saphire, A.C., M.D. Bobardt, Z. Zhang, G. David, and P.A. Gallay, *Syndecans serve as attachment receptors for human immunodeficiency virus type 1 on macrophages.* J Virol, 2001. **75**(19): p. 9187-200.

172. Arthos, J., C. Cicala, E. Martinelli, K. Macleod, D. Van Ryk, D. Wei, . . . A.S. Fauci, *HIV-1 envelope protein binds to and signals through integrin alpha4beta7, the gut mucosal homing receptor for peripheral T cells.* Nat Immunol, 2008. **9**(3): p. 301-9.

173. Geijtenbeek, T.B., D.S. Kwon, R. Torensma, S.J. van Vliet, G.C. van Duijnhoven, J. Middel, . . . Y. van Kooyk, *DC-SIGN, a dendritic cell-specific HIV-1-binding protein that enhances trans-infection of T cells.* Cell, 2000. **100**(5): p. 587-97.

174. Wilen, C.B., J.C. Tilton, and R.W. Doms, *HIV: Cell Binding and Entry*, in *Cold Spring Harb Perspect Med*. 2012.

175. Leonard, C.K., M.W. Spellman, L. Riddle, R.J. Harris, J.N. Thomas, and T.J. Gregory, *Assignment of intrachain disulfide bonds and characterization of potential glycosylation sites of the type 1 recombinant human immunodeficiency virus envelope glycoprotein (gp120) expressed in Chinese hamster ovary cells.* J Biol Chem, 1990. **265**(18): p. 10373-82.

176. Moebius, U., L.K. Clayton, S. Abraham, S.C. Harrison, and E.L. Reinherz, *The human immunodeficiency virus gp120 binding site on CD4: delineation by quantitative equilibrium and kinetic binding studies of mutants in conjunction with a high-resolution CD4 atomic structure.* J Exp Med, 1992. **176**(2): p. 507-17.

177. Olshevsky, U., E. Helseth, C. Furman, J. Li, W. Haseltine, and J. Sodroski, *Identification of individual human immunodeficiency virus type 1 gp120 amino acids important for CD4 receptor binding.* J Virol, 1990. **64**(12): p. 5701-7.

178. Trkola, A., T. Dragic, J. Arthos, J.M. Binley, W.C. Olson, G.P. Allaway, . . . J.P. Moore, *CD4-dependent, antibody-sensitive interactions between HIV-1 and its co-receptor CCR-5.* Nature, 1996. **384**(6605): p. 184-7.

179. Shaik, M.M., H. Peng, J. Lu, S. Rits-Volloch, C. Xu, M. Liao, and B. Chen, *Structural basis of coreceptor recognition by HIV-1 envelope spike.* Nature, 2019. **565**(7739): p. 318-323.

180. Buzon, V., G. Natrajan, D. Schibli, F. Campelo, M.M. Kozlov, and W. Weissenhorn, *Crystal structure of HIV-1 gp41 including both fusion peptide and membrane proximal external regions.* PLoS Pathog, 2010. **6**(5): p. e1000880.

181. Chan, D.C., D. Fass, J.M. Berger, and P.S. Kim, *Core structure of gp41 from the HIV envelope glycoprotein.* Cell, 1997. **89**(2): p. 263-73.

182. Melikyan, G.B., R.M. Markosyan, H. Hemmati, M.K. Delmedico, D.M. Lambert, and F.S. Cohen, *Evidence that the transition of HIV-1 gp41 into a six-helix bundle, not the bundle configuration, induces membrane fusion.* J Cell Biol, 2000. **151**(2): p. 413-23.

183. Chernomordik, L.V. and M.M. Kozlov, *Mechanics of membrane fusion.* Nat Struct Mol Biol, 2008. **15**(7): p. 675-83.

184. Munoz-Barroso, I., S. Durell, K. Sakaguchi, E. Appella, and R. Blumenthal, *Dilation of the human immunodeficiency virus-1 envelope glycoprotein fusion pore revealed by the inhibitory action of a synthetic peptide from gp41.* J Cell Biol, 1998. **140**(2): p. 315-23.

185. Harrison, S.C., *Mechanism of membrane fusion by viral envelope proteins.* Adv Virus Res, 2005. **64**: p. 231-61.

186. Magnus, C., P. Rusert, S. Bonhoeffer, A. Trkola, and R.R. Regoes, *Estimating the stoichiometry of human immunodeficiency virus entry.* J Virol, 2009. **83**(3): p. 1523-31.

187. Lehmann, M.J., N.M. Sherer, C.B. Marks, M. Pypaert, and W. Mothes, *Actin- and myosin-driven movement of viruses along filopodia precedes their entry into cells.* J Cell Biol, 2005. **170**(2): p. 317-25.

188. Sherer, N.M., J. Jin, and W. Mothes, *Directional spread of surface-associated retroviruses regulated by differential virus-cell interactions.* J Virol, 2010. **84**(7): p. 3248-58.

189. Miyauchi, K., Y. Kim, O. Latinovic, V. Morozov, and G.B. Melikyan, *HIV enters cells via endocytosis and dynamin-dependent fusion with endosomes.* Cell, 2009. **137**(3): p. 433-44.

190. Bukrinsky, M., *A Hard Way to the Nucleus*, in *Mol Med*. 2004. p. 1-5.

191. Suzuki, Y. and R. Craigie, *The road to chromatin - nuclear entry of retroviruses.* Nat Rev Microbiol, 2007. **5**(3): p. 187-96.

192. Mortuza, G.B., L.F. Haire, A. Stevens, S.J. Smerdon, J.P. Stoye, and I.A. Taylor, *High-resolution structure of a retroviral capsid hexameric amino-terminal domain.* Nature, 2004. **431**(7007): p. 481-5.

193. Warrilow, D., G. Tachedjian, and D. Harrich, *Maturation of the HIV reverse transcription complex: putting the jigsaw together.* Rev Med Virol, 2009. **19**(6): p. 324-37.

194. Fassati, A. and S.P. Goff, *Characterization of intracellular reverse transcription complexes of human immunodeficiency virus type 1.* J Virol, 2001. **75**(8): p. 3626-35.

195. McDonald, D., M.A. Vodicka, G. Lucero, T.M. Svitkina, G.G. Borisy, M. Emerman, and T.J. Hope, *Visualization of the intracellular behavior of HIV in living cells*, in *J Cell Biol*. 2002. p. 441-52.

196. Nermut, M.V. and A. Fassati, *Structural Analyses of Purified Human Immunodeficiency Virus Type 1 Intracellular Reverse Transcription Complexes*, in *J Virol*. 2003. p. 8196-206.

197. Ambrose, Z. and C. Aiken, *HIV-1 Uncoating: Connection to Nuclear Entry and Regulation by Host Proteins.* Virology, 2014. **0**: p. 371-9.

198. Schaller, T., K.E. Ocwieja, J. Rasaiyaah, A.J. Price, T.L. Brady, S.L. Roth, . . . G.J. Towers, *HIV-1 capsid-cyclophilin interactions determine nuclear import pathway, integration targeting and replication efficiency.* PLoS Pathog, 2011. **7**(12): p. e1002439.

199. Arhel, N.J., S. Souquere-Besse, S. Munier, P. Souque, S. Guadagnini, S. Rutherford, . . . P. Charneau, *HIV-1 DNA Flap formation promotes uncoating of the pre-integration complex at the nuclear pore.* Embo j, 2007. **26**(12): p. 3025-37.

200. Rasaiyaah, J., C.P. Tan, A.J. Fletcher, A.J. Price, C. Blondeau, L. Hilditch, . . . G.J. Towers, *HIV-1 evades innate immune recognition through specific cofactor recruitment.* Nature, 2013. **503**(7476): p. 402-405.

201. Butler, S.L., M.S. Hansen, and F.D. Bushman, *A quantitative assay for HIV DNA integration in vivo.* Nat Med, 2001. **7**(5): p. 631-4.

202. Hu, W.S. and H.M. Temin, *Genetic consequences of packaging two RNA genomes in one retroviral particle: pseudodiploidy and high rate of genetic recombination.* Proc Natl Acad Sci U S A, 1990. **87**(4): p. 1556-60.

203. Rhodes, T., H. Wargo, and W.S. Hu, *High rates of human immunodeficiency virus type 1 recombination: near-random segregation of markers one kilobase apart in one round of viral replication.* J Virol, 2003. **77**(20): p. 11193-200.

204. Delviks-Frankenberry, K., A. Galli, O. Nikolaitchik, H. Mens, V.K. Pathak, and W.S. Hu, *Mechanisms and factors that influence high frequency retroviral recombination.* Viruses, 2011. **3**(9): p. 1650-80.

205. Levy, D.N., G.M. Aldrovandi, O. Kutsch, and G.M. Shaw, *Dynamics of HIV-1 recombination in its natural target cells.* Proc Natl Acad Sci U S A, 2004. **101**(12): p. 4204-9.

206. Hemelaar, J., E. Gouws, P.D. Ghys, and S. Osmanov, *Global trends in molecular epidemiology of HIV-1 during 2000-2007.* Aids, 2011. **25**(5): p. 679-89.

207. Bushman, M.D.M., C.M. Farnet, and D. F, *Human immunodeficiency virus type 1 preintegration complexes: studies of organization and composition.* 1997.

208. Bishop, P.O.B., B. Bowerman, H.E. Varmus, and M. J, *Retroviral integration: structure of the initial covalent product and its precursor, and a role for the viral IN protein.* 1989.

209. Ao, Z., K. Danappa Jayappa, B. Wang, Y. Zheng, S. Kung, E. Rassart, . . . X. Yao, *Importin alpha3 interacts with HIV-1 integrase and contributes to HIV-1 nuclear import and replication.* J Virol, 2010. **84**(17): p. 8650-63.

210. Hearps, A.C. and D.A. Jans, *HIV-1 integrase is capable of targeting DNA to the nucleus via an importin alpha/beta-dependent mechanism.* Biochem J, 2006. **398**(3): p. 475-84.

211. Matreyek, K.A. and A. Engelman, *The requirement for nucleoporin NUP153 during human immunodeficiency virus type 1 infection is determined by the viral capsid.* J Virol, 2011. **85**(15): p. 7818-27.

212. Matreyek, K.A. and A. Engelman, *Viral and Cellular Requirements for the Nuclear Entry of Retroviral Preintegration Nucleoprotein Complexes*, in *Viruses*. 2013. p. 2483-511.

213. Goujon, C., O. Moncorge, H. Bauby, T. Doyle, C.C. Ward, T. Schaller, . . . M.H. Malim, *Human MX2 is an interferon-induced post-entry inhibitor of HIV-1 infection.* Nature, 2013. **502**(7472): p. 559-62.

214. Varmus, J.M.C., H.H. Stephen, and E. Harold, *Retroviruses.* 1997.

215. Lewinski, M.K., D. Bisgrove, P. Shinn, H. Chen, C. Hoffmann, S. Hannenhalli, . . . F.D. Bushman, *Genome-wide analysis of chromosomal features repressing human immunodeficiency virus transcription.* J Virol, 2005. **79**(11): p. 6610-9.

216. Schroder, A.R., P. Shinn, H. Chen, C. Berry, J.R. Ecker, and F. Bushman, *HIV-1 integration in the human genome favors active genes and local hotspots.* Cell, 2002. **110**(4): p. 521-9.

217. Fujinaga, K., T.P. Cujec, J. Peng, J. Garriga, D.H. Price, X. Grana, and B.M. Peterlin, *The ability of positive transcription elongation factor B to transactivate human immunodeficiency virus transcription depends on a functional kinase domain, cyclin T1, and Tat.* J Virol, 1998. **72**(9): p. 7154-9.

218. Zhou, M., M.A. Halanski, M.F. Radonovich, F. Kashanchi, J. Peng, D.H. Price, and J.N. Brady, *Tat modifies the activity of CDK9 to phosphorylate serine 5 of the RNA polymerase*

II carboxyl-terminal domain during human immunodeficiency virus type 1 transcription. Mol Cell Biol, 2000. **20**(14): p. 5077-86.

219. Daugherty, M.D., D.S. Booth, B. Jayaraman, Y. Cheng, and A.D. Frankel, *HIV Rev response element (RRE) directs assembly of the Rev homooligomer into discrete asymmetric complexes.* Proc Natl Acad Sci U S A, 2010. **107**(28): p. 12481-6.

220. Daugherty, M.D., B. Liu, and A.D. Frankel, *Structural basis for cooperative RNA binding and export complex assembly by HIV Rev.* Nat Struct Mol Biol, 2010. **17**(11): p. 1337-42.

221. Tahirov, T.H., N.D. Babayeva, K. Varzavand, J.J. Cooper, S.C. Sedore, and D.H. Price, *Crystal structure of HIV-1 Tat complexed with human P-TEFb.* Nature, 2010. **465**(7299): p. 747-51.

222. Ono, A. and E.O. Freed, *Cell-type-dependent targeting of human immunodeficiency virus type 1 assembly to the plasma membrane and the multivesicular body.* J Virol, 2004. **78**(3): p. 1552-63.

223. Ono, A., S.D. Ablan, S.J. Lockett, K. Nagashima, and E.O. Freed, *Phosphatidylinositol (4,5) bisphosphate regulates HIV-1 Gag targeting to the plasma membrane.* Proc Natl Acad Sci U S A, 2004. **101**(41): p. 14889-94.

224. Saad, J.S., J. Miller, J. Tai, A. Kim, R.H. Ghanam, and M.F. Summers, *Structural basis for targeting HIV-1 Gag proteins to the plasma membrane for virus assembly.* Proc Natl Acad Sci U S A, 2006. **103**(30): p. 11364-9.

225. Hogue, I.B., J.R. Grover, F. Soheilian, K. Nagashima, and A. Ono, *Gag induces the coalescence of clustered lipid rafts and tetraspanin-enriched microdomains at HIV-1 assembly sites on the plasma membrane.* J Virol, 2011. **85**(19): p. 9749-66.

226. Moore, M.D., O.A. Nikolaitchik, J. Chen, M.L. Hammarskjold, D. Rekosh, and W.S. Hu, *Probing the HIV-1 genomic RNA trafficking pathway and dimerization by genetic recombination and single virion analyses.* PLoS Pathog, 2009. **5**(10): p. e1000627.

227. Nikolaitchik, O.A., K.A. Dilley, W. Fu, R.J. Gorelick, S.H. Tai, F. Soheilian, . . . W.S. Hu, *Dimeric RNA recognition regulates HIV-1 genome packaging.* PLoS Pathog, 2013. **9**(3): p. e1003249.

228. Lu, K., X. Heng, L. Garyu, S. Monti, E.L. Garcia, S. Kharytonchyk, . . . M.F. Summers, *NMR detection of structures in the HIV-1 5'-leader RNA that regulate genome packaging.* Science, 2011. **334**(6053): p. 242-5.

229. Ehrlich, L.S., B.E. Agresta, and C.A. Carter, *Assembly of recombinant human immunodeficiency virus type 1 capsid protein in vitro.* J Virol, 1992. **66**(8): p. 4874-83.

230. Schur, F.K., W.J. Hagen, M. Rumlova, T. Ruml, B. Muller, H.G. Krausslich, and J.A. Briggs, *Structure of the immature HIV-1 capsid in intact virus particles at 8.8 A resolution.* Nature, 2015. **517**(7535): p. 505-8.

231. Tedbury, P.R. and E.O. Freed, *The role of matrix in HIV-1 envelope glycoprotein incorporation.* Trends Microbiol, 2014. **22**(7): p. 372-8.

232. Checkley, M.A., B.G. Luttge, and E.O. Freed, *HIV-1 envelope glycoprotein biosynthesis, trafficking, and incorporation.* J Mol Biol, 2011. **410**(4): p. 582-608.

233. Murakami, T. and E.O. Freed, *Genetic evidence for an interaction between human immunodeficiency virus type 1 matrix and alpha-helix 2 of the gp41 cytoplasmic tail.* J Virol, 2000. **74**(8): p. 3548-54.

234. Tedbury, P.R., S.D. Ablan, and E.O. Freed, *Global rescue of defects in HIV-1 envelope glycoprotein incorporation: implications for matrix structure.* PLoS Pathog, 2013. **9**(11): p. e1003739.

235. Demirov, D.G., A. Ono, J.M. Orenstein, and E.O. Freed, *Overexpression of the N-terminal domain of TSG101 inhibits HIV-1 budding by blocking late domain function.* Proc Natl Acad Sci U S A, 2002. **99**(2): p. 955-60.

236. Martin-Serrano, J., T. Zang, and P.D. Bieniasz, *HIV-1 and Ebola virus encode small peptide motifs that recruit Tsg101 to sites of particle assembly to facilitate egress.* Nat Med, 2001. **7**(12): p. 1313-9.

237. VerPlank, L., F. Bouamr, T.J. LaGrassa, B. Agresta, A. Kikonyogo, J. Leis, and C.A. Carter, *Tsg101, a homologue of ubiquitin-conjugating (E2) enzymes, binds the L domain in HIV type 1 Pr55(Gag).* Proc Natl Acad Sci U S A, 2001. **98**(14): p. 7724-9.

238. Henne, W.M., N.J. Buchkovich, and S.D. Emr, *The ESCRT pathway.* Dev Cell, 2011. **21**(1): p. 77-91.

239. Hurley, J.H. and P.I. Hanson, *Membrane budding and scission by the ESCRT machinery: it's all in the neck.* Nat Rev Mol Cell Biol, 2010. **11**(8): p. 556-66.

240. Joshi, A., U. Munshi, S.D. Ablan, K. Nagashima, and E.O. Freed, *Functional replacement of a retroviral late domain by ubiquitin fusion.* Traffic, 2008. **9**(11): p. 1972-83.

241. Sette, P., K. Nagashima, R.C. Piper, and F. Bouamr, *Ubiquitin conjugation to Gag is essential for ESCRT-mediated HIV-1 budding.* Retrovirology, 2013. **10**: p. 79.

242. Schubert, H.L., Q. Zhai, V. Sandrin, D.M. Eckert, M. Garcia-Maya, L. Saul, . . . C.P. Hill, *Structural and functional studies on the extracellular domain of BST2/tetherin in reduced and oxidized conformations.* Proc Natl Acad Sci U S A, 2010. **107**(42): p. 17951-6.

243. Kaplan, A.H., J.A. Zack, M. Knigge, D.A. Paul, D.J. Kempf, D.W. Norbeck, and R. Swanstrom, *Partial inhibition of the human immunodeficiency virus type 1 protease results in aberrant virus assembly and the formation of noninfectious particles.* J Virol, 1993. **67**(7): p. 4050-5.

244. Frank, G.A., K. Narayan, J.W. Bess, Jr., G.Q. Del Prete, X. Wu, A. Moran, . . . S. Subramaniam, *Maturation of the HIV-1 core by a non-diffusional phase transition.* Nat Commun, 2015. **6**: p. 5854.

245. Keller, P.W., R.K. Huang, M.R. England, K. Waki, N. Cheng, J.B. Heymann, . . . A.C. Steven, *A two-pronged structural analysis of retroviral maturation indicates that core formation proceeds by a disassembly-reassembly pathway rather than a displacive transition.* J Virol, 2013. **87**(24): p. 13655-64.

246. von Schwedler, U.K., T.L. Stemmler, V.Y. Klishko, S. Li, K.H. Albertine, D.R. Davis, and W.I. Sundquist, *Proteolytic refolding of the HIV-1 capsid protein amino-terminus facilitates viral core assembly.* Embo j, 1998. **17**(6): p. 1555-68.

247. Bhatti, A.B., M. Usman, and V. Kandi, *Current Scenario of HIV/AIDS, Treatment Options, and Major Challenges with Compliance to Antiretroviral Therapy.* Cureus. **8**(3).

248. Gulick, T.R.K. and G. Peter, *HIV Antiretroviral Therapy.* 2019.

249. Cihlar, T. and A.S. Ray, *Nucleoside and nucleotide HIV reverse transcriptase inhibitors: 25 years after zidovudine.* Antiviral Res, 2010. **85**(1): p. 39-58.

250. Lavie, A., I. Schlichting, I.R. Vetter, M. Konrad, J. Reinstein, and R.S. Goody, *The bottleneck in AZT activation.* Nat Med, 1997. **3**(8): p. 922-4.

251. Nakashima, H., T. Matsui, S. Harada, N. Kobayashi, A. Matsuda, T. Ueda, and N. Yamamoto, *Inhibition of replication and cytopathic effect of human T cell lymphotropic virus type III/lymphadenopathy-associated virus by 3'-azido-3'-deoxythymidine in vitro.* Antimicrob Agents Chemother, 1986. **30**(6): p. 933-7.

252. Doong, S.L., C.H. Tsai, R.F. Schinazi, D.C. Liotta, and Y.C. Cheng, *Inhibition of the replication of hepatitis B virus in vitro by 2',3'-dideoxy-3'-thiacytidine and related analogues.* Proc Natl Acad Sci U S A, 1991. **88**(19): p. 8495-9.

253. Prokofjeva, M.M., S.N. Kochetkov, and V.S. Prassolov, *Therapy of HIV Infection: Current Approaches and Prospects.* Acta Naturae, 2016. **8**(4): p. 23-32.

254. Hooker, D.J., G. Tachedjian, A.E. Solomon, A.D. Gurusinghe, S. Land, C. Birch, . . . N.J. Deacon, *An in vivo mutation from leucine to tryptophan at position 210 in human immunodeficiency virus type 1 reverse transcriptase contributes to high-level resistance to 3'-azido-3'-deoxythymidine.* J Virol, 1996. **70**(11): p. 8010-8.

255. Larder, B.A., G. Darby, and D.D. Richman, *HIV with reduced sensitivity to zidovudine (AZT) isolated during prolonged therapy.* Science, 1989. **243**(4899): p. 1731-4.

256. Deval, J., J. Courcambeck, B. Selmi, J. Boretto, and B. Canard, *Structural determinants and molecular mechanisms for the resistance of HIV-1 RT to nucleoside analogues.* Curr Drug Metab, 2004. **5**(4): p. 305-16.

257. Naeger, L.K., N.A. Margot, and M.D. Miller, *ATP-dependent removal of nucleoside reverse transcriptase inhibitors by human immunodeficiency virus type 1 reverse transcriptase.* Antimicrob Agents Chemother, 2002. **46**(7): p. 2179-84.

258. de Bethune, M.P., *Non-nucleoside reverse transcriptase inhibitors (NNRTIs), their discovery, development, and use in the treatment of HIV-1 infection: a review of the last 20 years (1989-2009).* Antiviral Res, 2010. **85**(1): p. 75-90.

259. Usach, I., V. Melis, and J.E. Peris, *Non-nucleoside reverse transcriptase inhibitors: a review on pharmacokinetics, pharmacodynamics, safety and tolerability.* J Int AIDS Soc, 2013. **16**: p. 1-14.

260. Fletcher, R.S., K. Syed, S. Mithani, G.I. Dmitrienko, and M.A. Parniak, *Carboxanilide derivative non-nucleoside inhibitors of HIV-1 reverse transcriptase interact with different mechanistic forms of the enzyme.* Biochemistry, 1995. **34**(13): p. 4346-53.

261. Ren, J., J. Milton, K.L. Weaver, S.A. Short, D.I. Stuart, and D.K. Stammers, *Structural basis for the resilience of efavirenz (DMP-266) to drug resistance mutations in HIV-1 reverse transcriptase.* Structure, 2000. **8**(10): p. 1089-94.

262. Zhou, Z., M. Madrid, J.D. Evanseck, and J.D. Madura, *Effect of a bound non-nucleoside RT inhibitor on the dynamics of wild-type and mutant HIV-1 reverse transcriptase.* J Am Chem Soc, 2005. **127**(49): p. 17253-60.

263. Das, K., J. Ding, Y. Hsiou, A.D. Clark, Jr., H. Moereels, L. Koymans, . . . E. Arnold, *Crystal structures of 8-Cl and 9-Cl TIBO complexed with wild-type HIV-1 RT and 8-Cl TIBO complexed with the Tyr181Cys HIV-1 RT drug-resistant mutant.* J Mol Biol, 1996. **264**(5): p. 1085-100.

264. Das, K., S.G. Sarafianos, A.D. Clark, Jr., P.L. Boyer, S.H. Hughes, and E. Arnold, *Crystal structures of clinically relevant Lys103Asn/Tyr181Cys double mutant HIV-1 reverse transcriptase in complexes with ATP and non-nucleoside inhibitor HBY 097.* J Mol Biol, 2007. **365**(1): p. 77-89.

265. Hsiou, Y., J. Ding, K. Das, A.D. Clark, Jr., P.L. Boyer, P. Lewi, . . . E. Arnold, *The Lys103Asn mutation of HIV-1 RT: a novel mechanism of drug resistance.* J Mol Biol, 2001. **309**(2): p. 437-45.

266. Margolis, A.M., H. Heverling, P.A. Pham, and A. Stolbach, *A review of the toxicity of HIV medications.* J Med Toxicol, 2014. **10**(1): p. 26-39.

267. Paik, S., S. Sen, N. Era, B. Saha, and S.K. Tripathi, *Fatal Nevirapine-Induced Toxic Epidermal Necrolysis in a HIV Infected Patient.* J Clin Diagn Res, 2016. **10**(3): p. Fd03-6.

268. Scott, L.J. and C.M. Perry, *Delavirdine: a review of its use in HIV infection.* Drugs, 2000. **60**(6): p. 1411-44.

269. Sheran, M., *The nonnucleoside reverse transcriptase inhibitors efavirenz and nevirapine in the treatment of HIV.* HIV Clin Trials, 2005. **6**(3): p. 158-68.

270. Roberts, N.A., J.A. Martin, D. Kinchington, A.V. Broadhurst, J.C. Craig, I.B. Duncan, . . . et al., *Rational design of peptide-based HIV proteinase inhibitors.* Science, 1990. **248**(4953): p. 358-61.

271. Gulick, R.M., J.W. Mellors, D. Havlir, J.J. Eron, C. Gonzalez, D. McMahon, . . . J.A. Chodakewitz, *Treatment with indinavir, zidovudine, and lamivudine in adults with human immunodeficiency virus infection and prior antiretroviral therapy.* N Engl J Med, 1997. **337**(11): p. 734-9.

272. Hammer, S.M., K.E. Squires, M.D. Hughes, J.M. Grimes, L.M. Demeter, J.S. Currier, . . . M.A. Fischl, *A controlled trial of two nucleoside analogues plus indinavir in persons with human immunodeficiency virus infection and CD4 cell counts of 200 per cubic millimeter or less. AIDS Clinical Trials Group 320 Study Team.* N Engl J Med, 1997. **337**(11): p. 725-33.

273. Kempf, D.J., K.C. Marsh, J.F. Denissen, E. McDonald, S. Vasavanonda, C.A. Flentge, . . . et al., *ABT-538 is a potent inhibitor of human immunodeficiency virus protease and has high oral bioavailability in humans.* Proc Natl Acad Sci U S A, 1995. **92**(7): p. 2484-8.

274. Kumar, G.N., A.D. Rodrigues, A.M. Buko, and J.F. Denissen, *Cytochrome P450-mediated metabolism of the HIV-1 protease inhibitor ritonavir (ABT-538) in human liver microsomes.* J Pharmacol Exp Ther, 1996. **277**(1): p. 423-31.

275. Vacca, J.P., B.D. Dorsey, W.A. Schleif, R.B. Levin, S.L. McDaniel, P.L. Darke, . . . E. Roth, *L-735,524: an orally bioavailable human immunodeficiency virus type 1 protease inhibitor.* Proc Natl Acad Sci U S A, 1994. **91**(9): p. 4096-100.

276. Ghosh, A.K., H.L. Osswald, and G. Prato, *Recent Progress in the Development of HIV-1 Protease Inhibitors for the Treatment of HIV/AIDS.* J Med Chem, 2016. **59**(11): p. 5172-208.

277. Bold, G., A. Fassler, H.G. Capraro, R. Cozens, T. Klimkait, J. Lazdins, . . . M. Lang, *New aza-dipeptide analogues as potent and orally absorbed HIV-1 protease inhibitors: candidates for clinical development.* J Med Chem, 1998. **41**(18): p. 3387-401.

278. Sham, H.L., D.J. Kempf, A. Molla, K.C. Marsh, G.N. Kumar, C.M. Chen, . . . D.W. Norbeck, *ABT-378, a highly potent inhibitor of the human immunodeficiency virus protease.* Antimicrob Agents Chemother, 1998. **42**(12): p. 3218-24.

279. Mitsuya, H., K. Maeda, D. Das, and A.K. Ghosh, *Development of protease inhibitors and the fight with drug-resistant HIV-1 variants.* Adv Pharmacol, 2008. **56**: p. 169-97.

280. Turner, D., J.M. Schapiro, B.G. Brenner, and M.A. Wainberg, *The influence of protease inhibitor resistance profiles on selection of HIV therapy in treatment-naive patients.* Antivir Ther, 2004. **9**(3): p. 301-14.

281. Doyon, L., S. Tremblay, L. Bourgon, E. Wardrop, and M.G. Cordingley, *Selection and characterization of HIV-1 showing reduced susceptibility to the non-peptidic protease inhibitor tipranavir.* Antiviral Res, 2005. **68**(1): p. 27-35.

282. Weber, I.T. and J. Agniswamy, *HIV-1 Protease: Structural Perspectives on Drug Resistance.* Viruses, 2009. **1**(3): p. 1110-36.

283. Koh, Y., H. Nakata, K. Maeda, H. Ogata, G. Bilcer, T. Devasamudram, . . . H. Mitsuya, *Novel bis-tetrahydrofuranylurethane-containing nonpeptidic protease inhibitor (PI) UIC-94017 (TMC114) with potent activity against multi-PI-resistant human immunodeficiency virus in vitro.* Antimicrob Agents Chemother, 2003. **47**(10): p. 3123-9.

284. Tie, Y., P.I. Boross, Y.F. Wang, L. Gaddis, A.K. Hussain, S. Leshchenko, . . . I.T. Weber, *High resolution crystal structures of HIV-1 protease with a potent non-peptide inhibitor (UIC-94017) active against multi-drug-resistant clinical strains.* J Mol Biol, 2004. **338**(2): p. 341-52.

285. Choi, E., J.R. Mallareddy, D. Lu, and S. Kolluru, *Recent advances in the discovery of small-molecule inhibitors of HIV-1 integrase.* Future Sci OA, 2018. **4**(9).

286. Hazuda, D.J., P. Felock, M. Witmer, A. Wolfe, K. Stillmock, J.A. Grobler, . . . M.D. Miller, *Inhibitors of strand transfer that prevent integration and inhibit HIV-1 replication in cells.* Science, 2000. **287**(5453): p. 646-50.

287. Liao, C. and M.C. Nicklaus, *Tautomerism and magnesium chelation of HIV-1 integrase inhibitors: a theoretical study.* ChemMedChem, 2010. **5**(7): p. 1053-66.

288. Grinsztejn, B., B.Y. Nguyen, C. Katlama, J.M. Gatell, A. Lazzarin, D. Vittecoq, . . . R.D. Isaacs, *Safety and efficacy of the HIV-1 integrase inhibitor raltegravir (MK-0518) in treatment-experienced patients with multidrug-resistant virus: a phase II randomised controlled trial.* Lancet, 2007. **369**(9569): p. 1261-1269.

289. Demarest, J., M. Underwood, M. St Clair, D. Dorey, D. Brown, and A. Zolopa, *Short Communication: Dolutegravir-Based Regimens Are Active in Integrase Strand Transfer Inhibitor-Naive Patients with Nucleoside Reverse Transcriptase Inhibitor Resistance.* AIDS Res Hum Retroviruses, 2018. **34**(4): p. 343-346.

290. Shimura, K., E. Kodama, Y. Sakagami, Y. Matsuzaki, W. Watanabe, K. Yamataka, . . . M. Matsuoka, *Broad antiretroviral activity and resistance profile of the novel human immunodeficiency virus integrase inhibitor elvitegravir (JTK-303/GS-9137).* J Virol, 2008. **82**(2): p. 764-74.

291. Unger, N.R., M.V. Worley, J.J. Kisgen, E.M. Sherman, and L.M. Childs-Kean, *Elvitegravir for the treatment of HIV.* Expert Opin Pharmacother, 2016. **17**(17): p. 2359-2370.

292. Rathbun, R.C., S.M. Lockhart, M.M. Miller, and M.D. Liedtke, *Dolutegravir, a second-generation integrase inhibitor for the treatment of HIV-1 infection.* Ann Pharmacother, 2014. **48**(3): p. 395-403.

293. Reese, M.J., P.M. Savina, G.T. Generaux, H. Tracey, J.E. Humphreys, E. Kanaoka, . . . J.W. Polli, *In vitro investigations into the roles of drug transporters and metabolizing enzymes in the disposition and drug interactions of dolutegravir, a HIV integrase inhibitor.* Drug Metab Dispos, 2013. **41**(2): p. 353-61.

294. Ahmed, N., S. Flavell, B. Ferns, D. Frampton, S.G. Edwards, R.F. Miller, . . . R.K. Gupta, *Development of the R263K Mutation to Dolutegravir in an HIV-1 Subtype D Virus Harboring 3 Class-Drug Resistance,* in *Open Forum Infect Dis*. 2019.

295. Feng, Y., C.C. Broder, P.E. Kennedy, and E.A. Berger, *HIV-1 entry cofactor: functional cDNA cloning of a seven-transmembrane, G protein-coupled receptor.* Science, 1996. **272**(5263): p. 872-7.

296. Alkhatib, G., C. Combadiere, C.C. Broder, Y. Feng, P.E. Kennedy, P.M. Murphy, and E.A. Berger, *CC CKR5: a RANTES, MIP-1alpha, MIP-1beta receptor as a fusion cofactor for macrophage-tropic HIV-1.* Science, 1996. **272**(5270): p. 1955-8.

297. Connor, R.I., K.E. Sheridan, D. Ceradini, S. Choe, and N.R. Landau, *Change in coreceptor use correlates with disease progression in HIV-1--infected individuals.* J Exp Med, 1997. **185**(4): p. 621-8.

298. Schuitemaker, H., M. Koot, N.A. Kootstra, M.W. Dercksen, R.E. de Goede, R.P. van Steenwijk, . . . M. Tersmette, *Biological phenotype of human immunodeficiency virus type 1 clones at different stages of infection: progression of disease is associated with a shift from monocytotropic to T-cell-tropic virus population.* J Virol, 1992. **66**(3): p. 1354-60.

299. Tsamis, F., S. Gavrilov, F. Kajumo, C. Seibert, S. Kuhmann, T. Ketas, . . . T. Dragic, *Analysis of the mechanism by which the small-molecule CCR5 antagonists SCH-351125 and SCH-350581 inhibit human immunodeficiency virus type 1 entry.* J Virol, 2003. **77**(9): p. 5201-8.

300. Westby, M., M. Lewis, J. Whitcomb, M. Youle, A.L. Pozniak, I.T. James, . . . E. van der Ryst, *Emergence of CXCR4-using human immunodeficiency virus type 1 (HIV-1) variants in a minority of HIV-1-infected patients following treatment with the CCR5 antagonist maraviroc is from a pretreatment CXCR4-using virus reservoir.* J Virol, 2006. **80**(10): p. 4909-20.

301. Tilton, J.C., H. Amrine-Madsen, J.L. Miamidian, K.M. Kitrinos, J. Pfaff, J.F. Demarest, . . . R.W. Doms, *HIV type 1 from a patient with baseline resistance to CCR5 antagonists uses drug-bound receptor for entry.* AIDS Res Hum Retroviruses, 2010. **26**(1): p. 13-24.

302. Westby, M., C. Smith-Burchnell, J. Mori, M. Lewis, M. Mosley, M. Stockdale, . . . M. Perros, *Reduced maximal inhibition in phenotypic susceptibility assays indicates that viral*

strains resistant to the CCR5 antagonist maraviroc utilize inhibitor-bound receptor for entry. J Virol, 2007. **81**(5): p. 2359-71.

303. Joshi, S.B., R.E. Dutch, and R.A. Lamb, *A core trimer of the paramyxovirus fusion protein: parallels to influenza virus hemagglutinin and HIV-1 gp41.* Virology, 1998. **248**(1): p. 20-34.

304. Wild, C., T. Oas, C. McDanal, D. Bolognesi, and T. Matthews, *A synthetic peptide inhibitor of human immunodeficiency virus replication: correlation between solution structure and viral inhibition.* Proc Natl Acad Sci U S A, 1992. **89**(21): p. 10537-41.

305. Kilby, J.M., S. Hopkins, T.M. Venetta, B. DiMassimo, G.A. Cloud, J.Y. Lee, . . . M.S. Saag, *Potent suppression of HIV-1 replication in humans by T-20, a peptide inhibitor of gp41-mediated virus entry.* Nat Med, 1998. **4**(11): p. 1302-7.

306. Rimsky, L.T., D.C. Shugars, and T.J. Matthews, *Determinants of human immunodeficiency virus type 1 resistance to gp41-derived inhibitory peptides.* J Virol, 1998. **72**(2): p. 986-93.

307. Wei, X., J.M. Decker, H. Liu, Z. Zhang, R.B. Arani, J.M. Kilby, . . . J.C. Kappes, *Emergence of resistant human immunodeficiency virus type 1 in patients receiving fusion inhibitor (T-20) monotherapy.* Antimicrob Agents Chemother, 2002. **46**(6): p. 1896-905.

308. Burton, D.R. and L. Hangartner, *Broadly Neutralizing Antibodies to HIV and Their Role in Vaccine Design.* Annu Rev Immunol, 2016. **34**: p. 635-59.

309. Awi, N.J. and S.Y. Teow, *Antibody-Mediated Therapy against HIV/AIDS: Where Are We Standing Now?* J Pathog, 2018. **2018**.

310. Markham, A., *Ibalizumab: First Global Approval*, in *Drugs*. 2018. p. 781-5.

311. Rizza, S.A., R. Bhatia, J. Zeuli, and Z. Temesgen, *Ibalizumab for the treatment of multidrug-resistant HIV-1 infection.* Drugs Today (Barc), 2019. **55**(1): p. 25-34.

312. Blair, H.A., *Ibalizumab: A Review in Multidrug-Resistant HIV-1 Infection.* Drugs, 2020. **80**(2): p. 189-196.

313. Pace, C.S., M.W. Fordyce, D. Franco, C.Y. Kao, M.S. Seaman, and D.D. Ho, *Anti-CD4 monoclonal antibody ibalizumab exhibits breadth and potency against HIV-1, with natural resistance mediated by the loss of a V5 glycan in envelope.* J Acquir Immune Defic Syndr, 2013. **62**(1): p. 1-9.

314. Beccari, M.V., B.T. Mogle, E.F. Sidman, K.A. Mastro, E. Asiago-Reddy, and W.D. Kufel, *Ibalizumab, a Novel Monoclonal Antibody for the Management of Multidrug-Resistant HIV-1 Infection*, in *Antimicrob Agents Chemother*. 2019.

315. Toma, J., S.P. Weinheimer, E. Stawiski, J.M. Whitcomb, S.T. Lewis, C.J. Petropoulos, and W. Huang, *Loss of asparagine-linked glycosylation sites in variable region 5 of human*

immunodeficiency virus type 1 envelope is associated with resistance to CD4 antibody ibalizumab. J Virol, 2011. **85**(8): p. 3872-80.

316. Chomont, N., M. El-Far, P. Ancuta, L. Trautmann, F.A. Procopio, B. Yassine-Diab, . . . R.P. Sekaly, *HIV reservoir size and persistence are driven by T cell survival and homeostatic proliferation.* Nat Med, 2009. **15**(8): p. 893-900.

317. Siliciano, J.D., J. Kajdas, D. Finzi, T.C. Quinn, K. Chadwick, J.B. Margolick, . . . R.F. Siliciano, *Long-term follow-up studies confirm the stability of the latent reservoir for HIV-1 in resting CD4+ T cells.* Nat Med, 2003. **9**(6): p. 727-8.

318. Gupta, R.K., S. Abdul-Jawad, L.E. McCoy, H.P. Mok, D. Peppa, M. Salgado, . . . E. Olavarria, *HIV-1 remission following CCR5Delta32/Delta32 haematopoietic stem-cell transplantation.* Nature, 2019. **568**(7751): p. 244-248.

319. Hutter, G., D. Nowak, M. Mossner, S. Ganepola, A. Mussig, K. Allers, . . . E. Thiel, *Long-term control of HIV by CCR5 Delta32/Delta32 stem-cell transplantation.* N Engl J Med, 2009. **360**(7): p. 692-8.

320. Burton, D.R., R.L. Stanfield, and I.A. Wilson, *Antibody vs. HIV in a clash of evolutionary titans.* Proc Natl Acad Sci U S A, 2005. **102**(42): p. 14943-8.

321. Luciw, P.A., C. Cheng-Mayer, and J.A. Levy, *Mutational analysis of the human immunodeficiency virus: the orf-B region down-regulates virus replication.* Proc Natl Acad Sci U S A, 1987. **84**(5): p. 1434-8.

322. Niederman, T.M., B.J. Thielan, and L. Ratner, *Human immunodeficiency virus type 1 negative factor is a transcriptional silencer.* Proc Natl Acad Sci U S A, 1989. **86**(4): p. 1128-32.

323. Hammes, S.R., E.P. Dixon, M.H. Malim, B.R. Cullen, and W.C. Greene, *Nef protein of human immunodeficiency virus type 1: evidence against its role as a transcriptional inhibitor.* Proc Natl Acad Sci U S A, 1989. **86**(23): p. 9549-53.

324. Kim, S., K. Ikeuchi, R. Byrn, J. Groopman, and D. Baltimore, *Lack of a negative influence on viral growth by the nef gene of human immunodeficiency virus type 1.* Proc Natl Acad Sci U S A, 1989. **86**(23): p. 9544-8.

325. Kestler, H.W., 3rd, D.J. Ringler, K. Mori, D.L. Panicali, P.K. Sehgal, M.D. Daniel, and R.C. Desrosiers, *Importance of the nef gene for maintenance of high virus loads and for development of AIDS.* Cell, 1991. **65**(4): p. 651-62.

326. Deacon, N.J., A. Tsykin, A. Solomon, K. Smith, M. Ludford-Menting, D.J. Hooker, . . . J. Mills, *Genomic structure of an attenuated quasi species of HIV-1 from a blood transfusion donor and recipients.* Science, 1995. **270**(5238): p. 988-91.

327. Kirchhoff, F., T.C. Greenough, D.B. Brettler, J.L. Sullivan, and R.C. Desrosiers, *Brief report: absence of intact nef sequences in a long-term survivor with nonprogressive HIV-1 infection.* N Engl J Med, 1995. **332**(4): p. 228-32.

328. Hanna, Z., D.G. Kay, M. Cool, S. Jothy, N. Rebai, and P. Jolicoeur, *Transgenic mice expressing human immunodeficiency virus type 1 in immune cells develop a severe AIDS-like disease.* J Virol, 1998. **72**(1): p. 121-32.

329. Hanna, Z., D.G. Kay, N. Rebai, A. Guimond, S. Jothy, and P. Jolicoeur, *Nef harbors a major determinant of pathogenicity for an AIDS-like disease induced by HIV-1 in transgenic mice.* Cell, 1998. **95**(2): p. 163-75.

330. Zou, W., P.W. Denton, R.L. Watkins, J.F. Krisko, T. Nochi, J.L. Foster, and J.V. Garcia, *Nef functions in BLT mice to enhance HIV-1 replication and deplete CD4+CD8+ thymocytes.* Retrovirology, 2012. **9**: p. 44.

331. Campbell, E.M., R. Nunez, and T.J. Hope, *Disruption of the actin cytoskeleton can complement the ability of Nef to enhance human immunodeficiency virus type 1 infectivity.* J Virol, 2004. **78**(11): p. 5745-55.

332. Lundquist, C.A., M. Tobiume, J. Zhou, D. Unutmaz, and C. Aiken, *Nef-mediated downregulation of CD4 enhances human immunodeficiency virus type 1 replication in primary T lymphocytes.* J Virol, 2002. **76**(9): p. 4625-33.

333. Pizzato, M., A. Helander, E. Popova, A. Calistri, A. Zamborlini, G. Palu, and H.G. Gottlinger, *Dynamin 2 is required for the enhancement of HIV-1 infectivity by Nef.* Proc Natl Acad Sci U S A, 2007. **104**(16): p. 6812-7.

334. Simmons, A., V. Aluvihare, and A. McMichael, *Nef triggers a transcriptional program in T cells imitating single-signal T cell activation and inducing HIV virulence mediators.* Immunity, 2001. **14**(6): p. 763-77.

335. Cullen, B.R., *The role of Nef in the replication cycle of the human and simian immunodeficiency viruses.* Virology, 1994. **205**(1): p. 1-6.

336. Grzesiek, S., A. Bax, G.M. Clore, A.M. Gronenborn, J.S. Hu, J. Kaufman, . . . P.T. Wingfield, *The solution structure of HIV-1 Nef reveals an unexpected fold and permits delineation of the binding surface for the SH3 domain of Hck tyrosine protein kinase.* Nat Struct Biol, 1996. **3**(4): p. 340-5.

337. Grzesiek, S., A. Bax, J.S. Hu, J. Kaufman, I. Palmer, S.J. Stahl, . . . P.T. Wingfield, *Refined solution structure and backbone dynamics of HIV-1 Nef.* Protein Sci, 1997. **6**(6): p. 1248-63.

338. Lee, C.H., K. Saksela, U.A. Mirza, B.T. Chait, and J. Kuriyan, *Crystal structure of the conserved core of HIV-1 Nef complexed with a Src family SH3 domain.* Cell, 1996. **85**(6): p. 931-42.

339. Geyer, M. and B.M. Peterlin, *Domain assembly, surface accessibility and sequence conservation in full length HIV-1 Nef.* FEBS Lett, 2001. **496**(2-3): p. 91-5.

340. Harris, M., *The role of myristoylation in the interactions between human immunodeficiency virus type I Nef and cellular proteins.* Biochem Soc Trans, 1995. **23**(3): p. 557-61.

341. Bentham, M., S. Mazaleyrat, and M. Harris, *Role of myristoylation and N-terminal basic residues in membrane association of the human immunodeficiency virus type 1 Nef protein.* J Gen Virol, 2006. **87**(Pt 3): p. 563-71.

342. Kaminchik, J., R. Margalit, S. Yaish, H. Drummer, B. Amit, N. Sarver, . . . A. Panet, *Cellular distribution of HIV type 1 Nef protein: identification of domains in Nef required for association with membrane and detergent-insoluble cellular matrix.* AIDS Res Hum Retroviruses, 1994. **10**(8): p. 1003-10.

343. Yu, G. and R.L. Felsted, *Effect of myristoylation on p27 nef subcellular distribution and suppression of HIV-LTR transcription.* Virology, 1992. **187**(1): p. 46-55.

344. Wang, J.K., E. Kiyokawa, E. Verdin, and D. Trono, *The Nef protein of HIV-1 associates with rafts and primes T cells for activation.* Proc Natl Acad Sci U S A, 2000. **97**(1): p. 394-9.

345. Zheng, Y.H., A. Plemenitas, T. Linnemann, O.T. Fackler, and B.M. Peterlin, *Nef increases infectivity of HIV via lipid rafts.* Curr Biol, 2001. **11**(11): p. 875-9.

346. Chowers, M.Y., C.A. Spina, T.J. Kwoh, N.J. Fitch, D.D. Richman, and J.C. Guatelli, *Optimal infectivity in vitro of human immunodeficiency virus type 1 requires an intact nef gene.* J Virol, 1994. **68**(5): p. 2906-14.

347. Peng, B. and M. Robert-Guroff, *Deletion of N-terminal myristoylation site of HIV Nef abrogates both MHC-1 and CD4 down-regulation.* Immunol Lett, 2001. **78**(3): p. 195-200.

348. Alexander, M., Y. Bor, K.S. Ravichandran, M.L. Hammarskjöld, and D. Rekosh, *Human Immunodeficiency Virus Type 1 Nef Associates with Lipid Rafts To Downmodulate Cell Surface CD4 and Class I Major Histocompatibility Complex Expression and To Increase Viral Infectivity*, in *J Virol*. 2004. p. 1685-96.

349. Piguet, V., L. Wan, C. Borel, A. Mangasarian, N. Demaurex, G. Thomas, and D. Trono, *HIV-1 Nef protein binds to the cellular protein PACS-1 to downregulate class I major histocompatibility complexes.* Nat Cell Biol, 2000. **2**(3): p. 163-7.

350. Lubben, N.B., D.A. Sahlender, A.M. Motley, P.J. Lehner, P. Benaroch, and M.S. Robinson, *HIV-1 Nef-induced down-regulation of MHC class I requires AP-1 and clathrin but not PACS-1 and is impeded by AP-2.* Mol Biol Cell, 2007. **18**(9): p. 3351-65.

351. Greenberg, M.E., A.J. Iafrate, and J. Skowronski, *The SH3 domain-binding surface and an acidic motif in HIV-1 Nef regulate trafficking of class I MHC complexes.* Embo j, 1998. **17**(10): p. 2777-89.

352. Williams, M., J.F. Roeth, M.R. Kasper, T.M. Filzen, and K.L. Collins, *Human immunodeficiency virus type 1 Nef domains required for disruption of major histocompatibility complex class I trafficking are also necessary for coprecipitation of Nef with HLA-A2.* J Virol, 2005. **79**(1): p. 632-6.

353. Fackler, O.T., W. Luo, M. Geyer, A.S. Alberts, and B.M. Peterlin, *Activation of Vav by Nef induces cytoskeletal rearrangements and downstream effector functions.* Mol Cell, 1999. **3**(6): p. 729-39.

354. Saksela, K., G. Cheng, and D. Baltimore, *Proline-rich (PxxP) motifs in HIV-1 Nef bind to SH3 domains of a subset of Src kinases and are required for the enhanced growth of Nef+ viruses but not for down-regulation of CD4.* Embo j, 1995. **14**(3): p. 484-91.

355. Arold, S., P. Franken, M.P. Strub, F. Hoh, S. Benichou, R. Benarous, and C. Dumas, *The crystal structure of HIV-1 Nef protein bound to the Fyn kinase SH3 domain suggests a role for this complex in altered T cell receptor signaling.* Structure, 1997. **5**(10): p. 1361-72.

356. Bresnahan, P.A., W. Yonemoto, S. Ferrell, D. Williams-Herman, R. Geleziunas, and W.C. Greene, *A dileucine motif in HIV-1 Nef acts as an internalization signal for CD4 downregulation and binds the AP-1 clathrin adaptor.* Curr Biol, 1998. **8**(22): p. 1235-8.

357. Greenberg, M., L. DeTulleo, I. Rapoport, J. Skowronski, and T. Kirchhausen, *A dileucine motif in HIV-1 Nef is essential for sorting into clathrin-coated pits and for downregulation of CD4.* Curr Biol, 1998. **8**(22): p. 1239-42.

358. Foster, J.L., S.J. Denial, B.R.S. Temple, and J.V. Garcia, *Mechanisms of HIV-1 Nef Function and Intracellular Signaling.* J Neuroimmune Pharmacol, 2011. **6**(2): p. 230-46.

359. Narute, P.S. and T.E. Smithgall, *Nef Alleles from All Major HIV-1 Clades Activate Src-Family Kinases and Enhance HIV-1 Replication in an Inhibitor-Sensitive Manner*, in *PLoS One*. 2012.

360. Staudt, R.P., J.J. Alvarado, L.A. Emert-Sedlak, H. Shi, S.T. Shu, T.E. Wales, . . . T.E. Smithgall, *Structure, function, and inhibitor targeting of HIV-1 Nef-effector kinase complexes.* J Biol Chem, 2020. **295**(44): p. 15158-15171.

361. Shu, S.T., L.A. Emert-Sedlak, and T.E. Smithgall, *Cell-based Fluorescence Complementation Reveals a Role for HIV-1 Nef Protein Dimerization in AP-2 Adaptor Recruitment and CD4 Co-receptor Down-regulation.* J Biol Chem, 2017. **292**(7): p. 2670-2678.

362. Staudt, R.P. and T.E. Smithgall, *Nef homodimers down-regulate SERINC5 by AP-2-mediated endocytosis to promote HIV-1 infectivity.* J Biol Chem, 2020. **295**(46): p. 15540-15552.

363. Ye, H., H.J. Choi, J. Poe, and T.E. Smithgall, *Oligomerization is required for HIV-1 Nef-induced activation of the Src family protein-tyrosine kinase, Hck.* Biochemistry, 2004. **43**(50): p. 15775-84.

364. Alvarado, J.J., S. Tarafdar, J.I. Yeh, and T.E. Smithgall, *Interaction with the Src Homology (SH3-SH2) Region of the Src-family Kinase Hck Structures the HIV-1 Nef Dimer for Kinase Activation and Effector Recruitment**, in *J Biol Chem*. 2014. p. 28539-53.

365. Li, W.F., M. Aryal, S.T. Shu, and T.E. Smithgall, *HIV-1 Nef dimers short-circuit immune receptor signaling by activating Tec-family kinases at the host cell membrane.* J Biol Chem, 2020. **295**(15): p. 5163-5174.

366. Shi, H., C.M. Tice, L. Emert-Sedlak, L. Chen, W.F. Li, M. Carlsen, . . . T.E. Smithgall, *Tight-Binding Hydroxypyrazole HIV-1 Nef Inhibitors Suppress Viral Replication in Donor Mononuclear Cells and Reverse Nef-Mediated MHC-I Downregulation.* ACS Infect Dis, 2020. **6**(2): p. 302-312.

367. Wong, P. and E.G. Pamer, *CD8 T cell responses to infectious pathogens.* Annu Rev Immunol, 2003. **21**: p. 29-70.

368. Pawlak, E.N. and J.D. Dikeakos, *HIV-1 Nef: a master manipulator of the membrane trafficking machinery mediating immune evasion.* Biochim Biophys Acta, 2015. **1850**(4): p. 733-41.

369. Robinson, M.S., *Adaptable adaptors for coated vesicles.* Trends Cell Biol, 2004. **14**(4): p. 167-74.

370. Peden, A.A., V. Oorschot, B.A. Hesser, C.D. Austin, R.H. Scheller, and J. Klumperman, *Localization of the AP-3 adaptor complex defines a novel endosomal exit site for lysosomal membrane proteins.* J Cell Biol, 2004. **164**(7): p. 1065-76.

371. Traub, L.M., *Sorting it out: AP-2 and alternate clathrin adaptors in endocytic cargo selection.* J Cell Biol, 2003. **163**(2): p. 203-8.

372. Waguri, S., F. Dewitte, R. Le Borgne, Y. Rouille, Y. Uchiyama, J.F. Dubremetz, and B. Hoflack, *Visualization of TGN to endosome trafficking through fluorescently labeled MPR and AP-1 in living cells.* Mol Biol Cell, 2003. **14**(1): p. 142-55.

373. Wan, L., S.S. Molloy, L. Thomas, G. Liu, Y. Xiang, S.L. Rybak, and G. Thomas, *PACS-1 defines a novel gene family of cytosolic sorting proteins required for trans-Golgi network localization.* Cell, 1998. **94**(2): p. 205-16.

374. Crump, C.M., Y. Xiang, L. Thomas, F. Gu, C. Austin, S.A. Tooze, and G. Thomas, *PACS-1 binding to adaptors is required for acidic cluster motif-mediated protein traffic.* Embo j, 2001. **20**(9): p. 2191-201.

375. Dikeakos, J.D., K.M. Atkins, L. Thomas, L. Emert-Sedlak, I.J. Byeon, J. Jung, . . . G. Thomas, *Small molecule inhibition of HIV-1-induced MHC-I down-regulation identifies a temporally regulated switch in Nef action.* Mol Biol Cell, 2010. **21**(19): p. 3279-92.

376. Blagoveshchenskaya, A.D., L. Thomas, S.F. Feliciangeli, C.H. Hung, and G. Thomas, *HIV-1 Nef downregulates MHC-I by a PACS-1- and PI3K-regulated ARF6 endocytic pathway.* Cell, 2002. **111**(6): p. 853-66.

377. Hung, C.H., L. Thomas, C.E. Ruby, K.M. Atkins, N.P. Morris, Z.A. Knight, . . . G. Thomas, *HIV-1 Nef assembles a Src family kinase-ZAP-70/Syk-PI3K cascade to downregulate cell-surface MHC-I.* Cell Host Microbe, 2007. **1**(2): p. 121-33.

378. Wonderlich, E.R., J.A. Leonard, D.A. Kulpa, K.E. Leopold, J.M. Norman, and K.L. Collins, *ADP ribosylation factor 1 activity is required to recruit AP-1 to the major histocompatibility complex class I (MHC-I) cytoplasmic tail and disrupt MHC-I trafficking in HIV-1-infected primary T cells.* J Virol, 2011. **85**(23): p. 12216-26.

379. Yi, L., T. Rosales, J.J. Rose, B. Chowdhury, J.R. Knutson, and S. Venkatesan, *HIV-1 Nef binds a subpopulation of MHC-I throughout its trafficking itinerary and down-regulates MHC-I by perturbing both anterograde and retrograde trafficking.* J Biol Chem, 2010. **285**(40): p. 30884-905.

380. Owen, D.J. and P.R. Evans, *A structural explanation for the recognition of tyrosine-based endocytotic signals.* Science, 1998. **282**(5392): p. 1327-32.

381. Kasper, M.R., J.F. Roeth, M. Williams, T.M. Filzen, R.I. Fleis, and K.L. Collins, *HIV-1 Nef disrupts antigen presentation early in the secretory pathway.* J Biol Chem, 2005. **280**(13): p. 12840-8.

382. Schaefer, M.R., E.R. Wonderlich, J.F. Roeth, J.A. Leonard, and K.L. Collins, *HIV-1 Nef Targets MHC-I and CD4 for Degradation Via a Final Common β-COP–Dependent Pathway in T Cells*, in *PLoS Pathog*. 2008.

383. Glushakova, S., J. Munch, S. Carl, T.C. Greenough, J.L. Sullivan, L. Margolis, and F. Kirchhoff, *CD4 down-modulation by human immunodeficiency virus type 1 Nef correlates with the efficiency of viral replication and with CD4(+) T-cell depletion in human lymphoid tissue ex vivo.* J Virol, 2001. **75**(21): p. 10113-7.

384. Robinson, H.L. and D.M. Zinkus, *Accumulation of human immunodeficiency virus type 1 DNA in T cells: results of multiple infection events.* J Virol, 1990. **64**(10): p. 4836-41.

385. Lama, J., *The physiological relevance of CD4 receptor down-modulation during HIV infection.* Curr HIV Res, 2003. **1**(2): p. 167-84.

386. Michel, N., I. Allespach, S. Venzke, O.T. Fackler, and O.T. Keppler, *The Nef protein of human immunodeficiency virus establishes superinfection immunity by a dual strategy to downregulate cell-surface CCR5 and CD4.* Curr Biol, 2005. **15**(8): p. 714-23.

387. Ross, T.M., A.E. Oran, and B.R. Cullen, *Inhibition of HIV-1 progeny virion release by cell-surface CD4 is relieved by expression of the viral Nef protein.* Curr Biol, 1999. **9**(12): p. 613-21.

388. Skowronski, J., D. Parks, and R. Mariani, *Altered T cell activation and development in transgenic mice expressing the HIV-1 nef gene.* Embo j, 1993. **12**(2): p. 703-13.

389. Aiken, C., J. Konner, N.R. Landau, M.E. Lenburg, and D. Trono, *Nef induces CD4 endocytosis: requirement for a critical dileucine motif in the membrane-proximal CD4 cytoplasmic domain.* Cell, 1994. **76**(5): p. 853-64.

390. Craig, H.M., M.W. Pandori, and J.C. Guatelli, *Interaction of HIV-1 Nef with the cellular dileucine-based sorting pathway is required for CD4 down-regulation and optimal viral infectivity.* Proc Natl Acad Sci U S A, 1998. **95**(19): p. 11229-34.

391. Traub, L.M., *Tickets to ride: selecting cargo for clathrin-regulated internalization.* Nat Rev Mol Cell Biol, 2009. **10**(9): p. 583-96.

392. Pitcher, C., S. Honing, A. Fingerhut, K. Bowers, and M. Marsh, *Cluster of differentiation antigen 4 (CD4) endocytosis and adaptor complex binding require activation of the CD4 endocytosis signal by serine phosphorylation.* Mol Biol Cell, 1999. **10**(3): p. 677-91.

393. Chaudhuri, R., O.W. Lindwasser, W.J. Smith, J.H. Hurley, and J.S. Bonifacino, *Downregulation of CD4 by human immunodeficiency virus type 1 Nef is dependent on clathrin and involves direct interaction of Nef with the AP2 clathrin adaptor.* J Virol, 2007. **81**(8): p. 3877-90.

394. Doray, B., I. Lee, J. Knisely, G. Bu, and S. Kornfeld, *The gamma/sigma1 and alpha/sigma2 hemicomplexes of clathrin adaptors AP-1 and AP-2 harbor the dileucine recognition site.* Mol Biol Cell, 2007. **18**(5): p. 1887-96.

395. Chaudhuri, R., R. Mattera, O.W. Lindwasser, M.S. Robinson, and J.S. Bonifacino, *A basic patch on alpha-adaptin is required for binding of human immunodeficiency virus type 1 Nef and cooperative assembly of a CD4-Nef-AP-2 complex.* J Virol, 2009. **83**(6): p. 2518-30.

396. Kwon, Y., R.M. Kaake, I. Echeverria, M. Suarez, M. Karimian Shamsabadi, C. Stoneham, . . . X. Jia, *Structural basis of CD4 downregulation by HIV-1 Nef.* Nat Struct Mol Biol, 2020. **27**(9): p. 822-828.

397. Stumptner-Cuvelette, P., S. Morchoisne, M. Dugast, S. Le Gall, G. Raposo, O. Schwartz, and P. Benaroch, *HIV-1 Nef impairs MHC class II antigen presentation and surface expression.* Proc Natl Acad Sci U S A, 2001. **98**(21): p. 12144-9.

398. Schindler, M., S. Wildum, N. Casartelli, M. Doria, and F. Kirchhoff, *Nef alleles from children with non-progressive HIV-1 infection modulate MHC-II expression more efficiently than those from rapid progressors.* Aids, 2007. **21**(9): p. 1103-7.

399. Michel, N., K. Ganter, S. Venzke, J. Bitzegeio, O.T. Fackler, and O.T. Keppler, *The Nef protein of human immunodeficiency virus is a broad-spectrum modulator of chemokine receptor cell surface levels that acts independently of classical motifs for receptor endocytosis and Galphai signaling.* Mol Biol Cell, 2006. **17**(8): p. 3578-90.

400. Landi, A., V. Iannucci, A.V. Nuffel, P. Meuwissen, and B. Verhasselt, *One Protein to Rule them All: Modulation of Cell Surface Receptors and Molecules by HIV Nef*, in *Curr HIV Res*. 2011. p. 496-504.

401. Stove, V., I. Van de Walle, E. Naessens, E. Coene, C. Stove, J. Plum, and B. Verhasselt, *Human immunodeficiency virus Nef induces rapid internalization of the T-cell coreceptor CD8alphabeta.* J Virol, 2005. **79**(17): p. 11422-33.

402. Benito, J.M., M. Lopez, and V. Soriano, *The role of CD8+ T-cell response in HIV infection.* AIDS Rev, 2004. **6**(2): p. 79-88.

403. Lenschow, D.J., T.L. Walunas, and J.A. Bluestone, *CD28/B7 system of T cell costimulation.* Annu Rev Immunol, 1996. **14**: p. 233-58.

404. Chaudhry, A., S.R. Das, S. Jameel, A. George, V. Bal, S. Mayor, and S. Rath, *A two-pronged mechanism for HIV-1 Nef-mediated endocytosis of immune costimulatory molecules CD80 and CD86.* Cell Host Microbe, 2007. **1**(1): p. 37-49.

405. Swigut, T., N. Shohdy, and J. Skowronski, *Mechanism for down-regulation of CD28 by Nef.* Embo j, 2001. **20**(7): p. 1593-604.

406. Melian, A., E.M. Beckman, S.A. Porcelli, and M.B. Brenner, *Antigen presentation by CD1 and MHC-encoded class I-like molecules.* Curr Opin Immunol, 1996. **8**(1): p. 82-8.

407. Chen, N., C. McCarthy, H. Drakesmith, D. Li, V. Cerundolo, A.J. McMichael, . . . X.N. Xu, *HIV-1 down-regulates the expression of CD1d via Nef.* Eur J Immunol, 2006. **36**(2): p. 278-86.

408. Cho, S., K.S. Knox, L.M. Kohli, J.J. He, M.A. Exley, S.B. Wilson, and R.R. Brutkiewicz, *Impaired cell surface expression of human CD1d by the formation of an HIV-1 Nef/CD1d complex.* Virology, 2005. **337**(2): p. 242-52.

409. Baur, A.S., E.T. Sawai, P. Dazin, W.J. Fantl, C. Cheng-Mayer, and B.M. Peterlin, *HIV-1 Nef leads to inhibition or activation of T cells depending on its intracellular localization.* Immunity, 1994. **1**(5): p. 373-84.

410. Schrager, J.A. and J.W. Marsh, *HIV-1 Nef increases T cell activation in a stimulus-dependent manner.* Proc Natl Acad Sci U S A, 1999. **96**(14): p. 8167-72.

411. Pulkkinen, K., G.H. Renkema, F. Kirchhoff, and K. Saksela, *Nef associates with p21-activated kinase 2 in a p21-GTPase-dependent dynamic activation complex within lipid rafts.* J Virol, 2004. **78**(23): p. 12773-80.

412. Lu, X., X. Wu, A. Plemenitas, H. Yu, E.T. Sawai, A. Abo, and B.M. Peterlin, *CDC42 and Rac1 are implicated in the activation of the Nef-associated kinase and replication of HIV-1.* Curr Biol, 1996. **6**(12): p. 1677-84.

413. Wolf, D., V. Witte, B. Laffert, K. Blume, E. Stromer, S. Trapp, . . . A.S. Baur, *HIV-1 Nef associated PAK and PI3-kinases stimulate Akt-independent Bad-phosphorylation to induce anti-apoptotic signals.* Nat Med, 2001. **7**(11): p. 1217-24.

414. Heusinger, E. and F. Kirchhoff, *Primate Lentiviruses Modulate NF-κB Activity by Multiple Mechanisms to Fine-Tune Viral and Cellular Gene Expression.* Front Microbiol, 2017. **8**.

415. Pessler, F. and R.Q. Cron, *Reciprocal regulation of the nuclear factor of activated T cells and HIV-1.* Genes Immun, 2004. **5**(3): p. 158-67.

416. Kinoshita, S., B.K. Chen, H. Kaneshima, and G.P. Nolan, *Host control of HIV-1 parasitism in T cells by the nuclear factor of activated T cells.* Cell, 1998. **95**(5): p. 595-604.

417. Watkins, R.L., J.L. Foster, and J.V. Garcia, *In vivo analysis of Nef's role in HIV-1 replication, systemic T cell activation and CD4+ T cell loss*, in *Retrovirology*. 2015.

418. Emert-Sedlak, L., T. Kodama, E.C. Lerner, W. Dai, C. Foster, B.W. Day, . . . T.E. Smithgall, *Chemical library screens targeting an HIV-1 accessory factor/host cell kinase complex identify novel antiretroviral compounds.* ACS Chem Biol, 2009. **4**(11): p. 939-47.

419. Emert-Sedlak, L.A., P. Narute, S.T. Shu, J.A. Poe, H. Shi, N. Yanamala, . . . T.E. Smithgall, *Effector Kinase Coupling Enables High-Throughput Screens for Direct HIV-1 Nef Antagonists with Anti-retroviral Activity.* Chem Biol, 2013. **20**(1): p. 82-91.

420. Mujib, S., A. Saiyed, S. Fadel, A. Bozorgzad, N. Aidarus, F.Y. Yue, . . . M.A. Ostrowski, *Pharmacologic HIV-1 Nef blockade promotes CD8 T cell–mediated elimination of latently HIV-1–infected cells in vitro*, in *JCI Insight*.

421. Diehl, N. and H. Schaal, *Make yourself at home: viral hijacking of the PI3K/Akt signaling pathway.* Viruses, 2013. **5**(12): p. 3192-212.

422. Kumar, R., N. Khandelwal, R. Thachamvally, B.N. Tripathi, S. Barua, S.K. Kashyap, . . . N. Kumar, *Role of MAPK/MNK1 signaling in virus replication.* Virus Res, 2018. **253**: p. 48-61.

423. Sodhi, A., S. Montaner, and J.S. Gutkind, *Viral hijacking of G-protein-coupled-receptor signalling networks.* Nat Rev Mol Cell Biol, 2004. **5**(12): p. 998-1012.

424. Ingley, E., *Src family kinases: regulation of their activities, levels and identification of new pathways.* Biochim Biophys Acta, 2008. **1784**(1): p. 56-65.

425. Scheijen, B. and J.D. Griffin, *Tyrosine kinase oncogenes in normal hematopoiesis and hematological disease.* Oncogene, 2002. **21**(21): p. 3314-33.

426. Siveen, K.S., K.S. Prabhu, I.W. Achkar, S. Kuttikrishnan, S. Shyam, A.Q. Khan, . . . S. Uddin, *Role of Non Receptor Tyrosine Kinases in Hematological Malignances and its Targeting by Natural Products.* Mol Cancer, 2018. **17**(1): p. 31.

427. Darnell, J.E., Jr., *STATs and gene regulation.* Science, 1997. **277**(5332): p. 1630-5.

428. Weiss, A. and D.R. Littman, *Signal transduction by lymphocyte antigen receptors.* Cell, 1994. **76**(2): p. 263-74.

429. Bromann, P.A., H. Korkaya, and S.A. Courtneidge, *The interplay between Src family kinases and receptor tyrosine kinases.* Oncogene, 2004. **23**(48): p. 7957-68.

430. Pagano, M.A., E. Tibaldi, G. Palù, and A.M. Brunati, *Viral proteins and Src family kinases: Mechanisms of pathogenicity from a "liaison dangereuse".* World J Virol, 2013. **2**(2): p. 71-8.

431. Brown, M.T. and J.A. Cooper, *Regulation, substrates and functions of src.* Biochim Biophys Acta, 1996. **1287**(2-3): p. 121-49.

432. Bolen, J.B. and J.S. Brugge, *Leukocyte protein tyrosine kinases: potential targets for drug discovery.* Annu Rev Immunol, 1997. **15**: p. 371-404.

433. Willman, C.L., C.C. Stewart, T.L. Longacre, D.R. Head, R. Habbersett, S.F. Ziegler, and R.M. Perlmutter, *Expression of the c-fgr and hck protein-tyrosine kinases in acute myeloid leukemic blasts is associated with early commitment and differentiation events in the monocytic and granulocytic lineages.* Blood, 1991. **77**(4): p. 726-34.

434. Kawakami, Y., M. Furue, and T. Kawakami, *Identification of fyn-encoded proteins in normal human blood cells.* Oncogene, 1989. **4**(3): p. 389-91.

435. Veillette, A., M.A. Bookman, E.M. Horak, L.E. Samelson, and J.B. Bolen, *Signal transduction through the CD4 receptor involves the activation of the internal membrane tyrosine-protein kinase p56lck.* Nature, 1989. **338**(6212): p. 257-9.

436. Yamanashi, Y., S. Mori, M. Yoshida, T. Kishimoto, K. Inoue, T. Yamamoto, and K. Toyoshima, *Selective expression of a protein-tyrosine kinase, p56lyn, in hematopoietic cells and association with production of human T-cell lymphotropic virus type I.* Proc Natl Acad Sci U S A, 1989. **86**(17): p. 6538-42.

437. Dymecki, S.M., J.E. Niederhuber, and S.V. Desiderio, *Specific expression of a tyrosine kinase gene, blk, in B lymphoid cells.* Science, 1990. **247**(4940): p. 332-6.

438. Holtzman, D.A., W.D. Cook, and A.R. Dunn, *Isolation and sequence of a cDNA corresponding to a src-related gene expressed in murine hemopoietic cells.* Proc Natl Acad Sci U S A, 1987. **84**(23): p. 8325-9.

439. Corey, S.J. and S.M. Anderson, *Src-related protein tyrosine kinases in hematopoiesis.* Blood, 1999. **93**(1): p. 1-14.

440. Towler, D.A., J.I. Gordon, S.P. Adams, and L. Glaser, *The biology and enzymology of eukaryotic protein acylation.* Annu Rev Biochem, 1988. **57**: p. 69-99.

441. Resh, M.D., *Interaction of tyrosine kinase oncoproteins with cellular membranes.* Biochim Biophys Acta, 1993. **1155**(3): p. 307-22.

442. Kim, P.W., Z.Y. Sun, S.C. Blacklow, G. Wagner, and M.J. Eck, *A zinc clasp structure tethers Lck to T cell coreceptors CD4 and CD8.* Science, 2003. **301**(5640): p. 1725-8.

443. Amata, I., M. Maffei, and M. Pons, *Phosphorylation of unique domains of Src family kinases.* Front Genet, 2014. **5**.

444. Pérez, Y., M. Maffei, A. Igea, I. Amata, M. Gairí, A.R. Nebreda, . . . M. Pons, *Lipid binding by the Unique and SH3 domains of c-Src suggests a new regulatory mechanism*, in *Sci Rep*. 2013.

445. Arbesú, M., M. Maffei, T.N. Cordeiro, J.M. Teixeira, Y. Pérez, P. Bernadó, . . . M. Pons, *The Unique Domain Forms a Fuzzy Intramolecular Complex in Src Family Kinases.* Structure, 2017. **25**(4): p. 630-640.e4.

446. Spassov, D.S., A. Ruiz-Saenz, A. Piple, and M.M. Moasser, *A Dimerization Function in the Intrinsically Disordered N-Terminal Region of Src.* Cell Rep, 2018. **25**(2): p. 449-463.e4.

447. Pawson, T., *Protein modules and signalling networks.* Nature, 1995. **373**(6515): p. 573-80.

448. Pyper, J.M. and J.B. Bolen, *Identification of a novel neuronal C-SRC exon expressed in human brain.* Mol Cell Biol, 1990. **10**(5): p. 2035-40.

449. Musacchio, A., M. Noble, R. Pauptit, R. Wierenga, and M. Saraste, *Crystal structure of a Src-homology 3 (SH3) domain.* Nature, 1992. **359**(6398): p. 851-5.

450. Feng, S., C. Kasahara, R.J. Rickles, and S.L. Schreiber, *Specific interactions outside the proline-rich core of two classes of Src homology 3 ligands.* Proc Natl Acad Sci U S A, 1995. **92**(26): p. 12408-15.

451. Fukui, Y. and H. Hanafusa, *Requirement of phosphatidylinositol-3 kinase modification for its association with p60src.* Mol Cell Biol, 1991. **11**(4): p. 1972-9.

452. Pleiman, C.M., M.R. Clark, L.K. Gauen, S. Winitz, K.M. Coggeshall, G.L. Johnson, . . . J.C. Cambier, *Mapping of sites on the Src family protein tyrosine kinases p55blk, p59fyn, and p56lyn which interact with the effector molecules phospholipase C-gamma 2, microtubule-associated protein kinase, GTPase-activating protein, and phosphatidylinositol 3-kinase.* Mol Cell Biol, 1993. **13**(9): p. 5877-87.

453. Taylor, S.J. and D. Shalloway, *An RNA-binding protein associated with Src through its SH2 and SH3 domains in mitosis.* Nature, 1994. **368**(6474): p. 867-71.

454. Waksman, G., D. Kominos, S.C. Robertson, N. Pant, D. Baltimore, R.B. Birge, . . . J. Kuriyan, *Crystal structure of the phosphotyrosine recognition domain SH2 of v-src complexed with tyrosine-phosphorylated peptides.* Nature, 1992. **358**(6388): p. 646-53.

455. Songyang, Z., S.E. Shoelson, M. Chaudhuri, G. Gish, T. Pawson, W.G. Haser, . . . et al., *SH2 domains recognize specific phosphopeptide sequences.* Cell, 1993. **72**(5): p. 767-78.

456. Schaller, M.D., J.D. Hildebrand, J.D. Shannon, J.W. Fox, R.R. Vines, and J.T. Parsons, *Autophosphorylation of the focal adhesion kinase, pp125FAK, directs SH2-dependent binding of pp60src.* Mol Cell Biol, 1994. **14**(3): p. 1680-8.

457. Knighton, D.R., J.H. Zheng, L.F. Ten Eyck, V.A. Ashford, N.H. Xuong, S.S. Taylor, and J.M. Sowadski, *Crystal structure of the catalytic subunit of cyclic adenosine monophosphate-dependent protein kinase.* Science, 1991. **253**(5018): p. 407-14.

458. Yamaguchi, H. and W.A. Hendrickson, *Structural basis for activation of human lymphocyte kinase Lck upon tyrosine phosphorylation.* Nature, 1996. **384**(6608): p. 484-9.

459. Schindler, T., F. Sicheri, A. Pico, A. Gazit, A. Levitzki, and J. Kuriyan, *Crystal structure of Hck in complex with a Src family-selective tyrosine kinase inhibitor.* Mol Cell, 1999. **3**(5): p. 639-48.

460. Huse, M. and J. Kuriyan, *The conformational plasticity of protein kinases.* Cell, 2002. **109**(3): p. 275-82.

461. Chong, Y.P., T.D. Mulhern, and H.C. Cheng, *C-terminal Src kinase (CSK) and CSK-homologous kinase (CHK)--endogenous negative regulators of Src-family protein kinases.* Growth Factors, 2005. **23**(3): p. 233-44.

462. Okada, M., S. Nada, Y. Yamanashi, T. Yamamoto, and H. Nakagawa, *CSK: a protein-tyrosine kinase involved in regulation of src family kinases.* J Biol Chem, 1991. **266**(36): p. 24249-52.

463. Cooper, J.A., K.L. Gould, C.A. Cartwright, and T. Hunter, *Tyr527 is phosphorylated in pp60c-src: implications for regulation.* Science, 1986. **231**(4744): p. 1431-4.

464. Kmiecik, T.E. and D. Shalloway, *Activation and suppression of pp60c-src transforming ability by mutation of its primary sites of tyrosine phosphorylation.* Cell, 1987. **49**(1): p. 65-73.

465. Zheng, X.M., R.J. Resnick, and D. Shalloway, *A phosphotyrosine displacement mechanism for activation of Src by PTPα*, in *EMBO J.* 2000. p. 964-78.

466. Sicheri, F., I. Moarefi, and J. Kuriyan, *Crystal structure of the Src family tyrosine kinase Hck.* Nature, 1997. **385**(6617): p. 602-9.

467. Williams, J.C., A. Weijland, S. Gonfloni, A. Thompson, S.A. Courtneidge, G. Superti-Furga, and R.K. Wierenga, *The 2.35 A crystal structure of the inactivated form of chicken Src: a dynamic molecule with multiple regulatory interactions.* J Mol Biol, 1997. **274**(5): p. 757-75.

468. Xu, W., A. Doshi, M. Lei, M.J. Eck, and S.C. Harrison, *Crystal structures of c-Src reveal features of its autoinhibitory mechanism.* Mol Cell, 1999. **3**(5): p. 629-38.

469. Xu, W., S.C. Harrison, and M.J. Eck, *Three-dimensional structure of the tyrosine kinase c-Src.* Nature, 1997. **385**(6617): p. 595-602.

470. LaFevre-Bernt, M., F. Sicheri, A. Pico, M. Porter, J. Kuriyan, and W.T. Miller, *Intramolecular regulatory interactions in the Src family kinase Hck probed by mutagenesis of a conserved tryptophan residue.* J Biol Chem, 1998. **273**(48): p. 32129-34.

471. Arold, S.T., T.S. Ulmer, T.D. Mulhern, J.M. Werner, J.E. Ladbury, I.D. Campbell, and M.E. Noble, *The role of the Src homology 3-Src homology 2 interface in the regulation of Src kinases.* J Biol Chem, 2001. **276**(20): p. 17199-205.

472. Young, M.A., S. Gonfloni, G. Superti-Furga, B. Roux, and J. Kuriyan, *Dynamic coupling between the SH2 and SH3 domains of c-Src and Hck underlies their inactivation by C-terminal tyrosine phosphorylation.* Cell, 2001. **105**(1): p. 115-26.

473. Gonfloni, S., A. Weijland, J. Kretzschmar, and G. Superti-Furga, *Crosstalk between the catalytic and regulatory domains allows bidirectional regulation of Src.* Nat Struct Biol, 2000. **7**(4): p. 281-6.

474. Boggon, T.J. and M.J. Eck, *Structure and regulation of Src family kinases.* Oncogene, 2004. **23**(48): p. 7918-27.

475. Martin, G.S., *The hunting of the Src.* Nat Rev Mol Cell Biol, 2001. **2**(6): p. 467-75.

476. Mori, S., L. Rönnstrand, K. Yokote, A. Engström, S.A. Courtneidge, L. Claesson-Welsh, and C.H. Heldin, *Identification of two juxtamembrane autophosphorylation sites in the PDGF beta-receptor; involvement in the interaction with Src family tyrosine kinases.* Embo j, 1993. **12**(6): p. 2257-64.

477. Sieg, D.J., C.R. Hauck, and D.D. Schlaepfer, *Required role of focal adhesion kinase (FAK) for integrin-stimulated cell migration.* J Cell Sci, 1999. **112 (Pt 16)**: p. 2677-91.

478. Chan, P.C. and H.C. Chen, *p120RasGAP-mediated activation of c-Src is critical for oncogenic Ras to induce tumor invasion.* Cancer Res, 2012. **72**(9): p. 2405-15.

479. Masaki, T., M. Okada, M. Tokuda, Y. Shiratori, O. Hatase, M. Shirai, . . . M. Omata, *Reduced C-terminal Src kinase (Csk) activities in hepatocellular carcinoma.* Hepatology, 1999. **29**(2): p. 379-84.

480. Nakagawa, T., S. Tanaka, H. Suzuki, H. Takayanagi, T. Miyazaki, K. Nakamura, and T. Tsuruo, *Overexpression of the csk gene suppresses tumor metastasis in vivo.* Int J Cancer, 2000. **88**(3): p. 384-91.

481. Ponniah, S., D.Z. Wang, K.L. Lim, and C.J. Pallen, *Targeted disruption of the tyrosine phosphatase PTPalpha leads to constitutive downregulation of the kinases Src and Fyn.* Curr Biol, 1999. **9**(10): p. 535-8.

482. Chappel, J., F.P. Ross, Y. Abu-Amer, A. Shaw, and S.L. Teitelbaum, *1,25-dihydroxyvitamin D3 regulates pp60c-src activity and expression of a pp60c-src activating phosphatase.* J Cell Biochem, 1997. **67**(4): p. 432-8.

483. Somani, A.K., J.S. Bignon, G.B. Mills, K.A. Siminovitch, and D.R. Branch, *Src kinase activity is regulated by the SHP-1 protein-tyrosine phosphatase.* J Biol Chem, 1997. **272**(34): p. 21113-9.

484. Walter, A.O., Z.Y. Peng, and C.A. Cartwright, *The Shp-2 tyrosine phosphatase activates the Src tyrosine kinase by a non-enzymatic mechanism.* Oncogene, 1999. **18**(11): p. 1911-20.

485. Arregui, C.O., J. Balsamo, and J. Lilien, *Impaired integrin-mediated adhesion and signaling in fibroblasts expressing a dominant-negative mutant PTP1B.* J Cell Biol, 1998. **143**(3): p. 861-73.

486. Erpel, T., G. Alonso, S. Roche, and S.A. Courtneidge, *The Src SH3 domain is required for DNA synthesis induced by platelet-derived growth factor and epidermal growth factor.* J Biol Chem, 1996. **271**(28): p. 16807-12.

487. Schreiner, S.J., A.P. Schiavone, and T.E. Smithgall, *Activation of STAT3 by the Src family kinase Hck requires a functional SH3 domain.* J Biol Chem, 2002. **277**(47): p. 45680-7.

488. Lerner, E.C., R.P. Trible, A.P. Schiavone, J.M. Hochrein, J.R. Engen, and T.E. Smithgall, *Activation of the Src family kinase Hck without SH3-linker release.* J Biol Chem, 2005. **280**(49): p. 40832-7.

489. Meng, Y., D. Shukla, V.S. Pande, and B. Roux, *Transition path theory analysis of c-Src kinase activation.* Proceedings of the National Academy of Sciences, 2016. **113**(33): p. 9193.

490. Lee, C.H., B. Leung, M.A. Lemmon, J. Zheng, D. Cowburn, J. Kuriyan, and K. Saksela, *A single amino acid in the SH3 domain of Hck determines its high affinity and specificity in binding to HIV-1 Nef protein.* Embo j, 1995. **14**(20): p. 5006-15.

491. Wales, T.E., J.M. Hochrein, C.R. Morgan, L.A. Emert-Sedlak, T.E. Smithgall, and J.R. Engen, *Subtle Dynamic Changes Accompany Hck Activation by HIV-1 Nef and are Reversed by an Antiretroviral Kinase Inhibitor.* Biochemistry, 2015. **54**(41): p. 6382-91.

492. Moroco, J.A., J.J. Alvarado, R.P. Staudt, H. Shi, T.E. Wales, T.E. Smithgall, and J.R. Engen, *Remodeling of HIV-1 Nef Structure by Src-Family Kinase Binding.* J Mol Biol, 2018. **430**(3): p. 310-21.

493. Komuro, I., Y. Yokota, S. Yasuda, A. Iwamoto, and K.S. Kagawa, *CSF-induced and HIV-1-mediated distinct regulation of Hck and C/EBPbeta represent a heterogeneous susceptibility of monocyte-derived macrophages to M-tropic HIV-1 infection.* J Exp Med, 2003. **198**(3): p. 443-53.

494. Hanna, Z., X. Weng, D.G. Kay, J. Poudrier, C. Lowell, and P. Jolicoeur, *The pathogenicity of human immunodeficiency virus (HIV) type 1 Nef in CD4C/HIV transgenic mice is abolished by mutation of its SH3-binding domain, and disease development is delayed in the absence of Hck.* J Virol, 2001. **75**(19): p. 9378-92.

495. Briggs, S.D., E.C. Lerner, and T.E. Smithgall, *Affinity of Src family kinase SH3 domains for HIV Nef in vitro does not predict kinase activation by Nef in vivo.* Biochemistry, 2000. **39**(3): p. 489-95.

496. Choi, H.J. and T.E. Smithgall, *Conserved residues in the HIV-1 Nef hydrophobic pocket are essential for recruitment and activation of the Hck tyrosine kinase.* J Mol Biol, 2004. **343**(5): p. 1255-68.

497. Baur, A.S., G. Sass, B. Laffert, D. Willbold, C. Cheng-Mayer, and B.M. Peterlin, *The N-terminus of Nef from HIV-1/SIV associates with a protein complex containing Lck and a serine kinase.* Immunity, 1997. **6**(3): p. 283-91.

498. Collette, Y., H. Dutartre, A. Benziane, M. Ramos, R. Benarous, M. Harris, and D. Olive, *Physical and functional interaction of Nef with Lck. HIV-1 Nef-induced T-cell signaling defects.* J Biol Chem, 1996. **271**(11): p. 6333-41.

499. Dutartre, H., M. Harris, D. Olive, and Y. Collette, *The human immunodeficiency virus type 1 Nef protein binds the Src-related tyrosine kinase Lck SH2 domain through a novel phosphotyrosine independent mechanism.* Virology, 1998. **247**(2): p. 200-11.

500. Greenway, A.L., H. Dutartre, K. Allen, D.A. McPhee, D. Olive, and Y. Collette, *Simian Immunodeficiency Virus and Human Immunodeficiency Virus Type 1 Nef Proteins Show Distinct Patterns and Mechanisms of Src Kinase Activation*, in *J Virol*. 1999. p. 6152-8.

501. Yang, W.C., Y. Collette, J.A. Nunès, and D. Olive, *Tec kinases: a family with multiple roles in immunity.* Immunity, 2000. **12**(4): p. 373-82.

502. Mano, H., F. Ishikawa, J. Nishida, H. Hirai, and F. Takaku, *A novel protein-tyrosine kinase, tec, is preferentially expressed in liver.* Oncogene, 1990. **5**(12): p. 1781-6.

503. Tsukada, S., D.C. Saffran, D.J. Rawlings, O. Parolini, R.C. Allen, I. Klisak, . . . et al., *Deficient expression of a B cell cytoplasmic tyrosine kinase in human X-linked agammaglobulinemia.* Cell, 1993. **72**(2): p. 279-90.

504. Heyeck, S.D. and L.J. Berg, *Developmental regulation of a murine T-cell-specific tyrosine kinase gene, Tsk.* Proc Natl Acad Sci U S A, 1993. **90**(2): p. 669-73.

505. Tamagnone, L., I. Lahtinen, T. Mustonen, K. Virtaneva, F. Francis, F. Muscatelli, . . . K. Alitalo, *BMX, a novel nonreceptor tyrosine kinase gene of the BTK/ITK/TEC/TXK family located in chromosome Xp22.2.* Oncogene, 1994. **9**(12): p. 3683-8.

506. Hu, Q., D. Davidson, P.L. Schwartzberg, F. Macchiarini, M.J. Lenardo, J.A. Bluestone, and L.A. Matis, *Identification of Rlk, a novel protein tyrosine kinase with predominant expression in the T cell lineage.* J Biol Chem, 1995. **270**(4): p. 1928-34.

507. Yang, W.C., K.A. Ching, C.D. Tsoukas, and L.J. Berg, *Tec kinase signaling in T cells is regulated by phosphatidylinositol 3-kinase and the Tec pleckstrin homology domain.* J Immunol, 2001. **166**(1): p. 387-95.

508. Yang, W.C., M. Ghiotto, B. Barbarat, and D. Olive, *The role of Tec protein-tyrosine kinase in T cell signaling.* J Biol Chem, 1999. **274**(2): p. 607-17.

509. Ellmeier, W., S. Jung, M.J. Sunshine, F. Hatam, Y. Xu, D. Baltimore, . . . D.R. Littman, *Severe B Cell Deficiency in Mice Lacking the Tec Kinase Family Members Tec and Btk.* J Exp Med, 2000. **192**(11): p. 1611-24.

510. Tomlinson, M.G., L.P. Kane, J. Su, T.A. Kadlecek, M.N. Mollenauer, and A. Weiss, *Expression and function of Tec, Itk, and Btk in lymphocytes: evidence for a unique role for Tec.* Mol Cell Biol, 2004. **24**(6): p. 2455-66.

511. Rawlings, D.J., D.C. Saffran, S. Tsukada, D.A. Largaespada, J.C. Grimaldi, L. Cohen, . . . et al., *Mutation of unique region of Bruton's tyrosine kinase in immunodeficient XID mice.* Science, 1993. **261**(5119): p. 358-61.

512. Pal Singh, S., F. Dammeijer, and R.W. Hendriks, *Role of Bruton's tyrosine kinase in B cells and malignancies.* Mol Cancer, 2018. **17**(1): p. 57.

513. Siliciano, J.D., T.A. Morrow, and S.V. Desiderio, *itk, a T-cell-specific tyrosine kinase gene inducible by interleukin 2.* Proc Natl Acad Sci U S A, 1992. **89**(23): p. 11194-8.

514. Liao, X.C. and D.R. Littman, *Altered T cell receptor signaling and disrupted T cell development in mice lacking Itk.* Immunity, 1995. **3**(6): p. 757-69.

515. Ekman, N., A. Lymboussaki, I. Västrik, K. Sarvas, A. Kaipainen, and K. Alitalo, *Bmx tyrosine kinase is specifically expressed in the endocardium and the endothelium of large arteries.* Circulation, 1997. **96**(6): p. 1729-32.

516. Kaukonen, J., I. Lahtinen, S. Laine, K. Alitalo, and A. Palotie, *BMX tyrosine kinase gene is expressed in granulocytes and myeloid leukaemias.* Br J Haematol, 1996. **94**(3): p. 455-60.

517. Abassi, Y.A., M. Rehn, N. Ekman, K. Alitalo, and K. Vuori, *p130Cas Couples the tyrosine kinase Bmx/Etk with regulation of the actin cytoskeleton and cell migration.* J Biol Chem, 2003. **278**(37): p. 35636-43.

518. Zhang, R., Y. Xu, N. Ekman, Z. Wu, J. Wu, K. Alitalo, and W. Min, *Etk/Bmx transactivates vascular endothelial growth factor 2 and recruits phosphatidylinositol 3-kinase to mediate the tumor necrosis factor-induced angiogenic pathway.* J Biol Chem, 2003. **278**(51): p. 51267-76.

519. He, Y., Y. Luo, S. Tang, I. Rajantie, P. Salven, M. Heil, . . . W. Min, *Critical function of Bmx/Etk in ischemia-mediated arteriogenesis and angiogenesis.* J Clin Invest, 2006. **116**(9): p. 2344-55.

520. Jones, D., Z. Xu, H. Zhang, Y. He, M.S. Kluger, H. Chen, and W. Min, *Functional analyses of the bone marrow kinase in the X chromosome in vascular endothelial growth factor-induced lymphangiogenesis.* Arterioscler Thromb Vasc Biol, 2010. **30**(12): p. 2553-61.

521. Rajantie, I., N. Ekman, K. Iljin, E. Arighi, Y. Gunji, J. Kaukonen, . . . K. Alitalo, *Bmx Tyrosine Kinase Has a Redundant Function Downstream of Angiopoietin and Vascular Endothelial Growth Factor Receptors in Arterial Endothelium*, in *Mol Cell Biol*. 2001. p. 4647-55.

522. Palmer, C.D., B.E. Mutch, S. Workman, J.P. McDaid, N.J. Horwood, and B.M. Foxwell, *Bmx tyrosine kinase regulates TLR4-induced IL-6 production in human macrophages independently of p38 MAPK and NFkapp}B activity.* Blood, 2008. **111**(4): p. 1781-8.

523. Schaeffer, E.M., J. Debnath, G. Yap, D. McVicar, X.C. Liao, D.R. Littman, . . . P.L. Schwartzberg, *Requirement for Tec kinases Rlk and Itk in T cell receptor signaling and immunity.* Science, 1999. **284**(5414): p. 638-41.

524. Schneider, H., B. Guerette, C. Guntermann, and C.E. Rudd, *Resting lymphocyte kinase (Rlk/Txk) targets lymphoid adaptor SLP-76 in the cooperative activation of interleukin-2 transcription in T-cells.* J Biol Chem, 2000. **275**(6): p. 3835-40.

525. Gomez-Rodriguez, J., N. Sahu, R. Handon, T.S. Davidson, S.M. Anderson, M.R. Kirby, . . . P.L. Schwartzberg, *Differential expression of interleukin-17A and -17F is coupled to T cell receptor signaling via inducible T cell kinase.* Immunity, 2009. **31**(4): p. 587-97.

526. Ferrara, T.J., C. Mueller, N. Sahu, A. Ben-Jebria, and A. August, *Reduced airway hyperresponsiveness and tracheal responses during allergic asthma in mice lacking tyrosine kinase inducible T-cell kinase.* J Allergy Clin Immunol, 2006. **117**(4): p. 780-6.

527. Mano, H., *Tec family of protein-tyrosine kinases: an overview of their structure and function.* Cytokine Growth Factor Rev, 1999. **10**(3-4): p. 267-80.

528. Debnath, J., M. Chamorro, M.J. Czar, E.M. Schaeffer, M.J. Lenardo, H.E. Varmus, and P.L. Schwartzberg, *rlk/TXK Encodes Two Forms of a Novel Cysteine String Tyrosine Kinase Activated by Src Family Kinases*, in *Mol Cell Biol*. 1999. p. 1498-507.

529. Tomlinson, M.G., T. Kurosaki, A.E. Berson, G.H. Fujii, J.A. Johnston, and J.B. Bolen, *Reconstitution of Btk signaling by the atypical tec family tyrosine kinases Bmx and Txk.* J Biol Chem, 1999. **274**(19): p. 13577-85.

530. Hyvönen, M. and M. Saraste, *Structure of the PH domain and Btk motif from Bruton's tyrosine kinase: molecular explanations for X-linked agammaglobulinaemia.* Embo j, 1997. **16**(12): p. 3396-404.

531. Baraldi, E., K. Djinovic Carugo, M. Hyvönen, P.L. Surdo, A.M. Riley, B.V. Potter, . . . M. Saraste, *Structure of the PH domain from Bruton's tyrosine kinase in complex with inositol 1,3,4,5-tetrakisphosphate.* Structure, 1999. **7**(4): p. 449-60.

532. Wang, Q., E.M. Vogan, L.M. Nocka, C.E. Rosen, J.A. Zorn, S.C. Harrison, and J. Kuriyan, *Autoinhibition of Bruton's tyrosine kinase (Btk) and activation by soluble inositol hexakisphosphate.* Elife, 2015. **4**.

533. Macias, M.J., A. Musacchio, H. Ponstingl, M. Nilges, M. Saraste, and H. Oschkinat, *Structure of the pleckstrin homology domain from beta-spectrin.* Nature, 1994. **369**(6482): p. 675-7.

534. Fukuda, M., T. Kojima, H. Kabayama, and K. Mikoshiba, *Mutation of the pleckstrin homology domain of Bruton's tyrosine kinase in immunodeficiency impaired inositol 1,3,4,5-tetrakisphosphate binding capacity.* J Biol Chem, 1996. **271**(48): p. 30303-6.

535. Rameh, L.E., A. Arvidsson, K.L. Carraway, 3rd, A.D. Couvillon, G. Rathbun, A. Crompton, . . . L.C. Cantley, *A comparative analysis of the phosphoinositide binding specificity of pleckstrin homology domains.* J Biol Chem, 1997. **272**(35): p. 22059-66.

536. Chung, J.K., L.M. Nocka, A. Decker, Q. Wang, T.A. Kadlecek, A. Weiss, . . . J.T. Groves, *Switch-like activation of Bruton's tyrosine kinase by membrane-mediated dimerization.* Proc Natl Acad Sci U S A, 2019. **116**(22): p. 10798-10803.

537. Langhans-Rajasekaran, S.A., Y. Wan, and X.Y. Huang, *Activation of Tsk and Btk tyrosine kinases by G protein beta gamma subunits.* Proc Natl Acad Sci U S A, 1995. **92**(19): p. 8601-5.

538. Novina, C.D., S. Kumar, U. Bajpai, V. Cheriyath, K. Zhang, S. Pillai, . . . A.L. Roy, *Regulation of nuclear localization and transcriptional activity of TFII-I by Bruton's tyrosine kinase.* Mol Cell Biol, 1999. **19**(7): p. 5014-24.

539. Yao, L., P. Janmey, L.G. Frigeri, W. Han, J. Fujita, Y. Kawakami, . . . T. Kawakami, *Pleckstrin homology domains interact with filamentous actin.* J Biol Chem, 1999. **274**(28): p. 19752-61.

540. Yao, L., Y. Kawakami, and T. Kawakami, *The pleckstrin homology domain of Bruton tyrosine kinase interacts with protein kinase C.* Proc Natl Acad Sci U S A, 1994. **91**(19): p. 9175-9.

541. Amatya, N., T.E. Wales, A. Kwon, W. Yeung, R.E. Joseph, D.B. Fulton, . . . A.H. Andreotti, *Lipid-targeting pleckstrin homology domain turns its autoinhibitory face toward the TEC kinases.* Proc Natl Acad Sci U S A, 2019. **116**(43): p. 21539-21544.

542. Devkota, S., R.E. Joseph, S.E. Boyken, D.B. Fulton, and A.H. Andreotti, *An autoinhibitory role for the Pleckstrin Homology domain of ITK and its interplay with canonical phospholipid recognition.* Biochemistry, 2017. **56**(23): p. 2938-49.

543. Vihinen, M., L. Nilsson, and C.I. Smith, *Tec homology (TH) adjacent to the PH domain.* FEBS Lett, 1994. **350**(2-3): p. 263-5.

544. Cheng, G., Z.S. Ye, and D. Baltimore, *Binding of Bruton's tyrosine kinase to Fyn, Lyn, or Hck through a Src homology 3 domain-mediated interaction.* Proc Natl Acad Sci U S A, 1994. **91**(17): p. 8152-5.

545. Mano, H., K. Sato, Y. Yazaki, and H. Hirai, *Tec protein-tyrosine kinase directly associates with Lyn protein-tyrosine kinase through its N-terminal unique domain.* Oncogene, 1994. **9**(11): p. 3205-11.

546. Mano, H., Y. Yamashita, A. Miyazato, Y. Miura, and K. Ozawa, *Tec protein-tyrosine kinase is an effector molecule of Lyn protein-tyrosine kinase.* Faseb j, 1996. **10**(5): p. 637-42.

547. Rawlings, D.J., A.M. Scharenberg, H. Park, M.I. Wahl, S. Lin, R.M. Kato, . . . J.P. Kinet, *Activation of BTK by a phosphorylation mechanism initiated by SRC family kinases.* Science, 1996. **271**(5250): p. 822-5.

548. Andreotti, A.H., S.C. Bunnell, S. Feng, L.J. Berg, and S.L. Schreiber, *Regulatory intramolecular association in a tyrosine kinase of the Tec family.* Nature, 1997. **385**(6611): p. 93-7.

549. Joseph, R.E., D.B. Fulton, and A.H. Andreotti, *Mechanism and functional significance of Itk autophosphorylation.* J Mol Biol, 2007. **373**(5): p. 1281-92.

550. Park, H., M.I. Wahl, D.E. Afar, C.W. Turck, D.J. Rawlings, C. Tam, . . . O.N. Witte, *Regulation of Btk function by a major autophosphorylation site within the SH3 domain.* Immunity, 1996. **4**(5): p. 515-25.

551. Wilcox, H.M. and L.J. Berg, *Itk phosphorylation sites are required for functional activity in primary T cells.* J Biol Chem, 2003. **278**(39): p. 37112-21.

552. Morrogh, L.M., S. Hinshelwood, P. Costello, G.O. Cory, and C. Kinnon, *The SH3 domain of Bruton's tyrosine kinase displays altered ligand binding properties when auto-phosphorylated in vitro.* Eur J Immunol, 1999. **29**(7): p. 2269-79.

553. Laederach, A., K.W. Cradic, D.B. Fulton, and A.H. Andreotti, *Determinants of intra versus intermolecular self-association within the regulatory domains of Rlk and Itk.* J Mol Biol, 2003. **329**(5): p. 1011-20.

554. Laederach, A., K.W. Cradic, K.N. Brazin, J. Zamoon, D.B. Fulton, X.Y. Huang, and A.H. Andreotti, *Competing modes of self-association in the regulatory domains of Bruton's*

tyrosine kinase: intramolecular contact versus asymmetric homodimerization. Protein Sci, 2002. **11**(1): p. 36-45.

555. Pursglove, S.E., T.D. Mulhern, J.P. Mackay, M.G. Hinds, and G.W. Booker, *The solution structure and intramolecular associations of the Tec kinase SRC homology 3 domain.* J Biol Chem, 2002. **277**(1): p. 755-62.

556. Huang, K.C., H.T. Cheng, M.T. Pai, S.R. Tzeng, and J.W. Cheng, *Solution structure and phosphopeptide binding of the SH2 domain from the human Bruton's tyrosine kinase.* J Biomol NMR, 2006. **36**(1): p. 73-8.

557. Joseph, R.E., N.D. Ginder, J.A. Hoy, J.C. Nix, D.B. Fulton, R.B. Honzatko, and A.H. Andreotti, *Structure of the interleukin-2 tyrosine kinase Src homology 2 domain; comparison between X-ray and NMR-derived structures.* Acta Crystallogr Sect F Struct Biol Cryst Commun, 2012. **68**(Pt 2): p. 145-53.

558. Mallis, R.J., K.N. Brazin, D.B. Fulton, and A.H. Andreotti, *Structural characterization of a proline-driven conformational switch within the Itk SH2 domain.* Nat Struct Biol, 2002. **9**(12): p. 900-5.

559. Breheny, P.J., A. Laederach, D.B. Fulton, and A.H. Andreotti, *Ligand specificity modulated by prolyl imide bond Cis/Trans isomerization in the Itk SH2 domain: a quantitative NMR study.* J Am Chem Soc, 2003. **125**(51): p. 15706-7.

560. Colgan, J., M. Asmal, M. Neagu, B. Yu, J. Schneidkraut, Y. Lee, . . . J. Luban, *Cyclophilin A regulates TCR signal strength in CD4+ T cells via a proline-directed conformational switch in Itk.* Immunity, 2004. **21**(2): p. 189-201.

561. Pletneva, E.V., M. Sundd, D.B. Fulton, and A.H. Andreotti, *Molecular details of Itk activation by prolyl isomerization and phospholigand binding: the NMR structure of the Itk SH2 domain bound to a phosphopeptide.* J Mol Biol, 2006. **357**(2): p. 550-61.

562. Severin, A., R.E. Joseph, S. Boyken, D.B. Fulton, and A.H. Andreotti, *Proline isomerization preorganizes the Itk SH2 domain for binding to the Itk SH3 domain.* J Mol Biol, 2009. **387**(3): p. 726-43.

563. Benfield, A.P., B.B. Whiddon, J.H. Clements, and S.F. Martin, *Structural and energetic aspects of Grb2-SH2 domain-swapping.* Arch Biochem Biophys, 2007. **462**(1): p. 47-53.

564. Joseph, R.E. and A.H. Andreotti, *Conformational snapshots of Tec kinases during signaling.* Immunol Rev, 2009. **228**(1): p. 74-92.

565. Mao, C., M. Zhou, and F.M. Uckun, *Crystal structure of Bruton's tyrosine kinase domain suggests a novel pathway for activation and provides insights into the molecular basis of X-linked agammaglobulinemia.* J Biol Chem, 2001. **276**(44): p. 41435-43.

566. Brown, K., J.M. Long, S.C. Vial, N. Dedi, N.J. Dunster, S.B. Renwick, . . . G.M. Cheetham, *Crystal structures of interleukin-2 tyrosine kinase and their implications for the design of selective inhibitors.* J Biol Chem, 2004. **279**(18): p. 18727-32.

567. Joseph, R.E., T.E. Wales, D.B. Fulton, J.R. Engen, and A.H. Andreotti, *Achieving a Graded Immune Response: BTK Adopts Range of Active/Inactive Conformations Dictated by Multiple Interdomain Contacts.* Structure, 2017. **25**(10): p. 1481-1494 e4.

568. Hansson, H., P.T. Mattsson, P. Allard, P. Haapaniemi, M. Vihinen, C.I. Smith, and T. Hard, *Solution structure of the SH3 domain from Bruton's tyrosine kinase.* Biochemistry, 1998. **37**(9): p. 2912-24.

569. Márquez, J.A., C.I. Smith, M.V. Petoukhov, P. Lo Surdo, P.T. Mattsson, M. Knekt, . . . D.I. Svergun, *Conformation of full-length Bruton tyrosine kinase (Btk) from synchrotron X-ray solution scattering.* Embo j, 2003. **22**(18): p. 4616-24.

570. Antal, C.E., J.A. Callender, A.P. Kornev, S.S. Taylor, and A.C. Newton, *Intramolecular C2 Domain-Mediated Autoinhibition of Protein Kinase C βII.* Cell Rep, 2015. **12**(8): p. 1252-60.

571. Lietha, D., X. Cai, D.F. Ceccarelli, Y. Li, M.D. Schaller, and M.J. Eck, *Structural basis for the autoinhibition of focal adhesion kinase.* Cell, 2007. **129**(6): p. 1177-87.

572. Wu, W.I., W.C. Voegtli, H.L. Sturgis, F.P. Dizon, G.P. Vigers, and B.J. Brandhuber, *Crystal structure of human AKT1 with an allosteric inhibitor reveals a new mode of kinase inhibition.* PLoS One, 2010. **5**(9): p. e12913.

573. Shah, N.H., J.F. Amacher, L.M. Nocka, and J. Kuriyan, *The Src module: an ancient scaffold in the evolution of cytoplasmic tyrosine kinases.* Crit Rev Biochem Mol Biol, 2018. **53**(5): p. 535-63.

574. Joseph, R.E., I. Kleino, T.E. Wales, Q. Xie, D.B. Fulton, J.R. Engen, . . . A.H. Andreotti, *Activation loop dynamics determine the different catalytic efficiencies of B cell- and T cell-specific tec kinases.* Sci Signal, 2013. **6**(290): p. ra76.

575. Glaichenhaus, N., N. Shastri, D.R. Littman, and J.M. Turner, *Requirement for association of p56lck with CD4 in antigen-specific signal transduction in T cells.* Cell, 1991. **64**(3): p. 511-20.

576. Andreotti, A.H., R.E. Joseph, J.M. Conley, J. Iwasa, and L.J. Berg, *Multidomain Control Over TEC Kinase Activation State Tunes the T Cell Response.* Annu Rev Immunol, 2018. **36**: p. 549-578.

577. Stepanek, O., P. Draber, A. Drobek, V. Horejsi, and T. Brdicka, *Nonredundant roles of Src-family kinases and Syk in the initiation of B-cell antigen receptor signaling.* J Immunol, 2013. **190**(4): p. 1807-18.

578. Kurosaki, T., *Regulation of BCR signaling.* Mol Immunol, 2011. **48**(11): p. 1287-91.

579. Gaud, G., R. Lesourne, and P.E. Love, *Regulatory mechanisms in T cell receptor signalling.* Nat Rev Immunol, 2018. **18**(8): p. 485-497.

580. Readinger, J.A., G.M. Schiralli, J.K. Jiang, C.J. Thomas, A. August, A.J. Henderson, and P.L. Schwartzberg, *Selective targeting of ITK blocks multiple steps of HIV replication.* Proc Natl Acad Sci U S A, 2008. **105**(18): p. 6684-9.

581. Guendel, I., S. Iordanskiy, G.C. Sampey, R. Van Duyne, V. Calvert, E. Petricoin, . . . F. Kashanchi, *Role of Bruton's tyrosine kinase inhibitors in HIV-1-infected cells.* J Neurovirol, 2015. **21**(3): p. 257-75.

582. Tarafdar, S., J.A. Poe, and T.E. Smithgall, *The accessory factor Nef links HIV-1 to Tec/Btk kinases in an Src homology 3 domain-dependent manner.* J Biol Chem, 2014. **289**(22): p. 15718-28.

583. Collette, Y., S. Arold, C. Picard, K. Janvier, S. Benichou, R. Benarous, . . . C. Dumas, *HIV-2 and SIV nef proteins target different Src family SH3 domains than does HIV-1 Nef because of a triple amino acid substitution.* J Biol Chem, 2000. **275**(6): p. 4171-6.

584. Sengupta, S. and R.F. Siliciano, *Targeting the Latent Reservoir for HIV-1.* Immunity, 2018. **48**(5): p. 872-895.

585. Dionne, B., *Key Principles of Antiretroviral Pharmacology.* Infect. Dis. Clin. North Am, 2019. **33**(3): p. 787-805.

586. Sauter, D. and F. Kirchhoff, *Multilayered and versatile inhibition of cellular antiviral factors by HIV and SIV accessory proteins.* Cytokine Growth Factor Rev, 2018. **40**: p. 3-12.

587. Kestler, H., D.J. Ringler, K. Mori, D.L. Panicali, P.K. Sehgal, M.D. Daniel, and R.C. Desrosiers, *Importance of the nef gene for maintenance of high viral loads and for development of AIDS.* Cell, 1991. **65**: p. 651-662.

588. Watkins, R.L., J.L. Foster, and J.V. Garcia, *In vivo analysis of Nef's role in HIV-1 replication, systemic T cell activation and CD4(+) T cell loss.* Retrovirology, 2015. **12**: p. 61.

589. Mujib, S., A. Saiyed, S. Fadel, A. Bozorgzad, N. Aidarus, F.Y. Yue, . . . M.A. Ostrowski, *Pharmacologic HIV-1 Nef Blockade Enhances the Recognition and Elimination of Latently HIV-1 Infected CD4 T cells by Autologous CD8 T cells.* J. Clin. Invest. Insight, 2017. **2**(17): p. e93684.

590. Smithgall, T.E. and G. Thomas, *Small molecule inhibitors of the HIV-1 virulence factor, Nef.* Drug Discov Today: Technol, 2013. **10**: p. 523-529.

591. Aiken, C., J. Konner, N.R. Landau, M.E. Lenburg, and D. Trono, *Nef induces CD4 endocytosis: requirement for a critical dileucine motif in the membrane-proximal CD4 cytoplasmic domain.* Cell, 1994. **76**(5): p. 853-864.

592. Pawlak, E.N. and J.D. Dikeakos, *HIV-1 Nef: a master manipulator of the membrane trafficking machinery mediating immune evasion.* Biochim. Biophys. Acta, 2015. **1850**(4): p. 733-741.

593. Ramirez, P.W., S. Sharma, R. Singh, C.A. Stoneham, T. Vollbrecht, and J. Guatelli, *Plasma Membrane-Associated Restriction Factors and Their Counteraction by HIV-1 Accessory Proteins.* Cells, 2019. **8**(9): p. 1020.

594. Guiet, R., R. Poincloux, J. Castandet, L. Marois, A. Labrousse, C. Le, V, and I. Maridonneau-Parini, *Hematopoietic cell kinase (Hck) isoforms and phagocyte duties - from signaling and actin reorganization to migration and phagocytosis.* Eur. J. Cell Biol, 2008. **87**(8-9): p. 527-542.

595. Schindler, T., F. Sicheri, A. Pico, A. Gazit, A. Levitzki, and J. Kuriyan, *Crystal structure of Hck in complex with a Src family-selective tyrosine kinase inhibitor.* Mol. Cell, 1999. **3**(5): p. 639-648.

596. Moarefi, I., M. LaFevre-Bernt, F. Sicheri, M. Huse, C.-H. Lee, J. Kuriyan, and W.T. Miller, *Activation of the Src-family tyrosine kinase Hck by SH3 domain displacement.* Nature, 1997. **385**: p. 650-653.

597. Briggs, S.D., M. Sharkey, M. Stevenson, and T.E. Smithgall, *SH3-mediated Hck tyrosine kinase activation and fibroblast transformation by the Nef protein of HIV-1.* J. Biol. Chem, 1997. **272**: p. 17899-17902.

598. Trible, R.P., L. Emert-Sedlak, and T.E. Smithgall, *HIV-1 Nef selectively activates SRC family kinases HCK, LYN, and c-SRC through direct SH3 domain interaction.* J. Biol. Chem, 2006. **281**: p. 27029-27038.

599. Saksela, K., G. Cheng, and D. Baltimore, *Proline-rich (PxxP) motifs in HIV-1 Nef bind to SH3 domains of a subset of Src kinases and are required for the enhanced growth of Nef$^+$ viruses but not for down-regulation of CD4.* EMBO J, 1995. **14**(3): p. 484-491.

600. Emert-Sedlak, L., T. Kodama, E.C. Lerner, W. Dai, C. Foster, B.W. Day, . . . T.E. Smithgall, *Chemical library screens targeting an HIV-1 accessory factor/host cell kinase complex identify novel antiretroviral compounds.* ACS Chem. Biol, 2009. **4**(11): p. 939-947.

601. Emert-Sedlak, L.A., P. Narute, S.T. Shu, J.A. Poe, H. Shi, N. Yanamala, . . . T.E. Smithgall, *Effector Kinase Coupling Enables High-Throughput Screens for Direct HIV-1 Nef Antagonists with Antiretroviral Activity.* Chem. Biol, 2013. **20**(1): p. 82-91.

602. Courtney, A.H., W.L. Lo, and A. Weiss, *TCR Signaling: Mechanisms of Initiation and Propagation.* Trends Biochem. Sci, 2018. **43**(2): p. 108-123.

603. Readinger, J.A., G.M. Schiralli, J.K. Jiang, C.J. Thomas, A. August, A.J. Henderson, and P.L. Schwartzberg, *Selective targeting of ITK blocks multiple steps of HIV replication.* Proc. Natl. Acad. Sci. U. S. A, 2008. **105**(18): p. 6684-6689.

604. Tarafdar, S., J.A. Poe, and T.E. Smithgall, *The Accessory Factor Nef Links HIV-1 to Tec/Btk Kinases in an Src Homology 3 Domain-dependent Manner.* J Biol Chem, 2014. **289**(22): p. 15718-15728.

605. Shi, H., C.M. Tice, L. Emert-Sedlak, L. Chen, W.F. Li, M. Carlsen, . . . T.E. Smithgall, *Tight-Binding Hydroxypyrazole HIV-1 Nef Inhibitors Suppress Viral Replication in Donor Mononuclear Cells and Reverse Nef-Mediated MHC-I Downregulation.* ACS Infect. Dis, 2020. **6**(2): p. 10.

606. Devkota, S., R.E. Joseph, S.E. Boyken, D.B. Fulton, and A.H. Andreotti, *An Autoinhibitory Role for the Pleckstrin Homology Domain of Interleukin-2-Inducible Tyrosine Kinase and Its Interplay with Canonical Phospholipid Recognition.* Biochemistry, 2017. **56**(23): p. 2938-2949.

607. Joseph, R.E., T.E. Wales, D.B. Fulton, J.R. Engen, and A.H. Andreotti, *Achieving a Graded Immune Response: BTK Adopts a Range of Active/Inactive Conformations Dictated by Multiple Interdomain Contacts.* Structure, 2017. **25**(10): p. 1481-1494.

608. Lerner, E.C. and T.E. Smithgall, *SH3-dependent stimulation of Src-family kinase autophosphorylation without tail release from the SH2 domain in vivo.* Nat. Struct. Biol, 2002. **9**: p. 365-369.

609. Narute, P.S. and T.E. Smithgall, *Nef alleles from all major HIV-1 clades activate Src-family kinases and enhance HIV-1 replication in an inhibitor-sensitive manner.* PLoS. One, 2012. **7**(2): p. e32561.

610. Moroco, J.A., J.K. Craigo, R.E. Iacob, T.E. Wales, J.R. Engen, and T.E. Smithgall, *Differential sensitivity of Src-family kinases to activation by SH3 domain displacement.* PLoS One, 2014. **9**(8): p. e105629.

611. Collette, Y., S. Arold, C. Picard, K. Janvier, S. Benichou, R. Benarous, . . . C. Dumas, *HIV-2 and SIV nef proteins target different Src family SH3 domains than does HIV-1 Nef because of a triple amino acid substitution.* J. Biol. Chem, 2000. **275**(6): p. 4171-4176.

612. Osmanov, S., C. Pattou, N. Walker, B. Schwardländer, and J. Esparza, *Estimated global distribution and regional spread of HIV-1 genetic subtypes in the year 2000.* J Acquir Immune Defic Syndr, 2002. **29**(2): p. 184-90.

613. Moroco, J.A., J.J. Alvarado, R.P. Staudt, T.E. Wales, T.E. Smithgall, and J.R. Engen, *Remodeling of HIV-1 Nef Structure by Src-Family Kinase Binding.* J. Mol. Biol, 2018. **430**(3): p. 310-321.

614. Lee, C.-H., K. Saksela, U.A. Mirza, B.T. Chait, and J. Kuriyan, *Crystal structure of the conserved core of HIV-1 Nef complexed with a Src family SH3 domain.* Cell, 1996. **85**: p. 931-942.

615. Brazin, K.N., D.B. Fulton, and A.H. Andreotti, *A specific intermolecular association between the regulatory domains of a Tec family kinase.* J Mol Biol, 2000. **302**(3): p. 607-23.

616. Kueffer, L.E., R.E. Joseph, and A.H. Andreotti, *Reining in BTK: Interdomain Interactions and Their Importance in the Regulatory Control of BTK.* Front Cell Dev Biol, 2021. **9**: p. 655489.

617. Amatya, N., D.Y. Lin, and A.H. Andreotti, *Dynamic regulatory features of the protein tyrosine kinases.* Biochem Soc Trans, 2019. **47**(4): p. 1101-1116.

618. Mitchell, J.L., R.P. Trible, L.A. Emert-Sedlak, D.D. Weis, E.C. Lerner, J.J. Applen, . . . J.R. Engen, *Functional characterization and conformational analysis of the Herpesvirus saimiri Tip-C484 protein.* J. Mol. Biol, 2007. **366**(4): p. 1282-1293.

619. Greenway, A.L., H. Dutartre, K. Allen, D.A. McPhee, D. Olive, and Y. Collette, *Simian immunodeficiency virus and human immunodeficiency virus type 1 nef proteins show distinct patterns and mechanisms of Src kinase activation.* J. Virol, 1999. **73**(7): p. 6152-6158.

620. Alvarado, J.J., S. Tarafdar, J.I. Yeh, and T.E. Smithgall, *Interaction with the Src homology (SH3-SH2) region of the Src-family kinase Hck structures the HIV-1 Nef dimer for kinase activation and effector recruitment.* J Biol Chem, 2014. **289**: p. 28539-28553.

621. Berro, R., C. de la Fuente, Z. Klase, K. Kehn, L. Parvin, A. Pumfery, . . . F. Kashanchi, *Identifying the membrane proteome of HIV-1 latently infected cells.* J Biol Chem, 2007. **282**(11): p. 8207-18.

622. Charter, N.W., L. Kauffman, R. Singh, and R.M. Eglen, *A generic, homogenous method for measuring kinase and inhibitor activity via adenosine 5'-diphosphate accumulation.* J Biomol Screen, 2006. **11**(4): p. 390-9.

623. Shu, S.T., W.F. Li, and T.E. Smithgall, *Visualization of Host Cell Kinase Activation by Viral Proteins Using GFP Fluorescence Complementation and Immunofluorescence Microscopy.* Bio Protoc, 2021. **11**(13): p. e4068.

624. Engen, J.R., T.E. Wales, J.M. Hochrein, M.A. Meyn, 3rd, S. Banu Ozkan, I. Bahar, and T.E. Smithgall, *Structure and dynamic regulation of Src-family kinases.* Cell Mol Life Sci, 2008. **65**(19): p. 3058-73.

625. Santos, S.P., T.M. Bandeiras, A.F. Pinto, M. Teixeira, M.A. Carrondo, and C.V. Romão, *Thermofluor-based optimization strategy for the stabilization and crystallization of Campylobacter jejuni desulforubrerythrin.* Protein Expr Purif, 2012. **81**(2): p. 193-200.

626. Oshaben, K.M., R. Salari, D.R. McCaslin, L.T. Chong, and W.S. Horne, *The native GCN4 leucine-zipper domain does not uniquely specify a dimeric oligomerization state.* Biochemistry, 2012. **51**(47): p. 9581-91.

627. Nannenga, B.L. and T. Gonen, *The cryo-EM method microcrystal electron diffraction (MicroED).* Nat Methods, 2019. **16**(5): p. 369-379.

628. Till, M., A. Robson, M.J. Byrne, A.V. Nair, S.A. Kolek, P.D. Shaw Stewart, and P.R. Race, *Improving the success rate of protein crystallization by random microseed matrix screening.* J Vis Exp, 2013(78).

629. Tebo, A.G. and A. Gautier, *A split fluorescent reporter with rapid and reversible complementation.* Nat Commun, 2019. **10**(1): p. 2822.

630. Borgstahl, G.E., D.R. Williams, and E.D. Getzoff, *1.4 A structure of photoactive yellow protein, a cytosolic photoreceptor: unusual fold, active site, and chromophore.* Biochemistry, 1995. **34**(19): p. 6278-87.

631. Tebo, A.G., F.M. Pimenta, Y. Zhang, and A. Gautier, *Improved Chemical-Genetic Fluorescent Markers for Live Cell Microscopy.* Biochemistry, 2018. **57**(39): p. 5648-5653.